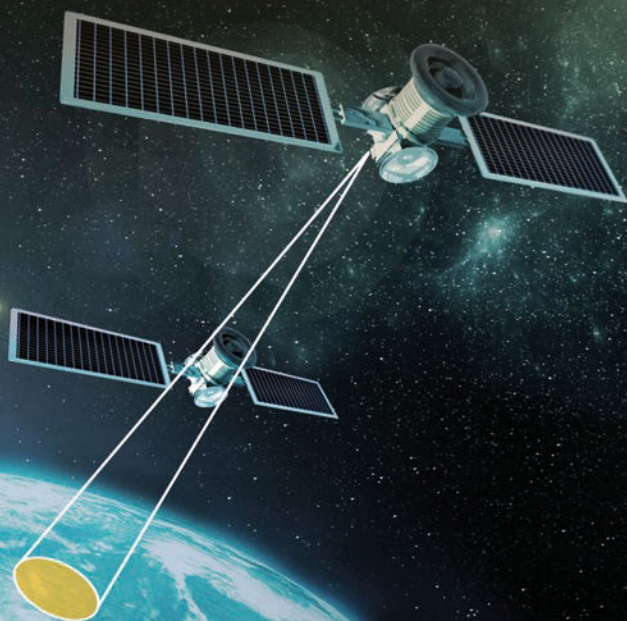


Christopher D. Lippitt
Douglas A. Stow
Lloyd L. Coulter *Editors*

Time-Sensitive Remote Sensing



 Springer

Time-Sensitive Remote Sensing

Christopher D. Lippitt • Douglas A. Stow
Lloyd L. Coulter
Editors

Time-Sensitive Remote Sensing

 Springer

Editors

Christopher D. Lippitt
University of New Mexico
Albuquerque
New Mexico
USA

Lloyd L. Coulter
San Diego State University
San Diego
California
USA

Douglas A. Stow
San Diego State University
San Diego
California
USA

ISBN 978-1-4939-2601-5

ISBN 978-1-4939-2602-2 (eBook)

DOI 10.1007/978-1-4939-2602-2

Library of Congress Control Number: 2015940549

Springer New York Heidelberg Dordrecht London
© Springer Science+Business Media New York 2015

This work is subject to copyright. All rights are reserved by the Publisher, whether the whole or part of the material is concerned, specifically the rights of translation, reprinting, reuse of illustrations, recitation, broadcasting, reproduction on microfilms or in any other physical way, and transmission or information storage and retrieval, electronic adaptation, computer software, or by similar or dissimilar methodology now known or hereafter developed.

The use of general descriptive names, registered names, trademarks, service marks, etc. in this publication does not imply, even in the absence of a specific statement, that such names are exempt from the relevant protective laws and regulations and therefore free for general use.

The publisher, the authors and the editors are safe to assume that the advice and information in this book are believed to be true and accurate at the date of publication. Neither the publisher nor the authors or the editors give a warranty, express or implied, with respect to the material contained herein or for any errors or omissions that may have been made.

Printed on acid-free paper

Springer is part of Springer Science+Business Media (www.springer.com)

Foreword

The maturity of remote sensing applications and technology has resulted in many innovative uses of satellite and airborne imagery. One particular use that has accelerated over the past few years is focused on time-sensitive remote sensing, which reduces the time for image acquisition, analysis, and product delivery. Bundling of these steps into an efficient remote sensing system has resulted in the capability to address questions for applications where the time from acquisition to information is critical.

While several broad applications benefit from time-sensitive remote sensing, one in particular is disaster response and recovery. Over the past 22 years there has been a remarkable change in the way we in the US emergency management and first responder community respond to disasters. Throughout my career, first with the National Aeronautics and Space Administration (NASA) and then with the Department of Homeland Security, Science and Technology (DHS/S&T), I have had the privilege to serve with first response teams using remote sensing technologies to aid the response and recovery operations of some of our worst national disasters. Throughout these events I have witnessed the convergence of technologically-maturing remote sensing capabilities and human effort to bring assistance to victims in need of relief. During the response to Hurricane Andrew in 1992 aerial imagery was acquired and processed primarily outside of the operational disaster response process to support the governor's request for Federal relief funds and to help put a face on the magnitude and extent of the event. At that time, digital multispectral scanner data could not be acquired at a spatial resolution adequate to address damage assessment requirements at a building level. Aerial photography was flown, processed overnight, printed and sent by special courier back to the governor's team building the damage assessment. In 1999, Hurricane Floyd resulted in extensive flooding that lasted several weeks. The duration of the event permitted the use of government satellite assets like Landsat and RADARSAT to provide a synoptic view of river systems in flood stage while airborne assets flew dedicated missions to detail the status of specific communities. These missions, again, were mostly outside of the operational disaster response, which focused on saving lives and property, but served to provide a compelling assessment of the magnitude of this disaster.

By 2003 the face of remote sensing had changed a great deal. Several commercial companies had made the shift to digital camera systems. Space Imaging had

launched Ikonos and DigitalGlobe had launched QuickBird, a new generation of satellites equipped with high spatial resolution sensor systems. When NASA's Shuttle Columbia suffered a disastrous failure that year on February 1st, remote sensing assets were soon brought in to assist the extensive ground search operations. Image-based products from satellite and airborne systems were constructed on a daily basis and used to target optimal search areas. During the response to Hurricane Katrina, realization of the importance of imagery to the response process resulted in imagery being used to generate specific products, including siting temporary housing on the Gulf Coast of Mississippi and flood extent in New Orleans.

During Hurricane Sandy the use of remote sensing had evolved to the point of incorporation into the operational response flow. Since hurricanes rarely occur without notice, the DHS Federal Emergency Management Agency (FEMA) was able to pre-position aerial assets for post event acquisitions by taking advantage of the strong partnership formed with the Civil Air Patrol and the National Oceanic and Atmospheric Administration (NOAA) to fly missions over the areas of greatest impact. The maturity and capabilities of digital cameras used by these organizations and the ability to get the images into operations quickly that they enabled were critical to the response effort. These digital images were used to expedite the rental assistance applications for over 44,000 victims of that storm.

The evolution of disaster response, briefly described above, demonstrates that as the gap between technology and information (for example radar backscatter and residential damage, respectively) becomes smaller, the more the disaster management community will rely on remote sensing as a critical tool during response. That is because disaster response, like several other applications, is fundamentally a time-sensitive process where having 75 % of the answer at the time the decision has to be made is better than 100 % after the fact. Furthermore, what the disaster events described above all demonstrate is the need for rapid access to current information about the status of human health and infrastructure so that response resources can be allocated in the best possible way to minimize suffering and loss. One of the best sources of *current* information following a disaster is remote sensing imagery acquired, processed, and delivered within the timeframe of the specific event underway.

This book provides a detailed discussion of the topic of time-sensitive remote sensing. It describes methods for improving the delivery of image data and the structuring of acquisition methods to optimize disaster assessment procedures such as change detection. It contains information on a new sensor system for characterizing fires and also presents information on technology that leverages pre-event and post-event imagery to improve the acquisition of field data for applications such as preliminary damage assessment and search and rescue.

Time-Sensitive Remote Sensing also describes ongoing governmental programs constructed by NOAA and NASA to facilitate the use of remote sensing for disaster response. These programs serve as a guide for other agencies and organizations with remote sensing missions to follow. Furthermore, this section provides an overview of the International Charter and the role it plays in accessing international remote sensing assets for disaster response.

Disasters resulting from different hazard types (i.e. fire, flood, earthquake, hurricane) all have different timelines for the event; the time in which the event is recognized, occurs, impact are manifest, and in which response must occur to be effective. Efficient response to these different hazards must work within the timeline of the particular disaster to protect life and preserve property. Time-sensitive remote sensing methods identify the timeframe of a particular application, such as disaster response, and seek to provide information within the window of that timeframe. The final section of *Time-Sensitive Remote Sensing* presents four applications that illustrate the use of remote sensing for earthquake, fire, and drought as well as an overview of several other hazards. It describes unique approaches in the use of imagery and delivery mechanisms to address these needs. Although primarily focused on the application of time-sensitive remote sensing for disasters it is important to recognize that this approach to remote sensing applies broadly to a range of applications where the status of phenomena or change in land cover at specific times are critical, including for example agriculture, infrastructure monitoring, and environmental assessment. The discussions presented in this volume have relevance to a wide range of applications.

As disaster response organizations mature their Standard Operating Procedures and adopt new technologies to improve response operations the demand for more accurate and rapid information will increase. Approaches to time-sensitive remote sensing will guide the development of innovative sensor technology and analysis techniques as data providers seek to meet the requirements of this unique application area. The discussions in this book are the start of what will surely be a long-term effort to realize the full potential of remote sensing for disaster response.

Department of Homeland Security, Science and Technology
Directorate (Retired), Washington, DC, USA

Bruce A. Davis

Contents

Remote Sensing Theory and Time-Sensitive Information	1
Christopher D. Lippitt and Douglas A. Stow	
Part I Methods	
Time-Sensitive Remote Sensing Systems for Post-Hazard Damage Assessment	13
Douglas A. Stow, Christopher D. Lippitt, Lloyd L. Coulter and Bruce A. Davis	
Repeat Station Imaging for Rapid Airborne Change Detection	29
Lloyd L. Coulter, Douglas A. Stow, Christopher D. Lippitt and Grant W. Fraley	
Rapid Fire Detection, Characterization and Reporting from VIIRS Data	45
Christopher D. Elvidge, Mikhail Zhizhin, Feng-Chi Hsu and Kimberly E. Baugh	
Application of Mobile Data Capture with Imagery Support	55
Michael E. Hodgson, Bruce A. Davis, Dexter Accardo, Haiqing Xu, Karen Beidel and Silvia E. Piovan	
Part II Programs	
The International Charter ‘Space and Major Disasters’	79
Brenda K. Jones, Timothy S. Stryker, Ahmed Mahmood and Gabriel R. Platzeck	
The Federal Oil Spill Team for Emergency Response Remote Sensing, FOSTERRS: Enabling Remote Sensing Technology for Marine Disaster Response	91
Ira Leifer, John Murray, Davida Streett, Timothy Stough, Ellen Ramirez and Sonia Gallegos	

LANCE, NASA’s Land, Atmosphere Near Real-Time Capability for EOS	113
Kevin J. Murphy, Diane K. Davies, Karen Michael, Christopher O. Justice, Jeffrey E. Schmaltz, Ryan Boller, Bruce D. McLemore, Feng Ding, Bruce Vollmer and Min M. Wong	
Part III Applications	
A Comprehensive Analysis of Building Damage in the 2010 Haiti Earthquake Using High-Resolution Imagery and Crowdsourcing	131
John S. Bevington, Ronald T. Eguchi, Stuart Gill, Shubharoop Ghosh and Charles K. Huyck	
Near-Real Time Delivery of MODIS-Based Information on Forest Disturbances	147
Robert A. Chastain, Haans Fisk, James R. Ellenwood, Frank J. Sapiro, Bonnie Ruefenacht, Mark V. Finco and Vernon Thomas	
The Use of NASA LANCE Imagery and Data for Near Real-Time Applications	165
Diane K. Davies, Kevin J. Murphy, Karen Michael, Inbal Becker-Reshef, Christopher O. Justice, Ryan Boller, Scott A. Braun, Jeffrey E. Schmaltz, Min M. Wong, Adam N. Pasch, Timothy S. Dye, Arlindo M. da Silva, Henry M. Goodman and Paul J. Morin	
Use of Satellite Image Derived Products for Early Warning and Monitoring of the Impact of Drought on Food Security in Africa	183
Christophe Sannier, Sven Gilliams, Frédéric Ham and Erwann Fillol	

Contributors

Dexter Accardo St. Tammany Parish of Homeland Security and Emergency Preparedness, Covington, LA, USA

Kimberly E. Baugh Cooperative Institute for Research in Environmental Sciences, University of Colorado, Boulder, CO, USA

Inbal Becker-Reshef Department of Geographical Sciences, University of Maryland, College Park, MD, USA

Karen Beidel Department of Geography, University of South Carolina, Columbia, SC, USA

John S. Bevington ImageCat Ltd., London, UK

Ryan Boller NASA Goddard Space Flight Center, Greenbelt, MD, USA

Scott A. Braun NASA Goddard Space Flight Center, Greenbelt, MD, USA

Robert A. Chastain RedCastle Resources Inc., Salt Lake City, UT, USA

Lloyd L. Coulter Department of Geography, San Diego State University, San Diego, CA, USA

Diane K. Davies Science Systems and Applications, Inc./Trigg-Davies Consulting Ltd, Malvern, UK

Bruce A. Davis Department of Homeland Security, Science and Technology Directorate (Retired), Washington, DC, USA

Feng Ding ADNET Systems, Inc., NASA Goddard Space Flight Center, Greenbelt, MD, USA

Timothy S. Dye Sonoma Technology, Inc., Petaluma, CA, USA

Ronald T. Eguchi ImageCat, Inc., Long Beach, CA, USA

James R. Ellenwood USDA Forest Service Forest Health Technology Enterprise Team, Fort Collins, CO, USA

Christopher D. Elvidge Earth Observation Group, NOAA National Geophysical Data Center, Boulder, CO, USA

Erwann Fillol Fundación Acción Contra el Hambre (ACF Spain), Madrid, Spain

Mark V. Finco RedCastle Resources Inc., Salt Lake City, UT, USA

Haans Fisk USDA Forest Service Remote Sensing Applications Center, Salt Lake City, UT, USA

Grant W. Fraley TerraPan Labs LLC, San Diego, CA, USA

Sonia Gallegos Naval Research Laboratory, NRL, Stennis Space Center, Hancock County, MS, USA

Shubharoop Ghosh ImageCat, Inc., Long Beach, CA, USA

Stuart Gill SecondMuse, Santa Fe, NM, USA

Sven Gilliams Vlaamse Instelling Technologish Onderzoek (VITO), Mol, Belgium

Henry M. Goodman NASA Marshall Space Flight Center, Huntsville, AL, USA

Frédéric Ham Fundación Acción Contra el Hambre (ACF Spain), Madrid, Spain

Michael E. Hodgson Department of Geography, University of South Carolina, Columbia, SC, USA

Feng-Chi Hsu Cooperative Institute for Research in Environmental Sciences, University of Colorado, Boulder, CO, USA

Charles K. Huyck ImageCat, Inc., Long Beach, CA, USA

Brenda K. Jones Earth Resources Observation and Science Center, U.S. Geological Survey (USGS), Sioux Falls, SD, USA

Christopher O. Justice Department of Geographical Sciences, University of Maryland, College Park, MD, USA

Ira Leifer Bubbleology Research International, Solvang, CA, USA

University of California, Santa Barbara, CA, USA

Christopher D. Lippitt Department of Geography and Environmental Studies, University of New Mexico, Albuquerque, NM, USA

TerraPan Labs LLC, San Diego, CA, USA

Ahmed Mahmood Canadian Space Agency (CSA), Saint-Hubert, QC, Canada

Bruce D. McLemore Honeywell Technology Solutions, Inc., 7515 Mission Drive, Seabrook, MD, USA

Karen Michael NASA Goddard Space Flight Center, Greenbelt, MD, USA

Paul J. Morin Polar Geospatial Center, University of Minnesota, Minneapolis, MN, USA

Kevin J. Murphy NASA Goddard Space Flight Center, Greenbelt, MD, USA

John Murray National Aeronautic and Space Agency, Langley Research Center, NASA, LRC, Hampton, VA, USA

Adam N. Pasch Sonoma Technology, Inc., Petaluma, CA, USA

Silvia E. Piovan Department of Historical Geographical and Antiquity Sciences, Geography Section, Università degli Studi di Padova, Padova, Italy

Gabriel R. Platzek INVAP S.E., Ciudad de Córdoba, Pcia. de Córdoba, Argentina (X5003DDY)

Ellen Ramirez National Oceanic and Atmospheric Administration, National Environmental Satellite, Data, and Information Service, NOAA, NESDIS, College Park, MD, USA

Bonnie Rufenacht RedCastle Resources Inc., Salt Lake City, UT, USA

Christophe Sannier Systèmes d'Information à Référence Spatiale (SIRS), Villeneuve d'Ascq, France

Frank J. Sapio USDA Forest Service Forest Health Technology Enterprise Team, Fort Collins, CO, USA

Jeffrey E. Schmaltz Science Systems and Applications, Inc., NASA Goddard Space Flight Center, Greenbelt, MD, USA

Arlindo M. da Silva NASA Goddard Space Flight Center, Greenbelt, MD, USA

Timothy Stough Jet Propulsion Laboratory, JPL, Pasadena, CA, USA

Douglas A. Stow Department of Geography, San Diego State University, San Diego, CA, USA

David Streett National Oceanic and Atmospheric Administration, National Environmental Satellite, Data, and Information Service, NOAA, NESDIS, College Park, MD, USA

Timothy S. Stryker U.S. Geological Survey (USGS), Reston, VA, USA

Vernon Thomas Cherokee Nation Technology, Fort Collins, CO, USA

Bruce Vollmer NASA Goddard Space Flight Center, Greenbelt, MD, USA

Min M. Wong Columbus Technologies and Services, Inc., NASA Goddard Space Flight Center, Greenbelt, MD, USA

Haiqing Xu Department of Geography, University of South Carolina, Columbia, SC, USA

Mikhail Zhizhin Cooperative Institute for Research in Environmental Sciences, University of Colorado, Boulder, CO, USA

Space Research, Institute, Russian Academy of Sciences, Moscow, Russia

Remote Sensing Theory and Time-Sensitive Information

Christopher D. Lippitt and Douglas A. Stow

Abstract

The role of time in remote sensing is complex and, particularly in the case of time-sensitive remote sensing, can impose substantial control on the utility of information derived using remote sensing techniques. A common vernacular is used to define the role of time in remote sensing as it is currently understood. The various manifestations of time in the remote sensing process are then evaluated in terms of their potential effect on the utility of information produced. The concept of information utility, which necessitates acknowledgment of remote sensing's role as a information production system, provides an orienting construct for evaluating the affect of time on the remote sensing process.

Keywords

Time-sensitive remote sensing · Remote sensing theory · Information utility

C. D. Lippitt (✉)

Department of Geography and Environmental Studies, University of New Mexico,
Albuquerque, NM 87131, USA

Tel.: +1 (505) 277-5485

e-mail: clippitt@unm.edu

D. A. Stow

Department of Geography, San Diego State University, San Diego, CA 92182-4493, USA

Tel.: +1 (619) 594-5498

e-mail: stow@mail.sdsu.edu

1 Theory in Remote Sensing

This chapter interrogates the role of time in the remote sensing process from a theoretical perspective. The myriad interactions between time and the remote sensing process are minimally addressed in most conceptual models of remote sensing, despite the control time can exert over the utility of the information produced by remote sensing (Lippitt et al. 2014). To effectively leverage the unique synoptic observation capabilities of remote sensing to produce time sensitive information, monitor transient phenomena, or accurately characterize the nature of dynamic changes, a coherent body of knowledge prescribing methodological best practices is critical. This body of knowledge will necessarily be based on empirical tests and practical experience deploying various remote sensing systems, but just as necessarily, a common vernacular, conceptualization of remote sensing, and common understanding and active debate of the role of remote sensing in science and society. This book and the theoretical treatment of time in the remote sensing process presented in this chapter are intended to contribute to and (hopefully) facilitate expansion of the body of knowledge relating to the use of remote sensing to inform time-sensitive decisions and, accordingly, expand the utility of remote sensing to some of societies' most pressing challenges.

To date, remote sensing has been primarily an engineering exercise focused on the design, implementation, and testing of hardware and software systems to permit earth observation and mapping. The discipline's primary epistemology, academic culture, and mode of instruction are focused on what is resolvable at what precision using a given remote sensing approach. Knowledge is generated through empirical testing, comparison to some standard, and rigorous validation. The ability of remote sensing to do various tasks has advanced substantially as a product of this empirical approach and many technological innovations from a multitude of disciplines.

It is fair to say that remote sensing approaches now play a primary data collection role in earth science disciplines (e.g., Hartmann et al. 2013). The persistent role of remote sensing in intelligence and war fighting (Stanley 1981), coupled with its many civilian applications (Mondello et al. 2006) have helped make remote sensing into a broad and well funded discipline that spans a variety of academic departments, industries, and branches of government. Like geographic information systems (GIS), remote sensing is a technology that is used (i.e., a tool), but is also a profession that is practiced (e.g., photogrammetry, image analyst), and an academic discipline that exists formally in academic journals, degree specializations, and professional societies.

The broad utility of remote sensing as a tool and the subsequent demand for trained professionals may help explain why the discipline has largely focused on improvement of the ability to resolve targets or measure properties; those improvements, even if incremental, have tangible benefits with quantifiable value. The ability to resolve novel targets or to make measurements with improved precision expands the use of remote sensing into new application domains, prompts the creation of new remote sensing companies, and ultimately contributes to better data and better

science. In 2011 remote sensing was a 7 billion US\$ per year industry projected to grow at between 9–14 % per year for the next decade (Mondello et al. 2011).

Remote sensing employs laws (e.g., Boltzman's, Wien's, Planck's) and theory (e.g., particle, wave) from physics, but there are few examples of work seeking generalized principles of remote sensing in the literature. The few examples of published works about the nature of remote sensing that do exist (e.g., Phinn et al. 2003; Schott 2007; Strahler et al. 1986; Woodcock and Strahler 1987) conceptualize what might be called remote sensing theory and have had a measurable impact on the discipline, whether by citation rate or pervasiveness of the concepts in use today. However, these seminal references minimally address the role and importance of time as a key element of remote sensing theory. While examples of published works are rare, the promise of theory in remote sensing science is significant (Lippitt et al. 2014; NASA 2013).

This chapter attempts to contribute to the small but important body of remote sensing theory and establishes the foundations for the theme of this book—time-sensitive remote sensing. Specifically, it seeks to contribute toward what Lippitt et al. (2014) refer to as “a paucity of methodological prescription and theory vis-à-vis information timeliness.” Conceptualizations of time in the remote sensing literature and their related terminology are reviewed and followed by a discussion of the various ways in which time plays a critical role in determining the utility of remote sensing derived information.

2 Conceptualizing Time in Remote Sensing

Remote sensing of materials, objects, or phenomena necessarily requires consideration of when to observe, such that the timing of acquisition is aligned to optimize target or phenomenon observations and possibly coordinated with ancillary (e.g., ground) observations. While perhaps obvious, this simple principle can become challenging to implement when phenomena are transient; coordination of assets to be located over the scene, prediction of the appropriate time to observe, adapting to changing conditions, etc., all present operational challenges to this most rudimentary temporal question in remote sensing—when to acquire. Beyond when to acquire, the timeliness (Lippitt et al. 2014) of remote sensing derived information presents a second critical temporal question. While neither of these questions has received a great deal of attention in the remote sensing literature, both are fundamental to the utility of remote sensing, as a tool, profession, and discipline.

Like most scientific disciplines, remote sensing has a nomenclature, a set of terms that are accepted by its practitioners to enable discussion of concepts efficiently and precisely. The small subset of terms relating to time provide a window into how remote sensing has, to date, conceptualized time in the remote sensing process. These conceptualizations of time, codified by terminology, help elucidate appropriate remote sensing methods and, subsequently, increase the value of remote sensing as

a tool and the intellectual merit of remote sensing as a discipline. They represent generalized truths about the role of time in remote sensing. Terminology relating to time is reviewed and new terms useful for conceptualizing and communicating time in the remote sensing process are proposed.

2.1 Temporal Resolution

Temporal resolution, which is defined by Jensen (2007, p. 17) as “how often the sensor records imagery of a particular area”, is the only theoretical concept of time that is widely accepted in the remote sensing literature. The concept of temporal resolution explains well the operation of satellite-based sensors; orbits, whether polar or geostationary, enable repeated observation of earth surface locations at a predictable interval. For airborne sensors, however, it is far less clear how to define their temporal resolution beyond being more variable and flexible than satellites, except perhaps in the context of routine surveillance. Despite not always being quantifiable and its variable applicability to sensors, the concept of temporal resolution has proved indispensable to remote sensing.

Temporal resolution can be defined quantitatively as the number of observations per unit time, characterizing temporal sampling frequency or the time interval between successive observations. The term has not, however, necessarily implied regular intervals between those observations in common use. In the case of regular sampling intervals, temporal resolution can be described by a single frequency. Any deviation from that single frequency can be considered modulation (M) of the temporal resolution, quantifiable as:

$$M = \frac{R_{\max} - R_{\min}}{R} \quad (1)$$

where R is the temporal resolution in units of observations per unit time, R_{\max} the maximum temporal resolution and R_{\min} the minimum temporal resolution. Modulation provides a measure of the degree of variation in temporal resolution and makes its quantitative description possible even in cases where frequency varies.

2.2 Timeliness

The concept of timeliness, defined by Lippitt et al. (2014, p. 6817) as “the time between information request and the use of that information to inform a decision”, provides a more quantitative meaning than the conventional definition of timeliness that simply means the state of being timely. Timeliness situates remote sensing in a decision support context by describing the amount of time required to produce, deliver, and ingest remote sensing derived information. While broader acceptance of the term remains to be seen, timeliness provides a concept that is critical to the use of remote sensing to answer time-sensitive questions.

Timeliness quantifies the amount of time required to deliver information to a user once that user requests the information, where that user could be a human or automated system (Lippitt et al. 2014). It seems, however, that there are several categories of timeliness that might be useful to describing the time required for various tasks. Lippitt et al. (2014) allude to these categories, but do not specify them. Acquisition time (TA) describes the amount of time required to collect remote sensing of a given target from the request for that acquisition, analysis time (TR) the time required to process collected data into an information product, and transmission time (TC) the time required to move data or information between systems or persons. Collectively, these determine the timeliness of a given remote sensing system (RSS). By definition, minimizing timeliness is of primary concern to time-sensitive remote sensing applications.

2.3 Capacity

The ability of a remote sensing system to produce information within a given time-period (i.e., timeliness) can be estimated by quantifying the capacity of a remote sensing system to observe ground area (i.e., sensor capacity), process data into information products (i.e., analyst capacity) and deliver data and information (i.e., channel capacity) (Lippitt et al. 2014). Capacity is a measure of volume (e.g., area, data quantity) per unit time. Conceptualization of all systems required to acquire, process, and distribute remote sensing data and information as a single remote sensing system where individual components of that system have a capacity that, in aggregate, determine the capacity of the system as a whole, enables the configuration of a remote sensing system to be explicitly linked to the timeliness of that system.

2.4 Time-Sensitive

Time-sensitive remote sensing, what many other authors have described as ‘real-time’ remote sensing (e.g., Ambrosia et al. 2003; Burkert et al. 2011; Cervone et al. 2006; Chen et al. 2011; Micheloni and Foresti 2006; Sannier et al. 2002), is described by Lippitt (2014, p. 6817) as “remote sensing applications where the utility of information changes as a function of the time inherent in the operation of the system.” The term time sensitive provides a nuanced clarification relative to real time with respect to describing expedited remote sensing applications, but more importantly it represents an advancement in remote sensing’s conceptualization of its role as an information production system. It makes clear that time-sensitive remote sensing, and arguably all remote sensing, necessarily must consider the user intended to employ that information if that information is to be of the most value. If the information arrives to late, its value is reduced or eliminated.

While time sensitivity is clearly defined, it seems that there are several ways in which remote sensing can be time sensitive. While many applications are sensitive to the amount of time required to produce and deliver information to a user (e.g.,

hazard response), others are sensitive to only a portion of the RSS. Observation of transient phenomena, for example, may make the utility of information sensitive to acquisition time, but not to analysis or transmission time. Monitoring algae blooms, for example, requires acquisition within a relatively short temporal window, but does not, for many scientific applications, necessitate expedited processing or delivery to a user, unless information is needed to guide in situ ocean surface measurements at the time of the bloom. Similarly, other applications may leverage archival data, making them sensitive to analysis and transmission time, but not to acquisition time. We can therefore consider applications to be acquisition time-sensitive, transmission time-sensitive, and/or analysis time-sensitive.

2.5 Window of Opportunity

Some applications do not fit the definition of time-sensitive provided by Lippitt et al. (2014), but are none-the-less sensitive to time. Monitoring of coastal processes or tidal boundary mapping, for example may require that acquisition be coordinated with specific tidal stages. In such a case, the time between the decision to acquire and the acquisition (i.e., acquisition time) does not affect the utility of the information produced, unless there is only one such observational opportunity. What does affect the utility of that information is the ability to acquire at the appropriate tidal stage, during what can be considered a window of opportunity. The utility of the information that such a RSS produces is not sensitive to the amount of time inherent in the acquisition, transmission, or analysis of remote sensing data, but it is sensitive to the ability to observe transient phenomena at a specific point in time.

3 Time and Information Utility

Information derived from remote sensing sources has some amount of utility or value that varies as a function of the quality of the information produced and the user's timely employment of that information in a decision process (Lippitt et al. 2014). Measurement or quantification of utility necessarily requires consideration of the effect of that information on a decision process, compared to it not informing that decision process. Quantification of the utility of information derived from remote sensing sources is challenging due to the many factors affecting the information itself (e.g., accuracy, timeliness), its combination and weighting with other information sources, how it is presented to a user, and how it is employed. Nonetheless, it provides a concept and clear rationale for the configuration of RSSs—to maximize the utility of the information produced in its intended decision context. Time-sensitive remote sensing, by definition, makes the utility of remote sensing information sensitive to the timeliness of delivery, but the utility of information is affected by time, in some way, for all remote sensing.

3.1 Temporal Resolution

Temporal resolution is a measure of temporal sampling density, in the same way that sampling density in a spatial context determines the scale of phenomena observed (Turner et al. 1989). Temporal resolution must therefore be matched to the temporal scale of the phenomena being measured, making the affect of temporal resolution on the utility of remote sensing derived information idiosyncratic to the application and/or phenomena under observation. The higher or finer the actual and potential temporal resolution of a RSS the more likely that critical timeliness can be achieved. Higher/finer temporal resolution also increases the potential utility of an RSS to adequately capture the dynamics of processes or phenomena.

Turner et al. (2008) call for an increase in temporal and spatial resolution in satellite remote sensing systems, but there are technological limits that necessitate the tradeoff of spatial resolution and spatial coverage, such that increases in temporal resolution require reduction in spatial resolution. Systems like the NOAA Advance Very High Resolution Radiometer (AVHRR) and Aqua/Terra Moderate Resolution Imaging Spectrometer (MODIS) have relatively high temporal sampling frequency (e.g., one to four observations per day), but do so at relatively coarse spatial resolution (250 m–8 km). Commercial high spatial resolution satellites offer the promise of high temporal resolution (Hodgson et al. 2010) through their pointability and through constellations of platforms carrying identical sensors (Tyc et al. 2005). Since pointability involves variable look angles, it introduces variability in apparent surface radiance and emittance, and view geometries that are unsuitable for many types of time series analyses.

3.2 Timeliness

Timeliness has a clear affect on the utility of information produced from remote sensing (Lippitt et al. 2014). The magnitude of that affect is a product of the time sensitivity of the information that informs decision-making or knowledge formulation tasks. In many cases, information derived from a RSS that does not meet critical timeliness requirements has no utility, even if it is highly accurate and/or precise. Conversely, information that does meet critical timeliness requirements may be sufficiently inaccurate or imprecise to yield wrong decisions. Even in cases that do not fit the definition of time-sensitive remote sensing, the timeliness of information delivery still affects the utility of the information produced (Phinn et al. 2003). As an example, monitoring land cover change for planning and decadal projections, may require results within months or years of the decision to employ remote sensing techniques to obtain that information. Current technological, administrative, and analysis practices regularly produce information within these time scales, not meeting the definition of time-sensitive remote sensing put forth in Lippitt et al. (2014), but that information nonetheless must be delivered within some time frame to be of use for decision-making. Decline in the utility of such information to inform planning decisions is gradual relative to the time scales of current remote sensing technology

and practice, but contractual obligations, policy cycles, and a range of other potential factors make timeliness a fundamental control on information utility in all cases.

3.3 Window of Opportunity

The time at which remotely sensed data are captured can determine the utility of information derived from such data. If the window of opportunity to capture a process or phenomenon of interest is missed, resultant information products may have no utility. In some cases, time of acquisition represents a continuous control on information utility by contributing to the timeliness of information delivery. Similarly, analysis and transmission time can act as binary or continuous controls on information utility, but binary control (i.e., useful/not useful) is limited to time-sensitive remote sensing applications where analysis or transmission time alone are greater than the timeliness requirements of a given user case. Timeliness is often a binary control on information utility to a particular user, in cases where information delivery cannot take place before a decision is made. The affect of timeliness on information utility is user and use specific; utility may be reduced to zero for one user tasked with a given decision (e.g., land manager with a report due), but that information may still be of use to others or to that same user for a different application (e.g., next years report).

Recently implemented and tested missions, both spaceborne (e.g., Davies et al. 2009; Ip et al. 2006) and airborne (e.g., Ambrosia et al. 2003), have begun to explicitly consider the timeliness of information delivery in their design by designing sensor, transmission, and analysis systems in concert. These systems produce and deliver data and information and, therefore, meet the definition of RSS proposed by Lippitt et al. (2014). This change in practice represents a profound change in conceptualization from remote sensing as a data collection technique to remote sensing as an information production system; so profound that one of the first operational missions to adopt this orthodoxy, MODIS, has been adjectivalised to “MODIS-ize” to describe this change in approach. MODIS-izing, which is essentially the adoption of the Lippitt et al. (2014) definition of RSS, has been demonstrated by MODIS and related programs to lead to dramatic reductions in the time required to deliver remote sensing derived information (i.e., timeliness).

4 Conclusions

Time is implicit in the remote sensing process. Collection, transmission, analysis, and even light traveling from the ground to a sensor, all take time. All phenomena observed are inherently transient at some temporal scale. The role of time in the remote sensing process is complex and idiosyncratic to the application, but not so complex that clear trends and dependencies cannot be observed or generalized. The

terminology and concepts reviewed here likely represent a subset of the myriad ways in which time affects the utility of remote sensing derived information, but none-the-less represent a promising body of knowledge on which to build.

The concept of information utility, which necessitates acknowledgment of remote sensing's role as a information production system, provides an orienting construct for evaluating the affect of time and other factors on the remote sensing process. While utility is difficult to empirically measure or quantify and is thus, for now, a theoretical concept, it permits interrogation and generalization of the affect of various factors on remote sensing. In this chapter, utility provides a concept for evaluating the affect of time on the remote sensing process.

Unlike the majority of remote sensing research, this chapter does not test, observe, or measure. Instead it takes a meta-view and theoretical approach to understanding the role of time in the remote sensing process. The chapters that follow provide valuable methodological insights and document useful applications of time-sensitive remote sensing.

References

- Ambrosia VG, Wegener SS, Sullivan DV, Buechel SW, Dunagan SE, Brass JA, Stoneburner J, Schoening SM (2003) Demonstrating UAV-acquired real-time thermal data over fires. *Photogramm Eng Remote Sens* 69:391–402
- Burkert F, Butenuth M, Ulrich M (2011) Real-time object detection with sub-pixel accuracy using the level set method. *Photogramm Rec* 26:154–170
- Cervone G, Kafatos M, Napoletani D, Singh RP (2006) An early warning system for coastal earthquakes. *Natural hazards and oceanographic processes from satellite data*. Elsevier Science Ltd, Oxford, pp 636–642
- Chen N, Chen Z, Di L, Gong J (2011) An efficient method for near-real-time on-demand retrieval of remote sensing observations. *IEEE J Sel Top Appl Earth Obs Remote Sens* 4:615–625
- Davies DK, Ilavajhala S, Wong MM, Justice CO (2009) Fire information for resource management system: archiving and distributing MODIS active fire data. *IEEE Trans Geosci Remote Sens* 47:72–79
- Hartmann DL, Tank AMGK, Rusticucci M, Alexander LV, Brönnimann S, Charabi Y, Dentener FJ, Dlugokencky EJ, Easterling DR, Kaplan A, Soden BJ, Thorne PW, Wild M, Zhai PM (2013) Observations: atmosphere and surface. In Stocker TF, Qin D, Plattner GK, Tignor M, Allen SK, Boschung J, Nauels A, Xia Y, Bex V, Midgley PM (eds) *Climate change 2013: the physical science basis. Contribution of working group I to the fifth assessment report of the intergovernmental panel on climate change*. Cambridge University Press, New York
- Hodgson ME, Davis BA, Cheng Y, Miller J (2010) Modeling remote sensing satellite collection opportunity likelihood for hurricane disaster response. *Cartogr Geogr Inf Sci* 37:7–15
- Ip F, Dohm JM, Baker VR, Doggett T, Davies AG, Castano R, Chien S, Cichy B, Greeley R, Sherwood R, Tran D, Rabideau G (2006) Flood detection and monitoring with the autonomous sciencecraft experiment onboard EO-1. *Remote Sens Environ* 101:463–481
- Jensen JR (2007) *Remote sensing of the environment: an earth resource perspective*, 2nd edn. Prentice Hall, Upper Saddle River
- Lippitt CD, Stow D, Clarke K (2014) On the utility of models for time-sensitive remote sensing. *Int J Remote Sens* 35:6815–6841

- Michelsoni C, Foresti GL (2006) Real-time image processing for active monitoring of wide areas. *J Vis Commun Image Represent* 17:589–604
- Mondello C, Hepner GE, Williamson RA (2006) 10-year remote sensing industry forecast—phase IV—study documentation. *Photogramm Eng Remote Sens* 72:985–1000
- Mondello C, Hepner GE, Boerman S (2011) ASPRS ten-year remote sensing industry forecast phase VI. *Photogramm Eng Remote Sens* 77:1081–1095
- NASA (2013) Research opportunities in Space and Earth sciences—2013. In: NASA Research Announcement (NRA) soliciting basic and applied research proposals. National Aeronautics and Space Administration, Washington, D.C.
- Phinn SR, Stow DA, Franklin J, Mertes LAK, Michaelsen J (2003) Remotely sensed data for ecosystem analyses: combining hierarchy theory and scene models. *Environ Manage* 31:429–441
- Sannier CAD, Taylor JC, Plessis WD (2002) Real-time monitoring of vegetation biomass with NOAA-AVHRR in Etosha National Park, Namibia, for fire risk assessment. *Int J Remote Sens* 23:71–89
- Schott JR (2007) *Remote sensing: the image chain approach*, 2nd edn. Oxford University Press, New York
- Stanley RM (1981) *World War II photo intelligence*. Scribner, New York
- Strahler AH, Woodcock CE, Smith JA (1986) On the nature of models in remote-sensing. *Remote Sens Environ* 20:121–139
- Turner MG, Dale VH, Gardner RH (1989) Predicting across scales: theory development and testing. *Landscape Ecol* 3:7
- Turner, B. L., II and P. Robbins (2008). Land-change science and solitical ecology: similarities, differences, and implications for sustainability science. *Annu Rev Environ Resour* 33:295–316.
- Tyc G, Tulip J, Schulten D, Krischke M, Oxfort M (2005) The Rapideye mission design. *Acta Astronaut* 56:213–219
- Woodcock CE, Strahler AH (1987) The factor of scale in remote sensing. *Remote Sens Environ* 21:21

Part I Methods

Time-Sensitive Remote Sensing Systems for Post-Hazard Damage Assessment

Douglas A. Stow, Christopher D. Lippitt, Lloyd L. Coulter
and Bruce A. Davis

Abstract

Remote sensing can provide useful information in post-disaster assessments, depending on the type of hazard and when in the emergency response and recovery stage, the particular types of information are required. Three general types of post-disaster assessment can be defined, for which remote sensing may contribute to data gathering and information delivery: (1) large-area reconnaissance, situational awareness, and/or mapping of damage extent and severity (i.e., what communities suffered the most impact), (2) impact to family stability in terms of homes and businesses damaged or destroyed, and (3) impact to critical infrastructure such as roads, energy grids (electrical, gas and water), and public facilities.

This chapter provides a comprehensive perspective on the rationale and end-to-end design of time-sensitive remote sensing systems (TSRSS) that are able to provide timely information on magnitude and extent of damage immediately following hazard events in support of emergency management decision-making. An emphasis is placed on airborne platforms because of their greater flexibility and lower altitude of operation, which enables finer spatial resolution sensing

D. A. Stow (✉) · L. L. Coulter
Department of Geography, San Diego State University,
5500 Campanile Dr., San Diego, CA 92182, USA
Tel.: +1 (619) 594-5498
e-mail: stow@mail.sdsu.edu

C. D. Lippitt
Department of Geography and Environmental Studies,
University of New Mexico, Albuquerque, NM 87131, USA

B. A. Davis
Department of Homeland Security, Science and Technology Directorate (Retired),
Washington, DC 20528, USA

and greater control over imaging characteristics, as well as improved temporal tasking.

Remote sensing and related technologies associated with small aircraft, consumer grade digital cameras, and image processing procedures have matured substantially over the past decade and have been integrated into prototype TSRSS that are ready for operational and cost effective implementation for post-hazard damage assessment. Although some technology development in the area of image analysis still remains to be accomplished, the main limitations to implementation are institutional in nature (e.g., funding, technology coordination and acceptance, and government regulations). These limitations are worth overcoming so that TSRSS are implemented to save lives, aid in recovery, rehabilitation and remediation, and reduce clean-up costs associated with disasters.

Keywords

Hazards · Emergency response · Airborne remote sensing · Repeat station imaging · Change detection · Time sensitive

1 Introduction

Remote sensing (RS) imagery derived from airborne (suborbital) digital and earth observation satellite (orbital) systems (Visser and Darwood 2004) provide valuable sources of information about the location and severity of damage following major disasters (Stryker and Jones 2009). Disasters or hazards of a more geographically-extensive nature where remote sensing is particularly relevant include hurricanes, tornados, earthquakes, tsunamis, wildfires, floods, and terrorist events (Hodgson and Davis 1998). RS imagery has been underutilized and with limited effectiveness for these damage assessment tasks, largely because of a lack of technology integration, pre-event planning, and suitable data/information delivery systems. When effectively implemented, RS imagery can provide information on the degree, extent, and nature of damage to built and natural features which can be used to readily estimate the amount, distribution, and types of relief required.

Remote sensing can play multiple roles in post-disaster assessments, depending on the type of hazard and when in the various stages of emergency response and recovery particular types of information are required (Cutter 2003; Joyce et al. 2009). Three general types of post-disaster assessment can be defined, for which remote sensing may contribute to data gathering and information delivery: (1) large-area reconnaissance, situational awareness, and/or mapping of damage extent and severity (i.e., what communities suffered the most impact), (2) impact to family stability in terms of homes and businesses damaged or destroyed, and (3) impact to critical infrastructure such as roads, electrical grid, and public facilities. Another potential role of remote sensing is estimation of debris volumes for subsequent removal;

however minimal research and development activities have been conducted to evaluate, let alone operationalize such an implementation of remote sensing.

The goal of this chapter is to provide a comprehensive perspective on the rationale and end-to-end design of time-sensitive remote sensing systems (TSRSS) that are able to provide timely information on extent of damage and volume of debris immediately following hazard events in support of decision making by emergency managers. The objective is to describe the considerations and specifications for the components of the TSRSS in a manner that bridges the more theoretical treatment of TSRSS found in Chap. 1 with the more technical and applied material covered in Chap. 3. An emphasis is placed on airborne platforms because of their greater flexibility and lower altitude of operation, which enables finer spatial resolution sensing and greater control over imaging characteristics and timely acquisitions.

The proposed systems are based on theoretical, technical and applied aspects of: (1) time-sensitive remote sensing, (2) end-to-end airborne imaging systems, (3) precision image registration, (4) image change detection, (5) softcopy photogrammetry and light detection and ranging (LiDAR) for digital surface modeling, and (6) image and map delivery systems. All of these components of remote sensing are pertinent to effective damage assessments and are addressed in this chapter.

2 Information Requirements

Any remote sensing-based decision support system should be, first and foremost, responsive to users' information requirements (Phinn 1998). Information requirements of emergency response organizations need to be specified, in order to develop a TSRSS that provides appropriate information in a sufficiently reliable and timely fashion. National level emergency response organizations, e.g., the U.S. Department of Homeland Security (DHS), Federal Emergency Management Agency (FEMA), and regional and local emergency operations centers should be included as members of research teams to identify specific information requirements such as timeliness, accuracy and precision of damage assessments, cost constraints, and in-house technical capabilities. Their participation throughout any research involving the incorporation of advanced technologies to improve existing procedures is critical to successful implementation into operations.

Particularly important input from emergency response agencies is a determination of the types of hazards that have a reasonable probability of inflicting damage to a given jurisdictional area, as well as the types of built and natural features for which damage assessments are to be conducted. Damage and debris characteristics can be different for different types of hazards, as influenced by the nature of the disturbance associated with each type of hazard (e.g., water inundation for floods, high wind speeds for tropical storms, or ground shaking for earthquakes). For each hazard, the types of built features that may be damaged and the characteristics of damage will differ. Other important guidance from emergency managers is whether information

on damage is desired for all built features or some subset, such as critical infrastructure. Critical infrastructural features could include for instance, major transportation features, power generating facilities and transmission equipment, medical facilities, or any feature that if severely damaged, could result in massive secondary damage (e.g., fire and flooding). Determining which infrastructural features are truly critical, where they are located, and how damage would likely be manifested, in preparation for a potential disaster, can help guide the development and implementation of an effective TSRSS for post-disaster assessment.

3 Remote Sensing Roles, Strategies and Options

The most timely and arguably the most important information required for disaster response is associated with critical infrastructure, which affects emergency response communications and transportation, and the ability to provide timely medical care and to minimize secondary hazards (e.g., fires stemming from earthquake damage). Critical infrastructure features tend to be more localized, so site-specific damage information is needed in a very timely manner. However, access to critical infrastructure on the ground may be limited by road and bridge closures, so flexible airborne remote sensing data collection may provide the only source of information within a few hours of a major hazardous event.

Assessing the full extent and degree of damage, particularly to residential and other areas where rescues, evacuations, or triage need to occur becomes the focus, once critical infrastructure has been assessed. The spatial coverage requirements are more challenging than for assessing damage to critical infrastructure, though spatial resolution requirements are less stringent for this phase of post-damage assessment. Thus, both aircraft and satellite systems provide viable solutions to performing wide-area reconnaissance and mapping activities (Tralli et al. 2005), as long as the satellite acquisition opportunity is within the window of opportunity for the data to be valuable.

Different strategies and options exist for implementing remote sensing approaches to damage assessment. For example, a strategy for mapping the distribution and type of damage is to analyze only post-event imagery, while another is to compare post-event and extant imagery through the process commonly referred to as change detection. An advantage of the change detection approach is that damage is manifested as a land surface change that is more readily detectable than a single static view of damaged features that may be amorphous or may not have characteristic image signatures. A disadvantage is that the change detection process requires access to relatively recent pre-event imagery for areas with average land use change due to population growth and both dates of imagery must be precisely registered (co-aligned) to minimize false detections. Replicating sensors and view geometries is the most effective means for achieving precise image registration, as elaborated in Chap. 3 in the image pre-processing section (Coulter et al. 2003; Stow et al. 2003).

As is demonstrated by Lippitt et al. (2014), a TSRSS for post-hazard damage assessment must be carefully planned and constructed as an end-to-end system in a manner that attempts to minimize time to information delivery while meeting information accuracy and reliability requirements. Components of such an end-to-end system include: (1) planning of RS data capture, (2) RS data capture, (3) RS image transfer to processing facility, (4) geometric and radiometric processing, (5) image analysis and information extraction, and (6) data and information delivery to user. Associated with each component is a lapse of time and the total time for the system to generate the required information must be less than the maximum time for information to have utility in disaster response operations.

3.1 Pre-acquisition Planning

Pre-event planning of remote sensing data acquisition is important if timely and reliable information is to be generated, yet it is rare for such planning to be conducted, since most types of disasters are unpredictable, infrequent and episodic. In fact, a plan for the entire image capture, processing and delivery procedures should be prepared for disaster prone areas and particularly for critical infrastructural features (Lippitt et al. 2014). Flood, tornado, and particularly hurricane disasters are somewhat predictable through storm forecasts. For these more predictable events and their likely areal extents of damage, it is feasible to determine the coverage of satellite imaging assets hours to several days in advance of a likely disaster (Hodgson et al. 2010) and/or plan for effective airborne imagery acquisitions. Since it can be difficult to predict the location of likely damage and conduct pre-event planning for other types of hazardous events, preemptive planning should be conducted for areas such as major earthquake fault zones, hurricane prone regions, and wildland-urban interface zones subject to wildfires.

Whether or not image acquisition is conducted prior to or after a disaster event has occurred, some form of pre-acquisition planning is required, particularly for airborne imagery. Of all choices and considerations pertaining to planning RS image acquisition for damage and debris assessment, the most critical is the choice of platform and sensor. Determining the performance domains and specifications for airborne and satellite platforms and imaging and elevation measuring sensors should be based on information requirements derived from user surveys. The primary trade-off is normally between spatial resolution and extent of coverage, such that the lower the altitude of imaging, the finer the spatial resolution and the more limited the extent of coverage per frame or swath. Though greater operational flexibility exists for airborne systems, satellite sensing systems do not have to be mobilized and may be the first asset available for capturing post-event imagery. However, most post-disaster assessments require fine spatial resolution imagery that can only be provided today by commercial satellite sensing systems (e.g., GeoEye and WorldView) that have fairly limited spatial and temporal coverage and irregular viewing geometries over time. Given these factors and trade-offs, airborne imaging systems are likely to be the primary RSS of choice for most post-disaster damage assessments.

Once the choice of airborne platform and sensor has been made, the next pre-acquisition planning decisions pertain to altitude of operation (to achieve a desired spatial resolution). The flight altitude above ground level will also determine the extent of coverage per frame (for framing systems) or swath width (for line array or scanning systems). Based on the coverage characteristics and requirements for stereo or variable view perspectives that determine along-track overlap percentages, flight lines and imaging station locations can be established based on flight planning software tools. Variable view perspective (i.e., nadir and oblique viewing) can be obtained from vertical imagery captured with substantial overlap or by using multiple camera systems with nadir and off-nadir pointing sensors. The advantage of oblique or off-nadir view perspective is the ability to detect structural failure that may be difficult to observe from nadir-viewing perspectives.

There are many other factors to consider when acquiring airborne imagery, each of which affect the final image quality and utility. These include: camera orientation, speed of the aircraft (affects image blur and overall area covered), time of day (affects illumination and shadowing), flight line orientation (affects bi-directional reflectance across images), camera/lens specifications (affects viewing geometry and area covered), and supporting systems, e.g., global positioning system (GPS), inertial measurement units (IMU), gyro-stabilized mount, that affect the ability to accurately capture and geo-reference imagery. Each of these factors affects single date and repeat-pass imaging. Camera orientation pertains to whether nadir, oblique or dual-perspective image data are to be captured. Normally either color or infrared imagery would be captured, given the high spatial resolution nature of the information requirements and the likely manual image interpretation or hybrid approach where semi-automated routines are followed by manual image analysis and editing.

An important factor in guiding pre-acquisition planning is whether or not a change detection approach to damage assessment is to be conducted. If such an approach is to be implemented then the most reliable change analyses are based on multi-temporal airborne digital frame imagery collected through a patent pending strategy called repeat station imaging (RSI). Repeat station imaging involves returning the same (or similar) sensor to the same imaging stations (defined by specific horizontal and vertical positions) over time, replicating view geometry, and geometrically processing images on a frame-by-frame basis to maintain the benefits of replicated view geometry (Fig. 1). The RSI approach is further described in Chap. 3. This means that flight-line and image capture station locations (x-y-z position of where each image was captured) and information on the sensor type for pre-event acquisitions must be available or can be reliably estimated. The matched station approach is particularly useful for assessment of damage to critical infrastructural features, where even subtle damages to built features (e.g., cracks and slumping) may be important to detect. For areas prone to disasters, it may be prudent to collect and have available metadata (e.g., flight altitudes and image station locations) for the most recent and/or most suitable archived airborne image data sets.

For wide-area reconnaissance and situational awareness of damage extent and severity (i.e., urban areas and built features not associated with critical infrastructure), the key is to efficiently obtain extensive imagery coverage with a spatial resolution

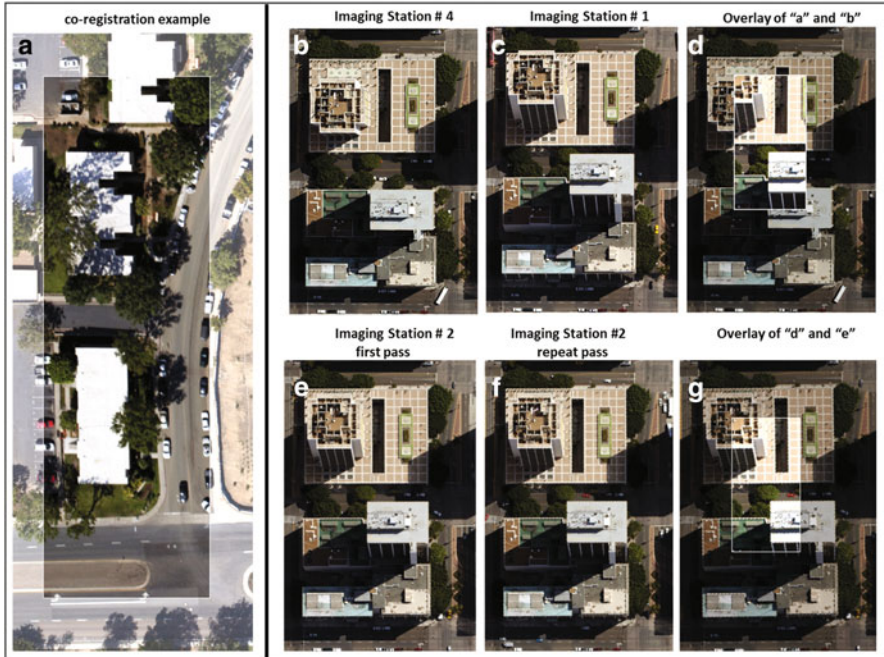


Fig. 1 a Time-2 image chip is displayed atop a lighter toned (i.e., washed-out) Time-1 image. The quality of the spatial co-registration between the 8 cm (3 in.) spatial resolution image sets is evident. A vehicle turning the corner is only present in the smaller image chip, and is not present in the larger chip. View angle differences between non-station matched images **b** & **c** are apparent, while view angle replication between station matched images **e** & **f** is demonstrated. Station matched images align precisely when co-registered **g**, compared to non-station matched images **d** which do not align well and are not appropriate for detailed change detection

and view geometry that are sufficient for determining the nature and extent of damage. Any knowledge of the spatial extent of hazard (e.g., from maps of flood extent or ground shaking magnitude) should be used to determine the area of image acquisition. Flight lines are then determined so as to optimize coverage for the desired areal extent.

Flight planning for image-based debris volume estimation can be conducted in a similar manner as for wide-area reconnaissance for damage assessment. A higher degree of along-track overlap in frames is likely since stereoscopic coverage is necessary for determining building/debris volumes. It may be that the same imagery would be used for both reconnaissance and debris volume estimation, such that the image capture requirements of the latter would dictate most of the flight planning specifications. The key consideration for whether this dual purpose usage of RS imagery is effective is the timing of acquisition, such that reconnaissance information can be derived in a sufficiently timely manner to enable rescue and evacuation efforts, while capturing a sufficiently stable debris field (i.e., the hazardous agent has subsided).

Finally, an often overlooked but critical aspect of pre-event planning is the mechanism and form in which remote sensing derived data and information products will be distributed to decision makers (Lippitt et al. 2014). Established responsibilities and protocols are required to ensure an efficient and coordinated response by first responders in various branches and levels of government (Alexander 2002). When coupled with the gravity of their charge to save lives and property, this structure requires that first responders know what information will come when, from whom it will come, and how to integrate that information into their response planning and coordination *before* the hazard occurs.

Collectively, pre-event planning represents the single most overlooked aspect of remote sensing for disaster response. Remote sensing based information collection following hazard events has typically been *ad hoc*, with collection, processing, and dissemination conducted by various private and public parties with minimal coordination. The end result of which is that a very small fraction of the information collected from remote sensing sources is typically exploited during the response phase of the disaster cycle.

3.2 Data Acquisition

Most decisions regarding image data acquisition should be made in pre-acquisition planning stages of the RSS implementation, preferably in advance of an actual disaster event. However, specific conditions during the post-hazard time frame will often require adjustments regarding timing and system configuration when actually acquiring airborne imagery. Factors such as weather (particularly cloud cover), airport runway, and air traffic conditions may necessitate deviation from pre-acquisition imaging plans, such as adjustments to flight plans and camera exposure settings.

While the choice of platform and sensor is made in pre-acquisition planning stages and some considerations pertaining to these TSRSS components were mentioned above, it is worth elaborating on some of the airborne platform and sensor system considerations that could prove to be useful in post-hazard image acquisitions. Unpiloted aircraft systems (UAS) and piloted light sport aircraft (LSA) are mobile, flexible and economical platforms that have great potential for supporting rapid damage assessment of critical infrastructural features (Ambrosia et al. 2003; Laliberte et al. 2010). These platforms can take-off and land in short distances and on a variety of surfaces, fly underneath most cloud cover, and most can be purchased and operated for very low cost when compared to traditional manned platforms. Their limitations are instability in turbulent atmospheric conditions, limited payload capacity and currently in the US, substantial regulatory limits on their operations. Small, high-wing aircraft (e.g., Cessna 172/182) are utilized by the US Civil Air Patrol, a volunteer group of private pilots who are funded by the US Air Force to support post-disaster imaging operations in addition to other mission responsibilities. Of greater utility for wide-area reconnaissance imaging are higher performance aircraft that can rapidly cover large areas and change altitude, with minimal need for refueling. Such aircraft are more expensive to operate, but cover ground quickly,

allowing for significantly reduced acquisition times and increased areal coverage (Lippitt et al. 2014).

Most airborne imaging for damage assessment is conducted with digital frame cameras, with some usage of digital line array sensors, while the use of metric film cameras and line scanner sensors is diminishing. The current trend with digital frame cameras is toward smaller, high-density arrays available (i.e., greater number of megapixels) at lower cost compared to large or medium format sensors, but still enabling high spatial resolution imaging and extensive areal coverage per frame. Another trend is more precise and lower cost global positioning and inertial measurement unit hardware, providing exterior orientation information for the location and view perspective of an airborne sensor. Similarly, cost reductions and performance enhancements of stabilized camera mounts help to ensure stable view perspectives.

The hardware component that has the potential to revolutionize time-sensitive remote sensing is the air-ground communications link. Such hardware enables images and/or image-derived maps (processed on-board) to be transmitted to a ground based command and control center for rapid product disseminate. These communication links tend to be prohibitively expensive and limited in range and frequency availability. Recent improvements in all of these characteristics offer great opportunity for remote sensing to contribute to the disaster response effort. An example of a relatively new development in airborne image transmission capability is the Real-time Airborne Management System (RAMS) developed by Pictometry, Inc. with support of the US Department of Homeland Security, Science and Technology Directorate specifically for post-disaster emergency response purposes.

To optimize the RSI image collection and subsequently improve the accuracy and efficiency of change detection processing, airborne data collection should be based on GPS (or other global navigation satellite system) triggering and flight line navigation systems. In the post-event image acquisition, x-y-z positions of flight lines and imaging stations, the digital frame camera, and exposure settings from a baseline collection need to be readily accessible and replicated to the extent possible. The approach enables view geometries and interior orientation properties of sensors to be replicated, which greatly simplifies and refines image-to-image co-registration. The biggest deterrents to implementing the RSI approach are (1) having access to the sensor originally used for baseline imaging and (2) the increasing availability of larger sensor array sizes at lower costs that make using the original sensor less attractive. Capturing images at nearly the same sun angle (or at least time of day) as the baseline image set is desirable, to minimize differences in shadows between image dates/times of acquisition. Scene features viewed from both nadir and off-nadir (i.e., oblique) perspectives may be required for definitive damage assessment. The RSI approach can be applied to either nadir or off-nadir view geometries.

3.3 Image Pre-processing

Image preprocessing considerations include geometric and radiometric corrections, and pre-analysis image enhancements. For geometric processing with single date

imagery, it is important to ascertain the level of georeferencing accuracy that is required for a particular time-sensitive task. Unlike traditional image products that often require accurate positioning so that they may be used with GIS data (or used to create GIS data), initial damage assessment immediately following a disaster tend to require less stringent geometric accuracy requirements. This is because the need to have a basic understanding of the extent and severity of the damage in a time frame to make critical decisions is more valuable than a perfectly registered image map. The level of positional accuracy required will depend on the intended application of the data and will primarily be affected by the image collection and supporting sensor systems (e.g., GPS & IMU) when employing a direct georeferencing approach. Geometric correction approaches that rely on reference datasets, significant human intervention, or computationally intensive optimization routines are rarely employed in a hazard response context due the expediency of direct project approaches in comparison.

The accuracy of direct projection is insufficient to enable change detection. The RSI approach may be employed to achieve precise (pixel-level) spatial co-registration between multitemporal image sets using automated techniques (Stow et al. 2003; Coulter et al. 2003; Coulter et al. 2013; Wyawahare et al. 2009) and coupled with direct projection to approximately locate detected changes. The co-registration accuracy of a large number and wide variety of data sets collected using the RSI approach have been tested and consistently found to have a co-registration accuracy within 1–2 pixels even with images having spatial resolution as fine as 8 cm (Coulter et al. 2003; Coulter and Stow 2008; Stow et al. 2003). Registration routines based on automatic control point generation and second-order polynomial warping functions can be implemented “on board” (i.e., images processed on the aircraft, immediately after acquisition) (Coulter et al. 2013; Du et al 2008; Zitova and Flusser 2003), when an RSI approach is used for image acquisition. The georeferencing accuracy of the matched image sets depends upon either the accuracy of the pre-event imagery (assuming that it was georeferenced ahead of time) or the accuracy afforded by the GPS/IMU systems on-board the aircraft at the time of acquisition. Achieving pixel-level spatial alignment between post-disaster imagery and existing ortho-rectified image mosaic products (such as the National Agriculture Imaging Program imagery) is not practical in most cases due to variable terrain and building feature distortions that can’t be corrected without ortho-rectifying the post-disaster images with high quality control data. However, flying at higher altitude in combination with a gyro-stabilized mount and long focal length lens can help to minimize geometric distortions caused by 3-D features.

Radiometric processing is useful for aligning digital number (DN) values between multitemporal image sets for reliable change detection. Automated global or local normalization techniques such as empirical line normalization and histogram matching routines can help to standardize image brightness values in like wavebands and therefore, reduce false positive change detections. For many time-sensitive remote sensing applications, however, radiometric preprocessing is minimized or omitted to reduce processing time. Identifying shadows and normalizing differences resulting from variations in shadow patterns between multitemporal image sets is also a critical

step for automated change detection, because shifting shadow areas can be observed as a false indication of “change” in the spectral characteristics between scenes (false positive).

3.4 Image Analysis

The value of a TSRSS for effective disaster response is the provision of remote sensing data that address the critical question at that time in the response timeline. Providing the data in a timely manner is only valuable if there are specific analytical approaches that extract reliable damage information from remote sensing imagery for use by incident commanders. When considering the use of remote sensing there is a difference between 2D mapping from image data to derive information regarding the distribution, severity and type of damage and estimating debris volume through measurements from digital surface models, with the latter discussed in the following section.

A repeat station imaging approach for assessing damage (particularly to critical infrastructure) is recommended, such that subtle, damage-associated changes to built structures are detected. The image analysis strategy incorporates a hybrid approach where apparent changes are automatically detected and delineated on the post-event image, and then an image analyst compares image pairs to determine if the apparent changes are actually associated with damage. Automated change detection routines can be pixel- or object-based, with the latter capable of incorporating shape and contextual information, along with image brightness changes. Simple change detection algorithms based on image brightness changes can be implemented “on board” in near real time, such that apparent change features are transmitted to a ground station along with the registered multitemporal image pair. Tools such as geographically linked cursors, graphical flicker and swiping, and color overlays allow image analysts to efficiently compare bi-temporal image pairs in a systematic fashion to delineate damage related changes. Image maps of delineated damage and annotation about the nature of damage is the likely information product that would be transferred to emergency response personnel.

An image analysis approach based solely on post-event imagery is most practical for wide-area reconnaissance and debris mapping purposes, because of the stringent and likely expensive requirement of acquiring an extensive baseline (pre-event) image data base. The primary goal is to determine the extent and severity of damage over inhabited areas, and locate buildings and infrastructure that may contain trapped victims, or could present a potential risk due to imminent collapse. A secondary goal is to prioritize possible evacuation, relief supply distribution points, and clean-up efforts. Depending on the type of disaster, specific information about the impact of the hazard may be extracted, such as extent and height of flood inundation, faults and fissures from earthquakes, and smoldering fires. Automated image classification of damage is relatively new to emergency response but holds great promise. Some of the more promising techniques could take advantage of supervised object-based (Stow et al. 2008) and/or machine-learning routines for delineating damaged features.

However, at this time the most reliable source of information on the severity and extent of damage will be generated from manual image interpretation by trained interpreters who have a background in damage assessment and emergency response. GIS layers such as land use and land cover, parcel boundaries and building footprints are extremely valuable in both manual and automated classification approaches.

3.5 Digital Surface Modeling and Analysis

Digital surface models derived from LiDAR, interferometric synthetic aperture radar (InSAR), or softcopy photogrammetric methods applied to optical stereo imagery may be used to detect damage that is not spectrally apparent and to measure heights and change in heights as a means for estimating debris volumes. LiDAR yields the most accurate (approximately 15 cm vertical accuracy) and detailed estimates of 3-D surface changes associated with structure loss or debris accumulation. However, InSAR yields very precise and accurate maps of changes in surface elevations. Simple and automated calculation of surface changes from LiDAR is likely to have errors associated with phenomenon such as differences in leaf-on and leaf-off condition of trees. Therefore, it may be necessary for the 3-D surface differencing to be used in combination with image-based detection of damage.

The generation of digital surface models from softcopy photogrammetry through the process called aerial triangulation may offer several advantages over LiDAR for hazard response; aerial cameras are more readily available than LiDAR sensors, aerial triangulation produces a single point cloud and digital surface model, without the need for filtering, dramatically reducing processing time when compared to LiDAR, and aerial triangulation enables a single dataset to provide both spectral and height information from a single acquisition. The primary advantages of LiDAR over aerial triangulation approaches is that LiDAR enables estimation of bare earth under canopies in addition to a first return surface model. Aerial triangulation via soft copy photogrammetry traditionally requires significant processing and analyst time to produce digital surface models comparable to those produced by LiDAR, although advances in automated feature detection and graphical processing unit (GPU)-based processing approaches are dramatically reducing the time associated with traditional aerial triangulation.

The estimation of feature heights by exploiting differences in single focal point view geometry is a well known in the fields of photogrammetry and computer vision. Traditionally, objects heights are estimated using soft copy photogrammetry, where the difference in the apparent horizontal position of objects (i.e., relief displacement) between two subsequent acquisitions can be used to calculated object height. Techniques borrowed from computer vision, including automated feature detection and high complexity matching algorithms, have enabled automation of the traditional bundle block adjustment employed by soft copy photogrammetry. This automation of feature extraction and correlation, traditionally the most time consuming aspect of soft copy photogrammetry, enables the calculation of heights for any feature identifiable from multiple perspectives (i.e., frames) in an expedited fash-

ion when compared to manual soft copy photogrammetry. Collectively, this means that the density of height estimates is limited only by the image data underlying it and permits aerial imagery to estimate height at densities comparable or surpassing LiDAR. GPU-enabled processing permits automated 3-D point cloud generation in minutes-hours for extremely large datasets (i.e., > 100 GByte), potentially offering a viable alternative to LiDAR for time-sensitive volumetric change mapping.

While efforts to compare the accuracy of point clouds generated from automated bundle block adjustment routines to those generated LiDAR and InSAR are ongoing, automated bundle block based estimates have been shown to be accurate within 40 % of the ground sampling distance (GSD) (Zhang et al 2011). An important research area is the assessment of the accuracy of volumetric change estimates produced using these techniques weighed against the time required to produce those estimates, leading to the identification of a workflow for operational estimation of volumetric change and ultimately the estimation of debris volume.

3.6 Data and Information Dissemination

An important (likely the most important) factor in effective disaster response is communication, and this is especially true and particularly challenging in the geospatial domain. Acquired image data must be communicated to analysts, processed, and then information products, in the form of maps, tables, or reports, must be communicated to decision makers or first responders on the ground. Transmission of data from the aircraft by wireless link is a critical first step to expedited information delivery, and expanding the range and functionality of wireless links is an important research area. More challenging however, is the management, distribution, and processing of those data and derived information products to relevant parties. The likely solution to this problem is a cloud based image distribution and processing services system that enable one-to-many data distribution and in-line processing. A cloud-based solution offers the potential to alleviate storage and bandwidth overhead of current distribution mechanisms in order to provide access to critical image data and analyses to thousands of users involved with emergency management operations. FEMA has recently taken steps to employ a cloud service for their GeoPortal to house the data and products that are generated during the response and recovery periods of a disaster. While the processing of remote sensing data has not matured to this environment, the creation of the GeoPortal has reduced the data and product communication problems apparent in other large scale disasters. Operating during the Hurricane Sandy response, this publically-available site allowed all levels of the incident command chain to access products and host products easily.

A systematic spatial reconnaissance strategy and use of graphical symbols and/or coded attributes by image interpreters to designate features that have been assessed and their damage status should be incorporated to ensure comprehensive and thorough assessments. Such symbology could build on developments for the National Grid and the Federal Geographic Data Committee standards.

3.7 Implementation

Planning and specifying the appropriate institutional arrangement(s) for implementing TSRSS for damage and debris assessment has been more challenging than developing the suitable RS technology. Appropriate arrangements should be based on the technical analyses and evaluations proposed above, along with cost and federal policy considerations. Most of the tasks and functions associated with each of the components of an end-to-end TSRSS could be incorporated into the Federal GeoCONOPS with specific SOPs to execute all aspects of an end to end TSRSS. For instance, FEMA currently relies on airborne remote sensing capabilities of the Civil Air Patrol, NOAA, and commercial remote sensing data providers. The DHS Customs and Border Protection rely on its Air and Marine Operations Surveillance System for airborne imaging and reconnaissance, whereas USGS contracts to commercial aerial survey firms for national airborne imagery data sets. Image processing and analysis functions could benefit from the expertise and tools of the private sector, but in-house personnel could be more responsive (i.e., “time-sensitive”) and have the application and geographic domain experience to enable more reliable interpretations. Open source and commercial delivery systems for geo-spatial data should be evaluated relative to federal data systems. These options are currently under investigation by Federal agencies with responsibility to provide analytical support and/or data during disaster incidents. Volunteers should also be considered as valuable and inexpensive assets for image processing and analysis components, particularly through the emerging crowd sourcing concept. Commercial service providers (e.g., Tomnod, Inc.) are attempting to systematize and operationalize this form of volunteer image analysis support for disaster response.

Any implementation of a TSRSS for damage and debris assessment requires training and technology transfer efforts. This would include support for implementing tools, processing and analysis strategies, and quality assurance. These could be conducted through hands-on training sessions, technical documentation, webinars and videos. Scenario and/or “dry run” tests should be conducted to work out and refine potential weak links in the flow of the TSRSS.

4 Conclusion

Remote sensing and related technologies associated with small aircraft, consumer grade digital cameras, and image processing procedures have matured substantially over the past decade and have been integrated into prototype TSRSS that are ready for operational and cost effective implementation for post-hazard damage assessment (Coulter et al. 2013). The potential exists for such TSRSS to save thousands of lives and millions of dollars in response and recovery operations by providing time-sensitive, situational awareness information that allows emergency responders to react in a more timely and effective manner. The emergency response community

in general has a greater appreciation for and proficiency with handling geographic data and information, and the time is ripe for the community to make a similar commitment to the direct incorporation of RS imagery into emergency operations centers.

The main limitations to implementation of remote sensing information for disaster assessment and recovery operations are institutional in nature. The culture of emergency response is changing and the use of technologies such as GIS and remote sensing are gaining acceptance. But there is currently a lack of demonstrated validity by remote sensing professionals to produce reliable products that address specific emergency response and recovery issues. Furthermore, funding limitations (or perception that the technology is too expensive), technology skepticism, avoidance, understanding, and government regulations and bureaucracies, are the main challenges to overcome for successful implementation of TSRSS for post-hazard assessment. Some research and development activities are still required to making TSRSS more reliable, but the primary need to fully realize their potential are: (1) a commitment by emergency response agencies to move forward with the development, implementation, and training of new techniques and methods based on remote sensing technologies, and (2) adjustments in policy and laws that will enable flexible, low-cost aircraft to operate in preparation for, during, and immediately after disaster events.

While the emphasis of the chapter has been on airborne systems, satellite imagery resources have and will continue to provide useful situational awareness information in support of emergency response during and following disasters. Satellite and classified airborne imaging assets are provided in the US during emergency events through the Interagency Remote Sensing Coordinating Cell (IRSCC) and by enabling access to the Eagle Vision One (EV1), a military-based commercial satellite imagery delivery capability programmed and funded by the U.S. Department of Defense. Future constellations of small satellites with miniaturized optical sensors may provide frequency of image coverage with sufficient time sensitivity and spatial resolution to meet the needs of emergency management organizations and personnel.

Acknowledgements The work was partially funded by the U.S. Department of Homeland Security and the Naval Postgraduate School at Monterey (Award Number G00009228) and by the National Science Foundation Directorate of Engineering, Infrastructure Management and Extreme Events (IMEE) program (Grant Number G00010529).

References

- Alexander D (2002) Principles of emergency planning and management. Oxford University Press, New York
- Ambrosia VG, Wegener SS, Sullivan DV et al (2003) Demonstrating UAV-acquired real-time thermal data over fires. *Photogramm Eng Remote Sens* 69:391–402
- Coulter L, Stow D (2008) Assessment of the spatial co-registration of multitemporal imagery from large format digital cameras in the context of detailed change detection. *Sensors* 8:2161–2173

- Coulter L, Stow D, Baer S (2003) A frame center matching approach to registration of high resolution airborne frame imagery. *IEEE Trans Geosci Remote Sens* 41(11):2436–2444
- Coulter L, Stow D, Lippitt, C, Dua S, Loveless B, Chavis C, Kumar S (2013) Rapid, high spatial resolution image assessment of post-earthquake damage. Final report to the Department of Homeland Security for a project conducted by San Diego State University and the Naval Postgraduate School, March 2013
- Cutter SL (2003) GI Science, disasters, and emergency management. *Trans GIS* 7:439–446
- Du Q, Raksuntorn N, Orduyilmaz A et al (2008) Automatic registration and mosaicking for airborne multispectral image sequences. *Photogramm Eng Remote Sens* 74(2):169–181
- Hodgson ME, Davis BA (1998) Remote sensing and GIS for hazards—foreword. *Photogramm Eng Remote Sens* 64:976–976
- Hodgson ME, Davis BA, Cheng Y et al (2010) Modeling remote sensing satellite collection opportunity likelihood for hurricane disaster response. *Cartogr Geog Info Sci* 37(1):7–15
- Joyce KE, Belliss SE, Samsonov SV et al (2009) A review of the status of satellite remote sensing and image processing techniques for mapping natural hazards and disasters. *Prog Phys Geogr* 33:183–207
- Laliberte AS, Herrick, JE, Rango A et al (2010) Acquisition, orthorectification, and object-based classification of unmanned aerial vehicle (UAV) imagery for rangeland monitoring. *Photogramm Eng Remote Sens* 76(6):661–672
- Lippitt CD, Stow DA, Clarke K (2014) On the utility of models for time-sensitive remote sensing. *Int J Remote Sens* 35:6815–6841
- Phinn SR (1998) A framework for selecting appropriate remotely sensed data dimensions for environmental monitoring and management. *Int J Remote Sens* 19:3457–3463
- Stow D, Coulter L, Baer S (2003) A frame centre matching approach to registration for change detection with fine spatial resolution multi-temporal imagery. *Int J Remote Sens* 24:3873–3879
- Stow D, Hamada Y, Coulter L et al (2008) Monitoring shrubland habitat changes through object-based change identification with airborne multi-spectral imagery. *Remote Sens Environ* 112:1051–1061
- Stryker T, Jones B (2009) Disaster response and the International Charter Program. *Photogramm Eng Remote Sens* 75:1242–1344
- Tralli DM, Blom RG, Zlotnicki V et al (2005) Satellite remote sensing of earthquake, volcano, flood, landslide and coastal inundation hazards. *ISPRS J Photogramm Remote Sens* 59:185–198
- Visser SJ, Dawood AS (2004) Real-time natural disasters detection and monitoring from smart earth observation satellite. *J Aerosp Eng* 17:10–19
- Wyawahare MV, Patil PM, Abhyankar HK (2009) Image registration techniques: an overview. *Int J Signal Process Image Process Pattern Recognit* 2(3):11–28
- Zhang Y, Xiong J, Hao L (2011) Photogrammetric processing of low-altitude images acquired by unpiloted aerial vehicles. *Photogramm Record* 26(134):190–211
- Zitova B, Flusser J (2003) Image registration methods: a survey. *Image Vision Computing* 21: 977–1000

Repeat Station Imaging for Rapid Airborne Change Detection

Lloyd L. Coulter, Douglas A. Stow, Christopher D. Lippitt and Grant W. Fraley

Abstract

Time-sensitive remote sensing requires that the steps between image collection and product delivery be expedited, as the utility of derived information decreases rapidly over time. A new approach for multitemporal image collection and co-registration, referred to as repeat station imaging (RSITM), is presented. RSI uses specific image collection and processing techniques to rapidly obtain precise geometric co-registration between airborne multitemporal images, and facilitates subsequent processes such as change detection and time sensitive information dissemination. RSI is based upon collecting multitemporal airborne imagery with matched view geometry, so that geometric alignment (or co-registration) between multitemporal images is simplified, rapid, and near pixel-level spatial accuracy. This chapter provides background information on the RSI approach and describes two applications for which RSI may be effectively employed. These applications include rapid post-disaster damage assessment and near real-time border monitoring. Both applications were developed and demonstrated as part of Department of Homeland Security (DHS) Science and Technology (S&T) funded projects. The approach is well suited for unmanned aircraft applications, with computers navigating the aircraft and camera shutter triggering accomplished automatically

L. L. Coulter (✉) · D. A. Stow
Department of Geography, San Diego State University,
San Diego, CA 92182-4493, USA
e-mail: lcoulter@geography.sdsu.edu

C. D. Lippitt
Department of Geography and Environmental Studies, University of New Mexico,
Albuquerque, NM 87131-0001, USA

C. D. Lippitt · G. W. Fraley
TerraPan Labs LLC, 330 A St Suite 29, San Diego, CA 92101, USA

as the aircraft passes predetermined camera stations. Aircraft and camera control may be implemented using global navigation satellite systems (GNSS) and other supporting systems.

Keywords

Image registration · Change detection · Airborne · Near real-time · Repeat station imaging · Disaster assessment · Infrastructure assessment · Rapid response · Monitoring

1 Introduction

Time-sensitive remote sensing often involves the use of image-based change detection to determine the status of features of interest in a scene (Lippitt et al. 2014). Through change detection, the characteristics of features in recent imagery are compared against the characteristics of the same features or locations in past imagery, offering significant benefits when compared to single date approaches. For example, change detection may be used to detect and verify a wide range of damage characteristics following an disaster (such as cracked bridges, damaged roadways, or swept away houses), rather than detecting only specific features such as building rubble in post-earthquake imagery (Gusella et al. 2005; Samadzadegan and Rastiveisi 2008; Hussain et al. 2011). Spatial co-registration (or alignment) of multitemporal imagery is an important prerequisite for change detection (Coppin et al. 2004; Lu et al. 2004). While co-registration of multitemporal imagery is helpful to human analysts and facilitates rapid interpretation, achieving precise co-registration is critical for semi-automated and fully automated image-based change detection. Without precise multitemporal image co-registration, the utility of change detection products is limited or nullified (Stow 1999). Even small errors in multitemporal image co-registration can result in falsely detected changes and omission of actual changes of interest (Townshend et al. 1992; Dai and Khorram 1998; Verbyla and Boles 2000). Further, achieving precise co-registration between ultra-high spatial resolution (e.g., 8 cm or 3 in) images for scenes with complex relief or built features using traditional techniques requires accurate ground control, detailed digital surface models, and can be time consuming or impractical to accomplish.

Our research team with the Center for Earth Systems Analysis Research (CESAR) at San Diego State University (SDSU) developed and demonstrated procedures for rapidly achieving precise spatial co-registration between ultra-high spatial resolution imagery. The approach is referred to as repeat station imaging (RSITM) (formerly frame center matching). It is based upon matching camera stations (both horizontal position and altitude) between multitemporal image acquisitions. When airborne image frames are captured from the same positions over time, they have similar view geometry and may be aligned by matching a limited number of control points

(e.g., 10–30) and applying a simple warping transformation. The RSI approach enables very precise (i.e., pixel-level) alignment between high spatial resolution multitemporal images, using automated and rapid procedures. Such multitemporal alignment has been demonstrated even with very fine spatial resolution imagery (e.g. 8 cm) for complex urban environments (Coulter et al. 2012a).

This chapter provides a background information on the RSI approach and describes two applications for which RSI may be effectively employed. These include rapid post-disaster damage assessment and near real-time border monitoring. For both applications, we have developed and demonstrated tools and techniques as part of two Department of Homeland Security (DHS) Science and Technology (S&T) funded projects.

2 Repeat Station Imaging

RSI image acquisition procedures that enable precise replication of camera station positions over time are described in Stow et al. (2003) and Coulter et al. (2003). RSI is most effectively accomplished through the use of a global navigation satellite system (GNSS) to aid the pilot/aircraft in maintaining the desired track and altitude (optionally using a barometric altimeter), and automatically trigger image capture at predetermined camera stations. Using GNSS-based aircraft navigation and camera triggering, camera station positions may be matched within meters (e.g., 10–20 m using non-differentially corrected GNSS). When repeat pass image frames from the same sensor are captured from nearly the same camera stations in the sky, there is virtually no parallax between the images, similar ground coverage is attained, and matched frames exhibit the same terrain or building related geometric distortions. In other words, multitemporal image frames are, with the exception of land cover change, essentially carbon copies of each other. Since scene-related geometric distortions (e.g., relief displacement) are virtually identical, only sensor related distortions such as those introduced by differences in aircraft roll and pitch are expected to be present between images. However, these systematic distortion differences can be corrected when station matched image frames are aligned using simple warping functions and a limited number of well distributed points (Stow et al. 2003; Coulter et al. 2003).

The repeat station imaging approach does not employ traditional photogrammetry techniques as part of the image-to-image co-registration process. Traditional photogrammetry techniques provide absolute positioning and attempt to remove distortions associated with the sensor, scene, and varying view geometries. Traditional photogrammetry techniques include removing lens distortion based on a camera calibration model, identifying the exact coordinates (XYZ) of ground control markers within the images, generating tie points between images, executing an aerial triangulation process that uses all information available (ground control, tie points,

camera model information, etc.) to determine the camera's 3-dimensional location and orientation, projecting the images onto the ground given the location/orientation of the camera, and removing terrain/feature distortions using digital surface models (DSM) or digital terrain models (DTM). The problems with traditional photogrammetry techniques are: (1) co-registration of multitemporal images requires highly accurate positioning of each image set independently, (2) traditional photogrammetry techniques rely on ancillary data such as ground control points and DSM/DTM, (3) the highest positional accuracy that can be achieved is dependent upon the quality of the ancillary data, and (4) human interaction is often required to generate high quality products. As a result, pixel-level co-registration between ultra-high spatial resolution (e.g., 8 cm), multitemporal image sets using traditional photogrammetric approaches for complex 3-dimensional scenes may not be possible or practical, and delivery of image products may be delayed by many hours to days.

Unlike traditional photogrammetry techniques, the RSI approach utilizes raw image frames as they are captured by a frame array sensor, and co-registers and aligns images on a frame-by-frame basis prior to any subsequent processing. The approach only requires that a small number of points be matched between multitemporal image frames. The benefits of RSI include simplified processing, as well as rapid and precise multitemporal image set generation.

Using the repeat station imaging technique, we have regularly achieved spatial co-registration within one to two pixels between multitemporal image sets, irrespective of spatial resolution or building/terrain variability within imaged scenes (Coulter and Stow 2005; Coulter and Stow 2008; Coulter et al. 2012a). These image sets ranged from 8 cm to 1 m spatial resolution, and included complex rural and urban scenes. For imagery with a spatial resolution of 8 cm, images may be expected to co-register with an accuracy of 0.15 m (6 in.). Even with misregistration on the order of four pixels with 8 cm spatial resolution (~ 0.3 m, or 1 ft), detailed changes may be detected.

Figures 1 and 2 illustrate the level of image co-registration achieved between two image frames with 8 cm spatial resolution simply by matching the imaging station, identifying matching points between multitemporal images, and applying a 2nd order polynomial warping function as part of the image registration process. The root mean square error (RMSE) of co-registration between these image frames is 1.3 pixels (10 cm) (Coulter et al. 2012a). Figure 1 shows the two full-frame 21 megapixel images collected with a Canon digital camera (a and b), as well as the co-registered frames (c). Figure 2 shows a subset of the two co-registered images with greater detail. Following co-registration, subsequent processing may include change detection analysis using the co-registered image frames, as well as georeferencing using direct projection techniques with GNSS and inertial measurement unit (IMU) data.

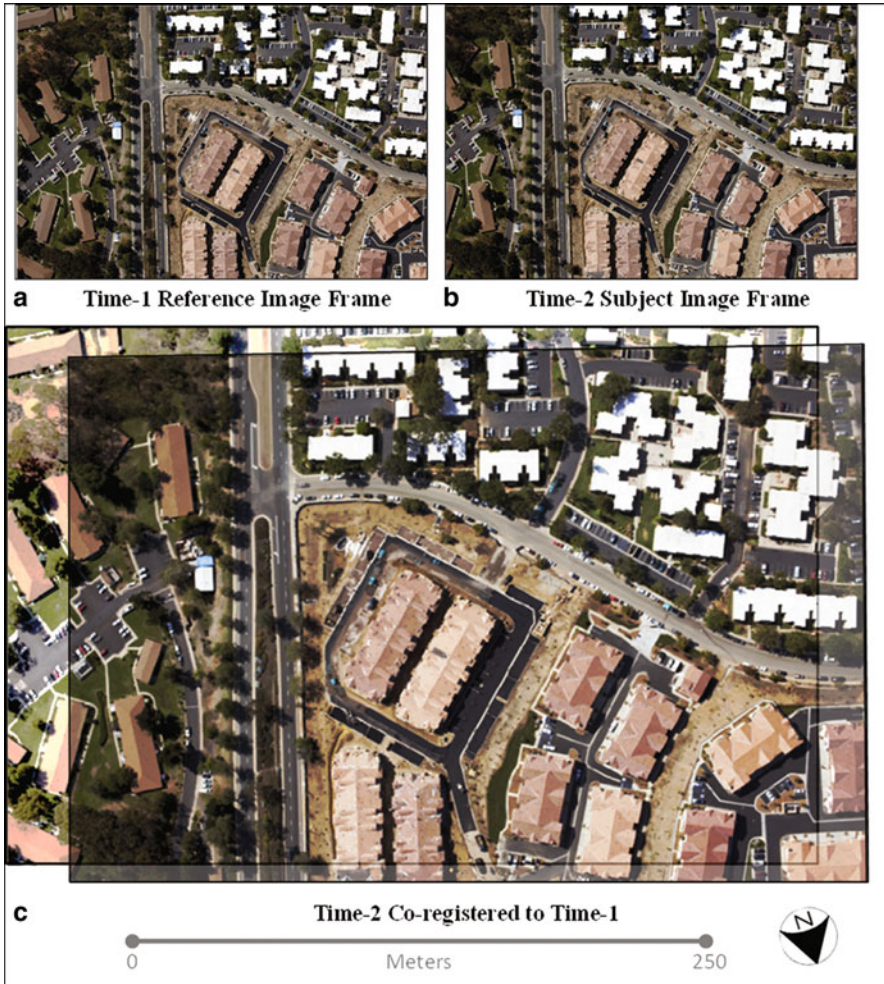


Fig. 1 Image co-registration example using repeat station images processed on a frame-by-frame basis. The 8 cm spatial resolution images from a multiple family residential area under construction are precisely aligned. The Time-2 image is displayed with darker tone. (Modified from: Coulter et al. (2012a). Reprinted with permission from the American Society for Photogrammetry & Remote Sensing, Bethesda, Maryland)

3 Bi-temporal Analysis—Rapid Post-earthquake Damage Assessment

Many post-hazard emergency response assessments can benefit greatly from access to high spatial resolution airborne imagery collected and provided to emergency response personnel in near real-time immediately following the disaster. However,



Fig. 2 A time-2 image chip is overlain on a time-1 image displayed in a lighter tone (i.e., washed-out). The quality of the spatial co-registration between the 8 cm (3 in) spatial resolution image sets is evident, as linear features such as street curbs, parking space paint lines, and roof edges are precisely aligned. A vehicle turning the corner is only present in the smaller image chip (half of the vehicle), while that vehicle was not present during collection of the larger image chip

identification of many damage features using visual or in particular semi-automated image analysis can be complicated due to the lack of information about the appearance and characteristics of buildings/infrastructure prior to the disaster (i.e., is the current state different than before). As part of a pilot project funded by DHS and lead by the Remote Sensing Center at the Naval Postgraduate School in Monterey, CA, our team refined procedures, developed tools, and demonstrated the collection and automated analysis of multitemporal airborne imagery for the purpose of rapidly identifying damage to critical infrastructure in the event of an earthquake in California (Coulter et al. 2013). The primary purpose of the project was to demonstrate the effectiveness of the approach for rapid image-based assessment. A live demonstration of the full image collection and processing flow was performed as part of the Research & Experimentation for Local & International Emergency and First-Responder (RELIEF) and Joint-Interagency Field Experiment (JIFX) exercises in August 2012 at Camp Roberts, CA.

The approach for rapid post-earthquake damage assessment exploited the RSI image collection and automated co-registration technique. The team designed and demonstrated a work flow that included: (1) pre-event planning (2) pre-disaster baseline image set collection at predetermined camera stations, (3) post-disaster image collection using the RSI approach, (4) precise and automated co-registration of corresponding multitemporal image frames, (5) automated change detection, and (6) dissemination of derived information to first responders. An operational system employing RSI could be configured several ways: (1) complete processing on-board an aircraft with wireless dissemination of change products from aircraft, (2) wireless data transmission of collected imagery from the aircraft to the ground (processing occurring on the ground), or (3) landing the aircraft and delivering imagery and/or

derived products without using wireless data transmission from the aircraft. The RELEIF/JIFX demonstration did not include wireless transmission (i.e., option 3 was used).

For the project, SDSU researchers developed routines for both automated image co-registration of repeat station image frames and automated change detection. The automated co-registration algorithm utilized camera station identification numbers to identify multitemporal image pairs collected from the same camera station and to initiate the frame-to-frame co-registration process. The co-registration routine used correlation windows to identify matching points between multitemporal image frames, and resampled the most recent image frame so that it aligned with the earlier collected reference image frame. The change detection algorithm was designed to function with images collected around the same time of day for purposes of the demonstration. The algorithm was used to identify and mask areas containing shadows so that changes in shadow positions over time would not be classified as change. Land cover changes of interest exhibited changes in brightness between images. Digital number (DN) value thresholding was applied to multitemporal difference images, along with post-classification filtering (majority filter, and clump and sieve operations) to detect land cover changes between multitemporal images.

As part of the team, TerraPan Labs LLC integrated SDSU's automated image co-registration and automated change detection procedures on top of their online image processing platform called "pan.io." The resulting tool, referred to as DeltaPan, enables image processing, visualization, and distribution of image products through a cloud-based infrastructure. For the project, Deltapan was utilized for rapid visualization of multitemporal imagery, automated co-registration and change detection processing, visualization of change detection products, change feature selection, documentation of an analyst's interpretation of the selected changes, and web-based dissemination of change detection products. A computer with internet access and an HTML 5 compliant web browser (e.g., Google Chrome) is utilized to operate the DeltaPan web-based pre-processing, analysis, and dissemination system, making it accessible to a large number of geographically distributed analysts.

DeltaPan simultaneously displays an early period (i.e., baseline or time-1) image, a more recent (i.e., time-2) image, and change products, along with an overview of the geographic location of all image pairs on top of a provided background image or web mapping service (Fig. 3). Default change detection parameters may be interactively adjusted by an analyst to highlight features of potential interest. Features of interest may then be selected (by adding an interactively controlled bounding box) and annotations may be entered describing the nature of the identified change.

The live demonstration of the rapid change assessment approach took place 15–16 August 2012 at Camp Roberts, CA as part of the JIFX and RELIEF event (Coulter et al. 2012b). For the demonstration, a light aircraft operated by research partner NEOS Ltd. utilized the RSI approach to collect multiple repeat pass images with 8 and 15 cm spatial resolutions. Between imaging passes, multiple targets (tarps, boxes, people, vehicles, building debris such as doors, and black duct tape representing asphalt cracks) were moved to simulate changes of interest. Selected sets of multitemporal image frames (and supporting airborne GPS data) were fed into automated image co-registration and change detection routines. Multitemporal image

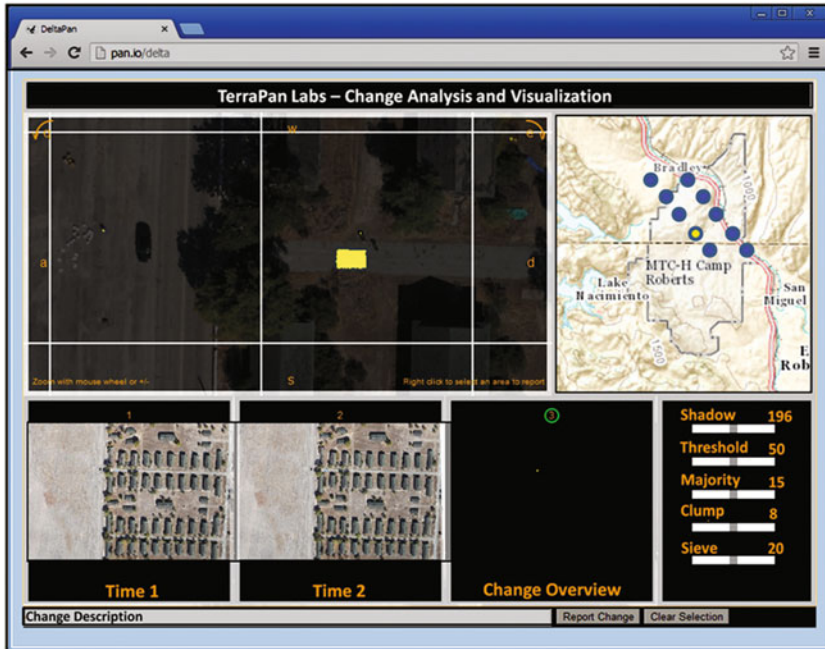


Fig. 3 User interface for the DeltaPan web-based, interactive change detection tool

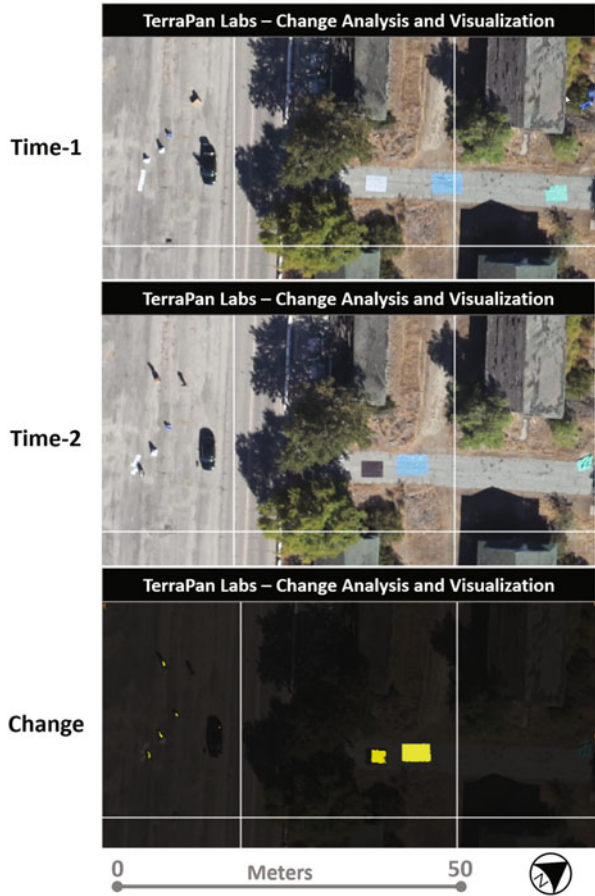
frames aligned very well, and detailed changes were detected. The detected changes were visually reviewed using the DeltaPan tool, and selected change examples and analyst interpretations were submitted via GeorSS feed to a common operating picture operated by Peak Spatial Enterprises. The common operating picture received a range of inputs from multiple projects participating in the event. An example set of time-1, time-2, and change image products from the RELIEF exercise is shown in Fig. 4.

In addition to the JIFX/RELIEF demonstration, SDSU researchers and partner NEOS Ltd. collected baseline imagery for the County and City of Monterey to facilitate implementation of the RSI approach for rapid damage assessment in the event of a major disaster such as an earthquake. Baseline imagery with 15 cm (6 in) spatial resolution was collected on 12–13 August 2012 for a large number critical infrastructure features identified by Monterey officials.

4 Time Series Analysis—Border Monitoring

In addition to bi-temporal analysis, the RSI approach may be utilized to precisely and automatically align a time series of multitemporal imagery for analysis that is time sensitive in nature. Regular monitoring of an area and rapid generation of

Fig. 4 Time-1, time-2, and change images as displayed in the DeltaPan viewer by TerraPan Labs LLC



information products may be important for applications such as disaster monitoring (e.g., flood, fire, etc.), search and rescue, border monitoring, battlefield monitoring, and wildlife monitoring. As part of the DHS S&T National Center for Border Security and Immigration (BORDERS), our team developed a novel approach for border monitoring that exploits repeat station image collection and co-registration. Using the approach, high temporal resolution image sets may be collected by repeatedly flying a racetrack pattern with high frequency (e.g., every 10 min). Figure 5 shows an example of a racetrack pattern with five image frames per flight line (for simplicity); however an actual racetrack flight pattern could include hundreds of frames per pass.

Following wide area, repeat pass image collection, precise co-registration achieved using RSI enables near real-time detection of features that move over time as part of a wide area surveillance solution. The wide area time series change indicator (WATSCIN) approach that our team developed as part of the BORDERS center is further described in Coulter et al. (2012c, d). The detection algorithm is based upon using the time series of images to determine the expected range of brightness



Fig. 5 Illustration of repeat pass, high temporal resolution imaging using a racetrack pattern. The location is Tecate, CA along the U.S./Mexico border

and/or spatial texture for each pixel. By comparing observed to expected values candidate change pixels are determined. However, the key point to note in this chapter is that we have demonstrated how several repeat pass image frames for scenes with complex terrain and land cover may be precisely and automatically aligned using the RSI approach. These co-registered, multitemporal image sets may subsequently be used with automated change detection algorithms to identify change anomalies associated with the movement of people, vehicles, and likely other features such as drug bundles or even animals for wildlife surveys. Feature detection results obtained in near real-time following automated image co-registration and change detection processing onboard an aircraft can prompt rapid response by authorities.

In September 2011, SDSU personnel worked with the U.S. Border Patrol to test the WATSCIN change detection approach. Three sites along the U.S./Mexico border in San Diego County were selected, and repeat pass imagery with 8 cm spatial resolution was collected at each. For a desert site, nine repeat pass image sets were collected with a frequency of one pass every 4 min. For grassland and chaparral sites, 13 repeat pass image sets were collected (also with a repetition of one pass every 4 min). SDSU and Border Patrol people and vehicles moved within the image scenes during the repeat pass collections. SDSU personnel co-registered corresponding multitemporal the image frames for each site using between 9–13 manually selected control points, and second order polynomial warping (at this point we had not automated the RSI co-registration procedures). The resulting nine co-registered frames for the desert site

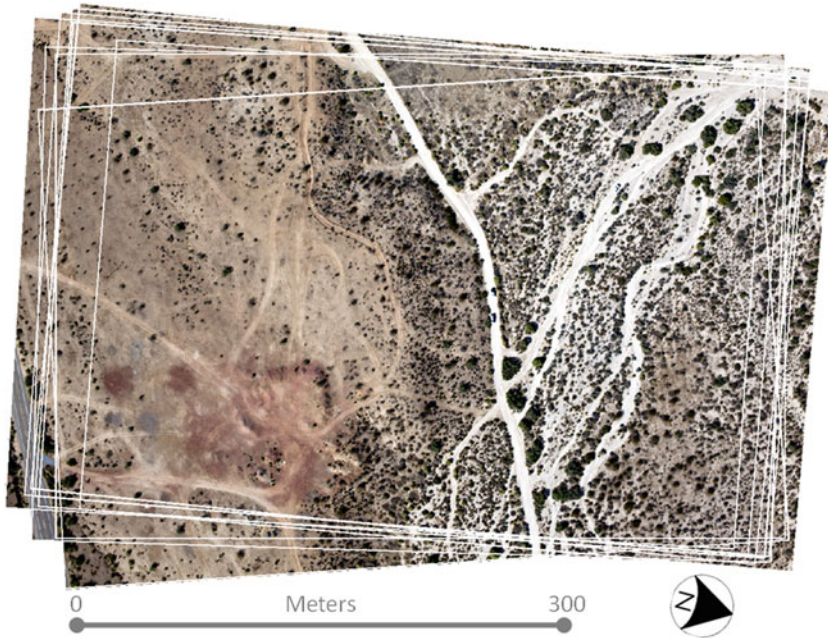


Fig. 6 Nine airborne image frames collected and co-registered using repeat station imaging techniques for a desert site in southeast San Diego County, CA. White lines indicate the extent of the individual repeat-pass image frames collected from the same camera station

are shown overlapping in Fig. 6, and extent of each frame is highlighted with white lines. For each site, the images were co-registered within two pixels (RMSE), and the WATSCIN change detection algorithm was utilized to detect people and vehicles that moved between imaging passes. The results of this time series image co-registration and change detection test are described in detail in Coulter et al. (2012c, d). Moving people and vehicles were detected with very high accuracy (63 of 64 people, and 11 of 11 vehicles were detected), with virtually no false detection. Figure 7 shows examples of selected detection results. For this test, image co-registration and change detection was accomplished by an analyst using a sequence of steps with commercial off the shelf software. However, the procedures are expected to be straightforward to automate.

5 Considerations

Through two DHS S&T projects, we demonstrated how the RSI approach may be used for rapid and automated image co-registration and change detection. The approach is well suited for unmanned aircraft applications, with computers nav-



Fig. 7 Detection results for people and vehicles in a single image collected for a desert site in southeast San Diego County, CA. A time series of precisely co-registered 8 cm imagery was used to accurately detect the people and vehicles. Detection results are shown as red with a color image backdrop, and was white with a black backdrop (i.e., binary). (Modified from: Coulter et al. (2012c). Reprinted with permission from the American Society for Photogrammetry & Remote Sensing, Bethesda, Maryland)

igating the aircraft and automatically triggering the camera as the aircraft passes predetermined camera stations, but can be implemented on any GNSS enabled aircraft.

There are several considerations regarding the use of RSI. RSI is ideally performed using the same camera system over time, so that there are no/limited variations in camera internal geometry and lens distortion (and therefore no need to correct for this). RSI requires the same flight lines and imaging stations to be repeated over time, which may be undesirable or unrealistic for some applications. In addition, factors such as wind speed, aircraft size, aircraft velocity, etc. may affect the accuracy with which camera station positions are matched. The specific accuracy with

which camera stations must be matched to obtain pixel-level co-registration depends upon factors such as the altitude of the aircraft, the 3-dimensional characteristics (e.g. terrain, buildings, vegetation) of the scene, and the spatial resolution of the imagery. All of these variables interact, and we have begun to develop an analytical model for determining collection requirements, given specific scene and image spatial resolution characteristics. In addition, variations in scene and/or shadow conditions over time could affect the ability to automatically match control points between RSI image pairs/sets.

6 Conclusions

Time-sensitive remote sensing requires all steps between image collection and product delivery to be expedited as the utility of derived information decreases rapidly over time. The repeat station imaging approach may be used to expedite geometric co-registration between airborne multitemporal images, and subsequent processes such as change detection and information dissemination. Further, RSI enables highly precise, pixel-level spatial co-registration between ultra-high spatial resolution (e.g., 8 cm) images for very detailed change detection. Rapidly achieving this level of spatial co-registration with such high spatial resolution imagery may not be possible or practical using other methods.

The scenario described above for rapid post-earthquake damage assessment requires baseline, pre-event imagery to be collected and available for change detection. Collecting pre-event imagery for a disaster that strikes without warning may be most appropriate for specific and predetermined critical infrastructure features, for which information is needed immediately following the disaster. Another consideration is that an aircraft with appropriate equipment and data must be ready to respond rapidly in the event of a disaster. Such an aircraft could be owned by a local municipality and serve multiple purposes (e.g., law enforcement reconnaissance, etc.), so that it is regularly used in the absence of any disaster. Alternatively, organizations such as the U.S. Civil Air Patrol who respond rapidly with aircraft following disasters could be prepared to collect RSI imagery for rapid assessment. In addition to pre-event and post-event imagery comparison, the RSI approach may also be used for repeated post-disaster imaging and monitoring, such as tracking the extent of rising flood waters or wildfire movement during the event. As exemplified by the border monitoring application described above, RSI is well suited for continuous monitoring missions, with frequent but intermittent imaging over wide areas.

Our team is taking steps to commercialize the RSI technology and make it available for a wide range of applications. This includes refining and demonstrating automated image co-registration and near real-time change detection, understanding image collection requirements, refining methods for more accurate repeat station image collection, and working with others who may benefit from the efficiency and precision of repeat station imaging.

Acknowledgments The work was partially developed by the National Aeronautics and Space Administration under Grant NAG13-99017 and Grant NCC13-03007. This material is also based upon work supported by the U.S. Department of Homeland Security under Award Number 2008-ST-061-BS0002 and by the Naval Postgraduate School in Monterey under contract number G00009228. Disclaimer: The views and conclusions contained in this document are those of the authors and should not be interpreted as necessarily representing the official policies, either expressed or implied, of the U.S. Department of Homeland Security.

References

- Coppin P, Jonckheere I, Nackaerts K, Muys B, Lambin E (2004) Digital change detection methods in ecosystem monitoring: a review. *Int J Remote Sens* 25(9):1565–1596
- Coulter L, Stow D (2005) Detailed change detection using high spatial resolution frame center matched aerial photography. In: Proceedings of the 20th Biennial Workshop on Aerial Photography, Videography, and High Resolution Digital Imagery for Resource Assessment, Weslaco, Texas, October 4–6, 2005
- Coulter L, Stow D (2008) Assessment of the spatial co-registration of multitemporal imagery from large format digital cameras in the context of detailed change detection. *Sensors* 8:2161–2173
- Coulter L, Stow D, Baer S (2003) A frame center matching approach to registration of high resolution airborne frame imagery. *IEEE Trans Geosci Remote Sens* 41(11):2436–2444
- Coulter L, Stow D, Kumar S, Dua S, Loveless B, Fraley G, Lippitt C, Shrivastava V (2012a) Automated co-registration of multitemporal airborne frame images for near real-time change detection. Proceedings of the ASPRS 2012 Annual Conference, Sacramento, CA, March 19–23, 2012
- Coulter L, Stow D, Fraley G, McCreight R, Lippitt C (2012b) Rapid, high spatial resolution image assessment of post-earthquake damage. Joint Inter-agency Field Experiment (JIFX) After Action Report, Experiment B-11, Camp Roberts, CA, August 15–16, 2012
- Coulter L, Stow D, Tsai YH, Lippitt C, Fraley G, McCreight R (2012c) Automated detection of people and vehicles in natural environments using high temporal resolution airborne remote sensing. Proceedings of the ASPRS 2012 Annual Conference, Sacramento, CA, March 19–23, 2012
- Coulter L, Stow D, Tsai YH, Chavis C, McCreight R, Lippitt C, Fraley G (2012d) A new paradigm for persistent wide area surveillance. Proceedings of the IEEE International Conference for Homeland Security Technologies, Waltham, MA, November 13–15.
- Coulter L, Stow D, Lippitt L, Dua S, Loveless B, Chavis C, Kumar S, Fraley G (2013) Rapid, high spatial resolution image assessment of post-earthquake damage. Final project report prepared for the Department of Homeland Security and the Naval Postgraduate School at Monterey, March 27, 2013, pp 270
- Dai X, Khorram S (1998) The effects of image misregistration on the accuracy of remotely sensed change detection. *IEEE Trans Geosci Remote Sens* 36(5):1566–1577
- Gusella L, Adams BJ, Bitelli G, Huyck CK, Mognol A (2005) Object-oriented image understanding and post-earthquake damage assessment for the 2003 Bam, Iran, earthquake. *Earthq Spectr* 21(S1):225–238
- Hussain E, Ural S, Kim K, Fu C, Shan J (2011) Building Extraction and Rubble Mapping for City Port-au-Prince Post-2010 Earthquake with GeoEye-1 Imagery and Lidar Data. *Photogrammetric Engineering and Remote Sensing* 77(10):1011–1023
- Lippitt CD, Stow DA, Clarke K (2014) On the nature of models for time sensitive remote sensing. *Int J Remote Sens* 35(18):6815–6841
- Lu D, Mausel P, Brondizio E, Moran E (2004) Change detection techniques. *Int J Remote Sens* 25(12):2365–2407

- Samadzadegan F, Rastiveisi H (2008) Automated detection and classification of damaged buildings, using high resolution satellite imagery and vector data. *The International Archives of the Photogrammetry, Remote Sensing and Spatial Information Sciences*, Vol XXXVII, Part B8, Beijing
- Stow D (1999) Reducing the effects of misregistration on pixel-level change detection. *Int J Remote Sens* 20(12):2477–2483
- Stow D, Coulter L, Baer S (2003) A frame centre matching approach to registration for change detection with fine spatial resolution multi-temporal imagery. *Int J Remote Sens* 24:3873–3879
- Townshend J, Justice C, Gurney C, McManus J (1992) The impact of misregistration on change detection. *IEEE Trans Geosci Remote Sens* 30(5):1054–1060
- Verbyla D, Boles S (2000) Bias in land cover change estimates due to misregistration. *Int J Remote Sens* 21(18):3553–3560

Rapid Fire Detection, Characterization and Reporting from VIIRS Data

Christopher D. Elvidge, Mikhail Zhizhin, Feng-Chi Hsu
and Kimberly E. Baugh

Abstract

Nightfire is a new fire product created by the National Oceanic and Atmospheric Administration (NOAA). The Nightfire algorithm detects and characterizes sub-pixel heat sources using multispectral data collected globally each night by the Suomi National Polar-orbiting Partnership (SNPP) Visible Infrared Imaging Radiometer Suite (VIIRS). The Nightfire algorithm is applied to two types of data streams. The global data stream has a 7–10 h latency that renders the data of low value to the first responder community. The second type of data stream comes from direct readout ground stations, where fire detection data can be available in less than 1 h. The Nightfire algorithm currently detects fires with high accuracy, however there are two areas where research and development (R&D) is needed to improve the value of VIIRS satellite fire detections to the first responder community. This includes refinement of the file format and file content, and improvements in the data delivery mechanisms. It should be possible to develop services that

C. D. Elvidge (✉)

Earth Observation Group, NOAA National Geophysical Data Center, Boulder, CO, USA
e-mail: chris.elvidge@noaa.gov

M. Zhizhin · F.-C. Hsu · K. E. Baugh

Cooperative Institute for Research in Environmental Sciences,
University of Colorado, Boulder, CO, USA
e-mail: mikhail.zhizhin@noaa.gov

M. Zhizhin

Space Research, Institute, Russian Academy of Sciences, Moscow, Russia

F.-C. Hsu

e-mail: feng-chi.hsu@noaa.gov

K. E. Baugh

e-mail: kim.baugh@noaa.gov

© Springer Science+Business Media New York 2015

C. D. Lippitt et al. (eds.), *Time-Sensitive Remote Sensing*,
DOI 10.1007/978-1-4939-2602-2_4

45

deliver graphics and text results to smartphones and other mobile devices used by the first responder community.

Keywords

SNPP · VIIRS · Fire detection · Gas flaring · Emergency response

1 Introduction

There is an urban legend that satellite sensors are so pervasive and powerful that pictures record your activities no matter where you go or what you do. This is clearly a legend easy to debunk. The high spatial resolution satellites are programmed every day with a limited set of sites where images will be collected, representing a small fraction of the earth's surface. Satellite sensors that collect global data on a daily basis have relatively coarse spatial resolution ($\sim 1 \text{ km}^2$) and very brief collection times for any particular spot on the earth's surface.

Another common misconception is that satellite data are available instantaneously. In fact, there is always some delay from the collection of satellite observations to their availability for analysis on the ground. One strategy for reducing the temporal latency of satellite observations is to collect data from a direct readout station. The core of such a facility is a satellite dish which is pointed at the satellite in order to collect the data broadcast. For geostationary satellites the position of the satellite remains fixed and the dish is stationary. Satellites which collect global data are typically in polar orbits. Ground stations for polar orbiting satellites have moving dishes that track the satellite from horizon to horizon.

This chapter examines the use of ground stations to accomplish near-real time detection and reporting of fires using nighttime infrared data collected by the Visible Infrared Imaging Radiometer Suite (VIIRS). Nighttime VIIRS data can be processed to estimate variables of interest to fire fighters and disaster managers, including fire temperature, source size and radiant heat. However, these observations are generally only available once per night, presenting a snapshot of the fire conditions at the time of the satellite overpass. A temporal latency comparison will be made for a specific disaster event involving a fire for the global data stream versus data from a ground station. The objective is to provide the reader with a solid understanding of the VIIRS fire detection capabilities and the limitations that are imposed by the sensor, the orbit, downlink, processing and delivery of fire detection data.

2 VIIRS Nightfire

The Nightfire algorithm detects and characterizes sub-pixel heat sources using multispectral data collected globally each night by the Suomi National Polar-orbiting Partnership (SNPP) Visible Infrared Imaging Radiometer Suite (VIIRS). The spec-

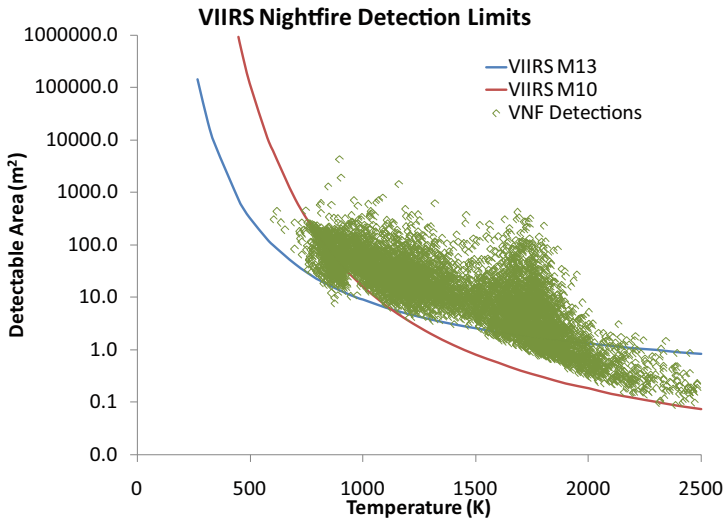


Fig. 1 Plot of Nightfire temperature versus source area estimates. The red line indicates the theoretical detection limit modeled based on the M10 detection limit. The blue line indicate the M13 detection limit

tral bands utilized span visible, near-infrared (NIR), short-wave infrared (SWIR) and mid-wave infrared (MWIR). Two independent fire detection algorithms are utilized. The first detector operates on SWIR band centered at 1.6 μm , commonly known as the VIIRS M10 band. Without solar input, the SWIR spectral band records sensor noise, punctuated by high radiant emissions associated with gas flares, biomass burning, volcanoes, and industrial sites like steel mills. The second detection algorithm identifies pixels containing hot sources using the two MWIR bands. Using a concept pioneer by Dozier (1981), Planck curve fitting of the heat source radiances yields temperature (K) and emission scaling factor (ESF). Additional calculations are done to estimate source size (m^2), radiant heat intensity (W/m^2) and radiant heat (MW). Use of M7, M8 and M10 spectral bands at night reduces scene background effects which are widely reported as problematic for fire algorithms based on MWIR and long-wave infrared (Giglio and Kendall 2001). High atmospheric transmissivity in the M10 spectral band reduces atmospheric effects on temperature and radiant heat retrievals. Nightfire retrieved temperature estimates for sub-pixel heat sources range from 600–6000 K (Elvidge et al. 2013). Output is in comma delimited value (CSV) and compressed Keyhole Markup Language (KMZ, used with Google Earth) formats.

Nightfire detection limits are defined by the minimal detectable radiance of the M10 and M13 spectral bands. Since the radiances detected in M10 are entirely from the heat source present in the pixel footprint, the minimal detectable radiance can be used to define the source area required to achieve a detection with the M10 band for any given temperature. Figure 1 shows a plot of a full day of Nightfire local maxima temperatures and source area estimates. Note there is a zone below the data cloud that is devoid of detections. If the source temperature is high, the

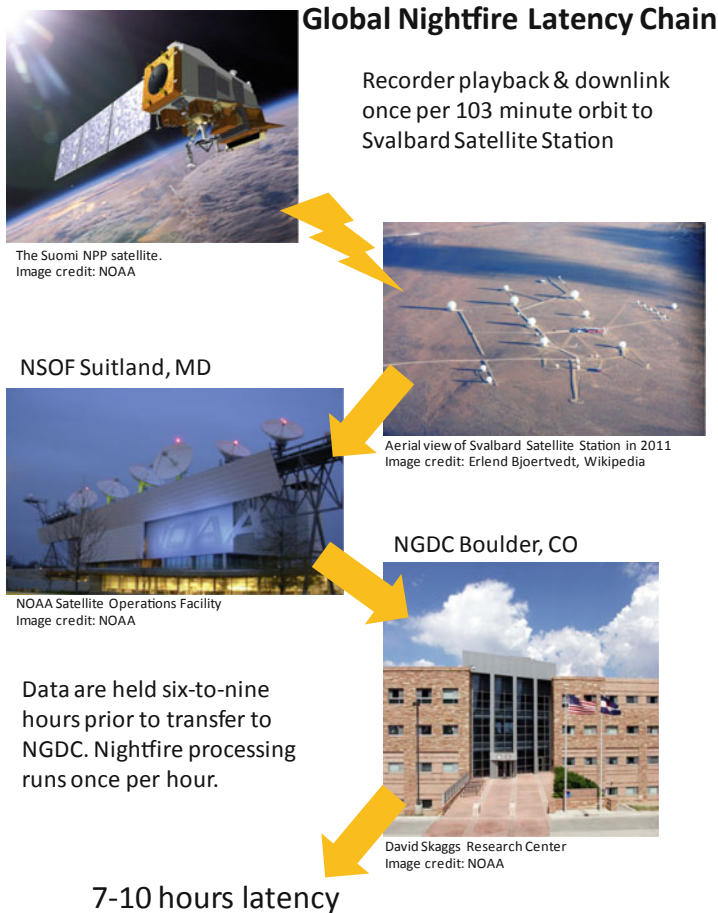


Fig. 2 Data for the global version of Nightfire are downloaded once per orbit to the Svalbard ground station for relay to the NOAA Satellite Operations Facility for initial processing. Data are delivered to NGDC after 6–7 h. NGDC runs Nightfire once per day on the previous day's data. The result is a 12–36 h temporal latency

source area required to get a detectable radiance is small. For instance, at 1800 °K a source size of 0.25 m² is sufficient to achieve detection. In contrast, if the source is 600 K it takes 1000 m² to achieve detection. The detection limit lines have been modeled using the typical detection limit at nadir Planck's Law is used to calculate the source size required to generate a detectable radiance for a range of temperatures. The modeled detection limit falls along the lower surface of the data cloud, indicating that Nightfire's detection limits closely match the theoretical limits based on the M10 detection limit. The lower detection limit for Nightfire is estimated at 500 K, the temperature at which a full pixel heat source would be required to generate an M10 detection at nadir.

3 Comparison of Two Nightfire Data Streams

The National Oceanic and Atmospheric Administration's (NOAA) National Geophysical Data Center (NGDC) currently operates the two Nightfire processing streams. Global nighttime VIIRS data are processed with Nightfire once per day from VIIRS Sensor Data Records that are delivered to NGDC from the NOAA National Satellite Operations Facility (NSOF) in Suitland, Maryland (Fig. 2). NSOF receives the full global data stream from the SNPP satellite which is downloaded once per orbit at the Svalbard ground station. The extreme north location of Svalbard is advantageous since the station has line of sight contact with the SNPP spacecraft on every orbit. The nighttime VIIRS data collections are on the descending node of the orbits (Fig. 3). The nighttime data are held on the spacecraft more than an hour before it is possible to download them at Svalbard. The SNPP data move quickly from Svalbard to the NSOF using undersea fiber optic cables. It takes about an hour for data to be processed from Raw Data Records (RDR) to Sensor Data Records (SDR) and Environmental Data Records (EDRs) at the NSOF. The National Weather Service receives the SDRs and EDRs from the NSOF in near-real time (e.g., seconds). However, the data are held in a data pool at the NSOF prior to delivery to the data centers for archive. The data NGDC receives for archive are generally 6–9 h old. The Earth Observation Group (EOG) pulls copies of the nighttime VIIRS data for Nightfire processing as they are arriving at NGDC. Thus, there is currently a 7–10 h latency range for the global Nightfire data to become available.

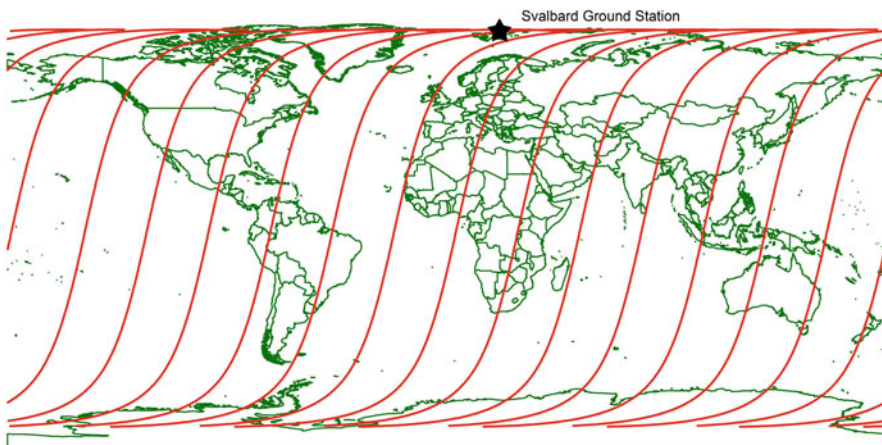


Fig. 3 Nighttime data are collected on the descending (southbound) side of the satellite orbits. Data are later downloaded at the Svalbard ground station while the satellite flies over the arctic. This results in a delay of more than an hour for the nighttime data to be downlinked



Fig. 4 Map showing the SNPP reception circle for the direct readout ground station operated by CIMSS

NGDC operates a second Nightfire processing stream designed to supply reduced temporal latency fire detection data over the continental U.S. (CONUS). In this case the SNPP data are being downloaded from direct readout stations operated by the University of Wisconsin, Cooperative Institute for Meteorological Satellite Studies (CIMSS). The SNPP broadcasts the data being collected by the sensors continuously. Direct readout ground stations receive SNPP data in real time via line of site reception. Figure 4 shows an outline of the CIMSS ground station reception circle. The Wisconsin ground station can collect SNPP data when the satellite passes through the reception circle. The data from the CIMSS and ground station are processed from RDR to SDR and are made available at an open access ftp site operated by CIMSS. NGDC has an automated process that checks the CIMSS site every 20 min and pulls any new nighttime data. The Nightfire algorithm runs on any newly retrieved data and the resultant CSV and KMZ files are posted to NGDC’s website. With these

Fig. 5 Data for the continental United States (CONUS) version of Nightfire are from direct readout ground stations operated by Cooperative Institute for Meteorological Satellite Studies (CIMSS) and Oregon State University (OSU). The dashed line represents the CIMSS ground station reception circle. Temporal latency ranges from 20–30 min

CONUS Nightfire Latency Chain



The Suomi NPP satellite.
Image credit: NOAA

Direct broadcast of real time data recorded by the CIMSS ground station in Madison, WI

CIMSS Processing and posting of data files typically requires 10 to 30 minutes.



SSEC satellite dish atop the AOSS building.
Photo credit: Jeff Miller

Nightfire processing runs as data arrive. Output files are posted on the internet without delay.

NGDC Boulder, CO



David Skaggs Research Center
Image credit: NOAA

20-100 minute latency

variables the temporal latency for Nightfire data over CONUS ranges from 40–100 min (Fig. 5).

4 Detection and Reporting of a Natural Gas Platform Blaze

On July 23, 2013 the Hercules 265 natural gas drilling platform lost control of a well in waters 250 ft deep, producing a plume of natural gas venting to the atmosphere. At 10:50 p.m. local time the plume ignited creating a fireball that persisted for several days (Fig. 6). The heat was so intense that crews sent to bring the well under control had to stay more than 200 ft away from the platform.

VIIRS collected data over the platform at 2:33 a.m. local time (CDT) on July 24, 2013. NGDC received the data from CIMSS 35 min later. The Nightfire data were available from NGDC’s web page at 4:26 CDT. The blaze was detected by VIIRS despite the presence of cloud cover. Nightfire indicated that the temperature was 1402 K and the size of the source was 108 m² (Figs. 6 and 7).



Fig. 6 The Hercules 265 natural gas drilling platform was on fire several days before collapsing. Photograph from the U.S. Coast Guard

5 Conclusions

While satellites are capable of detecting fires from space, there are several factors that limit the value of the observations to the disaster and fire management first responder communities. This includes long latencies for fire detection data deliveries, lack of an easily usable file format, and lack of information on fire characteristics such as size and temperature. Global satellite data streams have inbuilt delays due to storage of the data during orbit, data transmission, processing and release. These delays can be reduced by working with data collected by direct readout ground stations.

NGDC has made substantial progress in developing a new fire product, Nightfire, with specific estimates of temperature, source size and radiant heat. NGDC processes the global VIIRS data stream with the Nightfire algorithm and produces fire data with 7–10 h latency, much too slow for first responders. With tuning this could be reduced to 10 h latency, which is still slow for first responders. By running Nightfire at the NSOF it would be possible to get delivery time down to about 3 h.

NGDC also runs the Nightfire algorithm on VIIRS data collected from the University of Wisconsin direct readout ground station. This system currently runs with a latency range of 40–100 min. The latency could be further reduced by checking the CIMSS ftp sites for new files more frequently and by using a cluster approach to the data processing at NGDC. The Nightfire software can be installed at other ground station sites to provide low temporal latency fire detections in other parts of the world.

The areas that need more work to meet the needs of the first responder community are file formats and delivery mechanisms. It should be possible to deliver map

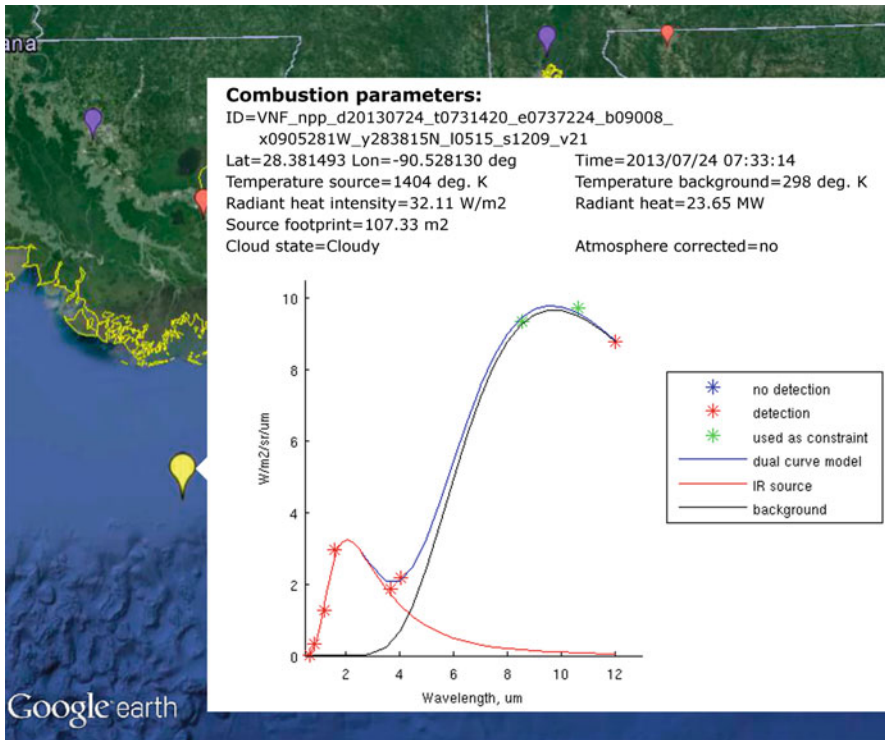


Fig. 7 The Hercules 265 blaze was detected by VIIRS at 02:33 local time (CDT). The detection data were available at NGDC’s web site within 2 h of the detection

graphics with embedded fire temperatures, sizes, and time stamps to smartphones and other mobile devices. Setting this up would require collaboration between a first responder community and the fire product producer.

Acknowledgments The Nightfire development is funded by NOAA’s Joint Polar Satellite System (JPSS) Proving Ground program and the U.S. Department of Homeland Security. NGDC is grateful to the University of Wisconsin Cooperative Institute for Meteorological Satellite Studies (CIMSS) for providing open access to the VIIRS data collected from their ground station.

References

Dozier J (1981) A method for satellite identification of surface temperature fields of sub-pixel resolution. *Remote Sens Environ* 11:221–229. doi:10.1016/0034-4257(81)90021-3
 Elvidge CD, Zhizhin M, Hsu F-C, Baugh K (2013) VIIRS nightfire: satellite pyrometry at night. *Remote Sens* 5(9):4423–4449. doi:10.3390/rs5094423
 Giglio L, Kendall JD (2001) Application of the Dozier retrieval to wildfire characterization—a sensitivity analysis. *Remote Sens Environ* 77:34–49

Application of Mobile Data Capture with Imagery Support

Michael E. Hodgson, Bruce A. Davis, Dexter Accardo, Haiqing Xu, Karen Beidel and Silvia E. Piovan

Abstract

Remote sensing technology and mobile devices are two data collection approaches that are proving invaluable in the disaster response phase of the hazard event. The adoption of these approaches is not universal and still faces significant challenges. The user community must understand the technology, learn how to acquire it, and be trained on its use before the disaster event. Much has been written about volunteered, unvolunteered, and crowd-sourcing of geospatial information for disaster

M. E. Hodgson (✉) · H. Xu · K. Beidel
Department of Geography,
University of South Carolina, Columbia, SC 29208, USA
e-mail: hodgsonm@sc.edu

H. Xu
e-mail: xu79@email.edu

K. Beidel
e-mail: kcbeidel@sc.edu

B. A. Davis
Department of Homeland Security,
Science and Technology Directorate, Washington, DC 20528, USA
e-mail: badavis@cableone.net

D. Accardo
St. Tammany Parish of Homeland Security and Emergency Preparedness,
510 East Boston St., Covington, LA 70433, USA
e-mail: daccardo@stpgov.org

S. E. Piovan
Department of Historical Geographical and Antiquity Sciences,
Geography Section, Università degli Studi di Padova,
via Del Santo 26, 35123 Padova, Italy
e-mail: silvia.piovan@unipd.it

response and recovery. While research in these areas continues, most U.S. federal and state agencies rely on authoritative data collected by authorized personnel. This research focuses on the use of geospatial technology with mobile devices by appointed users—those individuals with authorization to collect geospatial information for a governmental agency with authority in the disaster response process. This chapter describes a project to develop a web-app that allows appointed users to collect geospatial data in the field with Google Maps and user-supplied imagery and with pre-defined and user-defined structured forms. Although the original purpose focused on disaster response and recovery activities, such as the Urban Search and Rescue (USaR) house-to-house searches, the user-groups, purposes, and technologies rapidly changed in this two year project. Technology for the web environment rapidly changes, particularly for mobile devices. Our focus on the USaR teams changed to all parishes in the state of Louisiana. This project used an agile software development approach, which permitted the evolving nature of the user requirements. Without this agile approach the user community would not have adopted the application for emergency response.

Keywords

Remote sensing · Mobile applications · Disaster response · Web-GIS · WebApp

1 Introduction

During the initial days following a catastrophic disaster, federal, state and local response teams deploy to begin damage assessment and search and rescue operations. Multiple teams working over an extensive landscape using traditional data capture approaches of paper maps, clipboards, pencils and paper forms can often result in collecting redundant data for a geographic area and in errors translating from paper forms to the required format for submission up the incident command chain. Furthermore, the information gathered in the field is critical to the full understanding of the magnitude of the disaster incident as well as how field resources are being used and where additional resources are needed. Unfortunately, traditional methods of data capture and transmission of field data sometimes result in delay in this information being fully understood by all levels of incident command.

Disasters are recurring events and thus, in research, the concept of a hazard cycle is used to describe the sequential phases of a location that experiences repeated hazard events. The common phases described are event, response, recovery, planning/mitigation, warning—followed by another event. The response phase of the hazard cycle is the shortest phase (e.g. 3-days, but dependent on the scale of the event) and the recovery phase may last for days or months (and in some cases years). While considerable research has been and is still being conducted on crowd-sourced approaches for geospatial-enabled approaches in disasters (e.g. Goodchild and Glennon 2010; Merchant et al. 2011), the governmental (e.g., local, state, federal) process is

almost exclusively focused on the use of authorized personnel to collect geospatial information. In large part, the issues of quality, reliability, and liability restrict a governmental agency to using authoritative users for key data collection efforts.

The primary piece of information that disaster relief is based on is the Preliminary Damage Assessment, or PDA (GAO 1996). It is the first assessment of a community following a disaster and serves as the benchmark on which other information is built. It is the key component of information needed by a state to qualify for a Federal Disaster Declaration. The PDA identifies the impact, type, extent of disaster damages and impact on individuals. The PDA documents the damage by listing the number of residences that are destroyed or suffering major or minor damage; the estimated public assistance cost; and the estimated damage by county. The collection of PDA-data is a joint effort by both federal (i.e., FEMA) and state and county/parish staff. The thresholds for a Presidential Disaster Declaration are \$ 1.29 per capita statewide or \$ 3.23 per capita for a county.

Remotely sensed imagery is often viewed as a key part of planning and mitigation of natural disasters and without question, either the data/imagery or the derived products from remotely sensed data (e.g. land use/cover maps, digital elevation models) are very important. However, during disaster response operations aerial or satellite imagery is not commonly used (Hodgson et al. 2013) for several reasons. First, the post-event imagery must be collected and made available quickly and inexpensively to be useful enough in the disaster response or recovery operations to justify the cost. A recent survey of all state emergency management offices found only 16 % of states used imagery for mapping disaster extent and less than 8 % used imagery for other damage estimates (e.g. buildings, critical infrastructure, or transportation features) (Hodgson et al. 2013). Thirty percent of states expected the federal government to collect the post-event imagery regardless of whether the state requested it. Also, 54 % of the states expect the imagery to be collected and made available with no cost to the state. (Note: the general formula is the federal government will pay 75 % of image collection costs for disasters that have been declared under the Stafford Disaster Assistance and Emergency Relief Act of 2000.) The reasons for these statistics are many but chief among them may be the lack of appropriate tools to integrate the use of imagery into the decision making process in both the Incident Command HQ and in the field. How do these individuals obtain the imagery and utilize it on a portable device? Ideally, the field users would have both pre- and post-event imagery available. But how will they incorporate the imagery as a layer on a portable computing device, such as a tablet or smartphone?

While much research is focused on automated methods for extracting information from post-event imagery a very important use of imagery is simply for visual analysis. Automated approaches suffer from a variety of issues, including spatial resolution incompatibility, sun-angle, and spatial registration issues with pre- and post-event images (Tiede et al. 2011). The use of imagery for visual analysis may range from very simple 'backdrops' to other ancillary data (e.g. transportation networks, buildings, etc.) to more sophisticated uses such as classification of residential structure damage. Shortening the time it takes to build an understanding of the scope of a disaster is crucial in being able to direct resources quickly and efficaciously. Imagery is one of

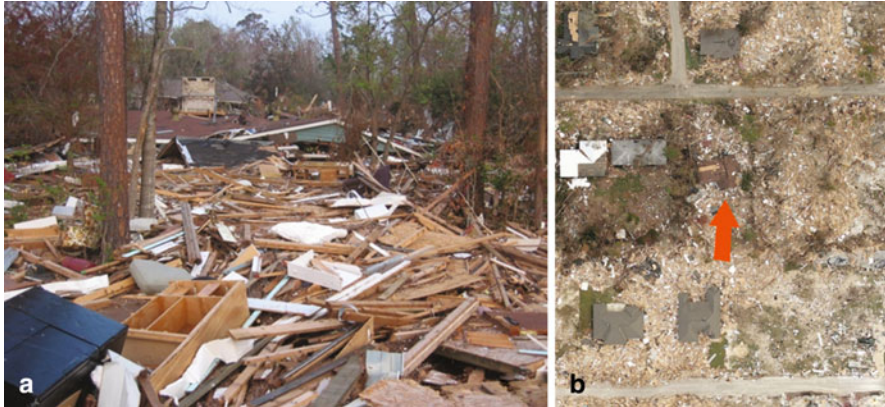


Fig. 1 Ground-level view (a) and aerial view from Pictometry (b) of a residential area impacted by Hurricane Katrina storm surge. (Image on the left courtesy of Bruce A. Davis)

the best ways to build that understanding and the key issue is delivering the imagery to response/recovery staff quickly, such as through the internet/cellular dissemination to field personnel.

There is a critical need for dynamic situational awareness during the first few days of a catastrophic disaster to enable response agencies at all levels to have an accurate, common operating picture of the incident to determine response resource needs and priority areas. Mobile applications can be a key element in the data acquisition process to improve situational awareness but, in general, have many challenges when used by disaster response communities (Clarke 2004). Data collection with mobile devices often takes place using tablets or cell phones (NOAA 2001; DeCapua 2007; Hodgson et al. 2013). While numerous ‘apps’ for collecting geospatial field information exist, a key need for authorized disaster response staff is the integration of pre- and post-event remotely sensed imagery. In some disasters, such as an earthquake or hurricane flood surge, a ground-level view of the disaster site after the event has occurred is very different than a vertical view (Fig. 1a and 1b). Importantly, a post-event observation may not provide important information on the pre-event structures. The post-event image may not show a residence that has been moved, or it may mislead staff where a multistory building has collapsed into a single story in an earthquake.

While many apps are now available for disaster response and recovery applications, few were actually created under the direction of a federal or state emergency response agency. These applications for iOS or Android devices are available in the online distribution portals, such as Google Play or App Store (American Red Cross 2014). Several GIS vendors (e.g., ESRI) have also developed ‘free’ apps (e.g., ArcGIS app) that can be used to collect geospatial information. Such apps are rarely ‘free’ but depend on licensing agreements for usage, storage of data online, or—worse—acceptance of product advertisements. Most importantly, such apps may not be usable in a disconnected mode (i.e., when the cellular connection or Wi-Fi connection is unavailable). Furthermore, data collected by local, state, or federal

response teams is normally confidential and therefore could not be stored in an unsecured IT architecture. Since these data are often part of the Preliminary Damage Assessment (PDA) used to qualify communities for disaster relief funds it is important that these data have credibility and a documented chain-of-custody handling to insure accuracy.

First response agencies at all levels share the requirement for tools that are tailored to their needs; that are easy to use in the field, operate in all conditions throughout incident response, and are affordable to acquire and maintain. The United States Department of Homeland Security (DHS), Science and Technology Directorate recently funded the development of a mobile app (i.e. the Mobile Image Analysis Toolkit), that meets these user requirements and those defined by DHS/FEMA, the State of Louisiana Governor's Office of Homeland Security and Emergency Preparedness (GOHSEP), and several parishes in Louisiana (especially the St. Tammany Parish Office of Homeland Security and Emergency). The design, implementation, and testing phases of this mobile app were conducted using the agile programming paradigm (Beck et al. 2001). The testing involved numerous state personnel and parishes in Louisiana and reviewers in other regions of the U.S. and Europe. The users for the application were a critical part of the design phase and provided important feedback on each step in the agile development process. The unique aspects of this project include the online/offline synchronization requirement, the pre- and post- imagery requirement, and the low-cost implementation strategy. The collection, editing, and even visibility of the data must be restricted to authorized users, necessitating a carefully orchestrated system of user management with defined roles.

The most important component of this project was the stakeholder. Any new technology 'solution' would not be used during the next disaster unless the stakeholder community had already adopted and trained with the solution. There is no time for training during a disaster and few if any response agencies will risk the collection of critical information with an untested and unproven technology. Furthermore, the application must be thoroughly tested to insure data integrity. Our approach to this challenge was to work directly with state and parish officials in Louisiana at several levels to help (1) define/refine their requirements, (2) customize a solution, and (3) train the administrators and field personnel with the technology solution. Through this process we gathered valuable feedback on the current version while training the end user community and preparing them to incorporate the technology when the product was ready.

An underlying factor in the design and implementation of the mobile application with server-side support was the continual evolution of the web-based and mobile-based technologies (hardware, software, and protocols). Because the cellular and tablet markets are rapidly evolving, the protocols and software technologies evolve too.

In the remainder of this chapter a discussion of the two key data elements in the application—pre- and post-event imagery and the user form. The use of an iterative development process (i.e. the agile software development method) and the software implementation are presented. Finally, the user testing, training, and application user manual are discussed.

2 Incorporating Pre- and Post-Event Imagery

Web-based distribution of imagery can be simple downloads of image files (e.g., in .jpg, .tif, .png form) or can incorporate web mapping services (e.g., Google Maps, Bing Maps). Web mapping services may be constructed in a *de facto* standard or organizational standard, such as the web mapping service (WMS) specification by the Open Geospatial Consortium (OGC). More problematic is the incorporation of imagery when the mobile device is disconnected (i.e., offline) from cellular or Wi-Fi networks. The mobile device application developed in this project incorporated imagery using the following three approaches:

- Downloading image tiles (.jpg format) from a centralized web server to be used in an offline mode,
- Employing Google Maps imagery in a connected mode,
- Incorporating user-supplied imagery as ‘pinned’ .jpg images on Google Maps.

Most counties and many states in the U.S. have online (or protected) repositories of image tiles covering their regions. These repositories are typically organized in a very structured set of ‘tiles’ (square regions) in a regular tessellation. For example, the tile boundaries in Richland County, SC are structured at three hierarchical levels of 5000-, 10,000-, and 20,000-foot tile boundaries for different spatial resolutions. Our approach allowed users to access these repositories by downloading the image tiles (and associated header file) to the mobile device for use in offline mode.

The DHS has recently (2013) created a formal project for requesting a commercial provider to collect post-event disaster imagery. These data will be hosted on the DHS Geospatial Information Infrastructure (GII) cloud architecture. Emergency response agencies with accounts will be able to access these images, and there are plans to test and evaluate image analysis tools within this architecture. The imagery will be disseminated either as separate .jpg files (as used by commercial providers in the past) or by a web mapping service in the form of tightly structured dynamic tiling schemes (e.g. Google Maps). Our implementation for post-event imagery is currently based on the ‘pinning’ (explicit georeferencing of an image with corner points) of such imagery on top of a Google Maps basemap or image.

2.1 The Form

The reason for delivering imagery to field teams is to enable them to navigate to a location or to assist them in the assessment of damage by collecting information about the structure under review. The mobile application data collection component is used to collect geographic position, attribute information, and ground-level photos of the position. Geographic position is based on either the GPS (actually the position may also be based on a global navigation satellite system (GNSS), depending on the newer receivers) or by the user designating a location on the map/imagery. The ‘form’ is the component that allows users to enter a structured set of attributes in pre-defined fields (e.g., textboxes, checkboxes, drop down lists, etc.)

2.2 PDA Form

The form created for the initial MIAT PDA application was based on the information needed by the state when applying for disaster assistance. Staff in the State of Louisiana GOHSEP office and St. Tammany Parish defined these requirements. The database and structured form was used to collect and store the key information for the PDA in a MySQL enterprise database.

In this project the information required for the PDA was collected in a pre-defined form. However, the user community also wanted many other forms (e.g., pet rescue, bridge conditions) and the list of forms was constantly changing. Thus, we implemented technology to allow users to define their own forms from a set of form elements (textboxes, data fields, checkboxes, and drop down lists). The development environment for a user-defined form was very simple. Other mobile applications have been developed that also allow user-defined forms (e.g., Aanensen et al. 2009). This ability to construct forms quickly and easily for the collection of attribute information is critical to the successful implementation of MIAT within state and local government agencies. As the maturity of MIAT use increases the application of the tool to a wider variety of problem sets grows requiring additional data collection forms. This capability also allows agencies to construct forms that address information gaps as disaster response operations unfold. Published from the server-side, the forms are instantly available to all field teams insuring that consistency in the data capture process is maintained by all personnel.

When the user-defined forms were demonstrated at the GOHSEP meeting in Baton Rouge and again at a Louisiana Emergency Preparedness Association meeting in Lake Charles, the increase in interest was marked (Fig. 2). While the PDA form was seen as useful, it was meeting a requirement imposed on the parishes by the state and federal authorities. Making their own forms allowed them to address important local issues. Parish officials suggested, for example, using it to monitor bridge conditions during ice storms, to record cemetery plots in areas prone to flooding, and to map facilities that were potential hazmat sites.

2.3 User Form

To test the flexibility of MIAT and its potential in non-emergency contexts, plans were made to test its data collecting potential in a different survey. In particular, MIAT will be tested during field activities of the 17th European Seminar on Geography of Water (GoW) (Padova, Italy, 22 June–3 July). In line with the main objectives of this seminar, the goal of the survey will be to collect information about the potential water-related landmarks of the Southern Venetian Plain. For this purpose, a new form called “GoW_2014_landmarks_point” was defined (Table 1a).



Fig. 2 Focus group and training of Parish directors in Lake Charles (a) and Baton Rouge (b)

3 Iterative Application Development Process

The best approximation of the software development cycle for this project would be the agile development approach (Beck et al. 2001). The classic waterfall design (Bell and Thayer 1976) has been criticized for many reasons but is clearly not appropriate for this project as (1) the requirements were loosely defined and (2) software technology changed during the project. The requirements for the mobile application could not be rigorously defined prior to beginning the software development/implementation; the needs of the clients/stakeholders both became more defined and evolved during development. In fact, the telecoms and group meetings enabled the stakeholders to assemble together and collectively discuss the requirements and context for implementation. These meetings forced the stakeholders to reach a consensus on the issues, the requirements, the implementation solutions, and the authorities. The final meeting was conducted at the Governor's Office of Homeland Security and Emergency Preparedness (GOHSEP) in Baton Rouge, Louisiana where both a focus group and some training took place (Fig. 2a and 2b).

Thus, we used an agile software design model to work with the stakeholders as the most important part of the project. The agile design required us to completely abandon one software solution (i.e., a custom ESRI iOS solution) because of (1) the stringent online database/server requirement and (2) the delays in the ESRI offline GIS mobile application. Our agile development cycle was composed of the following steps:

1. Initial set of requirements from Focus Group of Louisiana staff on PDA needs
2. Scoping of technology (server-side, mobile-side) availability
3. Scoping of business models (i.e., software licensing, cloud-server costs, local-server possibilities)
4. Mobile device support requirements
5. Integration of existing and near real-time imagery

Table 1 Example form for the 2014 European seminar on geography of water data collection exercise

Field name	Field type	Description of field	Example value(s)
Landmark_Name	TEXT	Identifies the landmark as univocally as possible	Idrovora vampadore
Date_of_Survey	DATE	Date of the survey, i.e. day month year	20 May 2014
Surveyor	TEXT	Name of the surveyor	Silvia E. Piovan
Surveyor_Contact	TEXT	Phone number or a email address	silvia.piovan@gmail.com
Description	TEXTAREA	Short description of the landmark	Built between 1880 and 1881, power of the pumps 400 HP
Age	DROP DOWN LIST	Defines the age of the landmark, e.g. Protohistorical, Roman Age, Middle Ages, Modern Age, Contemporary Age	Contemporary Age
Type	DROP DOWN LIST	Natural or historical of the landmark	Historical
Category	DROP DOWN LIST	Defines the type of the landmark, i.e. bridge, building, culvert, meander cutoff, pumping station, river diversion point, stone, water pond, other	Pumping station
Other	TEXT	“Other”, this “open” field allows the user to specify, the category. The administrator could be include a new category if it will become a common one	–
Preservation	DROP DOWN LIST	Defines the preservation condition of the landmark, i.e. bad, poor, good, excellent	Good
Enhancement	DROP DOWN LIST	Describes the enhancement condition of the landmark, i.e. absent, poor, good, excellent	Poor

6. Approaches to deploy software on mobile devices
7. Prototypes (ESRI and open-source)
8. In-house testing
9. Local user testing
10. International user testing
11. Revisit requirements and implementation strategies

We held two focus group meetings with Louisiana staff and numerous internal/DHS meetings. Some key requirements were defined in these two meetings:

Geospatial Location and Attributes The mobile application must be able to define positions based on the device location (e.g., GPS, GNSS) or pointing to an onscreen map or image. The application must have access to pre-event and post-event near real-time imagery.

Online and Offline Capabilities During a large scale disaster event the network connections (e.g., cellular or Wi-Fi) are often unavailable in the field. Furthermore, in the state of Louisiana, large rural areas had neither type of connectivity. The application had to address the need for offline data collection where the collected data would be synchronized when the user entered a Wi-Fi space.

Management of Users The use of the mobile data collection required a level of security that restricted data collection to authorized users. Furthermore, the set of authorized users should have different roles based on their collection/editing/proofing responsibilities and their geographic area of responsibility. The ‘role administrator’ assigns each user a role. The disaster Incident Commander must also have methods for assigning user roles.

Evolution of Software Application A number of significant software changes were required during development, and were envisioned as continuing to evolve. Deploying a device-dependent app would have required constant redeployment of the solution through the two main mobile device operating system portals, Google Play and the App Store. Thus, the development of new versions of the software in Objective C and Java for two operating systems would have been laborious and time consuming. Our solution quickly evolved from device-based apps into a single web-based app, where the code could be updated once and immediately made available to users from a server-side change. This approach also enabled the agency responsible for the information requirement to publish the data capture form for use by field teams and thereby control the process to insure consistency and accuracy.

4 Implementation Design

4.1 Technologies Used

The implementation of the mobile application requires both server-side and client-side code (Fig. 3a and 3b), a database on both sides, and a protocol for communication between the mobile device and server. During the design process the user community explicitly guided us to change the implementation plans from commercial software (e.g., SQL-Server, ESRI ArcGIS Online, ArcGIS for Mobile app) to open source software. The redirection was for two primary reasons: (1) the cost associated with a commercial solution itself with the uncertainty of future licensing/subscription

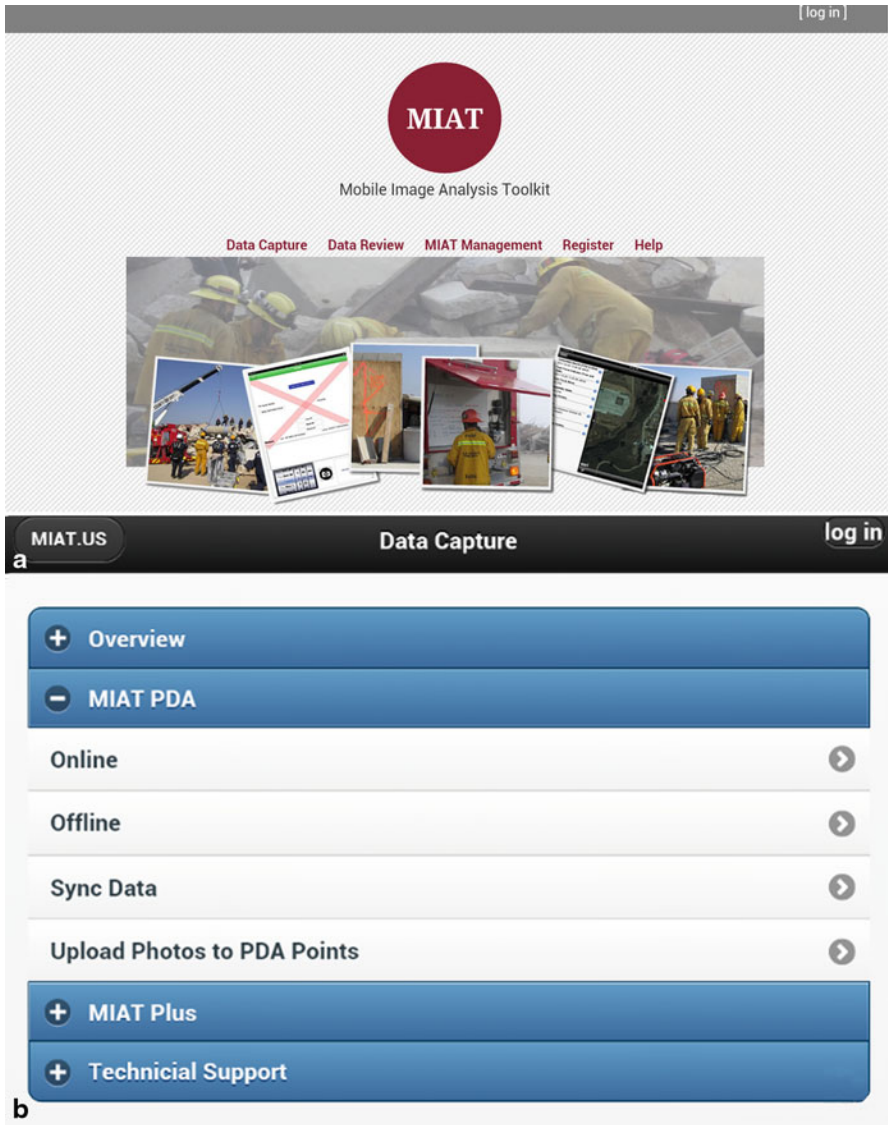


Fig. 3 Screen shot of MIAT home page on server side (a) in landscape mode and MIAT Data Capture app on client side (b) in portrait view (both running on 8” Tablet)

fees and (2) the lack of suitable commercial solution for offline use. These two issues impact operational sustainability of the tool and the utility of the tool for emergency response. Parish governments as well as state emergency management agencies work within very tight budgets. The ability to budget for a software license is difficult and when viable options exist for open source or ‘home grown’ software

developed from well understood and available tools then more and more governments are turning to this option. The guidance from the user community resulted in the use of the following technologies for an implementation: database (MySQL, IndexedDB), map (Google Maps API), programming languages (PHP, HTML5, CSS, JavaScript, jQuery, and jQuery Mobile), and communication (Ajax, JSON). These are tools that are well understood in government, industry, and academia. The ability of a local or state government to maintain a capability such as MIAT written in well understood languages is extremely valuable as it plans for continued development of the tool and long-term maintenance.

On the server side, MySQL 5.0 was used to store all user collected data. Additionally, the user profile (e.g., name, affiliation, email, operating state and county, and role) was stored in a protected table. This is the information that the user must provide to secure an active role using MIAT, and it is very valuable to the emergency management agency hosting the tool because they can review the data in the profile and compare it against an approved list of credentialed response personnel to avoid permitting unauthorized access to sensitive data. On the mobile device (client-side), an IndexedDB database within the browser cache was used to store user collected data for offline use. Pre-event and post-event image sets are stored in the file system on the mobile device. Communication between the mobile device and the server utilized the Ajax (Asynchronous JavaScript and XML) technique primarily in JSON (JavaScript Object Notation (JSON) format.

While the data creators and data editors roles could create and modify data, for the PDA app only the administrator role was allowed to ‘approve’ the final data. Thus, it was necessary to keep a record of the changes to each field for every location. We implemented methods for capturing the time and person changing each field for each record in the database.

4.2 User Maintenance

The authorization of each role required numerous trials and revisits with the stakeholders. After several iterations we settled on a hierarchy of user roles (Fig. 4). At the highest level, a super-administrator could modify all user roles, recover their passwords, and delete users. All other roles beneath the super-administrator were limited in scope to one state/county. Role-administrators would assign roles for users associated with their state/county. Data editors could modify any data for the state/region they were assigned; while data creators could collect data but only modify data they created. Data viewers could look at any data collected within their state/county but could not download or modify the data. After the initial registration a member waits to be assigned a role by the role-administrator before being allowed to access the mobile app.

We tested and implemented server-side functionality initially using Visual Studio and C# and subsequently using PHP. Visual Studio allowed for a simple implementation of user authentication with a login/password protocol and database hashing of passwords; however, because the code on the server-side and client-side both can utilize a login-authentication, we opted for a PHP/JavaScript solution.

MIAT Members

E-mail	Full name	County /Parish	Official Capacity	Phone #	Role	Save Change	Delete	Send Password

MIAT Data Viewers

E-mail	Full name	County /Parish	Official Capacity	Phone #	Role	Save Change	Delete	Send Password

MIAT Data Creators

E-mail	Full name	County /Parish	Official Capacity	Phone #	Role	Save Change	Delete	Send Password

MIAT Data Editors

E-mail	Full name	County /Parish	Official Capacity	Phone #	Role	Save Change	Delete	Send Password

MIAT Role Administrators

E-mail	Full name	County /Parish	Official Capacity	Phone #	Role	Save Change	Delete	Send Password
italy@miat.us	Silvia Piovani							
silvia.piovani@gmail.com		Padova	Colleague					

MIAT Super Administrators

E-mail	Full name	County /Parish	Official Capacity	Phone #	Role	Save Change	Delete	Send Password
hodgsonm@sc.edu	Michael E. Hodgson							

a

Registration for MIAT

Please fill out the form below. Select your state and your county/parish, and provide your official capacity there. Your application will be reviewed by a website administrator.

Your application will be reviewed by the website administrator. You will **not** be able to access any data on MIAT until the administrator has assigned a role to you.

Required

Email:

Password:

Confirm Password:

State:

County/Parish:

Official Capacity in County/Parish:

Terms and Conditions:
 I accept the [terms and conditions](#)

Optional

Full Name:

b

Fig. 4 MIAT user role assignment (a) and user registration (b)

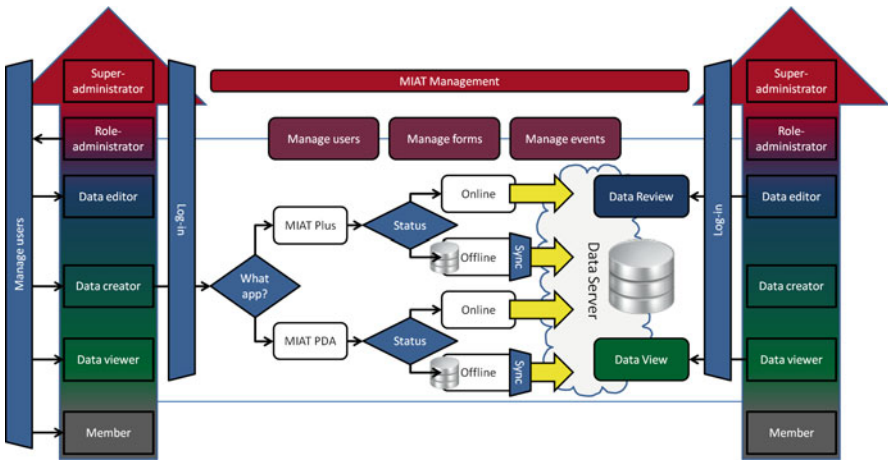


Fig. 5 MIAT Mobile app and supporting server-side software workflow illustration

4.3 Workflow

The typical workflow for each type of user is shown in Fig. 5. Users were required to register, be assigned to a role (Fig. 4a), and collect data in the field (Fig. 4b).

MIAT Mobile

County: St. Tammany

Event: Winter storm

Applicant Name: St Tammany

Contact Name: Dexter Accardo

Contact Number: 123 456 7890

Physical Address: 310 W 21st St

Project Name: Library Restoration

Category of Work: Construction

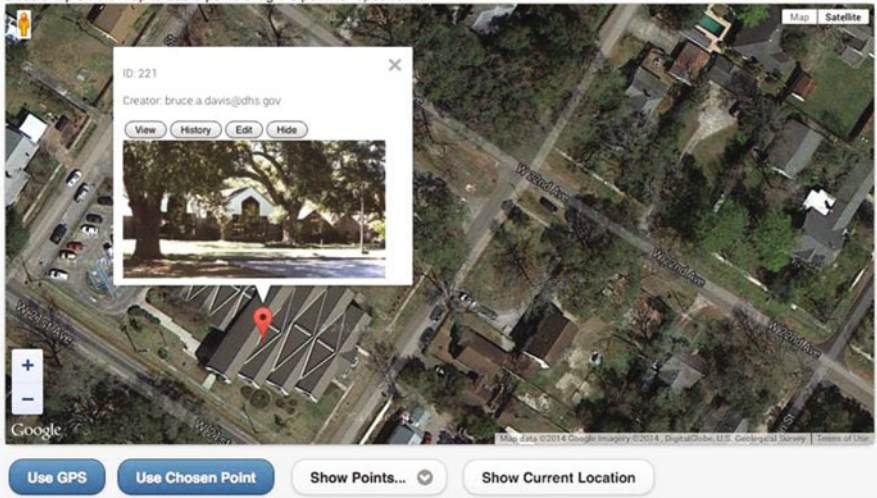
Work Completed (%): 10

Estimated Cost: 127655

Actual Cost: 176352

a

Double-tap on the map to add a point. Drag the point to reposition it.



b

Fig. 6 MIAT Mobile app: portion of PDA form (a) and data capture running on a tablet with observer location (b)

The data collected, which appeared as points on the onscreen map, included both the geographic location of the property (e.g., public buildings, residences) damaged by the disaster (using the device’s GPS or by directly selecting a location on an onscreen map) and the fields in the structured PDA form (Fig. 6a). In addition, the

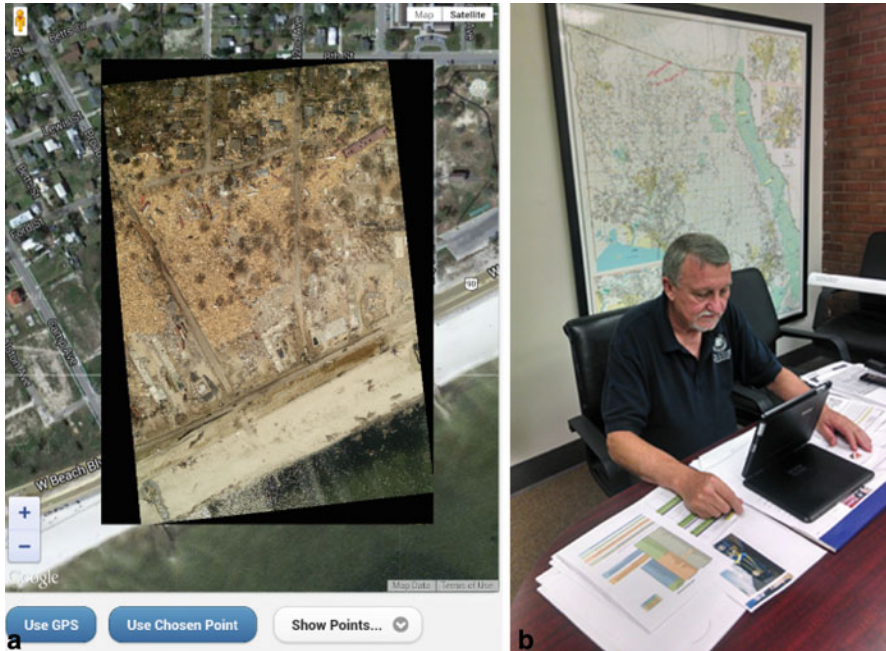
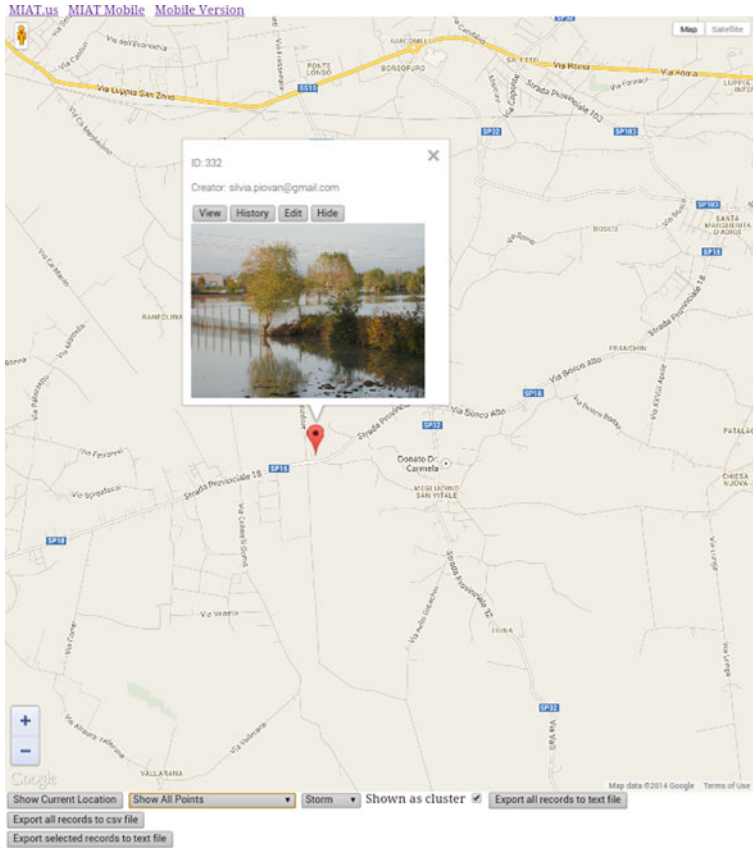


Fig. 7 MIAT Mobile app data capture screen illustrating a post-event (Hurricane Katrina in 2005) image from Pictometry overlaid on Google Maps imagery (a) while central staff observe field collections (b)

timestamps indicated when the data was collected and photos/videos were taken in the field. The interactive map in the application allowed user to see his/her location, previously collected points and photographs, and review the data collected (Fig. 6b). Post-event imagery could also be overlain on a Google Maps image base or a street/river network basemap (Fig. 7a). Command center staff can watch the data collection (if the field personnel synchronize their collected data or are operating in an online mode) (Fig. 7b). The display of points could also be restricted based on user criteria. After points were collected the data could be reviewed on desktop or mobile devices (Fig. 8). Finally, the data could be exported in several forms (e.g. databases, spreadsheets, or a shapefile) for consumption in other applications.

4.4 Device and Browser Independence

The MIAT app is designed for cross-platform use and the app has been tested to run fluently on many devices, browsers, and operating systems: iOS 6 and 7 (iPhone, iPad and iPod Touch), Android 4.2 (smartphones and tables), Windows Vista and Windows 7 (laptops and desktops). Compatible browsers based on our tests include but are not limited to Internet Explorer 10, Google Chrome, Firefox and Safari.



MIAT PDA Data

ID	Creator	Time Created	County	Applicant Name	Contact Name	Contact Number	Physical Address	Project Name	Category of Work	Work Completed (%)	Estimated Cost	Actual Cost
332	silvia.piovan@gmail.com	Sat, 17 May 2014 13:44:13 GMT	Padova	Silvia Piovan	Silvia Piovan					0	0	0

Fig. 8 Example MIAT data review page for proofing points already collected

An important requirement was the ability to use iOS and Android mobile tablets and phones and most browsers. We included checks for early versions of Internet Explorer and are not supporting versions earlier than IE9. Because tablets and phones, in particular, may be oriented either landscape or in portrait mode we designed a ‘fluid’ menu system that adapted to the device display resolution and orientation.

5 National/International Testing

We tested the use of the MIAT application in several places in the United States and in two European countries (Austria and Italy). Since the application was designed for U.S. states and counties (or county equivalents), we added international countries as ‘states’ and their immediate subdivisions as ‘counties’.

5.1 Testing in United States

All versions (initial concepts through alpha/beta/Version 1.0) were exhaustively tested in multiple states (District of Columbia, South Carolina, Louisiana, and Mississippi) in the U.S. Example imagery for offline use was created for Richland County, South Carolina, so most offline testing was conducted for this region. Both online and offline testing with various cellular service providers (e.g., AT&T, Verizon, T-Mobile) and Wi-Fi connections allowed thorough testing of connectivity and bandwidth issues. We also tested numerous platforms (desktop, laptop, tablet, and cell phones) using various operating systems (Windows, Android, iOS and Mac OS) and browsers (Internet Explorer, Safari, Chrome, and Firefox). While quantitative measures of disaster response improvement are not available, the overall evaluation of the tool was communicated to the team by end user emergency response agencies. In their review of MIAT, emergency response agencies generally measured the improvement in their operations based on improvement over existing methods for the collection of field information to support disaster assessment and search and rescue. The existing methods generally involved the use of paper forms with the transcription to digital spreadsheets later when the teams returned from the field. There was no dynamic update of a database as teams progressed through the disaster. They also did not have the benefit of post-event imagery to navigate through a confusing landscape. While each agency that used MIAT stated it would be an improvement over existing methods, an exact measure of this improvement was not possible chiefly because it was not used during an actual disaster response operation.

5.2 Testing in Austria

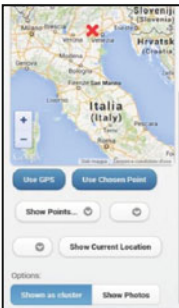
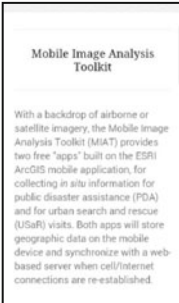
The online version of MIAT was tested on an Apple phone (an iPhone 5) and an Android Samsung Tab 3 8-in. tablet in Austria using various cellular providers (WOWWW!, Bob, Vodafone, Georg) for connectivity. The online testing worked flawlessly during testing in Salzburg, Austria. The offline version suffered some issues with one service provider while at the base of the Hohensalzburg Fortress.

5.3 Testing in Italy

Extensive testing of MIAT in Italy was by an Italian professor whose second language is English. This testing opportunity was also by a scientist not initially trained in

Table 2 Example list of important web site and application issues identified during testing

ISSUE	RESOLUTION
<p>“MIAT PDA, Online” and “MIAT Plus, MIAT Online” have different HMIs. Why?</p>	<p>Modify interfaces to be consistent.</p>
<p>There are no title for pages, so the user can forget if he/she is in MIAT PDA or in MIAT Plus.</p>	<p>Add consistent title to all pages.</p>
<p>The explanation of MIAT says that it provides “two free apps” (PDA and USaR). This is not evidenced neither in the lists of the 4 links “MIAT Mobile, MIAT ESRI, Mobile GIS Research, Related Sites” and in the MIAT Mobile menu. We need consistency.</p>	<p>Eliminate the references to the USaR app in this project and revise online description.</p>
<p>The “MIAT Plus, MIAT Online” has two buttons without label. The user cannot understand the meaning of those buttons.</p>	<p>Change text size for button widgets so text shows on all devices.</p>



the use of MIAT but relying on the user documentation and/or information on the interface. MIAT was tested in online mode and with a user-defined form using a Samsung Galaxy 3 cell phone. Testing in this international context was extremely helpful and identified both serious issues as well as issues that were simply overlooked by the users and developers that were ‘too’ familiar with the application (Table 2). Documentation of issues included graphic examples and textual descriptions. The MIAT team then reviewed the issues collectively and decided on resolutions. For example, a new user would quickly loose the workflow as the web/application pages either did not have titles or the title naming convention was not consistent. In a few instances the lag-time in cellular response necessitated letting the user know certain tools may require additional loading or processing time.

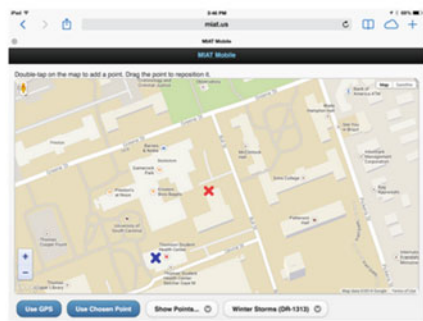
6 User Manual

The users of the PDA application are a mixture of many somewhat older staff and younger staff who may ‘learn’ an application in different manners (While differentiation by age may not be the perfect proxy for this learning style, we use it in this

should be indicated on the fourth button at the bottom of the map.

You can use the red GPS cross that marks your current position for your record if it is appropriate. If it not quite where you want it, double-tap the screen to position a point (a blue cross will appear). You can drag the blue cross until it is exactly where you want it.

Once you've identified your point, tap either the **Use GPS** (to use the red cross) or the **Use Chosen Point** (to use the blue cross) button beneath the map.



Tapping either button will open — in the same window — the PDA form, which you can then fill out. Ideally, some of the fields in the form would already be populated. You may edit these fields, add information

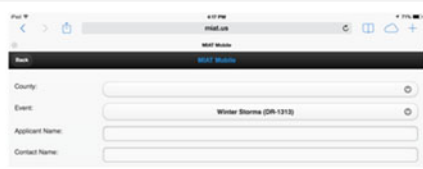


Fig. 9 Example portion of the online user’s manual for MIAT-PDA

article as most readers will understand the issue.) Traditional application users will be trained in a workshop or be instructed to follow the steps in a user-manual. Contemporary users of computing applications are conditioned to not read user-manuals or, at best, to rely on ‘Quick Start’ guides. For state/federal applications we will assume the user will be required to attend a short (e.g., 1-h) training course on the PDA application or instructed to follow a user-manual. We have created user manuals (Fig. 9) both for the use of the PDA application (online and offline versions) and for the installation/management of the entire server-side/client-side applications.

7 Discussion

The successful use of remote sensing technologies to improve disaster response and recovery depends on the entire remote sensing process working in an efficient manner. This process consists of tasking the optimal remote sensing assets, rapid acquisition of data, efficient and effective analysis, and effective delivery and use of the products. All four elements of this process have to be in place or the entire delivery of improved information is delayed. MIAT was developed to improve the capture of critical data in the field and to improve the use of remote sensing data as an

intelligent mapping of a post-disaster landscape. MIAT also helps response personnel to navigate to priority areas for execution of mission responsibilities. It leverages existing remote sensing databases resident with parishes and counties, states, and federal agencies and provides a means for field teams and Incident Commanders to better understand a changing disaster landscape and communicate this understanding to other agencies that may not be resident in the disaster. The ability for all levels of the incident command chain to see the same image of a disaster is a powerful tool. It allows everyone to understand the disaster at the same point in time and to come to agreement about priorities and allocation of resources. Within this context, MIAT uses remote sensing imagery and existing cartography to provide a dynamic update of response operations as they progress. From the Incident Command center, a regional facility to a national watch office, everyone with an account can monitor the collection of data by field teams and better understand the magnitude and extent of the disaster.

Throughout the development of MIAT the team worked with existing imagery over a few select test sites outside of a disaster response environment. During one opportunity (a field test with USaR personnel in the Los Angeles County Fire Department training site) the MIAT team participated in an exercise in which real-time remote sensing imagery was collected over a site designated by a response agency and then consumed by MIAT for use in the field by response personnel using tablets. This single test was successful and points to future possibilities as rapid data acquisition and transmission technologies combine with cloud computing architectures to offer emergency response agencies the opportunity for incorporation of image data into the operational response environment. As technologies to provide imagery improve and as technologies to consume image data for use with field-acquired information also improve, the push-pull of these two will move the national capability to respond to and recover from catastrophic disaster forward.

Acknowledgments This research was supported by funds from the Department of Homeland Security, Science and Technology Directorate.

References

- Aanensen DM, Huntley DM, Feil EJ, al-Own F, Spratt BG (2009) EpiCollect: linking smartphones to web applications for epidemiology, ecology and community data collection. *PLoS ONE* 4(9). doi:10.1371/journal.pone.0006968
- American Red Cross (2014) Red cross mobile apps. <http://www.redcross.org/prepare/mobile-apps>. Accessed 17 May 2014
- Beck K et al (2001) Manifesto for agile software development. Agile alliance meeting. <http://agilemanifesto.org/>. Accessed 17 May 2014
- Bell TE, Thayer TA (1976) Software requirements: are they really a problem? In: *Proceedings of the 2nd International Conference on Software Engineering*, IEEE Computer Society Press, Los Alamitos CA
- Clarke K (2004) Mobile mapping and geographic information systems. *Cartogr Geogr Info Sci* 31(3):131–136

- DeCapua C (2007) Applications of geospatial technology in international disasters and during Hurricane Katrina. Mississippi State University Coastal Research. http://www.gri.msstate.edu/research/katrinalessons/Documents/GeoSp_Tech_Applications.pdf. Accessed 4 Nov 2008
- GAO (1996) Disaster assistance: improvements needed in determining eligibility for public assistance. Testimony before the subcommittee on VA, HUD and independent agencies, committee on appropriations, U.S. Senate, GAO/T-RCED, pp 96–166
- Goodchild MF, Glennon JA (2010) Crowdsourcing geographic information for disaster response: a research frontier. *Int J Digit Earth* 3(3):231–241
- Hodgson ME, Battersby SE, Davis BA, Liu S, Sulewski L (2013) Geospatial data collection/use in disaster response: a united states nationwide survey of state agencies. In: Buchroithner MF, Pritchel N, Burghardt D (eds) *Cartography from pole to pole*. Springer-Verlag, Berlin, pp 407–419
- Merchant RM, Elmer S, Lurie N (2011) Integrating social media into emergency-preparedness efforts. *New Eng J Med* 365(4):289–290
- NOAA Coastal Services Center (2001) *Lessons Learned Regarding the Use of Spatial Data and Geographic Information Systems (GIS) during Hurricane Floyd*. U.S. National Oceanic and Atmospheric Administration, NOAA/CSC/20119-PUB. NOAA Coastal Service Center: Charleston
- Tiede D, Lang S, Fureder P, Holbling D, Hoffmann C, Zeil P (2011) Automated damage indication for rapid geospatial reporting. *Photogramm Eng Remote Sens* 77(9):933–942

Part II Programs

The International Charter ‘Space and Major Disasters’

Brenda K. Jones, Timothy S. Stryker, Ahmed Mahmood
and Gabriel R. Platzeck

Abstract

Responding to catastrophic natural disasters requires critical information. When lives and everyday activities are interrupted by crises such as earthquakes, landslides, volcanoes, hurricanes, and floods, timely satellite imagery and aerial photographs become invaluable tools in revealing post-disaster conditions and in aiding disaster response and recovery efforts. An international group of satellite data providers manages a cooperative program to provide emergency response satellite data to communities affected by major natural and anthropogenic disasters. The International Charter ‘Space and Major Disasters’ (“Charter”) draws on the capabilities and resources of fifteen space agencies and a number of cooperators to quickly provide imagery and supplemental information for relief efforts in response to major disasters. Repeatedly, the Charter and its resources have provided valuable assets in assisting with global disaster recovery activities.

B. K. Jones (✉)

Earth Resources Observation and Science Center, U.S. Geological Survey (USGS),
47914 252nd Street, Sioux Falls, SD 57198, USA
e-mail: bkjones@usgs.gov

T. S. Stryker

U.S. Geological Survey (USGS), 12201 Sunrise Valley Drive, Reston, VA 20192, USA
e-mail: tstryker@usgs.gov

A. Mahmood

Canadian Space Agency (CSA), 6767 Route de l’Aéroport, Saint-Hubert, QC J3Y 8Y9, Canada
e-mail: Ahmed.mahmood@asc-csa.gc.ca

G. R. Platzeck

INVAP S.E., Av. Colón 4050, Ciudad de Córdoba, Pcia. de Córdoba, Argentina (X5003DDY)
e-mail: gplatzeck@invap.com.ar

Keywords

International charter · Disaster response · Emergency response · Remote sensing

1 Introduction

When a disaster strikes, government agencies and relief organizations immediately begin to provide aid and make basic services available. These organizations require vital information that may not be readily available in order to assess public needs, such as the location of the most highly impacted populations. Remotely sensed satellite imagery can assist in providing critical information to the responding agencies, but it must be easily accessible and provided in a timely fashion.

The International Charter ‘Space and Major Disasters’ is an international, multi-agency consortium that provides satellite-derived disaster response imagery to any country that requires assistance, at no cost to the requestor. The provision of imagery is for response activities only. While distribution of imagery may be limited to select organizations, derived information products (e.g., damage assessment maps) may be shared among all responding agencies. In this chapter, the Charter’s history and operational policies will be presented, along with recent examples of Charter activations. We will describe activations that were completed in a timely fashion and others that were not, to demonstrate the importance of timely data delivery.

1.1 International Charter History

Many countries utilize satellites and conduct observations of the Earth’s surface for various applications. Additionally, the growing numbers of military and commercial systems have been increasingly important for supplementing data provided by civilian systems. Additional information is available via advanced aerial cameras, radio detection and ranging (RaDAR), light detection and ranging (LiDAR), and topographic measuring sensors. A major challenge to providing useful data and information for disaster response rests with the sheer abundance of observations collected by all of these Earth observation systems.

Magnifying the data volume problem is the importance of rapid analysis during emergency situations when quick response and rapid distribution of the information can save lives. The use of geospatial data during emergency response operations is distinct from the use of geospatial data in routine environmental operations (Brunner 2009). Hence, there is an immediate need to apply specialized skills to the event when disaster strikes. To deal with this issue, organizations have established groups to provide this kind of targeted response.

It has been documented that using a multi-sensor, multi-platform approach to remote sensing can provide the most comprehensive coverage of an event (Joyce 2009). To that purpose, the Charter organization, an international agreement among space and remote sensing agency members, provides multi-sensor, multi-platform space-based data and information to support relief efforts in the event of emergencies

Charter Members



Fig. 1 Current Charter member agencies

caused by natural and anthropogenic disasters. The data provided through the Charter are made available at no charge to the users for their use in the response effort. The Charter is an integrated earth observing system that maximizes data availability, providing first responders with timely access to satellite imagery for disaster monitoring and impact assessments. (Gitas 2008).

The Charter was conceived in connection with the third United Nations (UN) space conference, UNISPACE III, held in Vienna in July 1999. In the face of increasing destruction and damage to life and property caused by natural disasters and conscious of the benefits that space technologies can bring to rescue and relief efforts, the European Space Agency (ESA) and the French Centre National d’Études Spatiales (CNES) set out to establish the text of the Charter, which they themselves signed on 20 June 2000, while inviting other space agencies to do the same (Bessis et al. 2003). The Canadian Space Agency (CSA) was the first to come onboard and sign the Charter on 19 October 2000¹. These three founding space agencies then went on to establish the Charter’s implementing architecture. (Mahmood 2008).

The Charter membership (Fig. 1) grew accordingly:

- The U.S. National Oceanic and Atmospheric Administration (NOAA), and the Indian Space Research Organization (ISRO) became members in September 2001.

¹ International Charter Space and Major Disasters. June 6, 2013 http://www.disasterscharter.org/news?p_p_id=NiPortlet_WAR_DisasterCharter&p_p_lifecycle=0&p_p_state=normal&p_p_mode=view&p_p_col_id=column-1&p_p_col_count=1&_NiPortlet_WAR_DisasterCharter_articleId=NEWS-ITEM-20001020

- The Argentinian Comisión Nacional de Actividades Espaciales (CONAE) joined in July 2003.
- In 2005, the Japanese Aerospace Exploration Agency (JAXA) joined in February, the U.S. Geological Survey (USGS) joined in April as part of the U.S. membership, and the British National Space Centre/Disaster Monitoring Constellation (BNSC/DMCii) joined in November.
- The China National Space Administration (CNSA) joined in May 2007.
- The German Aerospace Center (DLR) joined in October 2010.
- The Korea Aerospace Research Institute (KARI) and the Brazilian Instituto Nacional de Pesquisas Espaciais (INPE) joined in 2011.
- The European Organisation for the Exploitation of Meteorological Satellites (EUMETSAT) joined in July 2012.
- Membership application of the Russian Federal Space Agency (ROSCOSMOS) was accepted in September 2010, and the formalities for Charter signature were completed in April 2013.

The Charter is governed by two entities, the Board and the Executive Secretariat. Both groups have a representative from all member agencies, with the Board being responsible for acceptance of new members, interaction with other international organizations, and other policy topics. The Executive Secretariat is responsible for the Charter's daily operations and related technical and administrative functions.

As part of its programmatic responsibilities, the Board has recently considered options for the Charter's further evolution. In 2012, the Board agreed to the implementation of Universal Access. Universal Access will allow any national disaster management authority to submit requests for emergency response support to the Charter. Proper procedures will have to be followed, but the affected country will not have to be a Charter member. This policy will benefit national users in countries beyond those of the Charter members, who were previously unable to make direct requests to the Charter during emergency situations.

2 International Charter Operations

There are four functional units that compose the operational response loop for a Charter activation (Fig. 2). The units are the Authorized User who requests the activation, the On-Duty Operator who is available 24 × 7 to receive the request, the Emergency On-Call Officer who begins the immediate tasking of satellite resources, and the Project Manager who manages the provision of data for the entire activation, ensuring that the value added provider generates the informational products that are required by the end-user to support their response efforts.

A Charter activation is requested by an Authorized User (AU). With the implementation of Universal Access, all countries have the opportunity to have their own AU. If they do not have a national AU, an AU from another country may submit the activation request on that nation's behalf. The activation request includes the type of event and the geographic location, including any information that will assist in the

Charter Operational Loop

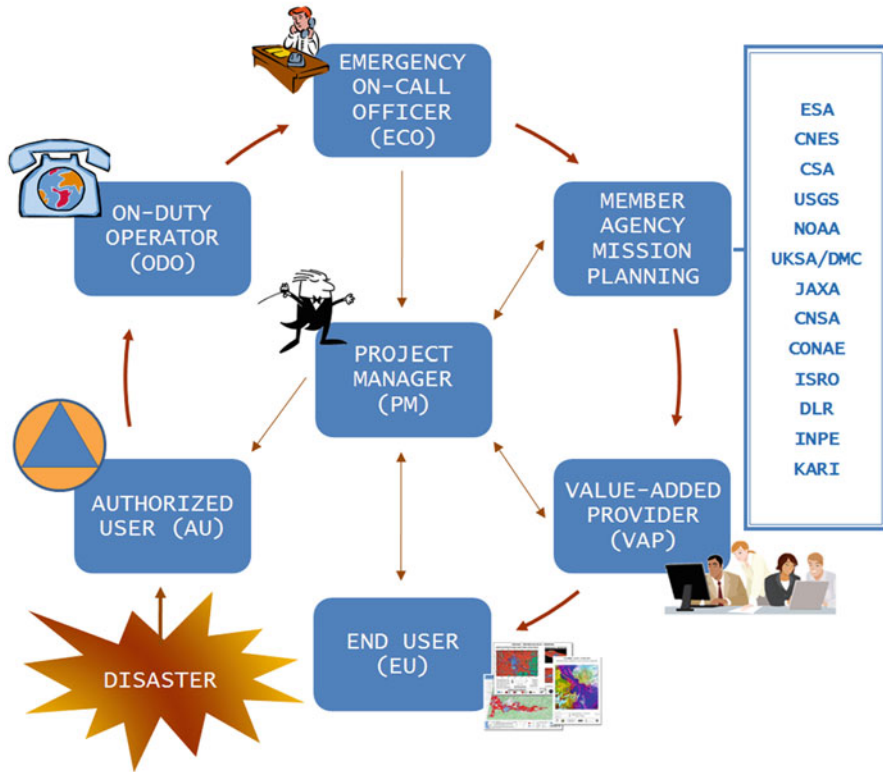


Fig. 2 Charter operational loop

tasking of appropriate sensors. The request is sent to the On-Duty Operator (ODO) in Frascati, Italy. The ODO position is permanently staffed at ESA, 24 × 7, 365 days a year. The ODO verifies that the requestor has the proper privileges to request an activation, logs the call, and proceeds to notify the Executive Secretariat members and the Emergency On-Call Officer (ECO).

The ECO is also available 24 × 7 and is responsible for immediate tasking of the appropriate satellites in response to the request for support. This is the level of operations that highlights the unified system that is in place among all of the member agencies. The ECO has 3 h from the time of notification to begin tasking satellites and coordinating with the mission planning staff of all the agencies that will be supplying data for the event. The initial tasking request is based on the information the ECO has about the satellite resources/sensors of the participating agencies and the type of event. The ECO sends these requests to the individual agencies and receives responses from the agencies in regards to the availability and appropriateness of the

Table 1 Chart showing type of Charter events by year from November 2000 to August 2014

		2000	2001	2002	2003	2004	2005	2006	2007	2008	2009	2010	2011	2012	2013	2014	Sub-totals
Solid Earth	Earthquake		3	1	3	5	3	2	5	4	3	5	5	3	4	1	47
	Landslide	1	1	2	2			1			4	2	2		1	2	18
	Volcano		1	1	2	2	1	1	2	3	3	2	2	1	3	2	26
Weather / Atmospheric	Storm/Hurricane**			1	2	3	6	1	8	8	7	11	2	9	6	3	67
	Ice/Snow hazard								1			1	1			1	4
	Flood/Ocean wave*		3	8	4	9	13	16	22	23	19	25	16	25	21	16	220
	Fire				5	1	2		4	2	4	1	3	2	2	3	29
Technological	Oil spill		3	2				4	3			1	1				14
	Others					1						3			1	1	6
Total / year		1	11	15	18	21	25	25	45	40	40	51	32	40	38	29	
TOTAL																	431

*includes solid earth related phenomenon of a tsunami
 **includes all wind type storms (hurricane, cyclone, typhoon and tornado)

these resources/sensors. The final satellite tasking choice is recommended by each agency for their respective resources/sensors. When the ECO has completed the initial tasking requests, created a dossier containing a history of the actions, and the resulting requested satellite collections, the ECO passes that information on to the Project Manager (PM).

Unlike the ODO and ECO, the PM is available only during normal local work hours. The PM is nominated by the Executive Secretariat based on geographic location of the disaster, disaster type, sensors needed to provide data, and the potential PMs that are available at the time of the disaster. Once appointed, the PM is responsible for coordinating the flow of imagery from the member agencies to the end user or value-added providers, reviewing requirements with the end user to ensure the appropriate collections are scheduled, and ensuring that the end user receives the data and/or products required to assist in the response operations. The following timelines are normally followed: in order for an activation to be accepted, a Charter activation request should be received within 10 days following the disaster event. The data acquisition planning is carried out for 15 days following the date of activation. The data/product deliveries are completed within 30 days of the activation date, when the activation is deemed closed. The PM submits a written report with user feedback to the Executive Secretariat within 45 days of the activation date.

In response to major disasters, the Charter has been activated 431 times between November 2000 and August 2014. The following chart shows the types of events by year (Table 1).

As shown in the figure on next page (Fig. 3), since 2004, most disasters covered by the Charter were caused by flooding. The other two principal hazards are storm/hurricanes and earthquakes. Activations for ice/snow hazards, technological hazards (e.g. oil spills, other) landslides and volcanic eruptions were relatively rare (around 18 % in total).

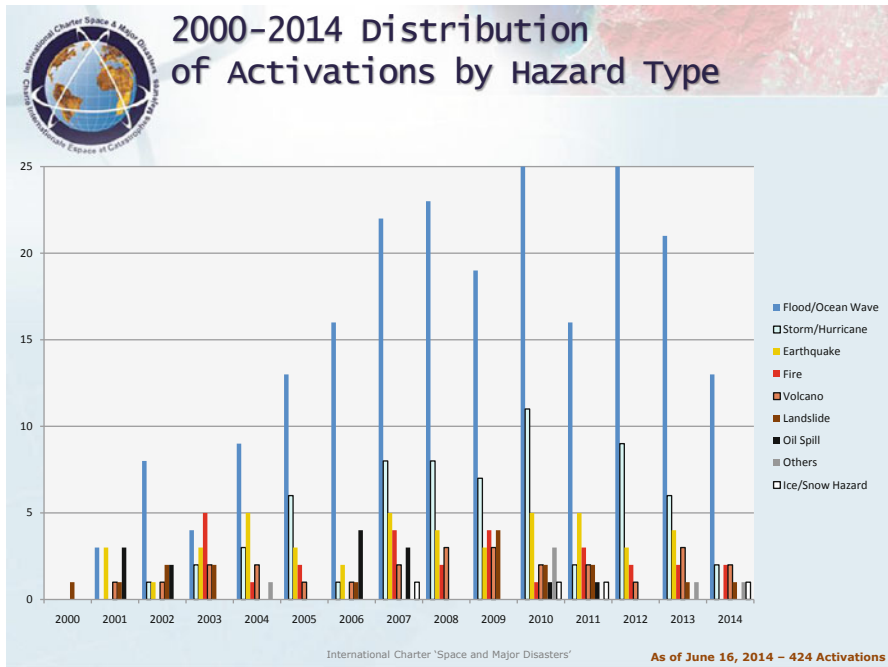


Fig. 3 2001–2013 Distribution of activations by hazard type

3 Activation Results

There are many factors that can affect the timeliness of data and product delivery, which in turn can affect the usefulness of the products in the actual response effort. For example, in September 2002, heavy rains caused flooding over the Gard department in the southeast of France. The water levels of the Gard, Gardon, and Vidourles Rivers rose quickly and the area was flooded. The Charter was activated the next day. On the day the Charter was activated, the SPOT 4 satellite was re-tasked to collect information on the flood event. The image was captured and the first products were made available within 38 h of the activation (Fig. 3). The re-tasking of the satellite and image interpretation and map production by the French value-added provider SERTIT were all very timely. However, the map product could not be fully utilized because the end user staff was unfamiliar with the satellite image-based map including the annotations, scale, projection, colour scheme, etc. (Fig. 4).

On December 26, 2004, an earthquake and resulting tsunami of great magnitude hit the countries bordering the Indian Ocean. The following day, the Charter was activated by the United Nations Institute of Training and Research’s Operational Satellite Applications Programme (UNOSAT), on behalf of the UN Office for the Coordination of Humanitarian Affairs (OCHA) and World Food Programme (WFP). The first information products were generated the same day and included base maps



Cartographie rapide des inondations dans le Gard le 10 septembre 2002

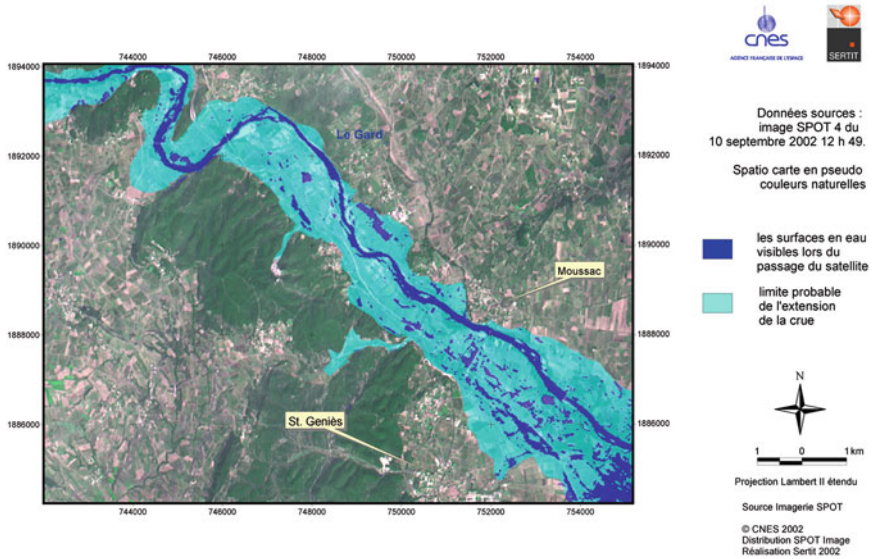


Fig. 4 Map showing the Gard river flooding in September 2002

made from Landsat 7 imagery and population maps. Same-day images of the tsunami showed the devastation that had been caused by the disaster (Fig. 5). Satellite collections that occur on the actual day of an unanticipated event, such as the Indian Ocean earthquake and tsunami, are generally a matter of luck rather than planning as it can often take at least several hours or days to task a satellite and have it in the proper orbit cycle for a collection.

On May 2, 2008, authorities evacuated hundreds of people from villages in southern Chile after a snowcapped volcano, considered dormant for thousands of years, erupted. The blast sent minor earthquakes rippling through the region. Ash from the eruption polluted water supplies and contaminated the air, prompting officials to hand out protective masks. Winds also carried ash over the Andes Mountains to neighboring Argentina. Based on a request from Chilean authorities, the Charter was activated on May 2 by the Argentinean AU.

To help track the dynamic geographic coverage of the ash, the Charter contributed several animated files produced from GOES-10 (NOAA) images, which are acquired every 15 min. The period of time covered by each resulting animation ranged from 6 to 12 h. There was a high demand for these animations, which were requested by sanitary teams in the field, as well as by the Civil Protection agencies in Argentina and Chile.

Following images are two snapshots taken randomly from one of the videos (Fig. 6). These images demonstrate the usefulness of real-time satellite data acquisitions.

Trinkat, Nicobar islands

Tsunami, 26 December 2004

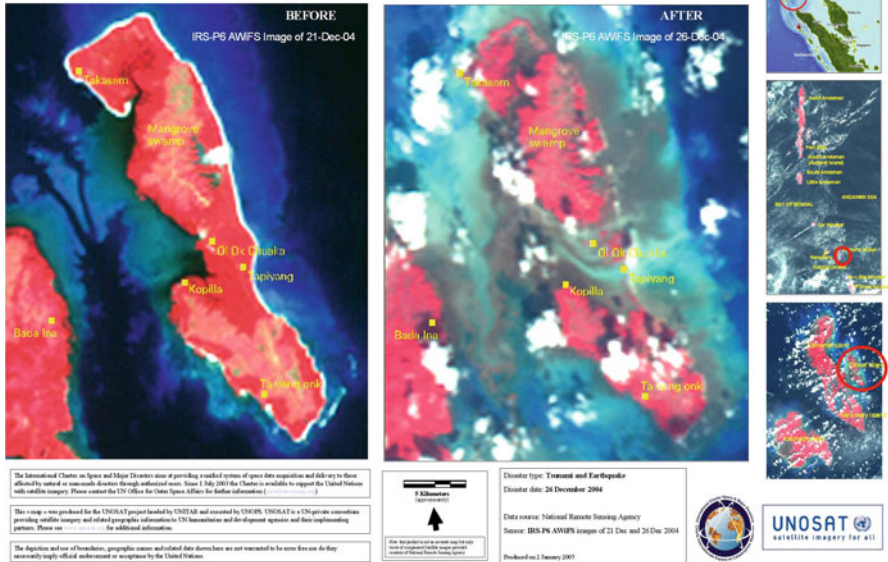
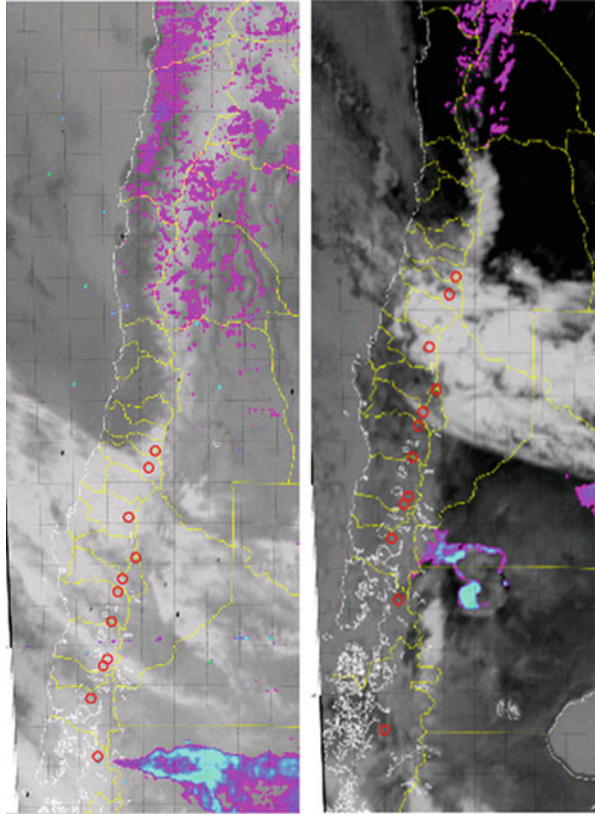


Fig. 5 Map showing pre- and post-event imagery of Trinkat Island, India. The post-event imagery was collected the day the tsunami struck. The image is rotated so north is up. (Copyright NRSC (2004))

Hurricane Gustav made landfall in the State of Louisiana on September 1, 2008, and the Charter was activated the next day. Even though participating space agencies anticipated the storm's landfall and the Charter was activated in a timely fashion, the first planned collections were biased towards the city of New Orleans, which in previous years had experienced severe storm-related flooding, rather than toward the inland areas that suffered the greatest impact due to high winds. The impact of the hurricane damaged the infrastructure and produced sustained electrical outages, which impeded communications between the PM and the end user about requirements and products, and delivery of products to responders in the field. Because satellite tasking cannot be instantaneous, there were also missed opportunities for collections of the inland impact area that could have been very useful. This example demonstrates that even with timely activation of the Charter, changing circumstances can affect the timeliness of acquisitions and delivery.

In July 2007, the Charter was activated for Hurricane Daman, predicted to make landfall on Vanua Levu, the second largest island of Fiji with a population of 130,000. Shortly before reaching the island, the storm shifted eastward and made a direct hit on the small island of Cikobia with 67 inhabitants. Although the Charter area of interest initially was the island of Vanua Levu, it had to be modified after the activation had started, to include the island of Cikobia. By the time the PM was nominated over the

Fig. 6 The ash can be identified on the *lower* part of each image as a magenta irregular shape, departing from a *red* circle that identifies the geographical position of the Chaitén Volcano. The images are rotated so north is up. (Image data courtesy of NOAA)



weekend, a scene had been captured and delivered, but the data were not used as the location of impact had changed and there was minimal damage to the island where the hurricane landfall actually occurred. This example also illustrates how changing circumstances can affect the results of satellite planning and tasking.

4 Conclusions

The applications of remotely sensed imagery for emergency response have varying degrees of success, dependent upon conditions that may or may not be within the control of the space agency responsible for satellite operations and observations. Success can depend on satellite location, amount of time needed to program a satellite, daily work schedules of personnel involved in the tasking process, and the amount of warning before an event occurs. The conditions may either allow for capturing an event at its peak, or can force a wait of several days before the images are available.

The Charter is addressing some new challenges as more user based communities become aware of the Charter and the services it offers. Many organizations outside of the immediate response community are beginning to look to the Charter for supplying their pre and post event imagery needs. The licensing restrictions that are in place for much of the data do not allow for easy, unrestricted data and product sharing. These requirements are being reviewed and addressed by each agency in regards to its own data distribution policy.

The Charter is also becoming more involved with other disaster response initiatives and programs. There is an increased need for improved communications in regards to support being provided for events, as more initiatives begin to provide products and services for disaster response. As an example, the Charter has a formal agreement with Sentinel Asia that allows the Asia Disaster Reduction Center to elevate its disaster response support calls to the Charter when more resources are needed for a successful response.

In conclusion, the Charter actively monitors its role in the response community and works to model an evolution process that will keep pace with the changing requirements and user base involved in disaster response.

Acknowledgments The authors would like to thank all member agencies of the International Charter 'Space and Major Disasters' for their contributions to the Charter and allowing access to the Charter materials used in this publication. Special thanks go to Amy McGuire, Satellite Data Services Specialist, Canadian Space Agency, for her assistance in providing edits and illustrations.

References

- Bessis J-L, Bequignon J, Mahmood A (2003) The international charter 'Space and Major Disasters' initiative. *Acta Astronaut* 54:183–190
- Brunner D, Lemoine G, Thoorens F-X, Bruzzone L (2009) Distributed geospatial data processing functionality to support collaborative and rapid emergency response. *IEEE J Sel Top Appl Earth Obs Remote Sens* 2(1):33–45
- Gitas I (2008) Contribution of remote sensing to disaster management activities: a case study of the large fires in the Peloponnese, Greece. *Int J Remote Sens* 29(6):1847–1853
- Joyce K, Belliss SE, Samsonov SV, McNeill SJ, Glassey PJ (2009) A review of the status of satellite remote sensing and image processing techniques for mapping natural hazards and disasters. *Prog Phys Geogr* 33(2):183–207
- Mahmood A, Shokr M (2008) Space measurements for disaster response: the international charter. In: Gad-el-Hak M (ed) *Large-Scale disasters prediction, control and mitigation*. Cambridge University Press, New York, pp 453–541

The Federal Oil Spill Team for Emergency Response Remote Sensing, FOSTERRS: Enabling Remote Sensing Technology for Marine Disaster Response

Ira Leifer, John Murray, Davida Streett, Timothy Stough, Ellen Ramirez and Sonia Gallegos

Abstract

Oil spills cause significant to devastating ecological, economic, and societal damage, requiring years to decades for recovery. In cases of floods such as those associated with Hurricane Katrina, both oil and marine debris can enter the ocean, with debris posing its own hazards and ecological damage. In other cases, massive debris introduction can occur from natural causes such as the great Japanese tsunami in 2011.

These disasters demand the best available technology for response, damage mitigation, and remediation efforts. Disaster response remote sensing can play an important role by greatly leveraging available resources and assets and in

I. Leifer (✉)

Bubbleology Research International, Solvang, CA 93463, USA

Tel.: +1 (805) 683-3333

e-mail: ira.leifer@bubbleology.com

University of California, Santa Barbara, CA 93106, USA

J. Murray

National Aeronautic and Space Agency, Langley Research Center,

NASA, LRC, Hampton, VA 23681, USA

D. Streett · E. Ramirez

National Oceanic and Atmospheric Administration, National Environmental Satellite, Data, and Information Service, NOAA, NESDIS, College Park, MD 20740, USA

T. Stough

Jet Propulsion Laboratory, JPL, Pasadena, CA 91109, USA

S. Gallegos

Naval Research Laboratory, NRL, Stennis Space Center, Hancock County, MS 39529, USA

mitigating consequences, as demonstrated during the Deepwater Horizon (DWH) oil spill in the Gulf of Mexico. The extent and persistence of DWH overwhelmed traditional airborne observers, ability to monitor the spill's development, with rapid response remote sensing filling critical response needs such as providing synoptic information on the spill. Still, incorporation of many remote sensing technologies faced significant challenges during the oil spill response.

To facilitate the sharing of remote sensing capabilities and to discuss improvements in disaster response, the Federal Oil Spill Team for Emergency Response Remote Sensing (FOSTERRS) interagency working group was created. Specifically FOSTERRS seeks to connect agency information on airborne and space borne asset's availability, limitations, capabilities and performance, and ancillary data needs to stake holders and responders. FOSTERRS comprises members from agencies with remote sensing assets and key end users, while outreaching to the larger community involved in marine disaster response and the development and implementation of remote sensing best practices.

Keywords

FOSTERRS · Oil spill response · Deepwater horizon

1 Introduction

1.1 Disaster Remote Sensing

There are a wide range of natural and anthropogenic disasters that have the potential to cause ecological, economic, health, and societal damage. Some natural disasters in which remote sensing is indispensable includes earthquakes tsunamis, tropical cyclones, severe weather, and wildfires. For a range of reasons, the most common anthropogenic disasters are related to oil; however, marine debris and industrial accidents can create significant problems. Recovering from these disasters can require years, decades, or longer. Responding to these disasters demands the best available technology for response, damage mitigation, and remediation efforts. When the scale of an unfolding disaster expands beyond the limits of human vision, remote sensing plays an increasingly important role.

Ongoing technological developments in remote sensing open new approaches and capabilities to responders. Critical challenges to new remote sensing technology acceptance for operational use lie in the responders' ability to use the output of the technology easily, quickly, and with confidence. These challenges require the rapid tasking of appropriate assets, delivery of useful data products in a timely manner to responders, and demonstration and validation of the data products. Note, useful product in an operational environment requires matching end-user needs so that specialized training for interpretation is not needed and preferably not using specialized software. In this regard, emergency response remote sensing is very different from academic remote sensing where time is not the driving constraint. In contrast, rapid

response remote sensing must emphasize speed and necessarily, accuracy while operating under the pressure cooker like situation that arises in the intense political media environment of a major disaster (Albaigés et al. 2006; Leifer et al. 2012). Unsurprisingly, marine disasters are more complex than terrestrial disasters due to the sea surface being a mobile interface with characteristics determined by ever-changing winds, waves, and currents. Further challenges arise from working at sea. When the disaster involves oil, additional complexities arise from its evolving physical and chemical properties—termed weathering—as it is advected on the ocean air-sea interface—affecting momentum and mass transfer between these two fluid bodies.

Remote sensing has tantalizing potential to improve greatly oil spill identification and mitigation (Fingas and Brown 1997). Remote sensing can survey areas that are vast and inaccessible and provide repeatable standardized data for interpretation, including automated space-based detection of spills that have not yet been reported. These benefits have justified resources for oil spill response remote sensing spanning more than half a century. Nearly two decades ago, Fingas and Brown (1997) concluded that its utility was limited and its potential was only partially tapped. Reviewing remote sensing during the Deepwater Horizon oil spill, Leifer et al. (2012) found this remains true today. In part this is because remote sensing can suffer from false positives and false negatives (Leifer et al. 2012). As a result, the automatic detection algorithms that have been developed, primarily for Synthetic Aperture Radar (SAR) data, suffer significant false positives unless multiple ancillary data are incorporated into the analysis (Espedal 1999).

1.2 Deepwater Horizon Oil Spill and Remote Sensing

The Deepwater Horizon oil spill was the largest accidental spill in modern history, releasing an estimated upper limit of 1.3×10^9 L oil and gas-oil equivalent (Joye et al. 2011). In addition, it also was exceptional in several other aspects, including its duration on the order of 100 days, release depth of 1300 m (Lehr et al. 2010), and maximum extent of tens of thousands of square kilometers (Fig. 1). Specifically, a typical oil spill releases fresh oil for a few days, after which the spilled oil ages—termed weathering, changing chemically and physically under the influence of winds, currents, waves, and sunlight (Reed et al. 1999). Given the time constraints of the duration of a typical oil spill, particularly those sensitive to unweathered oil, there are enormous challenges to mobilization in a sufficiently timely manner to demonstrate new remote sensing technologies. These challenges are logistical (including securing funding), bureaucratic (permission to operate in the area), and technical. In fact, the magnitude of these hurdles is a strong disincentive to trying. Thus, the persistence of emissions during the Deepwater Horizon oil spill provided ample mobilization time, enabling the application, demonstration, and development of a range of disaster remote sensing technologies.

Satellite assets are immediately available upon activation of the International Charter on Space and Major Disasters' ("Charter") Agreement, which requires all

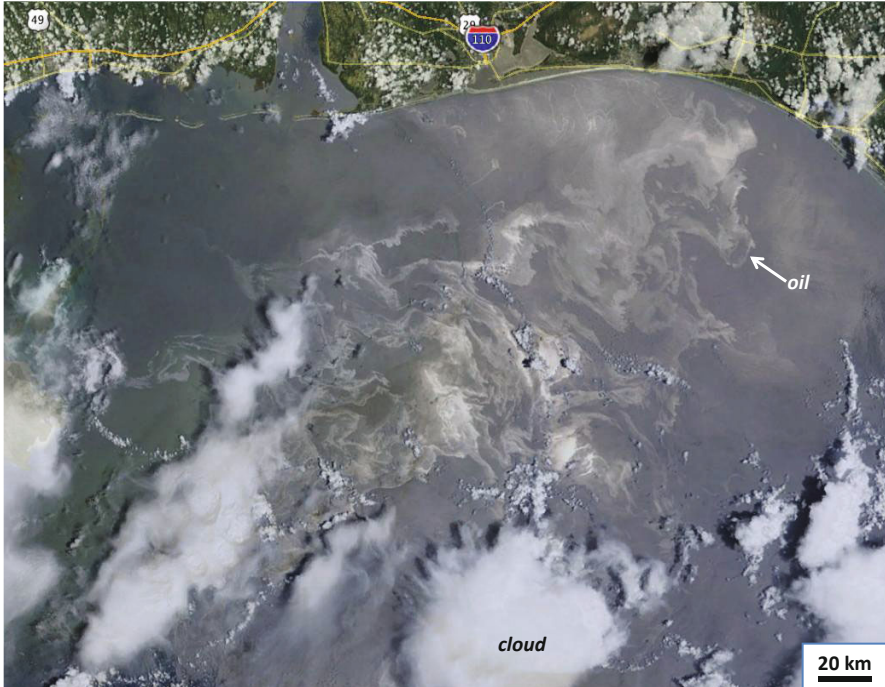


Fig. 1 MODIS Aqua image 11 June 2010, Gulf of Mexico (modis-today 2010). Most oil spills never cover such an extensive area, but remote sensing can be of critical benefit to both small and large oil spills. Size scale on figure.

participating countries and organizations to make available their space assets during events such as major oil spills (www.disasterscharter.org 2000). Through the Charter as well as open satellite instruments, extensive multispectral, high spatial resolution monochrome and moderate spectral-resolution, multispectral visible, thermal infrared SAR, and LIDAR (Light Detection and Ranging), data were available during oil spills (Leifer et al., 2012). However, the Charter is geared towards shorter events. Thus in the case of the Deepwater Horizon oil spill, the flow of new imagery was reduced after about 60 days (Bill Pichel, NOAA, Personal Communication 2014). Furthermore, in some cases, only lower-quality or lower-precision (i.e., 8-bit versus 16-bit) versions of higher quality, native products were available. Low quality satellite data can challenge analysis algorithms, reducing accuracy. As a result, modification of the Charter should be considered so that in the event of long-lived oil spills, agreements are in place to assure continued access to satellite data products. Furthermore Charter modifications should be considered that require providing the highest quality data.

Beyond space-based remote sensing data, airborne surface data can play an important role and have several advantages. Shortwave infrared hyperspectral and thermal infrared hyperspectral airborne data were collected during the Deepwater Horizon Oil Spill with the AVIRIS (Airborne Visual InfraRed Imaging Spectrometer) and

SEBASS (Spatially Enhanced Broadband Array Spectrograph) instruments, respectively, by the Jet Propulsion Laboratory, and Aerospace Corporation, respectively. Multispectral imagers, lidar, and SAR collected additional airborne data (Leifer et al. 2012). Several of these data were provided to the joint incident command during the spill.

Despite the wide diversity of remote sensing data that was collected during the Deepwater Horizon oil spill, only a subset was actually used operationally. As a result, the primary remote sensing lesson from the Deepwater Horizon spill, is that acceptance of new technology (i.e., incorporation into operational use, even in the presence of urgent needs—e.g., Fig. 1)—faces hurdles that range from challenging to impossible to surpass during an emergency (Bill Lehr, NOAA ORR, Personal Communication 2014). In fact, the appropriate time for incorporation of new technologies into response activities is during the interim calm period between major oil spills (Leifer et al. 2012). Another important consideration is that during the Deepwater Horizon oil spill, many remote sensing assets were tasked and the resultant data contributed significantly to the response; however, only a few agencies (e.g., NOAA) are mandated (and have budgets) for disaster response remote sensing. This can render contributions from some agencies difficult to maintain for long. Addressing this issue by developing a formal mechanism for wider, but manageable, participation would be beneficial.

In response, the Federal Oil Spill Team for Emergency Response Remote Sensing (FOSTERRS) interagency working group was created to facilitate collaboration and exchange of information on marine emergency response remote sensing. Ultimately, the goal of FOSTERRS is to improve the quality of disaster response information for stakeholders, leading to improved mitigation of the impacts of marine disasters.

1.3 Oil Spill Response Needs and Remote Sensing

The first information on an oil spill's location and extent typically arrives from a few, often-conflicting observations, commonly from airborne observers. These observations can suffer from confusion, in part, because first observations are frequently obtained from untrained individuals, although remote sensing is increasingly providing initial information. Importantly, both can yield false negatives and positives (Fingas and Brown 1997). Airborne observations are critical because of the overview perspective they have, whereas a nearby oil slick can be hidden from boat observers behind waves. Still, from the air, although many natural patterns mimic oil slicks (Leifer et al. 2012), airborne observers can cover far larger areas in a search.

These incoming data of uncertain quality can "obscure" from the responders the oil spill's true location and size (HAZMAT 1996); however, initial response decisions and resource allocation must be made based on the information that is available at the time.

Oil spill response remote sensing, and indeed general disaster remote sensing, must address a number of key questions in a timely manner, complementing the tradi-

tional “remote sensing” by “experienced eyes” on an airplane; however, experienced observers can require time to arrive at the potential spill location due to logistical considerations. Currently, experienced airborne observers are the preferred approach, where spatial patterns and appearance of oil slicks provide the information critical to identify false positives and thick oil. However, logistics and a shortage of trained personnel have strongly motivated the development of remote sensing approaches, both active and passive. Most passive approaches use reflected solar radiation or thermal emissions; active approaches use radar (SAR) or laser (lidar). Radar is all-weather, 24/7 technology, but requires winds to be in a range. Passive thermal and active laser can collect data underneath cloudy skies (for airplanes), while passive visible requires clear sunny skies (Leifer et al. 2012).

1.4 Oil Spill Remote Sensing Acceptance

First and foremost, for remote sensing to be used for oil spill response it must provide detection with few false positives for acceptance—mobilizing aircraft and observers is expensive, and false alarms are well known to contribute to complacency. In addition, remote sensing should enable an estimate of the spill’s magnitude so that the appropriate level of response assets can be tasked, preferably to more highly impacted areas or more ecologically sensitive areas. An example of this could involve discriminating thick from thin oil, to allocate resources to areas with thicker oil (Svejkovsky et al. 2012). Furthermore, remote sensing can address a number of other oil spill disaster response aspects from monitoring/ guiding mitigation strategies to ecosystem mapping to better triage response options. Even though remote sensing may be the only approach available to provide critical response information, it generally has not been incorporated into oil spill response for reasons discussed below. This reflects the reality that there are significant hurdles to acceptance above and beyond the technological readiness scale, discussed below in Sect. 3, and the more comprehensive operational readiness scale (Sauser et al. 2006).

Specifically, a new oil spill response technology must provide greater reliability than existing approaches, or lower the risk of failing to contribute to the efficacy of the oil spill response, again compared to existing and accepted approaches. Thus, technology acceptance requires a combination of demonstration, need, motivation, and clearly achievable goals. In addition, for remote sensing to be considered by responders, they must know about the existence and utility of remote sensing data products, and how to access them in a timely manner.

1.5 Deepwater Horizon Wakeup Call

Many applications of a wide range of remote sensing technologies have been demonstrated for oil spills over the years (Leifer et al. 2012). As noted, the greatest need is to identify thick oil to allocate resources best. These oil spill remote sensing approaches (passive and active) can discriminate to some extent between greater (thick)

and lesser (thin) oil sheens, albeit with differing confidence and a different understanding of what thick oil and thin oil means from a sensor and from an algorithm point-of-view. In contrast, from a responder point of view, thick oil has a practical definition—oil that is actionable, i.e., thick enough for effective use of mitigation strategies like oil booms and skimmers.

Currently, only hyperspectral imaging spectroscopy has demonstrated a quantitative capability to map oil volume by using unique diagnostic spectral features. These spectral features are diagnostic because only hydrocarbons exhibit these spectral features (Clark et al. 2010; Leifer et al. 2012). The use of hyperspectral imaging spectroscopy was developed during the Deepwater Horizon oil spill using data from AVIRIS (Airborne Visual Infrared Imaging Spectrometer). Deployment of AVIRIS is an example of development of a new remote sensing technology that was developed and demonstrated during the Deepwater Horizon oil spill (Clark et al. 2010; Leifer et al. 2012). Previously, there were indications that AVIRIS could remote sense oil in data collected during Hurricane Katrina (Greg Swayze, USGS, Personal Communication 2014), and in efforts to remote sensing methane (similar spectral features) for the Coal Oil Point seep field, offshore California where oil slicks are prevalent (Bradley et al. 2011). AVIRIS mobilization occurred exceedingly rapidly compared to normal missions that take months of planning, collecting its first data on May 6, approximately two weeks after the spill. AVIRIS flights then continued for an additional three weeks before critical maintenance required ending the first deployment, collecting more data in this period than in a normal year (Leifer et al. 2012). Unlike Deepwater Horizon, most oil spills release their oil in a few days, e.g., the Exxon Valdez, and after a few weeks, the remaining oil is heavily weathered (ASCE 1996)—chemically altered—without the key spectral features.

Other approaches, such as SAR long have been recognized as well-suited to identifying oil on water (Estes and Senger 1971–1973), with airborne SAR able to volumetrically analyze thick oil (Minchew et al. 2011) and current satellite SAR able to identify areas of thick oil (Garcia-Pineda et al. 2013). However, to reduce or eliminate false positives from analysis of SAR data, ancillary information often is needed (Espedal 1999; Fiscella et al. 2013). Fortunately, such ancillary information generally is available from other satellite data, ocean monitoring networks, or airborne and surface observers. For many years, SAR has been a part of advanced warning systems for oil spills integrated into the decision process for tasking airplanes and other survey assets to evaluate the need for a response (Topouzelis et al. 2007). During the Deepwater Horizon oil spill, satellite imagery from both SAR and MODIS (MODerate resolution Imaging SpectroRadiometer) played a key role in defining the extent of the oil spill (Leifer et al. 2012). MODIS is on the NASA Aqua and Terra satellites and has a daily revisit time with complete global mapping at 250-m resolution. Because, MODIS requires clear skies and clouds are common in the Gulf of Mexico, satellite SAR from a range of platforms provided important data.

There also are diagnostic thermal infrared (TIR) spectral features related to petroleum hydrocarbons (Byfield 1998). The only published example of the use of TIR spectral features for operational oil spill monitoring is by the EPA ASPECT

system (Shen and Lewis 2011). Instead, TIR remote sensing of oil has focused on sea surface temperature anomalies associated with thick oil (Salisbury et al. 1993); however, there are other causes of sea surface temperature anomalies that can result in false positives or negatives for oil slick detection (Leifer et al. 2012). Large thermal anomalies from thick oil are detectable by space-based (Tseng and Chiu 1994) and airborne sensors (Svejkovsky et al. 2012). The limitation of these systems to detect thick oil (thicker than 50–150 μm) was shown to relate to sensitivity; a sufficiently sensitive system showed TIR remote sensing of extremely thin oil slicks, to 1 μm (Grierson 1998). Airborne TIR remote sensing of oil by thermal anomaly detection has been used operationally to identify thick oil (Svejkovsky et al. 2012).

A novel remote sensing technology was demonstrated during the Deepwater Horizon oil spill using airborne and spaceborne lidar to observe submerged oil (Leifer et al. 2012); however, not on an operational basis. Further development of lidar oil spill remote sensing is needed to bring this capability into future oil spill response. In fact, although many remote sensing approaches were applied during the Deepwater Horizon oil spill, only some were used in an operational response mode (Leifer et al. 2012). For example, MODIS data were very useful for defining the spill extent when skies were clear and for sunglint viewing conditions, while satellite SAR provided important coverage when skies were cloudy.

Further development of these and other remote sensing technologies will continue to improve the quality of data products and provide more quantitative information on thickness to support future oil spill response. There also are operational improvements whose further development will improve the utility of remote sensing technologies. Specifically, new systems can incorporate realtime (or at least “time sensitive”) data analysis routines for processing during flight on manned or unmanned aircraft. Realtime data analysis can enable adaptive surveying. For example, AVIRIS Next Generation has a realtime data analysis capability that has been demonstrated for methane detection and could be modified for thick oil detection (Rob Green, Personal Communication, Jet Propulsion Laboratory 2014). Incorporation of unmanned aircraft (UAV) into future oil spill response could have benefits. UAV have longer dwell times than manned aircraft and can operate under poorer weather; however, there are concerns about multiple aircraft operations involving UAVs.

1.6 Marine Debris Remote Sensing

Marine debris is a large-scale problem threatening safe ship navigation, commercial and recreational fisheries, marine species, coastal habitat and other important ecosystems, as well as coastal economies. However, the scale of marine debris often precludes it being addressed effectively solely by ship and aircraft reconnaissance; yet operational response organizations lack the satellite-derived information and resources to mitigate this threat. Marine debris as a remote sensing issue ranges in complexity from large, dense debris fields (e.g., immediately following a tsunami) to ghost nets (lost fishing nets drifting in the ocean. Ghost nets entangle thousands of marine animals and debris). Post-tsunami or post-hurricane debris fields are easily

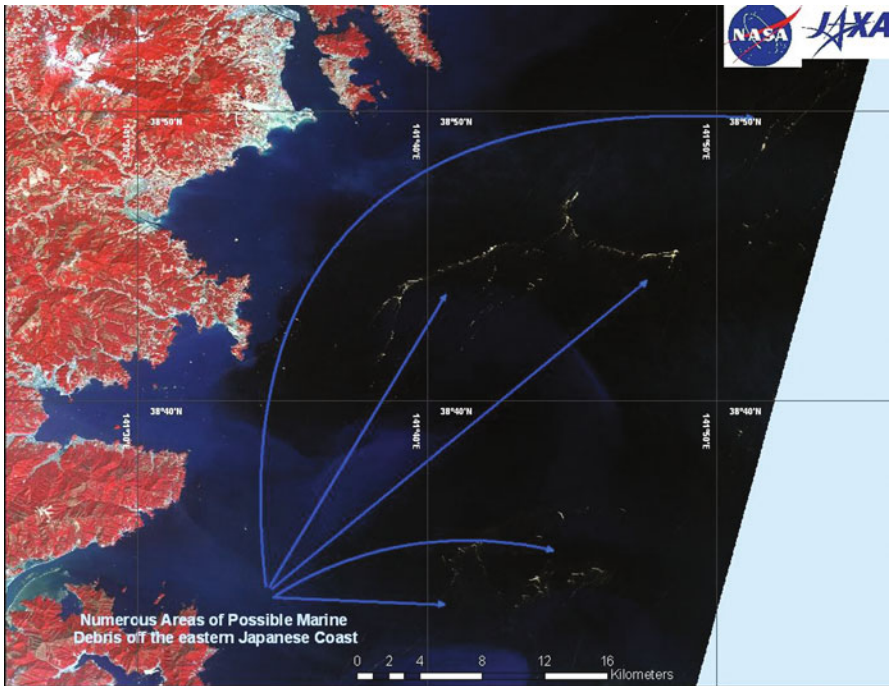


Fig. 2 Marine debris from the Tohoku Tsunami, offshore Japan. 15-m resolution image from the Advanced Spaceborne Thermal Emission and Reflection Radiometer (ASTER) on the Terra satellite from 14 March 2011 at 0119Z. Size scale on figure

detectable in satellite moderate resolution multispectral data, like ASTER (Fig. 2), or in SAR imagery, and can be used operationally. In contrast, ghost nets, which float near or even below the sea surface, will require the development of more sophisticated remote sensing techniques before they can be operationally addressed effectively.

2 FOSTERRS Mission and Team

Given the potential of remote sensing, there is a need to streamline remote sensing applications and data products between agencies maintaining assets and end users for marine disaster response. FOSTERRS is an interagency working group that was formed by the various elements of the disaster research and response community to facilitate an informed discussion to match oil spill response needs and remote sensing capabilities (See Fig. 3) by providing a readily accessible and informal forum for these discussions.

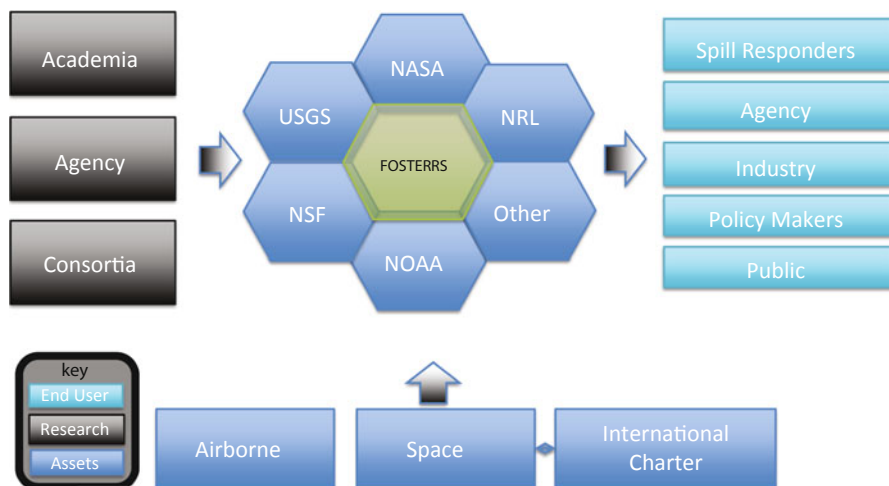


Fig. 3 FOSTERRS flowchart showing interactions and communication pathways between stakeholders

Specifically, FOSTERRS seeks to provide information on airborne and spaceborne asset availability, limitations, capabilities, and performance, to oil spill responders and other stakeholders.

To assimilate future remote sensing technologies into oil spill and other marine disaster response, the remote sensing information needs processing (manual, automated, or man-machine mix) and review with constant updating to aid decision making. Data products, including meta-data information, must be provided in a timely manner—i.e., before decisions must be made. In addition, data products need to meet responder needs in terms of utility and accessibility. FOSTERRS will expand interagency and academia dialogs through a range of communication approaches including teleconferences, workshops, conference special sessions, website, white papers, manuscripts, reports, etc.

Example FOSTERRS data products under development are shown in Table 1 and 2, listing space-based and airborne assets and their capabilities at the time of the Deepwater Horizon Oil Spill; however, some instruments, like SCIAMACHY and HICO, are no longer operational, while new assets have been and will be launched. Space assets have the ability to observe globally without need for mobilization, but may have long revisit times, limited coverage, poor to inadequate spatial resolution, and may require cloud-free skies, which can be rare in some parts of the globe. Deployment of satellite constellations, such as the Italian Space Agency's Cosmo-SkyMed (CONstellation of small Satellites for the Mediterranean basin Observation) of four identical SAR satellites (Covello et al. 2010), addresses these kinds of deficiencies. However, where logistics allow rapid deployment, airborne assets have significant advantages of tasking (such as to avoid clouds) and dramatically higher spatial resolutions.

Table 1 Summary of oil spill remote sensing relevant airborne sensors, 2010

Instrument	Region (bands)	Range (nm)	Platform	Resolution (m)	Cross track (pixels)	Primary link	Full name	Agency	Comment
AVIRIS	UV-NIR (224)	380–2500	Twin otter. ER-2	4.4–20	677	http://aviris.jpl.nasa.gov/	Airborne Visible Infrared Imaging Spectrometer	NASA/Jet Propulsion Laboratory	Whisk broom
HvMap	UV-NIR (128)	450–2480	Multiple	3–10	512	www.hyvi.sta.com	HYperspectral MAPPING	HyVista corp	Push broom
SEBASS	MIR, TIR (128)	2500–5200, 7500–13,500	Twin otter	2–7	128	www.aero.org/capabilities/documents/AER027_SEBASS_Final.pdf	Spatially Enhanced Broadband Array Spectrograph	The Aerospace corp	128 × 128 imaging element
ASPECT Multi-spectral	MIR, TIR(16)	3410–5330, 8730–11,360	Aero Commander 680 (twin engine)	1.1	1	http://www.epa.gov/NaturalEmergencies/flyinglab.htm	Airborne Spectra Photometric Environmental Collection Technology	EPA	Line scanner, flown at 1000 m
ASPECT FTIR	TIR (2048)	1266	Aero Commander 680 (twin engine)	9	1	http://www.epa.gov/NaturalEmergencies/flyinglab.htm	Airborne spectra photometric environmental collection technology	EPA	Fourier transform spectrometer
UAVSAR	L-band	1.2175–1.2975 GHz	Gulfstream 3	1.7–0.6 single look	9900	http://uavsar.jpl.nasa.gov/	Uninhabited aerial vehicle synthetic aperture radar	NASA/Jet Propulsion Laboratory	22–65° incidence angles

Table 1 (Continued)

Instrument	Region (bands)	Range (nm)	Platform	Resolution (m)	Cross track (pixels)	Primary link	Full name	Agency	Comment
HSRL	Vis, NIR(2)	522,1064	B200 or Learjet	–	1	http://science.larc.nasa.gov/hsrl/	High Spectral Resolution Lidar	NASA/Langley	
CHARTS	Vis, NIR(2)	532,1064	Twin engine	2/5 (Topographic hydro-graphic)	500	www.jalbtcx.org	Compact Hydrographic Airborne Rapid Total Survey, optech inc	US Army Corps of Engineers/JALBTCX	3 or 20 kHz sample, to 60 m, SHOALS 3000T20
CASI-1500	Vis-NIR (36)	375–1050	Twin engine	0.25–10	1500	www.jalbtcx.org	Compact Airborne Spectrographic Imager, ITRES	US Army Corps of Engineers/JALBTCX	Push broom, operates with CHARTS

UV Ultraviolet, Vis Visible, NIR Near Infrared, MIR Mid Infrared, TIR Thermal Infrared, JALBTCX Joint Airborne Lidar Bathymetry Technical Center of Expertise

Table 2 Summary of oil spill remote sensing relevant spaceborne sensors, 2010

Instrument (Satellite)	Bands (# bands)	Band range (nm)	Resolution (km)	Swath (km)	Revisit (days)	Rapid Response	Link	Acronym	Comment
Thematic Mapper (Landsat 5)	Vis nir, TIR (8 bands)	450–12,500	0.015–1.0	185	16	No	http://landsat.gsfc.nasa.gov/about/ http://landsat.usgs.gov/	Land satellite	
Enhanced Thematic Mapper (Landsat-7)	Vis, NIR TIR (7 bands)	450–12,500	0.03, 0.120	185	1–3/26	No	http://landsat.gsfc.nasa.gov/about/ http://landsat.usgs.gov/	Land satellite thematic mapper	Rapid revisit is for off-nadir Landsat 7 had scan line corrector failure
MODIS (Terra, Aqua)	Vis, MIR TIR (36 bands)	405–14,385	0.25, 0.5, 1.0	2330	1–2	Yes	http://modis.gsfc.nasa.gov/	Moderate resolution imaging spectroradiometer	120 m in TIR band
ASTER (Terra)	VNIR, NIR, TIR (14 bands)	520–11,650	0.015/0.03/0.09	60	4–16	No	http://asterweb.jpl.nasa.gov/	Advanced Spaceborne Thermal Emission and Reflection Radiometer	–
MISR (Terra)	Vis, NIR (4 Bands)	446.4–866.4	0.275–1.1	360	2–9	No	http://www-misr.jpl.nasa.gov/	Multiangle Imaging Spectro Radiometer	9 different, simultaneous along track viewing angles
MERIS (ENVISAT)	Vis-NIR (15 bands)	412.5–900	2.36 × 0.30–1.04 × 1.2	1150	3	–	http://miravi.co.esa.int/en/ http://www.esa.int/esa-EO/SEMWYN2VQID_index_0_m.html	Medium Resolution Imaging SpectroRadiometer	Bands can be reprogrammed

Table 2 (Continued)

Instrument (Satellite)	Bands (# bands)	Band range (nm)	Resolution (km)	Swath (km)	Revisit (days)	Rapid Response	Link	Acronym	Comment
HICO	Vis-NIR (90 bands)	400–1000	0.95	43	–	No	http://www.nasa.gov/mis-sion_pages/station/research/experiments/HICO.html	Hyperspectral Imager for the Coastal Ocean	International space station
Quickbird	Vis-NIR (4 bands)	450–900	0.0005/0.0026	16.5	1–3.5	Yes	http://www.digitalglobe.com http://www.satimaging.com/satellite/quickbird.htm	–	Panchromatic has higher resolution
AVHRR/3 (POES)	Vis, MIR, TIR (6 bands)	580–12,500	1.09	2440	0.5	No	http://noaa.nas.nasa.gov/NOAAASIS/ml/avhrr.html http://www.class.ngdc.gov/data_available/avhrr/index.htm	Advanced Very High Resolution Radiometer (polar-orbiting environmental satellites)	–
RadarSat 1	C-Band	5.3 GHz	0.008–0.1	50–500	24	Yes	http://www.asc-csa.gc.ca/eng/satellites/radarsat/	Radar satellite-1	–
RadarSat2	C-Band	5.405 GHz	0.003–0.100	20–1000	12	Yes	http://www.asc-csa.gc.ca/eng/satellites/Radarsat2/ http://gs.mdaacorporation.com/SatelliteData/Radarsat2/Features.aspx	Radar satellite-2	Left and right look halves revisit time
ASAR (ENVISAT)	C-Band	5.331 GHz	0.010–1.0	10–1000	35	Yes	http://envisat.esa.int/instruments/asar/	Advanced Synthetic Aperture Radar (ENVISAT)	Provides continuity with ERS-2

Table 2 (Continued)

Instrument (Satellite)	Bands (# bands)	Band range (nm)	Resolution (km)	Swath (km)	Revisit (days)	Rapid Response	Link	Acronym	Comment
ERS-SAR (ERS-2)	C-Band	5.330 GHz	0.006–0.030	5–100	3/35/168	Yes	http://earth.esa.int/ers/	European resource-sensing-synthetic aperture radar	Orbital adjustment with different repeat cycles mission ended 5 Sept. 2011
Cosmo SkyMed2	X-Band	9.6 GHz	0.001–0.1	10–200	0.5–1.25	Yes	http://www.telespazio.it/cosmo.html	Constellation of small satellites for mediterranean basin observation	A constellation of 4 satellites, steerable
PALSAR (ALOS)	L-Band	1.270 GHz	0.007–0.1	40/70–350	46/2	No	http://www.eorc.jaxa.jp/ALOS/en/about/palsar.htm	Phased array-type L-band synthetic aperture radar (advanced land observing satellite)	Multiple resolution modes, fast revisit by targeting
TerraSAR-X	X-Band	9.6 GHz	0.001–0.018	5–150	2.5	Yes	http://www.inforterra.de/terrasar-x-satellite	Terra synthetic aperture radar X-Band	Has twin, TanDEM-X satellite
CALiOP (CALIPSO)	Vis, NIR (2 bands)	532,1064	0.1	–	16	No	http://www-calipso.larc.nasa.gov/	Cloud aerosol lidar with orthogonal polarization (cloud-aerosol lidar and infrared pathfinder satellite observation)	Vertical resolution is (0.03–0.60 km)

Table 2 (Continued)

Instrument (Satellite)	Bands (# bands)	Band range (nm)	Resolution (km)	Swath (km)	Revisit (days)	Rapid Response	Link	Acronym	Comment
SCIAMACHY (ENVISAT)	UV, Vis, NIR (15 bands)	240–2380	30 × 240	3 × 132, 32 × 215, 1000	3	No	http://envisat.esa.int/instruments/sciamachy/	Scanning imaging absorption spectrometer for atmospheric CHartography (ENVIronmental SATellite)	1000 km for limb mode
ASMR-E (Aqua)	Microwave (12 bands)	6.925–89 GHz	6 × 4–74 × 43	1445	1	No	http://www.ghee.msfc.nasa.gov/AMSR/	Advanced microwave scanning radiometer-earth observing satellite	Ceased operation 4 Oct. 2011

Vis Visible spectrum, NIR Near infrared, UV Ultraviolet, TIR Thermal infrared. Repeat days is maximum

The FOSTERRS mission is to facilitate interagency and inter-institutional communication between agencies with remote sensing assets, responders, scientists, and end users. One important aspect of the FOSTERRS mission entails identifying critical technological needs and bottlenecks in technology acceptance.

The core FOSTERRS team incorporates representation for operations and science for agencies with relevant instrumental and platform assets (NASA, NOAA, USGS, NRL, NSF, contract laboratories) and key end-users (NOAA, USCG, etc.). FOSTERRS supports development of collaboration with a wide range of end-user agencies, entities, and researchers including industry and academic experts, and eventually international partners through outreach efforts. Through these collaborations, FOSTERRS facilitates interagency cooperation and communication between the various groups involved in marine disaster response to enable remote sensing best use.

3 Discussion and Conclusion

Remote sensing has demonstrated enormous potential to improve oil spill response in large magnitude spills, and as a triage tool for small spills, greatly leveraging available resources and compensating for the paucity of trained personnel, or for inaccessible oil spills. Moreover, while oil spill resources in the developing world are far less than those in countries like the US; satellite remote sensing provides global coverage, and oil spills can cross international boundaries.

As noted above, disasters of vast extent like the Japanese Tsunami and the Deepwater Horizon oil spill overwhelmed response systems and provided opportunities to demonstrate or field new remote sensing technologies. In contrast, typical, short duration and small-scale disasters fail to provide such opportunities. To apply a new and unproven technology to a typical spill-of-opportunity requires availability of key personnel and equipment, mobilization funding and logistics, and access to the disaster permitted by the incident command, whose priority is damage mitigation, rather than testing new technologies of unclear merit and accuracy.

Given the potential of remote sensing, its acceptance has been slow. In part this arises from the inherent conservatism of an oil spill response—tried and true approaches have less career risk. This is particularly true where a remote sensing approach has known false positives and negatives, or is untested. The Deepwater Horizon oil spill, by its magnitude and persistence, provided a unique opportunity to test many remote sensing technologies that would face logistical, bureaucratic, and technical hurdles requiring longer than a typical oil spill response lasts.

Technology adoption is distinct from the well-known technology readiness level (Ramirez-Marquez and Sauser 2009), which describes the process of development of a technology from inception of physical principles (TRL 1) through proven operational success (TRL 9), see Fig. 4. In order to interpret remote sensing products, an understanding of its limitations, signal to noise, and detection limits is necessary. Such criteria are criteria identified at TRL 2 and demonstrated at TRL 5/6. During

TRL9	Actual system "flight proven" through successful mission operations.	TRL9	Operational history demonstrating applicability for a wide range of conditions and oil spills
TRL8	Actual system completed and "flight qualified" through test and demonstration (ground or space)	TRL8	Actual system demonstrated and validated for an at sea oil spill
TRL7	System prototype demonstration in the relevant space or airborne environment	TRL7	Prototype demonstration and validation at sea – methods of validation
TRL6	System/subsystem model or prototype demonstration in a relevant environment	TRL6	Prototype demonstration and validation at sea or in a sea simulator – methods of validation
TRL5	Component and/or breadboard validation in relevant environment	TRL5	Component demonstration in the field (on oil)
TRL4	Component and/or breadboard in the laboratory environment	TRL4	Component demonstration in the laboratory (on oil)
TRL3	Analytical and experimental critical function and / or characteristic proof-of-concept	TRL3	Proof of Concept of basic principles in the laboratory (on floating oil)
TRL2	Technology concept and/or application formulated	TRL2	Formulation of application of basic principles in the environment (for an oil spill)
TRL1	Basic principles observed and reported	TRL1	Basic principles observed and theoretical basis described (for application to oil on water)

Fig. 4 *Left.* Technological Readiness Level chart and definitions from NASA (2012). *Right.* Proposed modification for oil spill technology

Deepwater Horizon, the response suffered from bandwidth limitations with individuals and institutions volunteering solutions at all levels of Technical Readiness Level. Given the resources, ideas that were not operational (TRL 9) were not considered seriously for incorporation into the response (Bill Lehr, NOAA, Pers. comm. 2014). Moreover, evaluating ideas took time, a most precious resource. For example, the BP Spill hotline for oil spill ideas from the public fielded about 60,000 calls in May which yielded about 10,000 suggestions, of which 700 were selected for further scrutiny; however, it is unclear if BP evaluated Technological Readiness Level in considering these suggestions. Providing a pre-screening survey to allow potential users to self evaluate the initial estimation of a technology's TRL would clearly be helpful to screening suggestions; a proposed modification of the Technological Readiness Ladder for Oil Spill Remote Sensing is shown in Fig. 4.

Low-level remote sensing products are not useful for response, which requires higher-level remote sensing products, such as thickness maps (Clark et al. 2010) or detection maps, that have reduced or eliminated false positives and negatives. The incorporation of complementary ancillary data, such as winds, can greatly improve the robustness of higher level remote sensing products (Espedal 1999). Thus, acceptance requires additional steps beyond operational readiness.

There can be considerable reticence in adopting new technologies given that using an un-approved technology has inherent risk for disaster response decision makers. As a result, acceptance requires demonstration on real oil spills that a new technology supports significantly better response decision making than accepted technologies in the real world. There clearly is a catch-22 for new technology needing field-testing to demonstrate utility and not being allowed for field-testing until said demonstration is performed. Opportunities to break this conundrum are presented by oil-on-water

exercises, such as conducted by NOFO, the Norwegian Clean Seas Association (McClimans et al. 2013), in Norwegian waters annually, and natural seepage, like the Coal Oil Point seep field, offshore California (Estes and Senger 1971–1973; Leifer et al. 2006), which releases more than a hundred barrels of oil daily (Clester et al. 1996). However, planned oil spills in US waters are politically very difficult (AP 1996). Thus, disasters like the Deepwater Horizon Oil Spill present a rare opportunity for collection of remote sensing data, which can help improve response to future oil spills.

Demonstration during an oil spill, and even one or several publications can be insufficient to gain acceptance—the threshold can be higher for new technology acceptance. Moreover, as noted above, turnaround time for final data products is key—oil in the marine environment is highly mobile, and information ages quickly. This distinguishes it from academic remote sensing, where old data is still useful data.

Fortunately, computational power continues to improve dramatically, allowing new capabilities to be built into next generation technologies. For example, the AVIRIS Next Generation instrument, AVIRIS NG has the potential to realtime map oil thickness. This realtime mapping capability was tested successfully on methane spectral features that have the same carbon-hydrogen stretch vibrations as oil during the summer of 2014 (Rob Green, Jet Propulsion Laboratory, Personal Communication 2014).

Among the many critical aspects needed to increase acceptance of new remote sensing technologies in disaster response, the most important is good communication between the various stakeholders. FOSTERRS mission is to improve these communications.

Clearly the appropriate time to integrate (i.e., gain acceptance) new technologies into disaster response is in the quiet interim between disasters, where acceptance requires spill responders to be provided with a good understanding of the benefits and limitations of new technologies, and under what conditions they can be applied. Hence the primary goal of FOSTERRS is to foster effective information exchange between the oil spill response community, agencies, researchers, and other stakeholders.

Although airborne and spaceborne remote sensing possesses great potential to improve marine disaster response, there are impediments to acceptance and integration of new technologies into response efforts. The best approach to facilitation of new technologies is through better information flow between oil spill response community, agencies, researchers, and other stakeholders. FOSTERRS, the Federal Oil Spill Team for Emergency Response Remote Sensing, comprised of members from NOAA, NASA, USGS, NRL, and academia was created to foster this critical information flow.

Acknowledgments Thanks are provided to the NASA Disasters Response Program of the NASA Applied Program, The NOAA's Gulf of Mexico Disaster Response Center and NOAA National Environmental Satellite, Data, and Information Service (NESDIS), and the Naval Research Laboratory. Special thanks are also for Brenda Jones, US Geological Survey, for help in the manuscript preparation.

References

- Albaigés J, Morales-Nin B, Vilas F (2006) The prestige oil spill: a scientific response. *Mar Pollut Bull* 53:205–207
- AP (1996) State postpones its plan to dump, burn oil in sea—Test delayed by fishermen’s concerns, logistics. *Seattle Times*. Seattle Times Company, Seattle
- ASCE (1996) State of the art review of modeling transport and fate of oil spill (task committee on modeling oil spills of the water resources engineering division). *J Hydraul Eng* 122:594–609
- Bradley EB, Leifer I, Roberts DA, Dennison PE, Washburn L (2011) Detection of marine methane emission with AVIRIS band ratios. *Geophys Res Lett* 38:L10702
- Byfield V (1998) Optical remote sensing of oil in the marine environment, School of Ocean and Earth Science. University of Southampton, Southampton, p 302
- Clark RN, Swayze GA, Leifer I, Livo KE, Kokaly R, Hoefen T, Lundeen S, Eastwood M, Green RO, Pearson N, Sarture C, McCubbin I, Roberts D, Bradley E, Steele D, Ryan T, Dominguez R, Team AAVIIS (2010) A method for quantitative mapping of thick oil spills using imaging spectroscopy, U.S. Department of the Interior, p 51
- Clester SM, Hornafius JS, Scepan J, Estes JE (1996) Quantification of the relationship between natural gas seepage rates and surface oil volume in the Santa Barbara Channel, (abstract). *EOS Am Geophys Union Trans* 77(46):F419
- Covello F, Battazza F, Coletta A, Lopinto E, Fiorentino C, Pietranera L, Valentini G, Zoffoli S (2010) COSMO-SkyMed an existing opportunity for observing the Earth. *J Geodyn* 49:171–180
- Espedal HA (1999) Satellite SAR oil spill detection using wind history information. *Int J Remote Sens* 20:49–65
- Estes JE, Senger LW (1971–1973) The multispectral concept as applied to marine oil spills. *Remote Sens Environ* 2:141–163
- Fingas MF, Brown CE (1997) Review of oil spill remote sensing. *Spill Sci Technol Bull* 4:199–208
- Fiscella B, Giancaspro A, Nirchio F, Pavese P, Trivero P (2013) Oil spill detection using marine SAR images. *Int J Remote Sens* 21:3561–3566
- García-Pineda O, MacDonald I, Hu C, Svejksvsky J, Hess M, Dukhovskiy D, Morey SL (2013) Detection of floating oil anomalies from the Deepwater Horizon oil spill with synthetic aperture radar. *Oceanography* 26:154–137
- Grierson IT (1998) Use of airborne thermal imagery to detect and monitor inshore oil spill residues during darkness hours. *Environ Manag* 2:905–912
- HAZMAT (1996) Aerial observations of oil at sea, NOAA, H.M.R.a.A.D., April 1996, p 15
- Joye SB, MacDonald IR, Leifer I, Asper V (2011) Magnitude and oxidation potential of hydrocarbon gases released from the BP oil well blowout. *Nat Geosci* 4:160–164
- Lehr B, Sky B, Possolo A, Allen AA, Boufadel M, Coolbaugh T, Daling P, Fingas M, French-McCay D, Goodmand R, Robert J, Khelifa A, Lambert P, Lee K, Leifer I, Mearns A, Overton E (2010) Oil budget calculator deepwater horizon: a report to the National Incident Command, November 2010, p 217.
- Leifer I, Luyendyk B, Broderick K (2006) Tracking an oil slick from multiple natural sources, Coal Oil Point, California. *Mar Pet Geol* 23:621–630
- Leifer I, Lehr WJ, Simecek-Beatty D, Bradley E, Clark R, Dennison P, Hu Y, Matheson S, Jones CE, Holt B, Reif M, Roberts DA, Svejksvsky J, Swayze G, Wozencraft J (2012) State of the art satellite and airborne marine oil spill remote sensing: application to the BP deepwater horizon oil spill. *Remote Sens Environ* 124:185–209
- McClimans T, Leifer I, Gjøvsund SH, Grimaldo E, Daling P, Leirvik F (2013) Pneumatic oil barriers: the promise of bubble rafts. *Proceedings of the Institution of Mechanical Engineers, Part M. J Eng Marit Environ* 227:22–38
- Minchew B, Jones C, Holt B (2011) Polarimetric analysis of backscatter from the deepwater horizon oil spill using L-band synthetic aperture radar. *IEEE Trans Geosci Remote Sens* 50:3812–3830

- modis-today (2010) MODIS Today: USA Composite, http://ge.ssec.wisc.edu/modis-today/index.php?satellite=t1&product=true_color&date=010_06_11_162&overlay_sector=false&overlay_state=true&overlay_coastline=true§or=USA7&resolution=50m. Accessed 2014
- NASA (2012) Technology Readiness Level, <http://www.nasa.gov/content/technology-readiness-level/-VDAbJSldVM2>. Accessed 2014
- Ramirez-Marquez JE, Sauser BJ (2009) System development planning via system maturity optimization. *Eng Manage, IEEE Trans* 56:533–548
- Reed M, Johansen O, Brandvik PJ, Daling P, Lewis A, Fiocco R, Mackay D, Prentki R (1999) Oil spill modeling towards the close of the 20th century: overview of the state of the art. *Spill Sci Technol Bull* 5:3–16
- Salisbury JW, D'Aria DM, Sabins Jr FF (1993) Thermal infrared remote sensing of crude oil slicks. *Remote Sens Environ* 45:225–231
- Sauser B, Ramirez-Marquez J, Verma D, Gove R (2006) From TRL to SRL: the concept of systems readiness levels. *Conference on Systems Engineering Research*, Los Angeles, p 10
- Shen SS, Lewis PE (2011) Deepwater horizon oil spill monitoring using airborne multispectral infrared imagery, SPIE. SPIE, Orlando, pp 80480H-80481–80480H-80416
- Svejkovsky J, Lehr W, Muskat J, Graettinger G, Mullin J (2012) Operational utilization of aerial multispectral remote sensing during oil spill response: lessons learned during the deepwater horizon (MC-252) spill. *Photogramm Eng Remote Sens* 78:1089–1102
- Topouzelis K, Karathanassi V, Pavlakis P, Rokos D (2007) Detection and discrimination between oil spills and look-alike phenomena through neural networks. *ISPRS J Photogramm Remote Sens* 62:264–270
- Tseng WY, Chiu LS (1994) AVHRR observations of persian gulf oil spills, *Geoscience and Remote Sensing Symposium, 1994. IGARSS '94. Surface and Atmospheric Remote Sensing: Technologies, Data Analysis and Interpretation* pp 779–782

LANCE, NASA's Land, Atmosphere Near Real-Time Capability for EOS

Kevin J. Murphy, Diane K. Davies, Karen Michael, Christopher O. Justice, Jeffrey E. Schmaltz, Ryan Boller, Bruce D. McLemore, Feng Ding, Bruce Vollmer and Min M. Wong

Abstract

NASA's Land, Atmosphere Near real-time Capability for EOS (Earth Observing System) (LANCE) provides global data and imagery from the Terra, Aqua and Aura satellites in less than 3 h from satellite observation to meet the needs of the near real-time (NRT) applications community. Science quality, or higher-level "standard" products are made available within 8–40 h of observation but application users, operational agencies, and even researchers often need data much sooner than what routine science processing offers. This chapter describes the architecture of LANCE and modifications made to achieve the nominal 3-h latency requirement.

K. J. Murphy (✉) · K. Michael · R. Boller · B. Vollmer
NASA Goddard Space Flight Center, Mail Code 423,
Building 32, 8800 Greenbelt Rd, 20771 Greenbelt, MD, USA
e-mail: Kevin.J.Murphy@nasa.gov

D. K. Davies
Science Systems and Applications, Inc./Trigg-Davies Consulting Ltd, Malvern, UK
e-mail: diane.k.davies@nasa.gov

C. O. Justice
Department of Geographical Sciences, University of Maryland, College Park, MD, USA

J. E. Schmaltz
Science Systems and Applications, Inc., NASA Goddard Space Flight Center,
Greenbelt, MD, USA

B. D. McLemore
Honeywell Technology Solutions, Inc., 7515 Mission Drive, Seabrook, MD, USA

F. Ding
ADNET Systems, Inc., NASA Goddard Space Flight Center, Greenbelt, MD, USA

M. M. Wong
Columbus Technologies and Services, Inc.,
NASA Goddard Space Flight Center, Greenbelt, MD, USA

Keywords

NASA · LANCE · Near real-time · AIRS · AMSR-E · MODIS · OMI · Rapid response · Worldview · GIBS · FIRMS

1 Introduction

NASA developed the Land, Atmosphere Near real-time Capability for EOS (Earth Observing System) (LANCE) in response to a growing need for timely satellite observations by applications users, operational agencies and researchers. Originally intended for long-term Earth science research, EOS capabilities were modified to deliver satellite data products with sufficient latencies, to meet the needs of near real-time (NRT) user communities. Latency is defined as the time from satellite observation to product delivery. All aspects, from geo-location (attitude and ephemeris) data to ground systems and in some cases, science algorithms, had to be modified to reach the 3 h latency requirement. This chapter describes how systems originally designed for long-term science research evolved into capabilities that can be used for NRT applications, such as those described in Chap. 11. Lessons learned from the development of LANCE are also conveyed.

2 Background

The first request for NRT products from the MODerate resolution Imaging Spectroradiometer (MODIS) instrument on the Terra satellite dates back to 2000 when the US Forest Service (USFS) requested MODIS fire detections within hours of acquisition, instead of the expected 7 day latency, to help manage wildland fires on the Idaho-Montana border. A team comprised of USFS, University of Maryland (UMD) and NASA Goddard Space Flight Center (GSFC) scientists assembled a series of customized images that demonstrated the significant contribution NRT MODIS imagery and data could make to wildfire suppression and emergency rehabilitation. The following April, the same team initiated the Rapid Response project, providing fire detection data and imagery from MODIS in NRT to the USFS Remote Sensing Applications Center in Salt Lake City, UT [<http://www.fs.fed.us/eng/rsac/>] and the National Interagency Fire Center in Boise, ID [<http://www.nifc.gov>] (Sohlberg et al. 2001; Quayle et al. 2004; Justice et al. 2002).

The Rapid Response System was built on experience gained with the MODIS Land 250 m Production System (Justice et al. 2000). Expedited data were received from the EOS Data and Operations System (EDOS) feed to the National Oceanic and Atmospheric Administration's (NOAA) NRT system. Initially, the imagery provided was in a swath-based, non-geo-referenced format for North America. By 2007, the

Rapid Response System was producing global swath-based imagery and data from the MODIS instruments on Aqua and Terra. Some of the most valuable products created included imagery based on the MODIS Corrected Reflectance algorithm, which provides 'true color' (i.e. natural-looking) images by removing gross atmospheric effects, such as Rayleigh scattering, from MODIS bands 1 through 7. Quasi-true-color images from bands 1-4-3 (as Red, Green, Blue), as well as false color band combination images were generated. Additional products included an expedited daily Normalized Difference Vegetation Index (NDVI) without cloud removal, expedited Land Surface Temperature (Pinheiro et al. 2007), and MODIS Band 31 (11 μm) brightness temperature.

As the Rapid Response image and information provision capability became more visible, news organizations, such as ABC, CBS, NBC, CNN, BBC, Washington Post and the New York Times, began requesting custom geo-referenced images for large newsworthy events. Users quickly realized that the imagery and data products produced by Rapid Response could be used for other tasks that required low latency products, including imagery for monitoring air quality, floods, dust storms, snow cover, agriculture, and for public education and outreach.

As the original system aged and the demand and expectations for NRT data increased, the NASA Earth Science Division (ESD) implemented an NRT capability that was closely aligned with the science-processing systems. NASA ESD sponsored the development of LANCE in 2009. The goal of LANCE was to provide a central point of access to high quality NRT data products imagery and data products for land and atmosphere studies (Michael et al. 2010). NRT algorithms used to produce LANCE products would keep in step with equivalent science algorithms and new data services would be offered. The system also needed to become more robust.

Originally, LANCE provided products from MODIS, Advanced Microwave Scanning Radiometer-EOS (AMSR-E), Atmospheric Infrared Sounder (AIRS), Microwave Limb Sounder (MLS) and Ozone Monitoring Instrument (OMI) instruments (see Box 1). In 2011, the AMSR-E instrument on the Aqua satellite malfunctioned and data provision was discontinued. Today, LANCE provides over 70 image and derived data products from the remaining instruments. On an average day, over 2 TB of NRT products (data and imagery) are downloaded. The demand for these products comes from applications users, operational agencies and scientists to support NRT research and applications in weather prediction, monitoring of natural hazards, agriculture, air quality, disaster relief and homeland security.

3 LANCE Architecture

The latency requirement for Level 2 products from LANCE is 180 min from instrument observation to product availability for users to download. Three hours was considered the minimum requirement to meet the needs of most of the NRT research and applications that were presented at the first LANCE User Working Group in

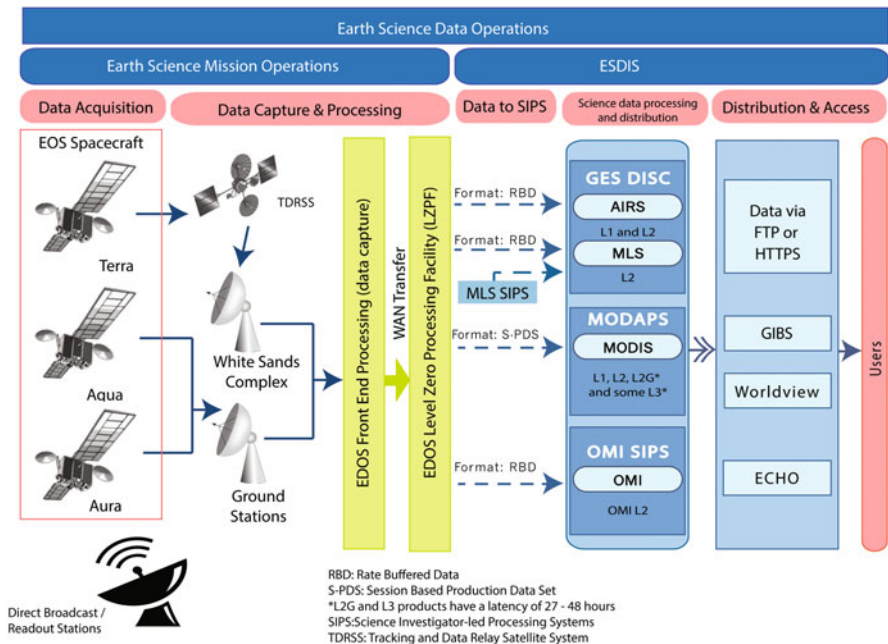


Fig. 1 The LANCE Architecture from Data Acquisition to Processing and Distribution

November 2010 (LANCCE 2010). These applications included monitoring floods, crops, volcanic clouds, fires and burned areas and some weather applications, where direct broadcast data were not available.

To achieve the latency requirements, many components of the EOS satellite operations, ground and science processing systems had to be made more efficient without compromising the quality of science data processing. For LANCE, this was achieved by creating a dual processing stream that leveraged components originally developed for science data processing and augmented them with features that allowed for more efficient processing within NASA’s Earth Observing System Data and Information System (EOSDIS). The main components of EOSDIS are: the EOS spacecraft and instruments; the ground systems, which are comprised of flight operations, data capture and Level 0 processing; and the science data segment that is responsible for producing near real-time data end user products. Figure 1 shows a simplified overview of the dataflow from satellite to users.

3.1 EOS Spacecraft and Instruments

At the time of writing all LANCE data originate from the Terra, Aqua, and Aura spacecraft. Box 1 provides a brief overview of the instruments.

Box 1. LANCE Instruments

AIRS (Atmospheric Infrared Sounder) was launched on Aqua in 2002. It is designed to support improved weather forecasting and climate research. It uses infrared sensing technology to create 3-dimensional maps of air and surface temperature, water vapor, and cloud properties.

AMSR-E (Advanced Microwave Scanning Radiometer-EOS) is a Japanese (JAXA) instrument launched on Aqua in 2002. LANCE provided AMSR-E data until the instrument failed in October 2011. It measured cloud properties, sea surface temperature, near-surface wind speed, radiative energy flux, surface water, ice and snow. JAXA began acquiring observations from AMSR2 in July 2012. LANCE plans to start releasing NRT products created from AMSR2 data in 2015.

MLS (Microwave Limb Sounder) was launched on Aura in 2004. It makes measurements of atmospheric composition, temperature, humidity and cloud ice that are needed to track the stability of the stratospheric ozone layer, help improve predictions of climate change and variability, and help improve understanding of global air quality.

MODIS (MODerate Resolution Imaging Spectroradiometer) was launched on Terra in 2000 and a second MODIS instrument was launched on Aqua in 2002. MODIS measures cloud properties and radiative energy flux, also aerosol properties; land cover and land use change, fires and volcanoes.

OMI (Ozone Monitoring Instrument) is a Dutch instrument launched on Aura in 2004. It measures various atmospheric constituents including ozone (column and profile), aerosols, clouds, surface ultraviolet (UV) irradiance, and a number of other trace gases. The Royal Dutch Meteorological Institute (KNMI) and NASA developed an NRT capability for the processing system that was integrated into LANCE.

3.2 EOSDIS Ground Systems

Once a satellite is launched, significant latency improvements can usually only be made at the ground system level, from data capture to the generation of products at distribution sites. Latency can best be minimized by downloading data transmitted directly from the satellite to the ground, however this limits geographic coverage. Direct Broadcast (DB) data can be downloaded by anyone with ground receiving equipment in direct line of sight to the satellite. Using DB, the wait-time associated with EOS ground station contacts is eliminated, thereby significantly reducing latency for these datasets (Huang et al. 2004; Urbanski et al. 2009). However, for global coverage, a different approach is required. This section describes the modifications made to the EOSDIS ground system to reduce latency for global NRT products.

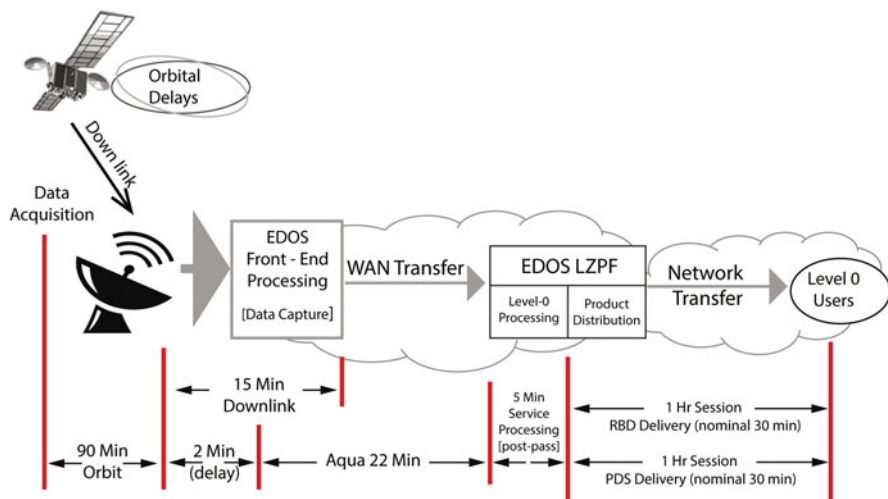


Fig. 2 The breakdown of latency from Aqua data acquisition to Level 0 users (including science teams and other expert users)

3.2.1 Data Capture

EDOS, under the management of the Earth Science Mission Operations (ESMO) Project, is responsible for capture and initial processing of science and engineering data from the EOS spacecraft. Data from Aqua and Aura instruments are downlinked to Polar Ground Stations in Alaska and Norway, nominally once per orbit. Terra data are downlinked to the White Sands complex in New Mexico, using Tracking and Data Relay Satellite System (TDRSS). In order to expedite data acquisition from Terra, ESMO added an additional TDRSS contact making two contacts per orbit. Downlinks from Terra are therefore more frequent and latency is less than for Aqua or Aura.

Once downlinked, satellite data are delivered as Rate Buffered Data (RBD) by Wide Area Network (WAN) high-rate lines to EDOS's Level Zero Processing Facility (LZPF) (Cordier et al. 2010). RBD contain data captured in a single spacecraft contact session that is sorted, processed and delivered in an expedited manner. Figure 2 shows the approximate breakdown of latency times from data acquisition. In 2011, EDOS implemented three major latency enhancements focused on decreasing the time taken to transfer data to the LZPF. These improvements resulted in a 51 % overall latency improvement for Terra MODIS and a 24 % overall latency improvement for Aqua MODIS.

At the LZPF, various Level 0 products are generated as agreed to by end users, and distributed to the respective data and processing centers. EDOS produces contact/session based data sets especially for LANCE NRT use; these are either RBD Sets or Session-based Production Data Sets (S-PDS) (S-PDS is identical to RBD except that it undergoes further processing to Level 0). The key difference between the NRT Level 0 products and those for standard science processing are the data used

to determine the precise location and tilt of the satellite. Standard products use definitive geo-location (attitude and ephemeris) data provided daily, whereas NRT products use predicted geo-location provided by the instrument's Global Positioning System (GPS) or an approximation of navigational data (depending on platform). Terra has an on-board GPS, therefore captured data can be processed immediately with its supplied predicted navigational data. However, Aqua and Aura do not have an on-board GPS, so for immediate processing it requires spacecraft housekeeping data and predicted ephemeris.

From LZPF, Level 0 data are distributed to the LANCE facilities for higher-level product generation after which they are made available to users.

3.2.2 LANCE Facilities: Expediting Data Processing

Level 0 data are processed into higher-level products at designated Science Investigator-led Processing Systems (SIPS). The LANCE science processing facilities are co-located at the Goddard Earth Sciences Data and Information Services Center (GES DISC), the OMI SIPS, the MODIS Adaptive Processing System (MODAPS) and the NASA Jet Propulsion Laboratory (JPL) MLS SIPS. This approach leverages the existing instrument science processing expertise and minimizes WAN transfer times.

The processes used by LANCE have been streamlined and adapted to work with data (both RBD and/or S-PDS) from LZPF as soon as they are downlinked from satellites or transmitted from ground stations, generally within 30 min to 2 h after observation.

3.2.2.1 MODIS NRT Data Processing

The difference between MODIS geolocation when using definitive vs. predicted attitude and ephemeris is routinely less than 100 m. However, there are situations, particularly before and after spacecraft maneuvers and during space weather events, when the difference can increase up to several kilometers. The recommendation from EOSDIS is to reprocess data when the definitive attitude and ephemeris data become available.

Routines used to derive Level 2 products, such as fire, snow, and sea ice products, do not make use of ancillary data and so their codes are identical to the ones used in standard operations. Those Level 2 products that require ancillary data have modified production rules to relax the requirements for ancillary data, thus reducing processing times. In the case of MODIS, the production rules to generate the Cloud Mask/Profiles and Level 2 Clouds were developed by the University of Wisconsin. The production rules for Level 2 Aerosols were developed to meet NRT requirements for NASA's ARCTAS (Arctic Research of the Composition of the Troposphere from Aircraft and Satellites) campaign. For Level 2 Land Surface Reflectance, the code uses the NOAA Global Forecast System (GFS) ancillary product rather than the Global Data Assimilation System (GDAS) data used in the standard processing version (Vermote et al. 2002). Prior to initiating production, the near real-time Product Generation Executive (PGE) codes were extensively science-tested and all products were compared to the baseline products generated by the standard processing (Fig. 3).

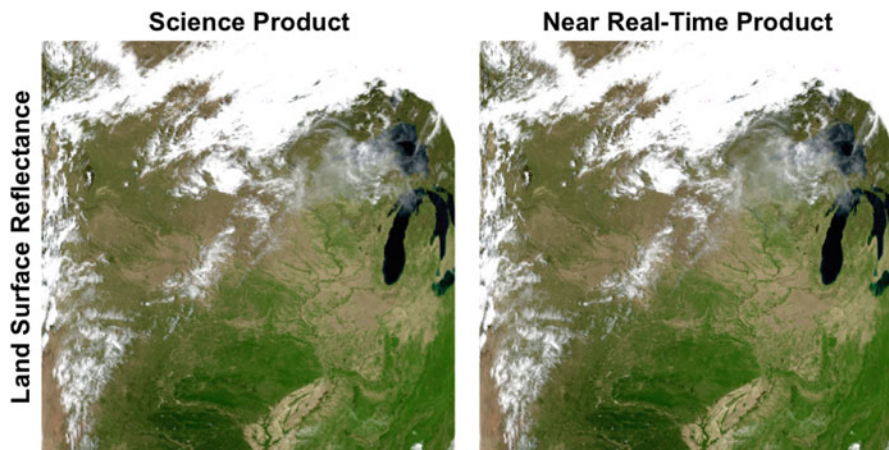


Fig. 3 In this side-by-side comparison of a standard and near-real time Land Surface Reflectance granule over the Midwest there appears to be no difference between the products. However, under close examination the near-real time view shows slightly more haze *West* of the Great Lakes

All PGE codes have been validated for use in LANCE MODIS by the Principal Investigators and are considered suitable for NRT applications. This process is repeated as new versions of the PGEs become available and are considered for inclusion in LANCE.

3.2.2.2 AIRS NRT Data Processing

For AIRS Level 1B products, the NRT system does not wait more than 5 min for the previous or subsequent granule data to be present before processing. This can cause small differences in radiances of Level 1B products between the NRT and routine processing, which uses calibration data from the previous and subsequent granules. These differences generally happen when AIRS leaves the range of a downlink station (usually 17 times/day) and are most visible in the first or last few scans of the granule, depending upon whether the previous or subsequent granule is missing. However, all of the radiances in a granule can be affected to some extent. For AIRS Level 2, the retrieval values of parameters in NRT products can differ from the routine products because of small differences in assumed surface pressure and/or differences in the radiances. Although it is rare, if the forecast surface pressure is not available when the NRT data are produced, the NRT algorithm assumes a surface pressure based on a digital elevation model rather than the more accurate forecast surface pressure. Differences in the assumed surface pressure tend to be small (~ 10 mbar) near the equator but can become larger (~ 70 mbar) during some synoptic weather events. These pressure differences can also lead to differences in the retrieved temperature and water vapor (Hearty et al. 2010). To meet the latency requirement of NRT data, retrievals of ice cloud properties are not included in the AIRS Level 2 NRT processing and subsequently products requiring these retrievals are not available in NRT. This

does not represent a loss of critical information for NRT data applications because the ice cloud properties are considered more climate-related information.

3.2.2.3 MLS NRT Data Processing

In the case of MLS, a modified Level 2 algorithm is used. The use of the standard MLS processing suite is not practical for processing a NRT data stream because of the large demands on computational resources and the inherent latency involved. Consequently, the NRT retrievals have been adapted to dramatically reduce the computational resource requirements compared to the standard product-processing suite. The NRT retrievals produce a subset of MLS products (Temperature O₃, CO, HNO₃, SO₂, H₂O, N₂O) using a reduced selection of the available MLS Level 1 radiances, coupled with lower fidelity forward model approximations, which also neglects line-of-sight temperature and concentration gradients. As a result, the faster processing algorithms result in a degradation in the NRT data quality compared to the standard products (Lambert et al. 2012).

3.2.2.4 OMI NRT Data Processing

OMI Level 1B processing software is provided by the KNMI (Royal Netherlands Meteorological Institute) and run by NASA. To expedite processing, a number of internal algorithms are bypassed in the Level 1 Processor as compared to the standard science processing. These include spectral calibration, solar stray light corrections, and some dark current corrections. This speeds up the Level 1B software by about 20 % as compared to standard processing. The Level 2 software also uses expedited production rules when selecting ancillary data. During NRT processing these rules use the most recent data available and do not wait for the best data, as is the basis of the production rules used in generating the standard products. This usually means using a snow and ice file that is 24–48 h old rather than one that is within the window of 24 h of measurements. (For more information please see the OMI NRT Data User Guide—<http://ozoneaq.gsfc.nasa.gov/media/docs/OMI-NRT-DUG.pdf>)

3.2.3 Distribution to End Users

As with data capture and data processing, the distribution of LANCE products leverages existing EOSDIS services, including: the earthdata.nasa.gov website; the EOS Clearing House (ECHO), a spatial and temporal metadata registry and order broker; the User Registration System (URS), that provides a single username and password for many EOSDIS resources; and the User Support Tool (UST) which is used to track and respond to user queries and comments. The centralized provision of these support services means users can benefit from the specialization of duties, for example a central user support tool allows experts from LANCE elements across the United States to focus on providing quality support to end users, while the distributed LANCE SIPS can focus on the data quality and data provision. This modular approach enables new capabilities (e.g. data from a new instrument) to be added to LANCE with relative ease.

LANCE products are made available to end-users through the LANCE SIPS facilities and distributed virtually through the NRT webpages on the earthdata.nasa.gov

Table 1 LANCE product categories by instrument

Instrument	Product categories	Average latency
AIRS	Radiances, temperature and moisture profiles, precipitation, dust, clouds and trace gases	75–140 min
MLS	Ozone, temperature, carbon monoxide, water vapor, nitric acid, nitrous oxide, sulfur dioxide	75–140 min
MODIS	Radiances, cloud/aerosols, water vapor, fire, snow cover, sea ice, land surface reflectance, land surface temperature	60–125 min (Latency range excludes daily LSR)
OMI	Ozone, sulfur dioxide, aerosols, cloud top pressure	100–165 min (Latency range excludes daily L3)

website. Both data files and imagery are provided. In keeping with NASA's Data and Information Policy, LANCE data are provided free of charge.¹

4 LANCE Products

LANCE creates expedited products that have a science heritage and a demonstrated utility for applications requiring NRT data. LANCE distributes lower level products such as calibrated geo-located radiances and higher-level products such as active fire locations and snow cover. Table 1 shows current NRT product categories by instrument.

Science team members oversee the development of expedited algorithms, and ensure that user feedback and evolving user needs translate into appropriate product modifications and new products. LANCE NRT data are archived in a rolling archive for a minimum of 7 days. If latency is not a primary concern, users are encouraged to use the standard science products, which are created using the best available ancillary, calibration and ephemeris information. Standard science quality products are an internally consistent, well-calibrated record of the Earth's geophysical properties to support science.

¹ However data supplied by international partners or other agencies may be restricted by a Memorandum of Understanding (MoU) with those organizations.

5 LANCE Services

5.1 Data File Distribution

Access to data files, predominantly in Hierarchical Data Format (HDF), but also as Binary Universal Format for Representation (BUFR) for AIRS Level 1B channel subsets, are distributed through File Transfer Protocol (FTP) and Hypertext Transfer Protocol Secure (HTTPS), and subscription services that push data to user's systems. Users register with the URS, to access to data from LANCE, as well as data from any of the other EOSDIS Distributed Active Archive Centers (DAAC). Once registered, users are notified of any missing data or delays in data processing, for example due to spacecraft maneuvers or downtime on one of the two data distribution servers.

5.2 Rapid Response

As mentioned in Sect. 2, the Rapid Response System was developed in response to the needs of the USFS for NRT fire products (Sohlberg et al. 2001) but It was soon realized that MODIS imagery was useful for a variety of applications and the scope of Rapid Response expanded to provide: global land swath images; geo-referenced images for "areas of interest" (referred to as subsets); gallery images; and hand-crafted imagery for newsworthy events or for public outreach. The success of Rapid Response imagery has been one of the main driving forces behind the development of GIBS and Worldview, both described below.

5.3 GIBS

Global Imagery Browse Services (GIBS) are a set of standard web services provided by EOSDIS to deliver daily global, full-resolution imagery via a variety of standard services and format, such as Web Map Tile Services (WMTS) and Keyhole Markup Language (KML). Full-resolution LANCE imagery products are provided to GIBS as 3-band (RGB GeoTIFFs) or 1-band (8 byte PNG) files through standard file delivery mechanisms (e.g. HTTPS or FTP) or through Web Coverage Services (WCS) and Web Mapping Services (WMS). GIBS processes this imagery into daily tiled, global images, which are then cataloged, archived, and immediately available for access through the GIBS services. GIBS provides a robust imagery management and distribution capability for LANCE imagery products. By leveraging common identifiers for imagery layers and corresponding data products, GIBS is able to interoperate with other EOSDIS resources like ECHO to facilitate data discovery and access.

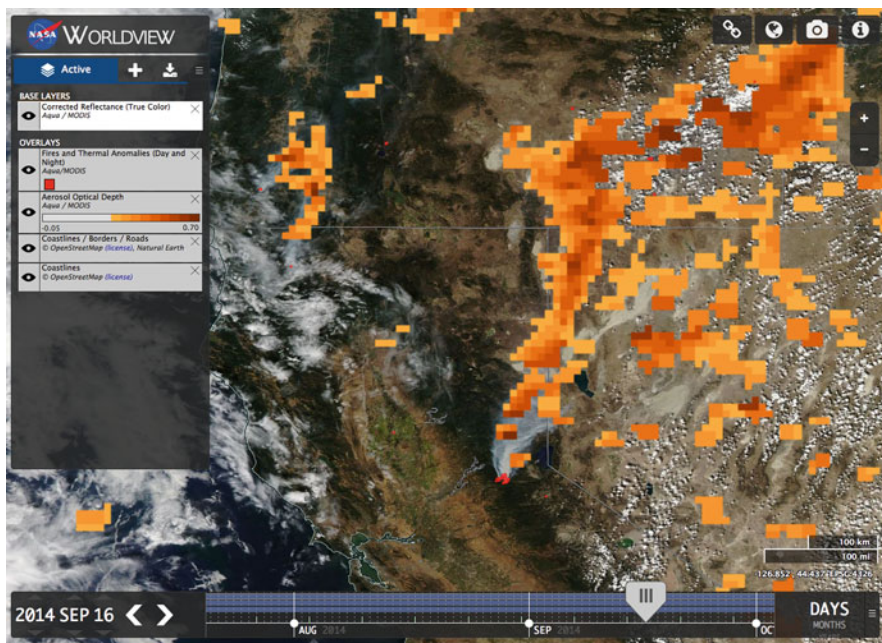


Fig. 4 Worldview showing wildfires burning in California on August 24th 2013. The base layer is a Corrected Reflectance (*true color*) image from Aqua’s MODIS instrument. This is overlaid with MODIS Fire and Thermal Anomalies shown as small *red* pixels and a carbon monoxide, in large pixels in varying shades of *red* and *orange*, from Aqua’s AIRS instrument

5.4 Worldview

Worldview is a web-based imagery browsing tool from EOSDIS which is designed for interactive visualization, discovery, and downloading of NASA data. By using GIBS to supply the imagery, Worldview users can quickly zoom, pan, and skip through time to visualize data from any spatial region and date of interest (Fig. 4). For high latitude use cases, imagery can be shown in Arctic and Antarctic polar stereographic map projections. The overall goal of the interface is to make imagery more accessible to all, including those not trained in remote sensing. Worldview has functionality to download the full-resolution imagery and the NRT data files from which it was created. The latter has been achieved in Worldview by combining the fast visual access of GIBS with searches of the ECHO metadata repository so that users can interactively browse imagery and link back to the source data.

Worldview was originally built with the NRT data user community in mind. New imagery is generally made available within 4 h of observation and most LANCE products are supported. In addition, selected products from NASA’s Socioeconomic Data and Applications Center (SEDAC) are viewable, such as population density and flood risk maps, to provide context for the NRT imagery. As Worldview continues to mature, it is expanding to include access to historical, standard science-quality

imagery for research-based use cases as well as enabling users to search for and download the underlying data through ECHO.

5.5 FIRMS

The Fire Information for Resource Management System (FIRMS) provides users with MODIS-derived hotspot/active fire locations. FIRMS data are delivered through email alerts, downloadable files, in shapefile and text file formats, or by querying the full archive of MODIS fire detections using the in Web Fire Mapper for visualization. FIRMS was originally developed at the University of Maryland, in partnership with Rapid Response under a NASA a grant from the NASA Applied Sciences Program (Davies et al. 2009).

6 Governance and Lessons Learned

LANCE is managed by NASA's Earth Science Data and Information System (ESDIS) but steered by a User Working Group (UWG) responsible for providing guidance and recommendations concerning a broad range of topics related to the LANCE system, capabilities, and services. The UWG represents the broad needs of the LANCE applications user communities, while maintaining close ties with the various Science Teams for the instruments included in LANCE. The UWG meets at least once a year to ensure that LANCE capabilities are aligned with the NRT community needs. UWG recommendations are made to ESDIS, and evaluated in terms of feasibility and cost of implementation.

LANCE capabilities are evolving based on user feedback. Significant enhancements include adding new LANCE NRT data products and providing the capability to visually select data for download.

Substantial reductions in latency have been realized by LANCE by adapting systems originally intended for science to produce NRT products. Future polar orbiting satellites could realize low latency data production earlier within their missions by focusing efforts on: (i) reducing the downlink time by using TDRSS and/or expanding the network of ground stations to include Antarctica; (ii) speeding up the delivery of Level 0 data to the appropriate processing facilities by using onboard processing of Level 0 data or once downlinked, using state-of-the-art computer networks to transmit the data; (iii) reducing the time required to create data products by using expedited algorithms that do not rely on science-quality ancillary data, or by creating products that are designed specifically for NRT (rather than science) applications; (iv) ensuring products are available in formats that are easily accessible and finally; (v) planning for low latency product generation earlier in the mission planning and development phases.

7 Conclusion

LANCE is evolving to meet the growing demand for NRT products. Under the guidance of the UWG, LANCE continues to improve, add new products and tools and expand its user base. Building on the existing EOSDIS capabilities, LANCE is a distributed system that keeps processing in the hands of the experts at designated facilities, while bringing everything together virtually on the LANCE NRT webpages on earthdata.nasa.gov.

With the exception of OMI, NRT capabilities were not considered a priority prior to launch of the spacecraft, so innovative ways have been sought to decrease latency in the ground system architecture and to expedite the processing of products. Looking to the future, LANCE can provide valuable lessons on what architecture works well and on how the delivery of global NRT products from other NASA missions might be achieved.

References

- Cordier G, McLemore B, Wood T, Wilkinson C (2010) EDOS evolution to support NASA future earth sciences missions. SpaceOps 2010 Conference Delivering on the Dream Hosted by NASA Marshall Space Flight Center and Organized by AIAA. American Institute of Aeronautics and Astronautics, Reston, Virginia, pp 1–9
- Davies DK, Ilavajhala S, Justice CO (2009) Fire information for resource management system: archiving and distributing MODIS active fire data. *Geosci Remote Sens, IEEE Trans* 47:72–79. doi:10.1109/TGRS.2008.2002076
- Hearty T, Hua X-M, Won Y-I, Savtchenko A, Theobald M, Vollmer B, Manning E, Olsen E (2010) AIRS Near Real Time (NRT) data products
- Huang H-L, Gumley LE, Strabala K, Li J, Weisz E, Rink T, Baggett KC, Davies JE, Smith WL, Dodge JC (2004) International MODIS and AIRS processing package (IMAPP): a direct broadcast software package for the NASA earth observing system. *Bull Am Meteorol Soc* 85:159–161. doi:10.1175/BAMS-85-2-159
- Justice C, Wolfe R, Desclotres J, Vermote E, Owens J, Masuoka E (2000) The availability and status of MODIS land data products. *Earth Obs* 12:10–17
- Justice CO, Townshend JRG, Vermote EF, Masuoka E, Wolfe RE, Saleous N, Roy DP, Morisette JT (2002) An overview of MODIS land data processing and product status. *Remote Sens Environ* 83:3–15. doi:10.1016/S0034-4257(02)00084-6
- Lambert A, Read WG, Froidevaux L, Schwartz MJ, Livesey NJ, Pumphrey HC, Manney GL, Santee ML, Wagner PA, Snyder W Van, Yanovsky I, Nguyen H, Cuddy DT, Perun VS, Martinez E (2012) Aura microwave limb sounder (MLS) version 3.4 Level-2 near-real-time data users guide. <http://mils.jpl.nasa.gov/data/NRT-user-guide-v34.pdf>. Accessed 8 April 2015
- LANCE User Working Group Meeting Report (2010) https://earthdata.nasa.gov/sites/default/files/field/document/UWG_Report_Final.pdf. Accessed 8 April 2015
- Michael K, Murphy K, Lowe D, Masuoka E, Vollmer B, Tilmes C, Teague M, Ye G, Maiden M, Goodman HM, Justice C (2010) Implementation of the land, atmosphere near real-time capability for EOS (LANCE). *Geosci Remote Sens Symp (IGARSS) 2010 IEEE Int.* doi:10.1109/IGARSS.2010.5650534
- Pinheiro ACT, Desclotres J, Privette JL, Susskind J, Iredell L, Schmaltz J (2007) Near-real time retrievals of land surface temperature within the MODIS Rapid Response System. *Remote Sens of Environ* 106:326–336. doi:10.1016/j.rse.2006.09.006

- Quayle B, Sohlberg R, Descloitres J (2004) Operational remote sensing technologies for wildfire assessment. *Geoscience and Remote Sensing Symposium. IGARSS'04. Proceedings 2004 IEEE Int 3:2245–2247* vol.3. doi: 10.1109/IGARSS.2004.1370809
- Sohlberg R, Descloitres J, Bobbe T (2001) MODIS land rapid response: operational use of Terra data for USFS wildfire management. *Earth Obs* 13:8–10
- Urbanski SP, Salmon JM, Nordgren BL, Hao WM (2009) A MODIS direct broadcast algorithm for mapping wildfire burned area in the western United States. *Remote Sens Environ* 113:2511–2526. doi:10.1016/j.rse.2009.07.007
- Vermote EF, El Saleous NZ, Justice CO (2002) Atmospheric correction of MODIS data in the visible to middle infrared: first results. *Remote Sens Environ* 83:97–111

Part III Applications

A Comprehensive Analysis of Building Damage in the 2010 Haiti Earthquake Using High-Resolution Imagery and Crowdsourcing

John S. Bevington, Ronald T. Eguchi, Stuart Gill,
Shubharoop Ghosh and Charles K. Huyck

Abstract

This chapter provides a detailed account of how technology, inspiration and collaboration were used to rapidly assess damage caused by the devastating January 12, 2010 Haiti earthquake. This was one of the first events where remote sensing technology (especially high spatial resolution imagery) was embraced in a truly operational sense to support post-disaster recovery planning. Sub-meter satellite imagery was available the day following the earthquake, and provided the first glimpse of the destruction caused by the earthquake. Days later, finer spatial resolution aerial imagery became available and provided even more detail on building damage. Together, these datasets allowed over 600 remote sensing experts and engineers to generate one of the most comprehensive assessments of earthquake building damage in the last decade. Furthermore, this information was shared with Haitian government in the form of a *Building Damage Assessment*

J. S. Bevington (✉)

ImageCat Ltd., 150 Minories, London EC3N 1LS, UK
e-mail: jb@imagecatinc.com

R. T. Eguchi · S. Ghosh · C. K. Huyck

ImageCat, Inc., 400 Oceangate, Long Beach, CA 90802, USA
e-mail: rte@imagecatinc.com

S. Ghosh

e-mail: sg@imagecatinc.com

C. K. Huyck

e-mail: ckh@imagecatinc.com

S. Gill

SecondMuse, 1002 Paseo de la Cuma Santa Fe, Santa Fe, NM 87501, USA
e-mail: stuart.gill@secondmuse.com

Report in support of the Post-Disaster Needs Assessment (PDNA) and Recovery Framework.

A unique crowd-sourcing initiative instigated by ImageCat in support of the World Bank's initial response to the disaster enabled reliable and timely information on damages to be generated. The chapter describes the various phases completed by the project team, including a Phase 1 damage assessment using satellite imagery and a Phase 2 assessment using aerial imagery. We discuss the World Bank-ImageCat-Rochester Institute of Technology remote sensing team's collection and analysis of very high spatial resolution aerial imagery over greater Port-au-Prince, which played a central role for the Phase 2 damage analysis. In addition, participation in the PDNA damage assessment with the United Nation's UNITAR/UNOSAT unit and the European Commission's Joint Research Centre is also discussed. The chapter concludes with a series of recommendations that are focused on better use of the technologies described in this study and a roadmap on how some of the products can be used for pre- and post-event planning for future devastating disasters.

Keywords

Crowdsourcing · Damage assessment · Earthquake · GEO-CAN · Remote sensing

1 Introduction

On January 12, 2010, a magnitude (M_w) 7.0 earthquake struck the Port-au-Prince region of Haiti. The epicenter was located immediately to the west of the city of Port-au-Prince at 18.443°N , 72.571°W , and a depth of 13 km. According to official estimates from the Haitian Government, the impacts caused by this event included 316,000¹ people killed, 300,000 injured, and 1.3 million people displaced (USGS 2010). In addition, significant damage to buildings, infrastructure and other critical services was observed as well as fatalities from localized tsunami waves. While not considered a *great* earthquake in seismological standards, this event was one of the deadliest earthquakes of the twenty-first century and spurred a unique remote-sensing based response.

On March 3, 2010, the World Bank and the Global Facility for Disaster Reduction and Recovery (GFDRR), working jointly with the United Nations Institute for Training and Research (UNITAR)—Operational Satellite and Applications Programme (UNOSAT), the European Commission (EC) through the Joint Research Centre (JRC) and the Centre National d'Information Geo-Spatial (CNIGS), submitted to the Government of Haiti the *Building Damage Assessment Report* (BDAR)

¹ This figure is disputed, with other estimates suggesting fewer than 100,000 killed (http://earthquake.usgs.gov/earthquakes/world/most_destructive.php).

that supports the Post Disaster Needs Assessment (PDNA) and Recovery Framework. This document contained technical assistance to support the reconstruction of damaged areas and contribute to the long-term national strategic development plan.

The BDAR report documented the results of substantial global technical assistance provided after the earthquake. The needs assessment was based on the best available data and information at the time of publication. Image analysts at UNITAR/UNOSAT and EC JRC had used manual photo-interpretation methods to classify buildings into different earthquake damage classes. Additionally, The World Bank/GFDRR had produced a building damage assessment using remotely-sensed imagery by commissioning the *GEO-CAN* (Global Earth Observation Catastrophe Assessment Network) community—a network of volunteer engineers and scientists coordinated by risk management consultants, ImageCat.

The Haiti event was illuminating in several respects. Firstly, unprecedented use of high and very-high spatial resolution remotely-sensed data² for the purpose of rapid damage assessment was documented. Although there have been many studies published where remote sensing technologies were instrumental in the assessment of post-disaster effects, this particular effort was unique in both scope and the rapidity at which these datasets were made available to the public and relief organizations. Very-high spatial resolution (VHR) imagery at a ground sampling distance of 15 cm was made available to a broad set of users which eventually led to multiple damage datasets being produced. These datasets were cross-compared in order to improve the accuracy and reliability of the final damage totals for Haiti. In developing these integrated damage datasets, significant benefits were accrued through the strong partnership formed among the three key organizations, i.e., the World Bank/GFDRR, the UN through its UNOSAT group, and the EC's Joint Research Centre. Although mandated several years ago to work together to prepare joint PDNA assessments, the Haiti earthquake is the first event in which technical collaboration took place.

Second, the speed at which these high spatial resolution imagery datasets were made available to end-users was phenomenal. Commercial satellite sensor, GeoEye-1 (50 cm spatial resolution), captured imagery of Port-au-Prince the day after the earthquake and GeoEye quickly made the image available to response agencies by distribution on Google Earth within days, allowing responders to quickly assess the most damaged areas. In addition to this, public, defense, and private airborne assets were contracted to fly targeted missions using a rich set of sensors, including very-high spatial resolution aerial optical and thermal infrared (IR) imagery and LIDAR. The World Bank led one such effort by commissioning Rochester Institute of Technology (RIT) to fly a seven-day aerial mission over the city and areas west of Port-au-Prince (the WB-IC-RIT Remote Sensing Mission). This mission, staged out of Aguadillo, Puerto Rico and Puerto Plata, Dominican Republic, captured long-wave, short-wave and micro-wave IR, optical (RGB), and LIDAR data over an area of 650 km² using Indigo Phoenix infrared imagers and one Geospatial Systems KCM-11 visible camera. In total, 60,764 individual raw images (1.1TB)

² When describing this study, we classify the resolution of satellite imagery (sub-meter) as “high spatial resolution” and that of aerial imagery (< 30 cm) as “very high spatial resolution”.

were transferred from the University of Puerto Rico at Mayaguez to RIT (Rochester, NY), where they were orthorectified and distributed to end-users. The eventual users of these data—besides ImageCat and the GEO-CAN community—included the UN, NGOs and US federal agencies, including the US Geological Survey who made the data available to responders through the International Charter for Space and Major Disasters. Because of the rapid collection of these key datasets, dissemination via online web services, and a very large network of people conducting analysis of the data, a full and comprehensive damage assessment was produced in less than two months.

Third, this effort was unique in that *crowdsourcing* was implemented on a large scale for the very first time to produce widespread post-disaster damage maps. Coordinated by ImageCat, over 600 engineering and scientific experts from 23 countries participated in an unprecedented mission to use VHR optical imagery to perform rapid damage assessments using the internet as the primary data delivery and display platform. These volunteers, driven by altruism to share their scientific and technical knowledge to help in any way, meant that the GEO-CAN was able to produce relatively complex damage maps and databases on over 30,000 collapsed and heavily-damaged buildings in a matter of days.

2 Timeline

A two-phased analysis was undertaken by GEO-CAN to develop a comprehensive building damage database using visual interpretations of satellite and aerial imagery. This approach was adopted to effectively utilize different imagery datasets as they became available (Table 1). Phase 1 involved identifying destroyed buildings through visual interpretation of GeoEye-1 satellite imagery, resulting in a points database. In Phase 2a and 2b (Table 1), VHR aerial imagery (15 cm) from the WB-IC-RIT and Google aerial missions was interpreted to delineate building footprints of collapsed or very heavily damaged buildings³. In addition, VHR imagery was visually interpreted to create land use information for Port-au-Prince and to estimate the total building area (square footage) of buildings that require significant repairs or reconstruction. The latter two products were required for financial assessment of rebuilding in the BDAR report.

³ Damage grades 4 and 5 represent Grade 4 and 5 of the European Macroseismic Scale 1998 (EMS-98; Grünthal 1998). These were used to classify buildings that were “very heavily damaged” or “destroyed”, respectively.

Table 1 Damage assessment timeline. A multi-phase approach was used to crowd-source the analysis of imagery from several sources: satellite imagery captured one day after the earthquake allowed a rapid overview of damage. A more detailed analysis followed when finer spatial resolution aerial imagery had been collected. Not included here was a further Phase 3 (liquefaction survey)

Start–end date	Duration	Description of activities	Imagery used	Coverage area (km ²)	Coverage communities
1/16/10–1/17/10	48 h	Phase 1: Detection of building damage (point locations)	Pre-event imagery: High-resolution satellite data served through Google Earth from various sources, including DigitalGlobe, GeoEye Post-event imagery: GeoEye-01 scenes (13 January 2010) 5V100113C0004594564 B523010701382M_001 567312.tif & 5V100113C0004594564 B523013801682M_001 567312.tif	~ 130	Port-au-Prince
1/18/10–1/26/10	8 days	Phase 2A—Delineation of damage (building footprints)	Pre-event imagery: high-resolution satellite data served through Google Earth from various sources- DigitalGlobe, GeoEye Post-event imagery: 15 cm Aerial imagery WB-IC-RIT remote sensing mission and Google	~ 350	Port-au-Prince
1/27/10–2/15/10	19 days	Phase 2B—Delineation of damage (building footprints)	Pre-event imagery: high-resolution data served through Google Earth from various sources- DigitalGlobe, GeoEye Post-event imagery: 15 cm Aerial imagery WB-IC-RIT remote sensing mission and Google	~ 200	Léogâne Carrefour Grand Goâve Petit Goâve Jacmel Hinche

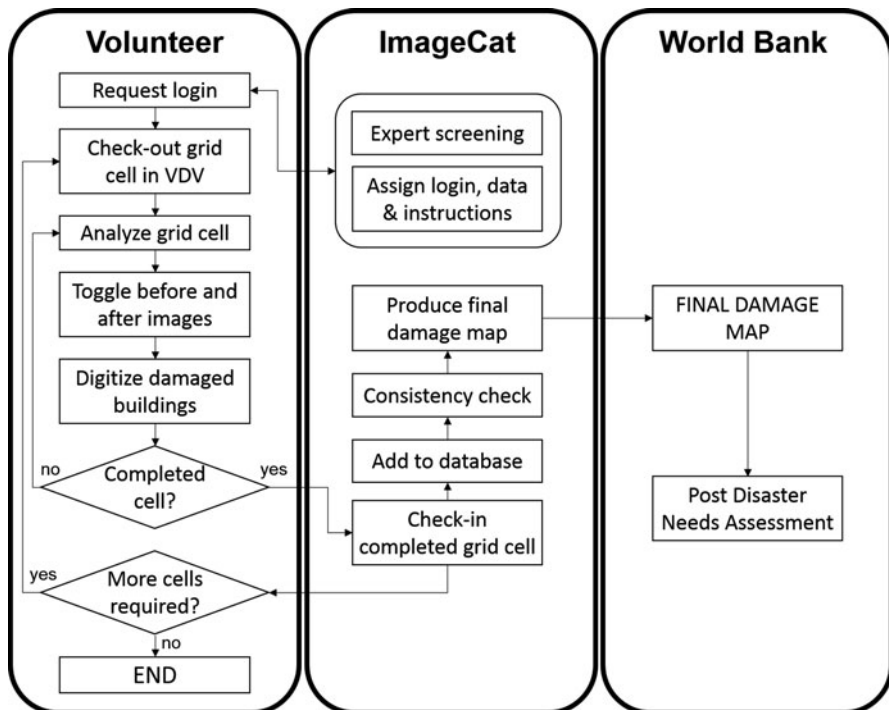


Fig. 1 The ImageCat/GEO-CAN Operational Workflow. Volunteers from the scientific community provided time and experience to analyze before and after earthquake imagery to assess damage to individual buildings. The online Virtual Disaster Viewer provided a portal for data collation, analysis and dissemination following a robust QA process

3 Damage Assessment Procedure

A multi-phased damage assessment was implemented to effectively utilize the GEO-CAN experts' experience in image analysis, earthquake engineering and other disciplines. Initially, the study area (including Port-au-Prince, Carrefour, Léogâne, Gressier, Petit-Goâve, Grand Goâve, and Jacmel) was divided into a grid of square cells, with volunteers using ImageCat's customized web platform, the Virtual Disaster Viewer (VDV), to check-out one cell at a time for analysis and check-in the completed cell, along with damage identified to all buildings within the cell. Each grid cell was automatically locked for editing by VDV until the cell was checked-in as completed. A rigorous quality assurance process followed to check submitted damage and provide additional training for analysts. The discussions below describe the analysis method used by each expert in assigning damage levels to each building.

Figure 1 shows the operational workflow that volunteers followed in the Phase 2 damage assessment. Volunteers registered their interest with the GEO-CAN ad-

ministrators. They provided information on their level of expertise in analyzing remotely-sensed imagery, and their experience in engineering, image analysis or other relevant disciplines. From this, administrators were able to assign grid squares to suit the analyst's experience level, with grid cells containing the most complex building configurations reserved for engineers, image analysts or the QA scientists at ImageCat.

On registration and declaration of their scientific background, each volunteer was provided with login credentials to VDV and training documentation. For the analysis, an analyst could check-out one grid cell at a time, which was then locked—it could not be reassigned—until it was checked-in as completed. Pre- and post-event satellite and aerial imagery was served through Google Earth and the analyst systematically worked around the grid cell, toggling between pre- and post-event imagery. Where changes in buildings were found, the building was assigned a damage level (either Grade 4 or 5 based on the EMS-98 damage scale). For Phase 2 analysis, the building perimeter was digitized as a polygon (using the pre-earthquake image for reference). This was done in order to estimate the total building area that would have to be replaced if the structure was beyond repair or a total loss. In addition to the building footprints and the assigned damage levels, a level of confidence for each damage assignment (0–100 %) was submitted to the GEO-CAN Administrator by the analyst.

4 Visual Damage Assessment

The Remote Sensing for Earthquake Scale⁴, which equates to the European Macro-Seismic Scale (EMS-98), was used to classify determinations of damaged and collapsed buildings. Although a prerequisite had been established for analysts to be trained GIS or remote sensing professionals, the protocol for identifying significant building damage was reviewed by each volunteer. Examples of the damage protocol were used to train volunteers to recognize the chaotic debris/rubble patterns of building damage that are frequently visible when a building collapses. The patterns are often influenced by the type of building materials used in construction and the type of building.

Collapsed buildings were often observed as being spectrally much brighter than the surrounding buildings and in many cases, had rough or more variegated textures. This was frequently seen in the images of Haiti due to prevalence of cement/concrete construction practices. However, analysts had to be careful that these signatures were not associated with materials in empty lots. Another example of the protocol involved looking for discontinuities in the before and after images of rectangular buildings. In toggling back and forth between two images, damaged buildings appear to shift suggesting that they may have collapsed. Despite the post-event data being

⁴ This building damage scale, developed for use with the Virtual Disaster Viewer (VDV), incorporated both engineering and remote sensing observations, with classes ranging from Indistinguishable to Collapse, and corresponds to the damage scales described in EMS-98 (Grünthal 1998).

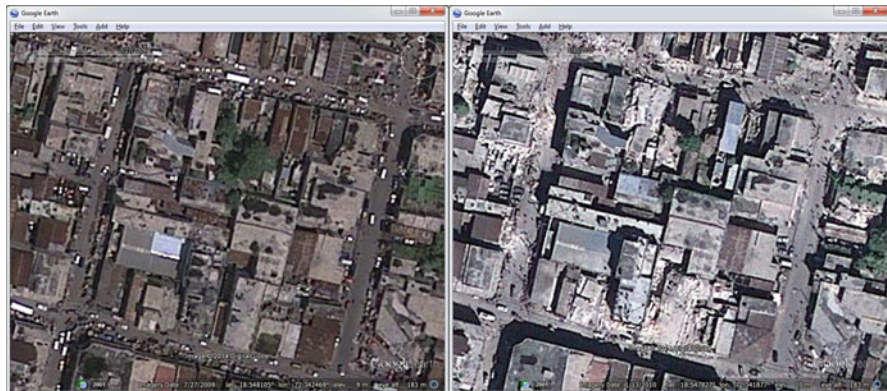


Fig. 2 Example of collapsed buildings as viewed in High-Resolution satellite imagery (50 cm) in Google Earth: Pre-event imagery is shown on the left and post-event imagery on the right. Signatures of damage include increased brightness of buildings, increased texture, offset roofs and irregular shadows (Google Earth 2014)

orthorectified, there were often mis-alignments between the pre- and post-event images served on Google Earth, meaning only a supervised approach (where human judgment could account for these discrepancies) was appropriate. The previous remote sensing experience of the analysts and protocols provided meant that analysts were able to differentiate between damage and differences in sensor and solar geometry, particularly the observational zenith angle. Changes in relative shadow heights also indicated possible soft-story failures or “pancaking.” This type of failure occurs when the bottom or lower story of a building is less robust than the upper stories and thus collapses completely under the load of the earthquake. It can be manifested in high-resolution images as a stair-step appearance on the side of the roof, or explosion of debris on the sides of the building. An interpreter can be trained to identify these conditions by toggling between before and after imagery. Examples of some of these failures are viewed in Google Earth as presented in Fig. 2. A more thorough discussion of the damage assessment methodology is provided in World Bank et al. (2013), Corbane et al. (2011) and Ghosh et al. (2011).

Once the analysis of each cell was complete, the user submitted their KML⁵ vector files containing point locations of collapsed buildings (Phase I), or polygon footprints of collapsed or heavily damaged structures (Phase II—see Table 1). Next, the user checked the grid cell back into VDV and registered the tile as completed. At this point, analysts had the opportunity to continue their involvement by analyzing a new cell. Administrators uploaded each set of observations to a central repository, where a thorough QA and consistency check was performed by ImageCat scientists. Once all cells were collated and checked (a total of 1384 cells (346 km²) and ~ 160,000 observations), the data were submitted to the World Bank.

⁵ Keyhole Markup Language (KML) files are used for expressing geographic information, primarily in Google Earth.

5 Results

Table 2 contains the final damage results for the Phase 2 GEO-CAN damage surveys for areas, including Port-au-Prince. Note that these totals solely reflect the work of the ImageCat/GEO-CAN team, and do not represent the joint final damage totals from the PDNA. (The GEO-CAN damage results were incorporated into the final PDNA report along with contributions from UNOSAT and JRC.) This table provides a tally of destroyed and heavily damaged of buildings by land-use type. Estimates of number of buildings classed in damage grade 1–3 are also provided. (More details on how these were statistically inferred can be found in World Bank et al. 2013; Corbane et al. 2011.) It also provides an estimate of the total floor area to be repaired or replaced, by damage grade and land-use type. By a large margin, the most floor area to be replaced or repaired was associated with housing units. An early estimate of the repair costs associated with all damaged buildings is also provided. Unit repair costs (\$/m²) for all land-use types were obtained from a report prepared by the Social Housing Promotion and Planning Institute of the Haiti Ministry of Social Affairs. These costs range from US\$ 40/m² for moderate to minor repairs to \$ 500/m² for complete replacement.

The total number of buildings with at least Grade 1 damage was estimated to be close to 160,000, with approximately 18 % (29,056) in Grade 4 and 5 (the damage levels identified in the image analysis). Of the 160,000 total, 90 % of buildings (142,654) were residential (low and high-density and informal/shanty), with approximately 5 % (7690) comprised of commercial, downtown or industrial buildings. From the Joint PDNA report (EC-JRC et al. 2010), it was estimated that close to 300,000 buildings in Haiti were affected by the earthquake.

The total amount of floor area to be repaired or replaced was estimated to be a little over 22 million m². Extensive repair or replacement was deemed to be required for 6.4 million m² (damage grades 3 through 5), with the vast majority were residential occupancy. The total repair and replacement costs were expected to exceed \$ 3.4 billion. Although the number of buildings with Grade 3 through 5 was lower than the total for Grades 1 and 2 (about a factor of 2.4), the estimated cost of repair or replacement of these buildings was ~ 80 % of the total cost. For higher damage grades, the likely action was not repair but replacement; replacement costs also include deconstruction and removal of debris, significantly adding to the total cost of replacement.

It should be noted that these damage totals were lower than those presented in the final PDNA damage assessment report. The PDNA reported a total of 298,739 buildings with damage. Of this total, about 60,000 buildings were identified by the joint World Bank/GEO-CAN-UNOSAT-JRC collaboration as having Grade 4 or 5 damage. The ImageCat/GEO-CAN repair/replacement cost estimate of \$ 3.4 billion was a little over half of the \$ 6.4 billion joint PDNA estimate. The reason for these discrepancies was that the ImageCat/GEO-CAN methodology emphasized accuracy over comprehensiveness, i.e., analysts were asked to only identify damage to buildings where there was a high degree of confidence in the assessment. Therefore, where damage was ambiguous or difficult to determine, these buildings were not

Table 2 Summary of damage and replacement statistics generated by the ImageCat/GEO-CAN damage assessment. These data were combined with the EC-JRC and UNOSAT damage observations for inclusion in the Building Damage Assessment Report that supported the Haiti Post-disaster Needs Assessment

	Damage grade (EMS-98)					
	Grade 1: negligible/ no visible damage	Grade 2: moderate damage	Grade 3: substantial damage	Grade 4: very heavy damage	Grade 5: destroyed	Total
	<i>Number of buildings</i>					
Residential (low density)	65,259	5675	10,404	4389	8852	94,579
Residential (high density)	14,909	1683	2645	1382	3187	23,807
Commercial	283	1039	992	646	1763	4724
Industrial	71	259	247	253	348	1178
Downtown	107	393	376	380	532	1788
Informal/ shanty	15,289	485	2427	1921	4146	24,268
Agricultural	6131	533	977	329	915	8886
Open land	64	6	10	4	9	93
<i>Total</i>	<i>102,114</i>	<i>10,074</i>	<i>18,078</i>	<i>9304</i>	<i>19,752</i>	<i>159,322</i>
	<i>Area (m²)</i>					
Residential (low density)	10,702,511	930,653	1,706,197	719,796	1,451,728	15,510,886
Residential (high density)	1,971,019	222,534	349,697	182,700	421,321	3,147,271
Commercial	44,212	162,112	154,743	100,776	275,028	736,871
Industrial	9460	34,688	33,112	33,851	46,562	157,674
Downtown	18,616	68,257	65,154	65,930	92,302	310,259
Informal/ shanty	966,255	30,675	153,374	121,407	262,027	1,533,738
Agricultural	503,980	43,824	80,345	27,044	75,213	730,406
Open land	5267	458	840	329	740	7633
<i>Total</i>	<i>14,221,319</i>	<i>1,493,201</i>	<i>2,543,461</i>	<i>1,251,834</i>	<i>2,624,922</i>	<i>22,134,737</i>
	<i>Replacement or repair cost (US\$)</i>					
Cost (US\$/m ²)	40	100	300	500	500	<i>Total</i>
<i>Total cost (millions)</i>	<i>569</i>	<i>149</i>	<i>763</i>	<i>626</i>	<i>1312</i>	<i>3420</i>

included in the GEO-CAN summaries. The end result of this approach was that the GEO-CAN values were highly reliable but did omit many buildings that had significant damage (CAR 2010).

6 Discussion and Recommendations

There were a number of successes of this remote sensing initiative. An independent geodatabase of damaged structures was produced in a timely manner—i.e. rapid enough to inform the PDNA process. The database of damaged structures and derived maps were distributed widely through the UN and donor networks to NGOs and other field operatives responding to the event. Establishing a global network of remote sensing experts meant that the interpretation process was carried out by experienced professionals.

The successes were largely because of a confluence of a number of key factors:

- i. **Image availability**—Satellite imagery was available the day after the event. This allowed preliminary damage estimates to be produced within a week of the disaster for the city of Port-au-Prince. Delivering data and maps in this time-frame allowed early insight into the unfolding humanitarian disaster, at a time where airport access and airspace was severely restricted, limiting the capacity for ground-based reconnaissance teams. Satellite remote sensing was a non-obtrusive technology that did not impede the essential search and rescue (SaR) or humanitarian relief operations. It also enabled a larger and more detailed damage assessment phase to be prepared and helped target the ground reconnaissance missions which followed the SaR activities. Even though the spatial resolution was less than that associated with the aerial imagery, satellite data was invaluable for the following reasons: rapid availability over a very large area, availability of pre-earthquake imagery, and inexpensive imagery (freely-available for responders under the International Charter). The subsequent WB-IC-RIT aerial remote sensing mission was key in providing timely data for the PDNA damage assessment. It also provided other data that had unique applications and uses (e.g., LIDAR was used to create digital elevation models used for flood risk assessment).
- ii. **Technology**—Web-based technologies allowed the distribution of huge volumes of data to analysts around the globe. Portals such as the Virtual Disaster Viewer and Google Earth meant that analysis could be distributed and results merged to form a large damage database
- iii. **Damage to local capacity**—The earthquake was particularly devastating for the Government of Haiti as a number of key governmental facilities were incapacitated by the event. Haiti's national center for geospatial information (CNIGS) was severely damaged, resulting in the deaths of a Director and other key staff. The comprehensive spatial data infrastructure and data and imagery archives were

also lost. This significantly reduced the capacity of local agencies to play a leading role in the response, meaning greater emphasis was placed on international bodies to support the geospatial response.

- iv. **Inter-agency collaborations**—A key factor in the success of the PDNA for Haiti was the agreement by all three main international responding organizations (World Bank, UNOSAT and JRC) to combine the different damage databases into one consolidated dataset. To accomplish this, extensive analysis by all parties was necessary in order to ensure consistency and complete but not overlapping coverage.
- v. **Altruism**—The humanitarian scale of the disaster was clearly evident. Combined with the fact that the US was on the same time zone and has a large Haitian diaspora meant that the event took prominence on 24 hour news channels in US and across the globe. The collective willingness of the engineering and scientific community to share their professional experience in some way to support response efforts meant that ImageCat could form the GEO-CAN community very rapidly, building on existing professional networks and connections.

Despite the success of the GEO-CAN damage assessment mission and other complementary missions, there are a number of lessons learned and recommendations for future events:

Outreach Thought should be given to how the various post-disaster databases or products can be used to address other needs, e.g., post-event rebuilding requirements, or establish post-event mitigation strategies and programs. For example, using aerial imagery to help meet cadastral data needs is a good example of how groups can leverage the cost of the initial data collection. Furthermore, more education and training is needed by the end-users of this data. A better understanding of the challenges and problems experienced by response organizations in this event will help to better integrate the different post-event products into existing workflows. Follow-up interviews highlighted how critical it is to have pre-event training, published metadata, and relationships with potential users ahead of a disaster.

Pre-event Preparation—Technical The use of crowdsourcing as a mechanism for performing damage assessments was clearly demonstrated in this event. However, the engineering and scientific community would benefit immensely from more pre-event training to effectively recognize earthquake damage from both satellite and aerial imagery. Damage assessments from nadir optical imagery fall short when evaluating special types of building collapse (such as soft-story failures) or quantifying damage that is less extensive than “collapsed” or “heavily damaged”. This was evident from subsequent detailed field assessments of damage in Port-au-Prince. In order to address this deficiency, we recommend that a detailed protocol be developed that utilizes both field surveys and oblique and vertical imagery, and that establishes where imagery should be collected and how much. This protocol should also consider, where possible, the level of ground shaking, the type of construction in the

affected regions, and the level of reliability needed in order to support key post-earthquake decisions. It is also recommended that additional research is conducted in order to develop—even at a high level—a factor which will allow the scaling of satellite damage assessments to a more accurate summary of damage, such as that afforded by VHR aerial imagery. Damage distributions inferred statistically for Grades 1 through 3 should be revisited to determine whether a fifth category representing “no damage” should be included to better balance overall damage estimates. It is anticipated that these advances could reduce the replacement cost discrepancies seen between the several damage surveys in Haiti.

Although following Haiti, each agency team utilized the same damage classification scale (EMS-98), the protocols used by each team to determine these damage grades have not been evaluated. There is a need to share best practice in this area to enable successful inter-agency collaboration in the future. The damage assessment protocols should also be extended to address other natural hazards and evaluate damage scales for other perils.

Pre-event Preparation—Operational In order to ensure consistent application of remote sensing methods in the next disaster, the three main organizations, with support from ImageCat and other groups, are pursuing the development of a set of Standard Operating Procedures (SOP). These SOPs are being designed to identify the requirements of key datasets and sensors, the appropriate set of protocols for determining the different levels of damage, procedures for integrating field observations and results with aerial or satellite damage assessments, and procedures for quantifying the reliability associated with the final datasets.

To ensure the sustainability of the GEO-CAN network as a viable entity that can be initiated following major disasters, a more formal structure should be investigated. As one of the key recommendations of this chapter, we recommend that a formal business plan be developed that will ensure that the GEO-CAN community is sustained for future events. Without such a plan, the network will continue as an informal list of scientists and engineers, called upon on sporadically. With investment, the network could be expanded to provide pre-event training, capacity-building exercises and workshops to share best practice globally.

The Haiti event was ground-breaking in the availability of satellite and aerial imagery. Numerous datasets were distributed to responders, NGOs and research organizations. However, in order to ensure that the appropriate imagery is available for the next event, we recommend that a “living” imagery fund be developed that can be used to (1) create pre-event, planning databases that will help to quantify the vulnerability of a city or area by establishing detailed building inventories on a building-by-building level (including structural type so that engineers can assess damage to building types with which they are familiar); (2) ensure that agreements with airborne data providers are in place well before the next event; (3) ensure that special imagery needs are met, e.g., LIDAR coverage, or oblique imagery in the case of earthquakes; and (4) prepare for future data collection missions (prepare for air space access in vulnerable nations, etc.); and (5) establish pre-event relationships with institutions and computing centers of excellence to support active dissemination

of data after a major disaster. Precise imagery specifications to support damage assessment are difficult to define before earthquake events due to the evolution in sensor and data hosting technologies, and the nature and location of the disaster event itself. An imagery fund, together with a committee of first responders would allow rapid decision making as to the best available data and response mechanism for the unfolding event. A multi-phased approach, as in Haiti, allows agile refinement of response in the days following the earthquake. However, close coordination of agencies in pre-event times will foster more successful post-event coordination.

7 Conclusion

This chapter provides insight into a dynamic and practical fusion of remote sensing technologies, imagery and scientists in support of the Government of Haiti following the devastating earthquake in 2010. The sheer scale of the event—covering over 1000 km², combined with accessibility restrictions in the days after the event, meant that ground-based efforts to assess damage were limited. It is difficult, therefore, to see how such a comprehensive picture of the damage could have been pieced together without the use of remote sensing or the support of the World Bank and dedication of the GEO-CAN volunteers.

References

- Cambridge Architectural Research Ltd (2010) Port-au-Prince earthquake damage assessment using pictometry. A report prepared for ImageCat, Inc., June 2010. http://www.eqclearinghouse.org/20100112-haiti/wp-content/uploads/2010/02/PaP_damage-assessment-using-Pictometry.pdf. Accessed 22 Sept 2013
- Corbane C, Saito K, Dell’Oro L, Gill SPD, Piard E, Huyck CK, Kemper T, Lemoine G, Spence RJS, Shankar R, Senegas O, Ghesquiere F, Lallemand D, Evans GB, Gartley RA, Toro J, Ghosh S, Svekla WD, Adams BJ, Eguchi R (2011) A comprehensive analysis of building damage in the 12 January 2010 Mw7 Haiti earthquake using high resolution satellite and aerial imagery. *Photogramm Eng Remote Sens* 77(10):997–1009
- European Commission-Joint Research Centre, United Nations Institute for Training and Research-Operational Satellite Applications Program, World Bank-Global Facility for Disaster Reduction and Recovery, Centre National d’Information Geo-Spatial (2010) Building damage assessment report—Haiti earthquake 12 January 2010, post-disaster needs assessment and recovery framework (PDNA) v3.0. 11 Mar 2010
- Ghosh S, Huyck C, Greene M, Gill S, Bevington J, Svekla W, DesRoches R, Eguchi R, (2011) Crowd-sourcing for rapid damage assessment: the global earth observation catastrophe assessment network (GEO-CAN). *Earthq Spectra* 27:S179–S198.
- Grünthal G (ed) (1998) European Macroseismic Scale 1998. *Cahiers du Centre Européen de Géodynamique et de Sismologie*, Vol 15. Conseil de l’Europe, Luxembourg
- United States Geological Survey (2010) Magnitude 7.0—Haiti region. <http://earthquake.usgs.gov/earthquakes/eqinthenews/2010/us2010rja6>. Accessed 22 Sept 2013

World Bank, GFDRR, ImageCat (2013) Final report: 2010 Haiti earthquake—post-disaster building damage assessment using satellite and aerial imagery interpretation, field verification and modeling techniques. Report produced for the World Bank/GFDRR by Image-Cat, Inc. http://www.imagecatinc.com/wp-content/uploads/2013/08/HAITI_EQ_Final_Report_12-22-10.pdf. Accessed 22 Sept 2013

Near-Real Time Delivery of MODIS-Based Information on Forest Disturbances

Robert A. Chastain, Haans Fisk, James R. Ellenwood, Frank J. Sapio, Bonnie Ruefenacht, Mark V. Finco and Vernon Thomas

Abstract

The Real-Time Forest Disturbance (RTFD) program of the Forest Service, U.S. Department of Agriculture (USFS) provides timely spatial information regarding changes in forest conditions to the Forest Health Protection (FHP) and State and Private Forestry (S&PF) community for improving aerial detection and forest health survey efficiency. The USFS Remote Sensing Applications Center (RSAC) creates CONUS-wide forest change geospatial layers for the RTFD program every 8 days during the growing season using image data from the Moderate Resolution Imaging Spectroradiometer (MODIS), and delivers these data to a web mapping application named the Forest Disturbance Monitor (FDM) developed by the USFS Forest Health Technology Enterprise Team (FHTET).

Differences in the timing, duration, and severity of disturbances in forested landscapes result in a broad array of possible types of forest change. Two effective remote sensing change detection approaches using MODIS satellite data are employed to detect and track quick and ephemeral change as opposed to gradually occurring disturbances in forest health. The first uses a statistical (Z-score)

H. Fisk (✉)

USDA Forest Service Remote Sensing Applications Center, 2222 West 2300 South,
Salt Lake City, UT 84119, USA
e-mail: hfisk@fs.fed.us

R. A. Chastain · B. Ruefenacht · M. V. Finco
RedCastle Resources Inc., Salt Lake City, UT, USA

J. R. Ellenwood · F. J. Sapio
USDA Forest Service Forest Health Technology Enterprise Team, Fort Collins, CO, USA

Vernon Thomas
Cherokee Nation Technology, Fort Collins, CO, USA

change detection approach designed to discern intraseasonal ‘quick’ changes in forest conditions caused by events such as defoliations or storm damage. The second approach uses trend analysis to identify areas where slower, multiyear changes occur in forested areas, such as bark beetle outbreaks and drought stress in the western coniferous forest biome.

Keywords

MODIS · Forest health monitoring · Forest insects and disease · Change detection · Z-score · Trend analysis

1 Introduction

There are about 749 million acres (303 million ha) of forested land in the contiguous United States. Forest ecosystems affect the global carbon cycle as well as regional hydrology and climate through their influence on water and energy budgets (Adams et al. 2010). A 2006 risk assessment, performed by FHTET, estimated that 58 million acres (23 million ha) of this land are at risk from 42 insect and disease risk agents, 13 of which are non-native. Drought and warming have been cited as drivers of extensive insect outbreaks occurring in western North America from Alaska to Mexico (Raffa et al. 2008). Other sources of forest stress and mortality include wind and ice storm damage, drought and other anomalous climatic conditions, fire, and flooding. The RTFD program has been implemented to detect and track changes in forest conditions across the conterminous 48 states (CONUS) in order to provide an early warning—similar to a smoke alarm—in an attempt to inform local and state forestry personnel so that they may respond with appropriate resources for management purposes.

Aerial detection surveys (ADS), which are a major component of the USFS Insect and Disease Survey (IDS), are conducted annually using a variety of light fixed and rotor wing aircraft. USFS, state and other federal cooperators work together to complete overview surveys in order to map current year forest injury. Some regions have been conducting ADS for more than 60 years; others have become more active within the last decade. Data collected during these surveys has proven useful in early detection of invasive species and for rapid response actions such as quarantine, control or eradication. The effects of endemic pest outbreaks are also recorded and provided to national and local area land managers, referenced in a variety of conditions and congressional reports to aid decision making. The RTFD program aims to enhance and supplement information for the current national Forest Health Protection (USDA, FHP) forest health IDS. Forest change data generated as part of the RTFD project allows a near real-time synoptic assessment of any region in the CONUS to determine where potential forest disturbance activity may be occurring prior to an actual aerial or ground survey. The RTFD data facilitates FHP survey community efforts, allowing for more cost effective and safe allocation of resources for aerial and/or ground survey.

2 Objective

The main objective of the RTFD program is to provide timely spatial information regarding changes in forest conditions to the Forest Health Protection (FHP) and State and Private Forestry (S&PF) communities to improve aerial detection and forest health survey efficiency. A broad array of potential changes can occur in a forested landscape, which can differ along both temporal and spatial dimensions. Any attempt to identify and track forest disturbances on a continental scale must be sufficiently flexible and comprehensive so that quick and ephemeral (e.g., frost damage or canopy defoliation) and gradually developing (e.g., forest degradation from drought and/or bark beetle) forest disturbances can be reliably detected. When attempting to detect and monitor forest disturbances using remote sensing image data and change detection methods, the spatial and temporal nature of these disturbances influence the selection of an appropriate sensor platform as well as the change detection methodology implemented.

Spatial data produced for the RTFD program highlight departures from expected forest conditions, which are identified using two distinct digital image change detection methodologies implemented in near real-time, using 16-day Moderate-resolution Imaging Spectroradiometer (MODIS) image composites that are updated every 8 days. The RTFD approach uses MODIS Aqua and Terra satellite imagery, as these data provide daily coverage, permitting frequent observations to follow developing disturbances and capture forest disturbances that may have a very finite temporal window. MODIS data includes visible, NIR, and MIR wavelength bands, permitting the calculation of spectral indices of vegetation greenness and vigor. These spatial data have been produced for the 2008 through 2013 growing seasons. In the eastern deciduous biome, the RTFD approach has detected and tracked forest tent caterpillar (*Malacosoma disstria*), winter moth (*Operophtera brumata*), fall webworm (*Hyphantria cunea*), and gypsy moth (*Lymantria dispar*) defoliation events in numerous locations. Beech Bark disease, caused by a complex of the beech scale (*Cryptococcus fagisuga*), and a fungi, primarily *Nectria coccinea* var. *faginata*, has been detected along the mortality front in the Great Lakes region. In the western coniferous biome, red attack and mortality associated with mountain pine beetle (*Dendroctonus ponderosae*) and spruce budworm activity (*Choristoneura occidentalis*) have been detected and tracked, as well as defoliation from pine butterfly (*Neophasia menapia*). Additionally, this approach has had significant success in tracking forest damage associated with tornadoes, hail, and ice storms.

Since 2009, a number of innovations and enhancements have been implemented to: (1) address challenges of detecting specific forest disturbance types in disparate regions of the CONUS, (2) address FHP and S&PF community data access needs, (3) deal with persistent cloud and other anomalies in composited MODIS imagery, and (4) enhance the detection of slowly occurring trends in forest degradation and mortality. Specific activities to address these needs and advance the RTFD program are discussed below.

- A quantitative retrospective assessment of 2010 RTFD results was performed to identify potential modifications to the RTFD approach in order to improve the effectiveness in detecting specific forest disturbance types in disparate regions of the CONUS. Various methodological alterations were assessed within six study areas wherein forest disturbances occurred during 2010—principally, the use of different vegetation indices and alterations in baseline definition. Bi-temporal Landsat change detection results acted as reference data to which RTFD Z-score change detection results were compared. Findings indicate that a one-size-fits-all paradigm is not the most effective approach to identify and track all types of forest disturbances across the CONUS. Specifically, two fundamental conclusions were drawn from this assessment: (1) the normalized difference vegetation index (NDVI) is a more effective change index for use in the eastern deciduous biome, with a baseline defined using per-pixel median values of NDVI from input imagery, and (2) the normalized difference moisture index (NDMI) is a more useful change index in the western coniferous biome, with a baseline defined using per-pixel maximum values of NDVI from input imagery.
- The web-based mapping application named the Forest Disturbance Monitor (FDM) was developed by FHTET to enable the FHP survey community to interact with the RTFD raster datasets and evaluate potential forest disturbances over large areas, thereby providing timely information for aerial survey resource allocation and related decision support.
- In 2012, the RTFD program added a key spatial data layer to the FDM interface—persistence of forest disturbance—to augment existing 16-day composited forest disturbance raster datasets. The persistence of forest disturbance data layer combines the results of the last three 16-day compositing period RTFD change products, to minimize the data noise inherent in individual compositing period change products which arise from persistent cloud cover and other MODIS data ephemera. The persistence of disturbance data layer classifies the number of times a pixel was disturbed over the last three compositing periods with different levels (standard deviations) of departure from expected RTFD values.
- Beginning in the 2013 season, a novel forest disturbance data product using time series trend analysis was created and delivered for each 16-day composite time frame to the FHP and S&PF user community via the FDM web mapping application. The forest disturbance trend data product employs a process that first computes a least squares regression model for each pixel location in a time 5-year time series raster image stack, then maps the trend slope for each pixel location in that raster stack. This technique enables the detection of long-term, gradual disturbances common with pine beetle and other non-defoliating forest disturbances more common in the western coniferous forests (Kennedy et al. 2007). In addition, a trend disturbance persistence data product was also produced that integrates the trend disturbance data from the previous three compositing period. To conform to the time-sensitive data delivery framework of the RTFD project, these data are incorporated into the FDM alongside the Z-score forest change data every 8 days.

3 Forest Change Detection Process

MODIS was launched by NASA in 1999 on board the on board the Terra satellite, followed by another MODIS instrument on the Aqua satellite in 2002. The orbital parameters of the Aqua and Terra satellites and swath size of the imagery collected allow these instruments to image most portions of the Earth's surface every day. The MODIS instruments capture 36 spectral bands ranging from 405 to 14,400 nm. MODIS data are employed for the current RTFD methodology to perform remote sensing-based forest change detection following two distinct approaches: (1) statistical two-date comparison of MODIS image composites, and (2) analysis of trends apparent in annual composited MODIS image data. The first approach is enabled through comparison of baseline image data constructed from a stack comprised of previous years of MODIS imagery with anniversary date image data from the current year. The baseline image data represent the expected condition of the forest, which is compared to the current year image data using a statistical "Z-score" method (Nielsen et al. 2008). The latter approach is implemented by mapping the slope from linear per-pixel regression models computed from the last 5 years of anniversary composited data. Both of these approaches utilize image products that are created by compositing 16-days of image data so that relatively cloud-free imagery can be used to perform change detections. These 16-day composites are updated every 8 days, so that timely information can be created to track developing forest disturbances. RTFD analysis is limited to forested pixels, which are defined using the FIA forest group type map (Ruefenacht et al. 2008).

3.1 Baseline Data Development

To create baseline raster datasets representing the expected forest health conditions for the Z-score change analysis, MOD09 8-day composited MODIS image data from a number of previous years are combined to produce 8-day (2008 and 2009), and 16-day (2010–2014 growing season) compositing periods. The decision to increase the length of MODIS compositing periods from 8- to 16-days was based on experience gained through producing RTFD datasets in a production setting. The 16-day compositing period provide an optimal balance between the timeliness of the information in the image composites and the ability to obtain cloud-free image data with which to detect forest disturbances. The 16-day compositing periods are staggered such that one begins every 8 days during growing season. The growing season is defined as Julian day 73 (March 14) through 313 (November 24). MODIS MOD09 (and MYD09) data are obtained in Hierarchical Data Format (HDF) format from the NASA Land Processes Distributed Active Archive Center (LPDAAC) and reprojected into Albers. A mask created using USGS multizone boundaries is applied to the MODIS tiles to perform separate digital change detections within finite regional areas.

Early in 2011, a quantitative retrospective assessment of 2010 RTFD results was performed to identify potential modifications to the analytical logic of the Z-score

change data methodology in order to improve detection efficiency. The findings of this retrospective assessment indicate that a one-size-fits-all paradigm is not the most effective approach to identify and track forest changes across the CONUS. Appropriate changes have been implemented in the RTFD approach for subsequent growing seasons to incorporate these findings. Two separate baseline composites of MODIS data are now produced for the Z-score forest change analysis. These baseline raster data sets include 3-year composites which are compiled by selecting the median (in the deciduous eastern biome) or maximum (in the coniferous western biome) NDVI value at every pixel location from an image stack comprised of temporally-adjacent Aqua and Terra 8-day composited reflectance images (MOD09). The image stacks therefore contain a total of 12 MODIS Aqua and Terra image inputs for 3-year baseline composites. The MODIS band 1–7 reflectance values from the image corresponding to the pixel-wise median or maximum NDVI value are then written to a new raster, which serves as the baseline image.

For the trend analysis forest change products, a completely different historical record is needed. For this analysis, the previous 4 years of MODIS data are pre-processed to match the current year 16-day composited MODIS data. This involves identifying maximum greenness values in both the MODIS Aqua and Terra image data. Composites of maximum NDVI values are first created for the Aqua and Terra images for the adjacent MOD09 (8-day) composites that fall within the 16-day compositing temporal window, then using these NDVI values in the eastern deciduous biome, and computing maximum NDMI values in the western coniferous biome. These greenness values are then rescaled to a 0–100 range, and stacked so that a per-pixel regression model can be computed by “drilling through” the past 5 years of NDVI (east) or NDMI (west) values (Fig. 1).

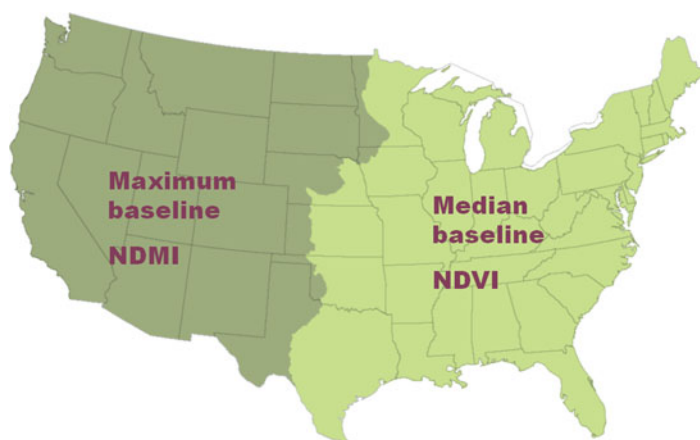


Fig. 1 A map showing the spatial extent of the greenness indices and baseline methods used to compute forest change data products for the RTFD program

3.2 Current Year Data Development

The incoming, or current year, image data is derived from daily MODIS MOD03 L2 swath data that is downloaded using a direct feed from an antenna on the roof of the RSAC building in Salt Lake City, UT. The first seven bands of the MODIS Level 2 Corrected Reflectance (CREFL) product are the source data used to create composited images based on image quality. Bands 1 and 2 have a spatial resolution of 250 m, and bands 3–7 have a spatial resolution of 500 m.

The native HDF data is transformed into GeoTiff formatted data in the geographic reference system (lat-long) using MRT, then reprojected into Albers equal area and combined into an 11 band image stack (six reflectance bands, along with day of year, sensor angle, sensor zenith, solar angle, and solar zenith). The NDVI is calculated for the daily images, and these data are masked based on viewing angle and cloud saturation.

After 16 days of imagery is collected, the maximum NDVI is used to select on a per-pixel basis from which input images the reflectance information will originate. The first step entails the creation of image masks, which are binary images where 0 represents areas where the sensor zenith is greater than 50 degrees or areas of super-saturated pixels. MODIS pixels that are associated with an image mask value of 0 are not considered for compositing. The next steps include the creation of band quality, mean focal standard deviation, and NDVI layers. The band quality layers are used as a shadow detector. Pixel values for layers 1, 2, and 4 are summed, with higher values indicating a higher band quality ranking. A 5×5 window is used to calculate an average focal standard deviation, which is calculated on all of the layers of the MODIS images. The band quality, mean focal standard deviation, and NDVI layers are used to determine which pixel to use for the compositing. For each pixel, a quality ranking is assigned by doing the following:

1. Identify the dates with the top three highest NDVI values and assign a ranking such as N—10, N—20, N—30 where N is equal to the number of MODIS images being used for the compositing multiplied by 10.
2. Identify the dates with the three lowest mean focal standard deviation values and assign a ranking such as N—10, N—20, N—30 where N is equal to the number of MODIS images being used for the compositing multiplied by 10.
3. Add the NDVI ranking and the mean focal standard deviation ranking to the band quality ranking.

Then, the following rules are followed to decide which of the three dates with the highest pixel quality value is used for the MODIS composite.

1. If a pixel has the highest pixel quality as compared to the pixels from the other two dates and a sensor zenith of less than or equal to 30 degrees, select the MODIS pixel from this date for the compositing.
2. If the first condition is not met, select the MODIS pixel from the date with the lowest sensor zenith.

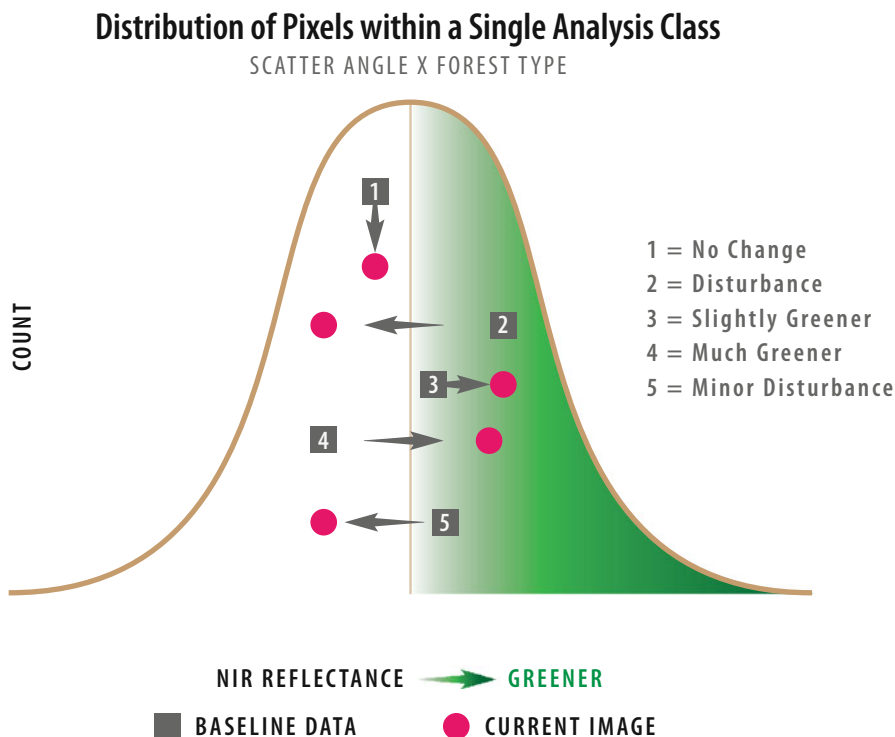


Fig. 2 A schematic illustration of the manner in which changes in forest conditions are identified using the statistical Z-score approach. This example illustrates how the relative positions in statistical space of NIR reflectance pixel values of baseline and current year MODIS imagery relate to apparent changes in the condition of a forested pixel

A clean-up process that uses a 3×3 majority filter is applied to the day of year data to avoid excessive speckle in the output imagery. After this filtering, the reflectance bands, four viewing geometry variables, and day of year pixel data are composited for the 16-day period. Outputs are masked to the 14 separate USGS multizones (Fig. 1), and a 250 m resolution 6-band reflectance image stack is produced, along with a 4-band viewing geometry image stack, and a day of year stack.

3.3 Forest Disturbance Detection

The RTFD program has evolved such that two separate CONUS-wide forest change geospatial layers are created every 8 days during the growing season that originate from two disparate change detection approaches. These two approaches are designed to identify very different types of forest disturbances: Quickly occurring events and slow trends of degradation and mortality. The first forest change geospatial layer entails a two-date statistical (Z-score) change detection approach designed to discern intraseasonal ‘quick’ changes in forest conditions caused by events such as defoliations or storm damage (Fig. 2), while the second geospatial layer is derived using a

trend analysis approach which is better suited to identify areas where slower, multiyear changes are occurring in forested areas. Bark beetle outbreaks in the western coniferous forest biome are a good example of this phenomenon.

The Z-score forest disturbance geospatial layer is derived by comparing a multiyear baseline image composite with current year image data in order to identify differences in the level of greenness for pixels identified as being forested by the FIA forest type group map. Statistical analysis classes are created by combining a static forest type group class and dynamic back-scattering angle class in a factorial manner. The primary purpose for separating forested area pixels into analysis classes is to control for the Bidirectional Reflectance Distribution Function (BRDF), which posits that the reflectance of a target is a function of both illumination and viewing geometry. Back-scattering angle is computed on a per-pixel basis from a MODIS viewing geometry image stack (sensor angle, sensor zenith, solar angle, and solar zenith) using a trigonometric expression taken from Vermote and Roy (2002), then a 6-class quantile classification scheme is implemented to separate these MODIS image pixels into analysis classes. The final statistical analysis classes result from a factorial combination of forest type-group and back-scattering angle quantile classes, which are used to calculate resistant Z-scores for only the forested pixels in the incoming MODIS image composite (Fig. 2).

After the analysis classes are defined for each incoming MODIS image composite, within-class resistant Z-scores are calculated using the following equation:

$$RZ_{cbi} = \frac{x_{cbi} - \tilde{x}_{cb}}{\tilde{\sigma}_{cb}} \quad (1)$$

Where RZ_{cbi} is the relative Z-score for pixel i in class c for band b . $\tilde{\sigma}_{cb}$ is the median absolute deviation (MAD), which is the median of the absolute values of the deviations of the median. The MAD represents a robust estimate of statistical dispersion that is more resilient to outliers than the standard deviation or variance.

Then, the detection of forest disturbances is performed by first calculating an anomaly score (ΔRZ) between current and baseline data using the following equation:

$$\Delta RZ_{cbi} = RZ_{cbi} - RZ_{cbi,baseline} \quad (2)$$

where ΔRZ_{cbi} is the anomaly score of pixel i in class c for band b , which represents the difference between the RZ computed for that pixel in the incoming image composite and the anniversary date baseline composite image (Fig. 2).

Finally, the Normalized Difference Vegetation Index (NDVI) is computed using the anomaly scores (ΔRZ s) calculated from the Red and NIR reflectance bands and used as a forest condition change index in the eastern deciduous biome:

$$\Delta NDVI = \frac{\Delta RZ_{NIR} - \Delta RZ_{RED}}{\Delta RZ_{NIR} + \Delta RZ_{RED}} \quad (3)$$

In the western coniferous biome, the Normalized Difference Moisture Index (NDMI) is computed using the anomaly scores (ΔRZ s) calculated from the NIR and MIR

reflectance bands and used as a forest condition change index:

$$\Delta NDMI = \frac{\Delta RZ_{NIR} - \Delta RZ_{MIR}}{\Delta RZ_{NIR} + \Delta RZ_{MIR}} Fi \quad (4)$$

The results of the Z-score disturbance detection methods are computed separately for all 14 USGS multizones in the CONUS are then merged together. The geographic pattern for the use of maximum and median values for baseline development as well as NDVI and NDMI for change indices can be seen in Fig. 1. The data range of the CONUS-wide RTFD change product is constrained using universal maximum and minimum values. A per-pixel maximum value from the Aqua and Terra disturbance detection result is calculated for use in the CONUS-wide forest change map to remove excess noise in these results and provide a more conservative estimate of departures in forest condition.

The trend analysis forest change detection approach is derived by performing a linear regression analysis on individual pixels within a stack of greenness values derived from each of the last 5 years of MODIS image data (Fig. 3a). The first step in the process of generating forest health trend analysis geospatial data for use in the RTFD program is to derive greenness values for the past 4 years as well as the current year from composited MODIS image data. A 16-day compositing period is used for this analysis so that these data match the overarching framework of the RTFD program. For the eastern half of the CONUS, NDVI is used to represent greenness, and NDMI is used as the greenness index in the western half of the CONUS. Five-year stacks of greenness are created, then per-pixel linear regression models are computed using this time series of greenness values through an application developed at the RSAC named the Time Series Trend Analysis Tool (TSTAT). The analysis performed by TSTAT returns slope, intercept, r-value, p-value, and standard error values. Finally, a land cover condition trend geospatial layer is derived using the slope of these pixel-wise regression models. In this layer, negative slope values indicate a decline or degradation in vegetative land cover types (Fig. 3b). In contrast, positive slope values indicate increased health or recovery in these land cover types (Fig. 3c).

3.4 Persistence of Forest Change

In addition to the 16-day Z-score and trend analysis forest disturbance datasets updated every 8 days, the temporal persistence of apparent changes in forest conditions is used to generate a CONUS-wide disturbance persistence product, which is developed by combining the results of the last three 16-day compositing period RTFD change products. To eliminate noise from the change products for the individual compositing periods which arise from persistent cloud cover and other MODIS data ephemera, a classification scheme was developed which combines the number of times a pixel was apparently disturbed in the last three compositing periods with different levels [standard deviations] of departure from expected RTFD values. The Persistence of Disturbance data product is made up of three basic classes: (1)

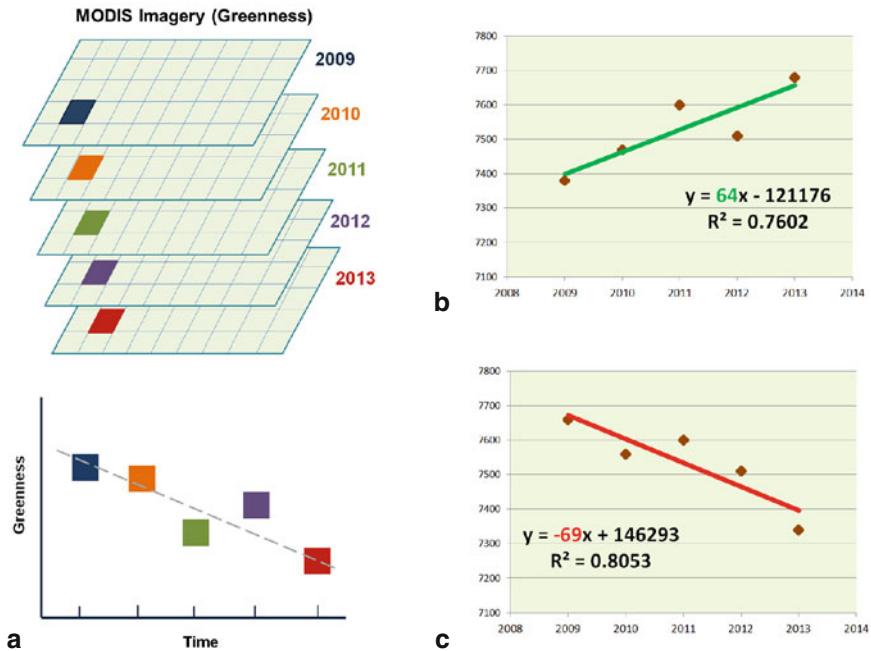


Fig. 3 Trends are derived by comparing pixel values from a 5 year stack of MODIS-derived greenness values (a). Linear regression model slope is mapped to represent trends in forest conditions, wherein a negative slope relates to a decline in greenness over time (b), and a positive slope is indicative of an increase in greenness over time (c)

persistent detectable disturbance, (2) persistent moderate disturbance and (3) persistent severe disturbance. These classes are based on a combination of the temporal persistence and the degree of departure from normal greenness. To be flagged as disturbed in the disturbance persistence raster layer, a pixel must have a value at least one standard deviation lower than the expected value for at least the last two out of three compositing periods. Successively more disturbed pixels that have RTFD values more than two standard deviations lower than the expected value in two or all three compositing periods are displayed in successively hotter colors. Figure 4 shows the difference between a single 16-day composite product and a three date persistence product.

4 Results

Comparison of the Z-score and linear trend analysis approaches for detecting and tracking forest changes confirms the premise that the Z-score method is preferable to identify rapid onset forest changes such as defoliation events typical in the eastern

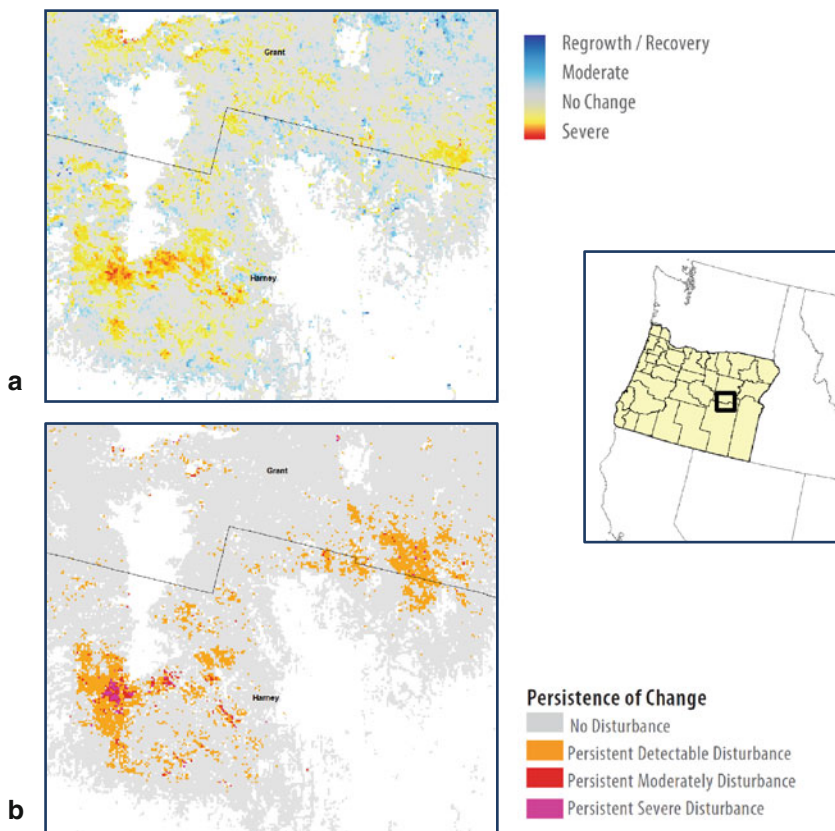


Fig. 4 Differences in the graphical appearance are readily apparent between **a** a 16-day Z-score forest change data from August 13–28, 2012 and **b** a three-date persistence forest change data product integrating data from July 28 through August 28, 2012 over an area in Central Oregon affected by a pine butterfly (*Neophasia menapia*) defoliation event. The persistence data product represents a cleaner, yet more spatially conservative, view of the defoliation event while highlighting the geographical “hotspot” of this forest disturbance

deciduous biome, whereas trend analysis is more suited for spatially characterizing gradual forest degradation and mortality events such as bark beetle infestations, which are more typical in the western coniferous biome. Comparison of these two remote sensing change detection approaches is facilitated by examining the forest change data products created in 2013 for different types of forest disturbances occurring in Colorado (Fig. 5), Utah (Fig. 6), and Pennsylvania (Fig. 7).

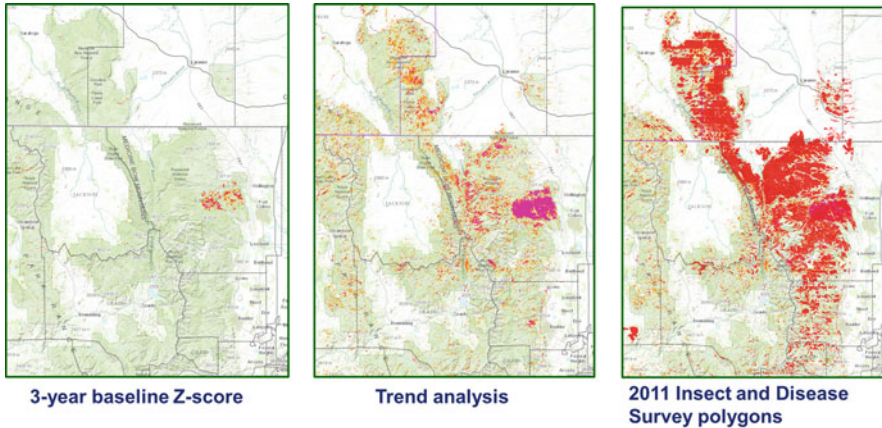


Fig. 5 Conifer decline and mortality related to drought and bark beetle activity in the front range of the Rocky Mountains in Colorado is well represented using trend analysis of MODIS data obtained between 2009 and 2013, whereas this forest decline is not detected using a change detection which compares Z-scores over two time periods. Aerial survey (IDS) polygon data corroborate the trend analysis results

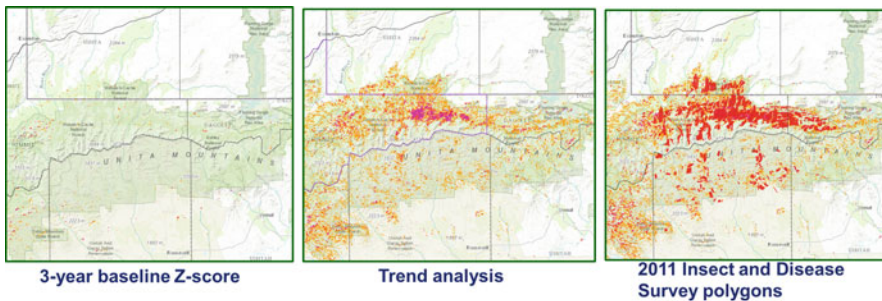


Fig. 6 Forest decline and mortality in the North Slope of the Uinta Mountains is well portrayed using trend analysis of MODIS data obtained between 2009 and 2013, whereas this forest decline is not detected using a change detection which compares Z-scores over two time periods. Aerial survey (IDS) polygon data corroborate the trend analysis results

5 Forest Change Data Delivery

The FHTET Forest Disturbance Monitor (FDM) is a web-based forest disturbance data delivery system designed specifically for the forest insect and disease survey for state, private, and National Forest end-users. This web application has been developed so that the FHP survey community may interact with the RTFD raster datasets to evaluate potential forest disturbances over large areas, thereby providing timely information for aerial survey resource allocation (Fig. 8). The forest disturbance products mapped with 250 m spatial resolution are created from 16-day MODIS

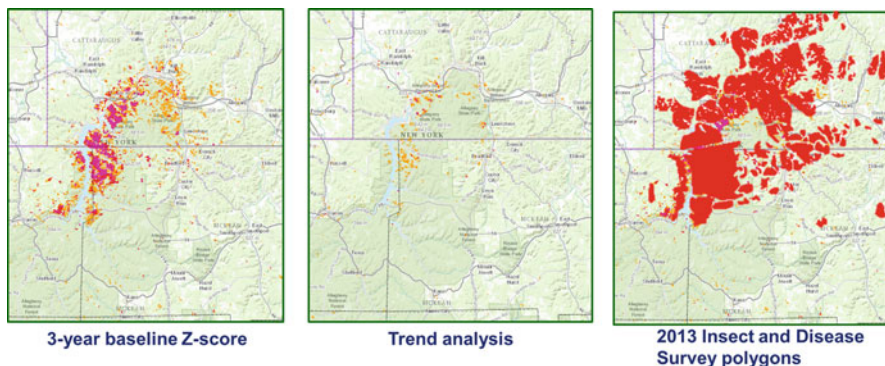


Fig. 7 A gypsy moth defoliation event that occurred in June and July of 2013 is quite evident in the Z-score forest change product which compares average forest conditions in 2010–2012 with forest conditions during an anniversary date range in 2013. This defoliation event is not detected very well by an analysis of trend in forest conditions between 2009 and 2013. Aerial survey (IDS) polygon data from 2013 corroborate the results of the Z-score analysis

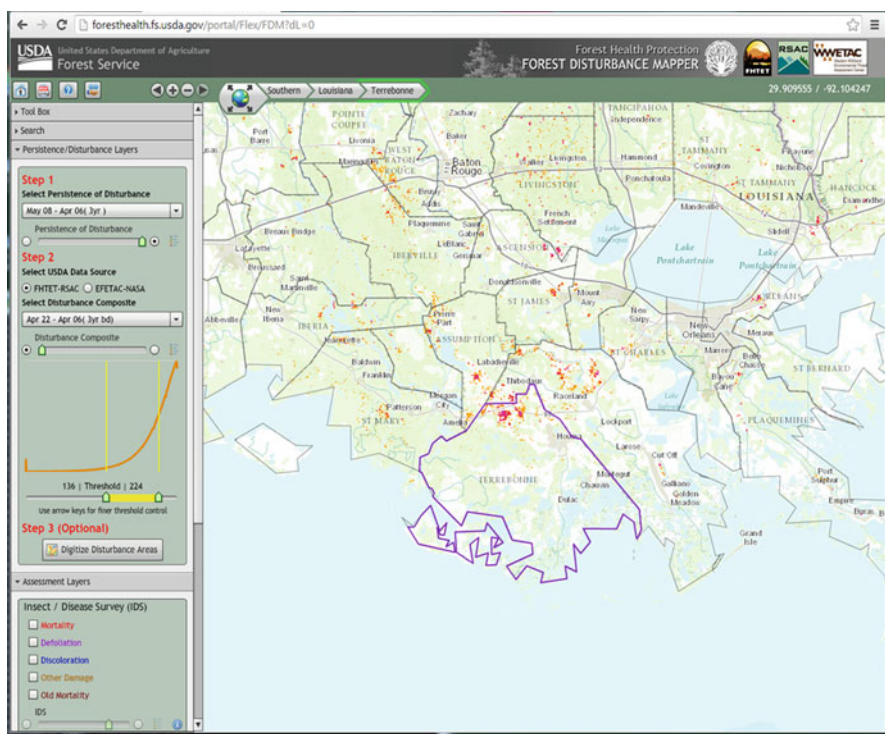


Fig. 8 View of the FDM web mapping application graphical user interface

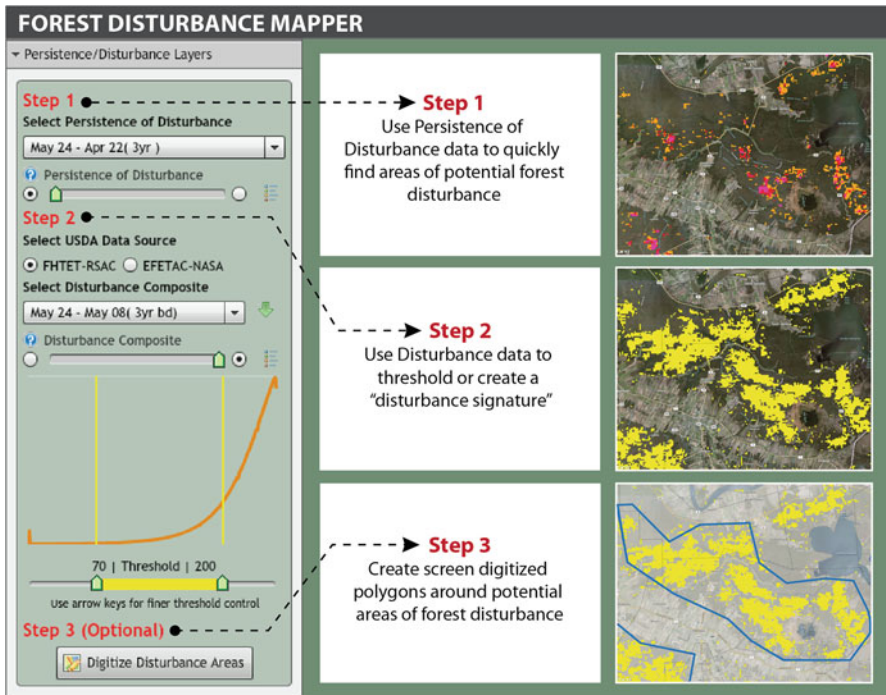


Fig. 9 Illustration of the three-step process for the FDM user interface

composites updated every 8 days. The FDM application is integrated into overall forest health monitoring activities, and enhances the ability to allocate and plan aerial and ground forest health survey missions. The FDM graphical user interface (GUI) facilitates an intuitive three-step process that allows the user to: (1) quickly scan and assess large areas for potential forest disturbances; (2) create spatial forest disturbance signatures using the FDM disturbance composite threshold tool; and (3) create screen digitized, downloadable data that can be used in aerial and ground survey missions as well as GIS analysis (Fig. 9). Key functionalities of the FDM also include the capacity to create and download spatial data to upload into Digital Aerial Sketch-mapping (DASM) units, usage in ground survey units such as pads and/or mobile units, or use in GIS analysis and map making. Additionally, the FDM contains data layers such as past IDS data, drought and past disturbances from fire, storm damage, and land use changes that can be leveraged for decision support.

The first step in the FDM process is to examine the Persistence of Disturbance data. These data serve as the initial targeting layer allowing the user to quickly locate potential forest disturbance over a wide area, and acts as a reference for thresholding the continuous disturbance data. Compared to the continuous forest disturbance data (Disturbance Composite in the FDM), the persistence of forest disturbance data represents a more conservative spatial estimate of a potential forest disturbance. An important advantage of the persistence of change data is that the incidence of false positives related to atmospheric contamination and other data ephemera is reduced.

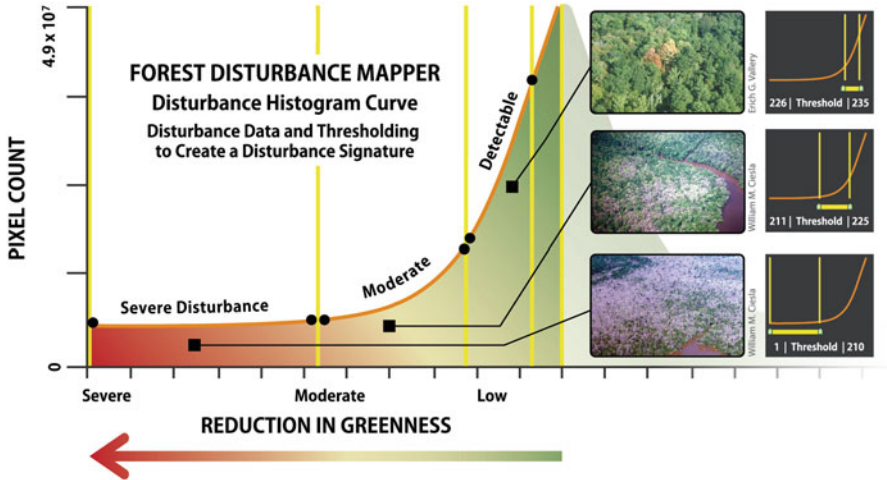


Fig. 10 Explanation of the disturbance data histogram manipulated using the threshold slider bar in Step 2 of the FDM process to create forest disturbance signatures

The second step in the FDM process involves direct interaction with the 3-year Z-score and 5-year trend analysis data products using the FDM Histogram Threshold Tool (Fig. 9). This tool is used to develop forest disturbance signatures by reclassifying the continuous Z-score and trend analysis Disturbance Composite data in real time. The thresholding is accomplished by adjusting the left and right slider located just under the histogram graphic tool. Any adjustment made to the histogram slider is updated immediately in the viewer allowing the user to quickly create a disturbance signature that best represents the potential disturbance area. All pixels that fall within the adjusted range between the left and right slider are displayed in the viewer frame. Because these forest change data products are delivered to the FDM as “below-normal” (lower than expected Z-score results and negative slope trend analysis results) data stretched to an 8-bit value range, the actual data values are only meaningful on an interval scale. The data rescaling enhances the signal for the negative departures from expected (“normal”) forest health conditions, and allows finer thresholding for the classification of apparent forest disturbances. Different levels of departure from normal forest conditions are located at different positions within the disturbance composite histogram (Fig. 10). The FDM Histogram Threshold Tool allows the user to select specific threshold ranges that best represent a potential forest disturbance. The severity of forest damage varies for different types of forest disturbances, as does the threshold range that best captures these disturbances in the forest disturbance data. Histogram positions located toward the left-hand tail have a much greater departure from an expected forest health condition, and represent areas of severe disturbance such as fires, storm damage and extreme insect and disease activity. Similarly, moderate severity disturbance values are typically found near the middle of the data histogram, and the more subtle or detectable disturbances are associated

with the right side shoulder portion of the histogram. The data user may also choose to examine a similar forest change dataset produced by Eastern Forest Environmental Threat Assessment Center (EFETAC) and NASA personnel (Hargrove et al. 2009) during this step.

In the third step, the user creates generalized polygons around the area of potential disturbance using the (thresholded) forest disturbance areas as a guide. These polygons are downloaded and utilized in the DASM systems that are used onboard aircraft during aerial survey missions. These polygons contain attribute data based on the disturbance data including the creation date, the data source, the name and date range of the disturbance composite data, and the threshold range. The user may also assign additional attributes, such as the rationale for the polygon's delineation, and the hypothesized (or verified) causal agent of disturbance.

6 Discussion

The unique mission of the RTFD program is to produce timely forest disturbance detection spatial data specifically for use by the FHP and S&PF forest health survey to improve aerial and ground detection planning efficiency. The RTFD program has been providing spatial data to this community since 2009, and has been incorporated into the FDM web application since 2010. The RTFD data production and FDM web-based application are designed to work in concert with each other to provide a vertically integrated and seamless service to the FHP and S&PF forest health survey community, and are continually evolving based on new technologies, user requirements, and data improvements. A principal lesson learned over the past 5 years of RTFD implementation is that a one-size-fits-all approach is not optimal for identifying the myriad of disturbance types observed across the forests of the continental United States. Specifically, a statistical (Z-score) two-date change detection approach is more effective for identification of quick and severe changes in forest health or condition (such as deciduous forest defoliation events), whereas trend analysis is apparently a more optimal approach to detect and track slowly developing degradation and mortality events in coniferous forests such as bark beetle or drought.

The relatively coarse spatial resolution of MODIS data and remnant atmospheric noise often found in these image data impede very accurate mapping of sometimes subtle forest disturbances. The RTFD datasets instead attempt to identify larger area (> 64 acres) 'hotspots' of apparent forest change. Moreover, an attempt is made to limit the amount of false positives (commission error) in these change data, sometimes at the expense of an increase in the amount of omission error in these data. The danger is that too many false positives in these data may lead the RTFD user community to tend to disregard the value in these data, which would consequently limit the efficacy of the entire RTFD program. The implementation of categorical data describing the persistence of forest disturbance has proven to be quite useful as both a spatially and graphically conservative estimate of forest disturbances. When combined with the continuous disturbance data from the individual compositing

periods using the tools available in the web-based FDM, these data sets provide timely and powerful information to the RTFD user community.

The overarching goal of the RTFD program is not to produce spatially accurate maps of forest disturbances, but rather to deliver as rapidly as possible spatial data that serve as an alarm to personnel with local knowledge and access so that they can obtain more detailed information (both spatial and causal) regarding a forest disturbance event. With a primary aim to be as time-sensitive as possible with respect to the delivery of these spatial data, our desired timing is to have the RTFD forest change data available for consumption on the FDM web mapping application within 3 days after the end of a MODIS compositing period. Creation of the MODIS image data composites begins at midnight of the last date of the compositing period, and the goal is to have this processing completed within 2 days afterward. The analysis which is then performed on these data to produce forest change spatial data should ideally be completed and delivered to the FDM web mapping application within 3 days after the end of a compositing period. Actual performance for the 2014 growing season indicates that this goal has been achieved, with an mean data delivery time of 2.7 days (range = 2–6 days; StdDev = 1.2 days). Weekly updates of RTFD forest change data delivered in a timely manner help IDS survey specialists to monitor forest disturbances throughout the field season. Areas of interest can be selected to target specific areas that have potential insect and disease issues for an ADS survey. The IDS specialist can fly these areas to confirm these target areas and sketchmap the fine scale boundaries for the disturbance agent.

References

- Adams HD, Macalady AK, Breshears DD, Allen CD, Stephenson NL, Saleska SR, Huxman TE, McDowell NG (2010) Climate-induced tree mortality: earth system consequences. *EOS Trans Am Geophys Union* 91(17):153–154
- Hargrove WW, Spruce JP, Gasser GE, Hoffman FM (2009) Toward a national early warning system for forest disturbances using remotely sensed canopy phenology. *Photogr Eng Remote Sens* 75(10):1150–1156
- Kennedy RE, Cohen WB, Schroeder TA (2007) Trajectory-based change detection for automated characterization of forest disturbance dynamics. *Remote Sens Environ* 110:370–386
- Nielsen EM, Finco MV, Hinkley E (2008). Change detection in image time-series affected by directional reflectance and phenological variability: application to forest disturbance monitoring. In: Proceedings of the 2008 IEEE International Geosciences and Remote Sensing Symposium, Boston, 6–11 July 2008
- Raffa KF et al (2008) Cross-scale drivers of natural disturbances prone to anthropogenic amplification: the dynamics of bark beetle eruptions. *Bioscience* 58(6):501–517
- Ruefenacht B, Finco MV, Nelson MD, Czaplewski R, Helmer EH, Blackard JA, Holden GR, Lister AJ, Salajano D, Weyeremann D, Winterberger K (2008) Conterminous U.S. and Alaska Forest Type Mapping Using Forest Inventory and Analysis Data. USDA Forest Service—Forest Inventory and Analysis (FIA) Program & Remote Sensing Applications Center (RSAC)
- Vermote EF, Roy DP (2002) Land surface hot-spot observed by MODIS over Central Africa. *Int J Remote Sens* 23:2141–2143

The Use of NASA LANCE Imagery and Data for Near Real-Time Applications

Diane K. Davies, Kevin J. Murphy, Karen Michael,
Inbal Becker-Reshef, Christopher O. Justice, Ryan Boller,
Scott A. Braun, Jeffrey E. Schmaltz, Min M. Wong,
Adam N. Pasch, Timothy S. Dye, Arlindo M. da Silva,
Henry M. Goodman and Paul J. Morin

Abstract

NASA's Land, Atmosphere Near real-time Capability for EOS (Earth Observing System) (LANCE) supports users interested in monitoring and analyzing a wide variety of natural and man-made phenomena in Near Real-Time (NRT). This chapter provides descriptions of how LANCE products are being used and key lessons learned about delivering these products to end-users. The applications of

K. J. Murphy (✉) · K. Michael · R. Boller · S. A. Braun · A. M. da Silva
NASA Goddard Space Flight Center, Building 32, 8800 Greenbelt Rd., Greenbelt, MD 20771,
USA

e-mail: kevin.j.murphy@nasa.gov

D. K. Davies

Science Systems and Applications, Inc./Trigg-Davies Consulting Ltd, Malvern, UK

e-mail: diane.k.davies@nasa.gov

I. Becker-Reshef · C. O. Justice

Department of Geographical Sciences, University of Maryland, College Park, MD, USA

J. E. Schmaltz

Science Systems and Applications, Inc., NASA Goddard Space Flight Center, Greenbelt, MD,
USA

M. M. Wong

Columbus Technologies and Services, Inc., NASA Goddard Space Flight Center, Greenbelt, MD,
USA

A. N. Pasch · T. S. Dye

Sonoma Technology, Inc., Petaluma, CA, USA

H. M. Goodman

NASA Marshall Space Flight Center, Huntsville, AL, USA

P. J. Morin

Polar Geospatial Center, University of Minnesota, Minneapolis, MN, USA

LANCE data and imagery described in this chapter include: agricultural monitoring, volcano monitoring, aerosol forecasting, short-term weather forecasting, supplying ships with ice conditions, planning flights near hurricanes, monitoring air quality, and the use of fire email alerts to warn of illegal fires in protected forests.

Keywords

NASA · LANCE · Near real-time · AIRS · AMSR-E · MLS · MODIS · OMI · Worldview · FIRMS · Agricultural monitoring · Volcanic activity · Aerosol forecasts · Short-term weather forecasting · Sea-ice conditions · Hurricanes · Air quality · Fire

1 Introduction

LANCE provides near real-time data and imagery for over 70 products from MODerate Resolution Imaging Spectroradiometer (MODIS), Atmospheric Infrared Sounder (AIRS), Microwave Limb Sounder (MLS) and Ozone Monitoring Instrument (OMI). Scientists, operational agencies, government and non-government organizations use LANCE products for a wide range of purposes. This chapter provides examples of these applications and summarizes key lessons learned about delivering products to end-users. An overview of the LANCE system and a description of the LANCE services used to distribute data and imagery is provided in Chap. 8.

2 LANCE Services

LANCE products are primarily distributed as Hierarchical Data Format (HDF) data files for analysis and as imagery for visualization. In addition, MODIS active fire data are provided through the Fire Information for Resource Management System (FIRMS). LANCE services include: FTP/HTTPS file distribution, Rapid Response (RR), Worldview, Global Imagery Browse Services (GIBS) and FIRMS. These services are described in Chap. 8 on LANCE, and summarized in Table 1.

3 Use of LANCE Products

This section describes eight examples of how LANCE products are used. The use of Near Real-Time (NRT) satellite-derived products is a relatively new field; the examples described in this chapter, and summarized in Table 2, serve to illustrate the broad utility of NRT products across a range of disciplines.

Table 1 LANCE services

		LANCE service	NRT product	Targeted user/Use
Data	Download data	FTP/HTTPS file distribution	HDF data files	Remote sensing experts, scientists
		FIRMS FTP/HTTPS	MODIS active fire data. File formats: TXT, SHP	Fire/natural resource managers, conservationists
	Data via subscription	HDF	HDF data files	Remote sensing experts, scientists, and modelers who want data daily
		FIRMS fire email alerts	MODIS-derived hotspot/active fire location coordinates with optional map (Format: NRT, daily or weekly alerts with CSV file)	Notification of hotspots/fires in user-specified area. Fire managers and field staff/practitioners
Visualize	Rapid response imagery	Subsets	GIS-ready satellite data. MODIS geo-referenced, geographically subsetted images	For rapid assessment of same area on multiple days. Excellent in poor bandwidth areas
		MODIS NRT (orbit swath) images	Swath images for each 5-min interval for MODIS data	Quick look prior to granule (data) download
		Gallery images	Geo-referenced MODIS imagery for interesting events and phenomena in GIS compatible format	Public outreach and Media: press, blogs and social media
	All LANCE imagery	Worldview	Imagery from AIRS, MLS, MODIS and OMI. Image subsets as JPEG, PNG, GeoTIFF and KMZ	Google maps type tool to interactively browse and download global imagery as well as search for underlying data through the EOS clearing house (ECHO)
		GIBS	Imagery via standard services e.g. Web Map Tile Services (WMTS), Tiled Web Map Service (TWMS) and KML	Web mapping, geographic information system (GIS), and mobile applications
	MODIS fire data	FIRMS web fire mapper	Interactive global web map service for MODIS hotspot/active fire data	Understanding fire patterns over time for any area/date query

Table 2 Use of LANCE: Summary of examples described in this chapter

Application	LANCE NRT Product	Organization accessing products from LANCE	Use/End users
Global agricultural monitoring	MODIS HDF data	Global Agricultural Monitoring (GLAM) UMD	USDA—FAS, agricultural monitoring systems in Europe, China, UN FAO
Monitoring volcanic clouds and detecting pre-eruptive volcanic degassing globally	OMI HDF data (SO ₂ and aerosol index)	UMD, and NOAA OSPO	Support to aviation control -US FAA, European SACS. Airlines receiving advisories for operational decisions. USGS volcano observatories, VAACs
Aerosol forecasts	MODIS HDF data	Scientists at GSFC	NASA aircraft campaigns
Short-term weather forecasting	AMSR-E HDF	SPoRT at NASA MSFC	NWS forecast offices
Getting the latest ice conditions to ships in Antarctica	MODIS rapid response imagery	Polar Geospatial Center	US Antarctic program's science ships and research vessels
Planning optimal flights near hurricanes	MODIS and AIRS imagery in worldview	Hurricane and severe storm sentinel mission	NASA GSFC, HS3 mission
Air quality decision support assessments	GIBS imagery	US EPA AirNow-Tech Navigator	Air quality monitoring agencies and air monitoring/forecasting community
Identifying illegal burning within protected forests	FIRMS fire email alerts	FCD, Belize	Park staff/Friends for Conservation and Development

3.1 NRT Data: HDF Files Distributed by FTP and HTTPS

3.1.1 MODIS Data for Global Agricultural Monitoring

Monitoring global agricultural production from space was made possible with the launch of the Earth Resources Technology Satellite (ERTS-1) (later renamed Landsat 1) in the 1970s and subsequently in the early 1980s with the Advanced Very High Resolution Radiometer (AVHRR) on the NOAA satellite series. Techniques for agricultural monitoring using remote sensing were developed through the joint NASA-United States Department of Agriculture (USDA) Large Area Crop Inventory Experiment (LACIE) and later, the joint program for Agriculture and Resources Inventory Surveys Through Aerospace Remote Sensing (AgRISTARS) Program. Time-series observations from the AVHRR using the Normalized Difference Vegetation Index (NDVI) proved to be extremely useful for monitoring vegetation, crop development and condition during the growing season at national to global scales (Justice et al. 1985; Tucker et al. 1981). Significant improvements for vegetation monitoring came

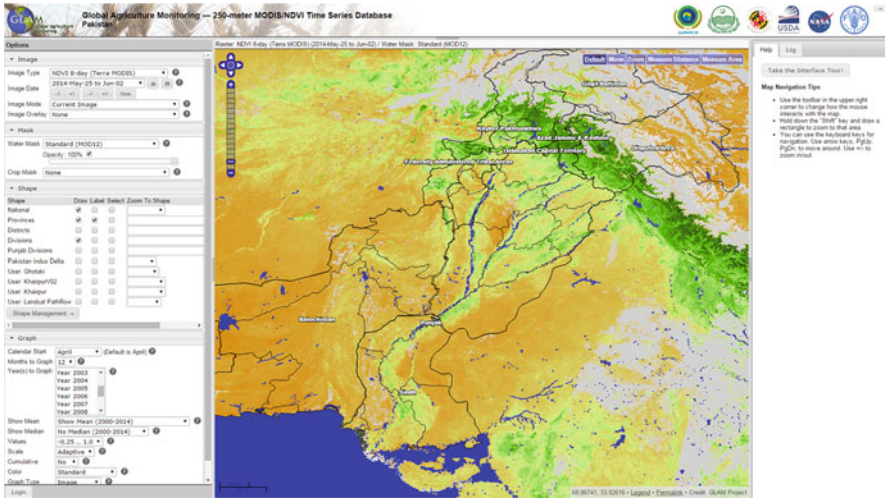


Fig. 1 LANCE MODIS NDVI data available through GLAM interface within 24 h of last date composite

with the MODIS instrument (Justice et al. 2002). The USDA Foreign Agricultural Service (FAS), which undertakes global agricultural production monitoring, uses global satellite data as one of their inputs. MODIS Vegetation Index data were incorporated into the FAS Crop Explorer through the Global Agriculture Monitoring (GLAM) System (Becker-Reshef et al. 2010). The requirements for agricultural production monitoring are time-sensitive. The MODIS Adaptive Processing System (MODAPS) which generates the MODIS data primarily for land-science users waits for all data to be available before processing NDVI composites, which results in delayed availability (Masuoka et al. 2011). The development of the NRT MODIS data from the LANCE system provided a significant improvement in timeliness of delivery critical for agricultural monitoring. These LANCE data have been integrated into the GLAM system and NDVI composites are provided to USDA as well as to the international agricultural community within 24 h of the last day of composite. Research is being developed to extend the use of NRT MODIS data for estimation of crop yield (Becker-Reshef et al. 2010). In addition to the USDA FAS system, there are other global agricultural monitoring systems in Europe, China and at the United Nations Food and Agriculture Organization (UN FAO), which are coordinated through the G-20 GEOGLAM initiative of GEO (Group on Earth Observations). All of these systems use MODIS data and take advantage of the LANCE system to access them. Efforts are underway to make the case for a similar NRT capability to be generated from the Suomi National Polar-orbiting Partnership (S-NPP) Visible Infrared Imager Radiometer Suite (VIIRS) system providing continuity with MODIS data (Justice et al. 2013) (Fig. 1).

3.1.2 OMI Data for Volcano Monitoring

OMI Sulfur Dioxide (SO₂) and Aerosol Index products from LANCE are used in monitoring volcanic clouds and detecting pre-eruptive volcanic degassing globally (Carn et al. 2008; Krueger et al. 2009). This information is used to support the US Federal Aviation Administration (FAA) goal of a safe and efficient national air space. NRT observations of SO₂ and volcanic ash are incorporated into data products compatible with decision support tools in use at Volcanic Ash Advisory Centers (VAACs) in Washington and Anchorage and at the United States Geological Survey (USGS) Volcano Observatories. The VAACs provide Volcanic Ash Advisories to airlines for their operational decisions. This information includes the location and forecasted movement of the visible ash clouds. The data are pulled from LANCE by NOAA National Environmental Satellite Data and Information Service (NESDIS), Office of Satellite and Product Operations (OSPO)—Satellite Products and Service Division (SPSD) and fed in to an operational OMI NRT SO₂ image and data products distribution system, that was developed between 2007 and 2010 in a NASA sponsored collaboration between University of Maryland, Baltimore County and the NOAA SPSD. This system creates automated volcanic eruption alarms that are sent to the Washington and Anchorage VAACs, and produces volcanic cloud subsets for multiple regions of interest. These are provided through the website: <http://satepsanone.nesdis.noaa.gov/pub/OMI/OMISO2/index.html>. This site provides access to different graphical products derived from OMI, intended to facilitate rapid access to global volcanic cloud data. Detailed maps of volcanic regions are provided to show degassing activity, which is useful for monitoring emissions that may be a precursor to eruptive activity (Carn et al. 2008). OMI NRT SO₂ data from LANCE are also ingested into a European support to aviation control service web site: <http://sacs.aeronomie.be/nrt>.

When the automated system detects an SO₂ cloud, an alert is sent out to hundreds of subscribers via email. Public web alerts are also automatically generated and can be viewed at <http://so2.gsfc.nasa.gov>.

3.1.3 GEOS-5 Global Aerosol Forecasting System

Aerosols are tiny airborne particles that affect climate through the absorption and scattering of solar and thermal radiation, which affects cloud and precipitation formation. Aerosol is also a common type of air pollution, affecting health, transporting pollution across international borders and across the oceans. Scientists at NASA Goddard Space Flight Center (GSFC) have developed a computer model for ingesting satellite data to provide global NRT forecasts of common aerosol types such as desert dust, salt from the oceans, smoke from fires, sulfates from volcanoes and particulate matter pollution.

The Goddard Earth Observing System Model, Version 5 (GEOS-5) is the latest version of the NASA Global Modeling and Assimilation Office (GMAO) Earth system model. The aerosol module in GEOS-5 is based on a version of the Goddard Chemistry, Aerosol, Radiation, and Transport (GOCART) model (Chin et al. 2002) and source and sink processes are modeled for dust, sulfate, sea salt, and black and organic carbon aerosols. Figure 2 depicts a sample initial condition for the aerosol

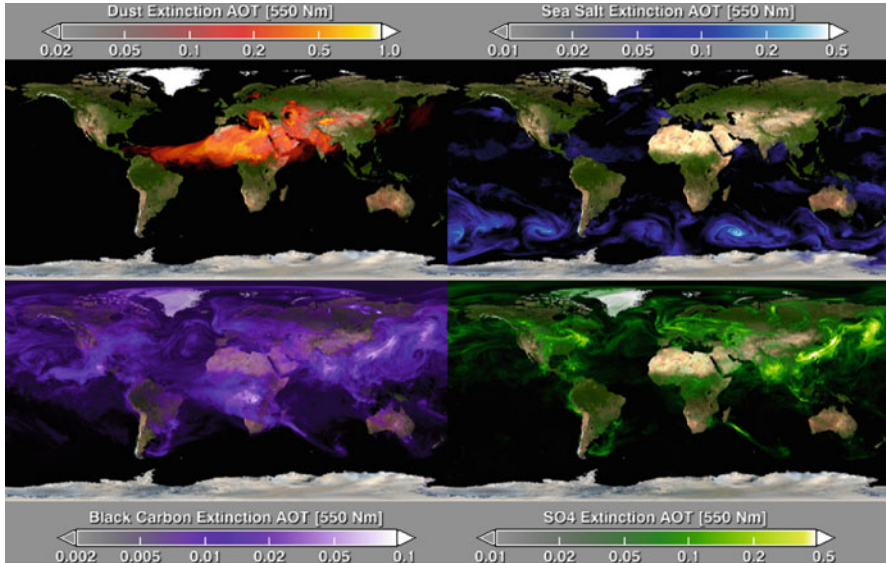


Fig. 2 GEOS-5 aerosol optical depth analysis valid 12 UTC on May 29, 2013 for dust, sea salt, back carbon and sulfate aerosols. These images are available on the GEOS-5 WMS server: http://www.map.nasa.gov/cgi-bin/viewer.cgi?project=e572.inst1_2d_hwl_Nx

forecast starting on 12 UTC May 29, 2013 based on NRT satellite data provided by LANCE.

NRT MODIS data provided by LANCE plays a critical role in the GEOS-5 aerosol forecasts. Daily biomass burning emissions are derived from MODIS radiative power retrievals (Darmanov and da Silva 2013) and cloud-cleared MODIS reflectances are the main ingredients of the aerosol forecasting and data assimilation system.

The GMAO runs the global GEOS-5 Data Atmospheric Data Assimilation system in near real-time, producing twice daily 5 day forecasts with a nominal spatial resolution of 25 km. These forecasts have been used to support numerous NASA aircraft campaigns (e.g., CRAVE, TC⁴, ARCTAS, TIGERZ, GLOPAC, DISCOVER-AQ, ATTREX, HS3; more information on these campaigns can be found at: <http://www.espo.nasa.gov/missions.php>). A number of recent studies highlight the application of GEOS-5 with GOCART aerosols (Nowottnick et al. 2010, 2011; Colarco et al. 2010; Aquila et al. 2012; Randles et al. 2013; Bian et al. 2013). GEOS-5 forecast data files and images are available on-line from the GMAO website (<http://gmao.gsfc.nasa.gov>).

3.1.4 Advanced Microwave Scanning Radiometer Data for Short-Term Weather Forecasting

Spaceborne passive microwave radiometers have been observing the Earth in near polar, sun-synchronous orbits since the 1970s with the launch of the Electronically Scanning Microwave Radiometer (ESMR) aboard the Nimbus-5 satellite. Over the

last 40+ years a series of US satellites have carried increasingly more sophisticated instruments. They include the Scanning Multichannel Microwave Radiometer (SMMR), Special Sensor Microwave Imager (SSM/I), Special Sensor Microwave Imager Sounder (SSM/IS) and the Advanced Microwave Scanning Radiometer for Earth Observing System (AMSR-E). Launched in 2002, the AMSR-E flew aboard the NASA Aqua satellite. After over 9 years of service, the AMSR-E instrument failed in Oct 2011, but not before the LANCE system was able to demonstrate cases where NRT uses of passive microwave data were beneficial to the weather forecasting community. Fortunately, the Japan Aerospace Exploration Agency (JAXA) operates a similar instrument, the Advanced Microwave Scanning Radiometer-2 (AMSR2), launched on the Global Change Observation Mission—Water (GCOM-W1) satellite in May 2012. LANCE is planning to ingest and process AMSR2 data in NRT.

AMSR-E was designed to detect water in all its state phases (ice, water, vapor) in the environment. As such, the AMSR-E instrument monitored the water processes that exert a strong influence on climate and weather. The environmental properties that can be measured by AMSR-E include precipitation, oceanic water vapor, cloud water, near-surface ocean wind speed, sea surface temperature, soil moisture, snow cover, snow water equivalent, sea ice concentration and sea ice speed and direction. AMSR-E provided global coverage of the Earth's surface and atmosphere from its near-polar orbit aboard the Aqua satellite. The steady stream of data were continually downlinked and distributed through LANCE, which is managed by NASA Earth Science Data and Information System (ESDIS) project (see LANCE Chap. 8).

The Short-term Prediction Research and Transition (SPoRT) Center at the NASA Marshall Space Flight Center (MSFC) used the AMSR-E products to provide a variety of geophysical products to the National Weather Service (NWS) forecast offices. The SPoRT Center is a research to operations focused project whose objective is to provide the end-to-end transition of modeling and data assimilation techniques, nowcasting tools, and NASA satellite derived data products for improved short-term weather forecasting (Jedlovec 2013). SPoRT works closely with the NWS to provide new applications and data sets that can be incorporated into the NWS forecasters procedures for developing their short-term forecasts. SPoRT used the AMSR-E data sets to provide weather products to help diagnose convective weather events.

SPoRT collaborated with NWS to identify and provide NRT AMSR-E estimated rainfall rates and the percentage of convective storms to the forecasters. An example of the use of NRT AMSR-E is depicted in Fig. 3. This figure shows a strong line of thunderstorms passing through the southeastern U.S. on 10 December 2008. Figure 3a identifies the instantaneous rain rates and Fig. 3b highlights which of the storms are convectively active. The highest convection and the heaviest rains are concentrated along the cold front, particularly in west-central Alabama and east-central Mississippi. The NWS forecasters use these products to analyze current conditions and to improve prediction (in weather forecast models) of clouds and precipitation.

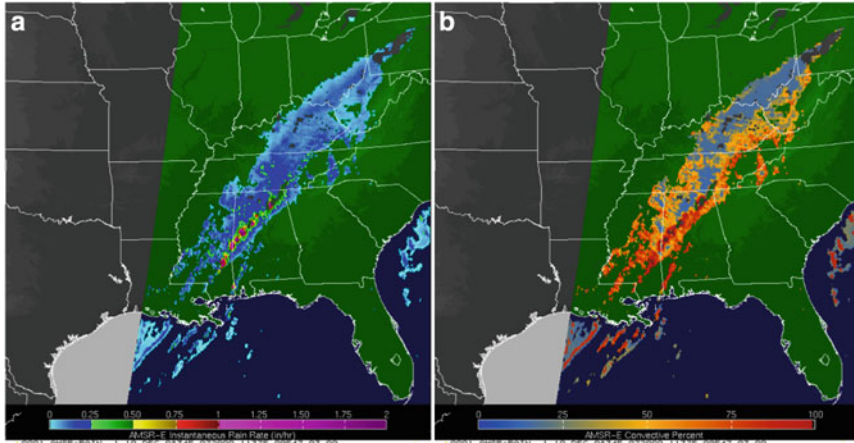


Fig. 3 AMSR-E microwave observations “see” through the cloud cover to identify areas of the most intense rainfall. AMSR-E products show estimated rainfall rates (a) and (b) convective percent of storms on 10 December 2008. Colors indicate rainfall rates in excess of 1 in/h and identify the strongest convective cells along the leading edge of the front

3.2 Rapid Response Imagery: Supplying Ships in Antarctica Ice Conditions Information

Rapid Response images are regularly seen in press releases and on television for newsworthy events but they are useful for a wide range of applications. This example comes from long-time users at the Polar Geospatial Center (PGC) that routinely use NRT MODIS imagery, along with other remotely sensed datasets, to provide ships and stations in the Antarctic with up-to-date information on sea ice conditions.

Antarctica is covered by the world’s largest ice sheet and surrounded by sea ice. The sea ice is very dynamic and changes day-to-day and hour-to-hour. The US Antarctic Program has two science vessels, a resupply container ship, a fuel tanker and an icebreaker—to allow resupply access to McMurdo station. When conditions are challenging, the US Antarctic Program’s Antarctic Research and Supply Vessels ask PGC for imagery and maps outlining the location and type of sea ice in their area. This information needs to be current and delivered rapidly to ships and stations with limited internet connectivity. To obtain the most up-to-date maps of sea ice, the team at PGC use the latest MODIS image, created by combining information from bands 3, 6, and 7 (Fig. 4) that differentiates clouds from the snow and ice, and overlay it with other imagery. The final maps are provided to the captain and science teams onboard the research vessel. With this information a research vessel can plot a route that will save time and money and meet science goals by avoiding the need to reduce speed to maneuver around sea ice. MODIS NRT images are routine but critical source of information used by the US Antarctic Program fleet.

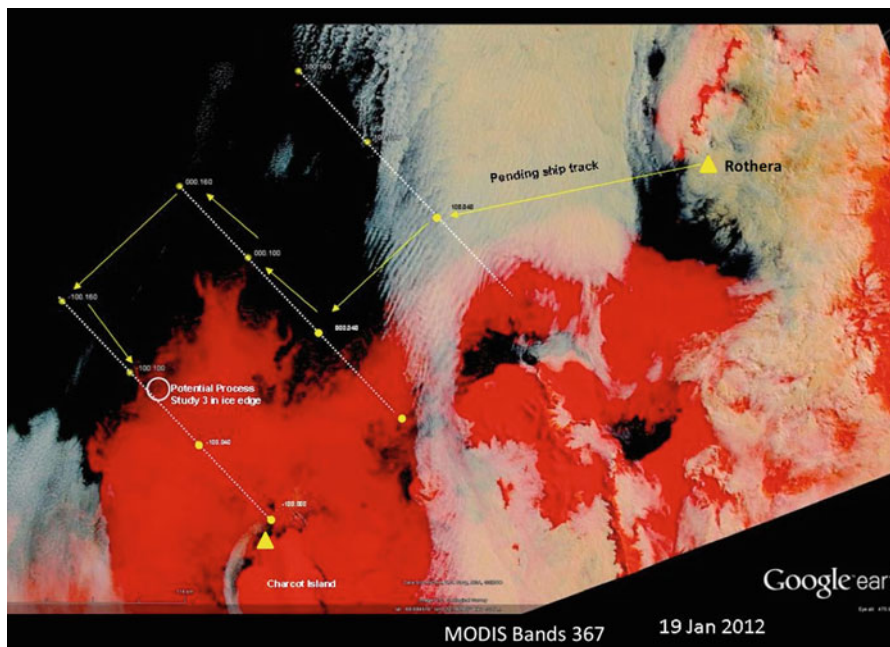


Fig. 4 Map of sea ice in the Antarctic on January 19, 2012. Using a Rapid Response MODIS image combining bands 3, 6, and 7 it is possible to differentiate sea ice from clouds. Red shades indicate ice, while tan shades indicate clouds. Such information can be overlaid in Polar View (<http://www.polarview.org>), an earth observation portal that combines the latest satellite imagery for the poles. These data are routinely used to help ships safely plot their course through icy waters. Image credit: Paul Morin. (originally reproduced in Murphy et al. 2012)

3.3 Worldview: Planning Optimal Flights Near Hurricanes

As described in Chap. 8, Worldview (<https://earthdata.nasa.gov/worldview>) was originally designed as an interactive map client tailored to the NRT applications community. An example of this within NASA is the Hurricane and Severe Storm Sentinel (HS3), a 5-year airborne investigation to study the processes that govern hurricane formation and intensification. HS3 uses a pair of Global Hawk unmanned aerial vehicles (UAVs) equipped with scientific instruments to measure both the large-scale environment around a storm and the internal processes within the storm itself. Of particular interest is the effect of the Saharan Air Layer—a dry, warm, and dusty air mass—on hurricanes in the Atlantic basin.

While HS3 is an airborne mission designed to collect data within and in close proximity to a hurricane, NRT satellite data plays an important role in deciding exactly where the aircraft should fly. In particular, the ability to interactively examine satellite observations of aerosols, humidity, and clouds in the vicinity of a storm can be critical for pre-flight and in-flight route adjustments based on the most recent data available.

Although the system was not fully operational in time for HS3's first deployment in 2012, the potential of using LANCE data fed into Worldview/GIBS can be illustrated using the case of Hurricane Nadine, a long-lasting storm that was active from September 10—October 3, 2012, and heavily sampled by HS3. The HS3 team began planning for a September 11–12 flight into Nadine as early as September 8. Between September 9 and 11 (Fig. 5), a major dust outbreak from the Sahara was moving rapidly westward on the eastern and northern sides of the cloud system that became Nadine. MODIS Aerosol Optical Depth (AOD) and numerical weather prediction data were used to estimate the likely extent of the Saharan Air Layer for the day of flight and to design a flight pattern that both sampled the storm and the portion of the Saharan air closest to the storm (Fig. 6). With the addition of AIRS temperature and humidity data in 2013, the HS3 team will be making Worldview/GIBS a core tool in their forecasting and flight planning processes for their deployments in 2013 and 2014.

3.4 GIBS: Providing Imagery to EPA AirNow-Tech Navigator

As described in Chap. 8, GIBS is a relatively new Earth Observing System Data and Information System (EOSDIS) capability that provides NRT imagery through a set of standard services that can be used in a variety of desktop, online, or mobile mapping tools. An illustration of this is the integration of GIBS into AirNow-Tech, a decision support system developed by the US Environmental Protection Agency (EPA). The EPA's AirNow program provides the public with easy access to national ambient air quality. The public AirNow.gov website uses the Air Quality Index (AQI), a standardized index for reporting air quality based on health effects for ground-level ozone (O_3), fine particulate matter ($PM_{2.5}$), and other pollutants.¹ AirNow.gov provides NRT hourly AQI conditions and daily AQI forecasts with maps of interpolated AQI levels on national, regional, and local spatial scales.

AirNow-Tech, is a password-protected, interactive website and decision support system for managing ambient air quality and meteorological data submitted to AirNow. AirNow-Tech is a data management tool for air monitoring agencies and includes an analysis tool for querying and mapping air quality and meteorological information across agencies. Access to AirNow-Tech is available to all partner air monitoring agencies and other technical users in the ambient air monitoring and forecasting community (e.g., multi-state organizations, EPA staff, and third-party scientists). Sonoma Technology, Inc. (STI) operates AirNow and AirNow-Tech for the EPA.

AirNow-Tech Navigator (hereafter, Navigator) is an interactive spatial analysis GIS tool within AirNow-Tech that allows users to display spatial plots of air quality data and surface weather conditions. Navigator uses standardized geospatial web services; such as Open Geospatial Consortium (OGC) compliant Web Mapping Services (WMS) and Web Mapping Tile Services (WMTS), to display air quality and

¹ For more information about the AQI, go to <http://www.airnow.gov>.

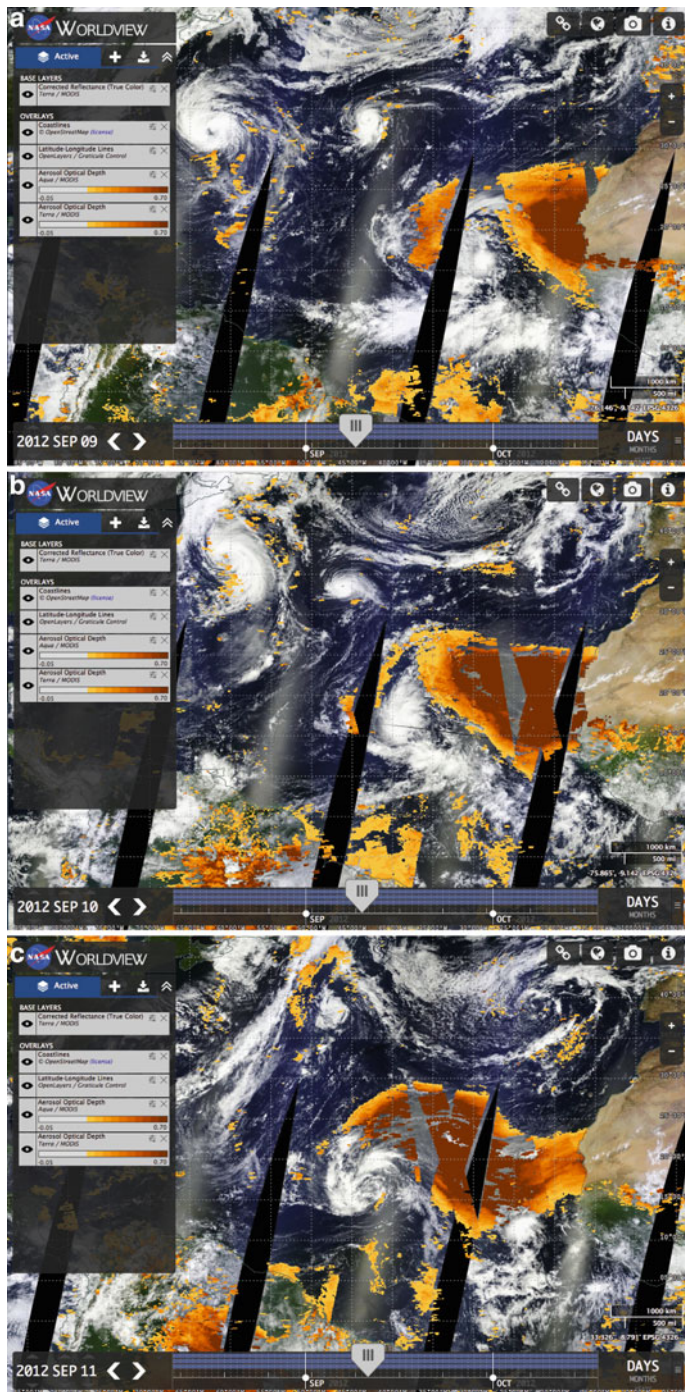


Fig. 5 Sept. 9–11, 2012 in NASA worldview displaying Hurricane Nadine as observed from the Terra and Aqua spacecraft; the MODIS corrected reflectance product provides the “true color” imagery while MODIS aerosol optical depth (*orange*) shows a large dust plume

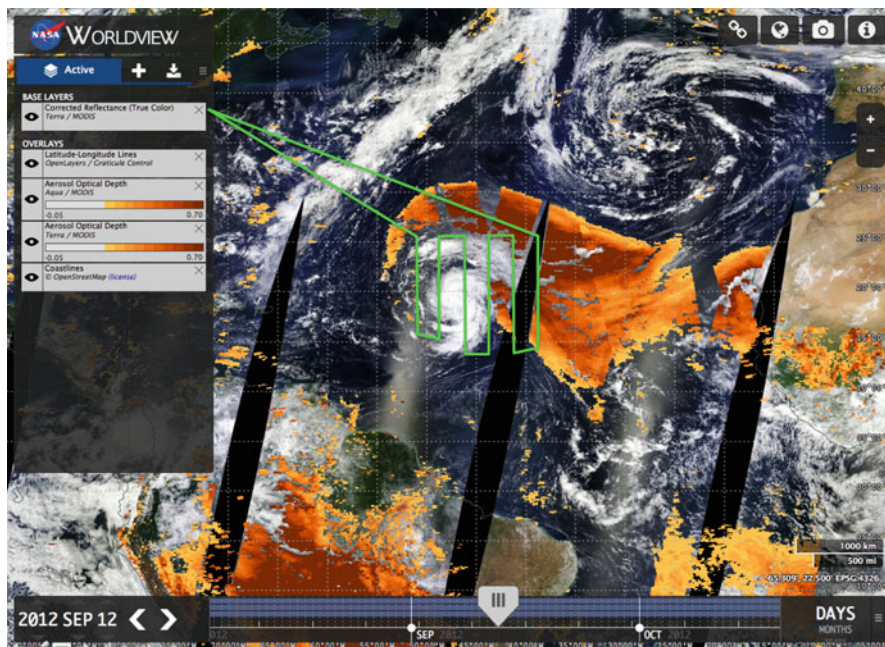
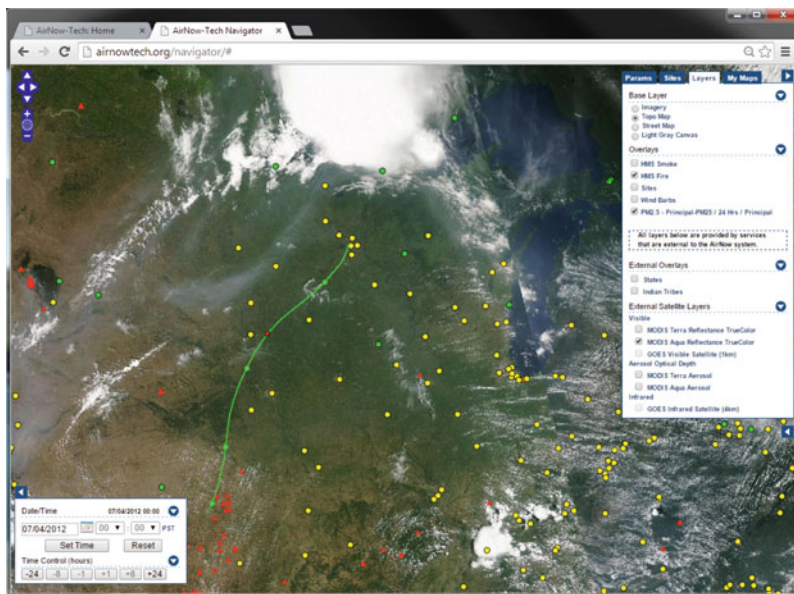


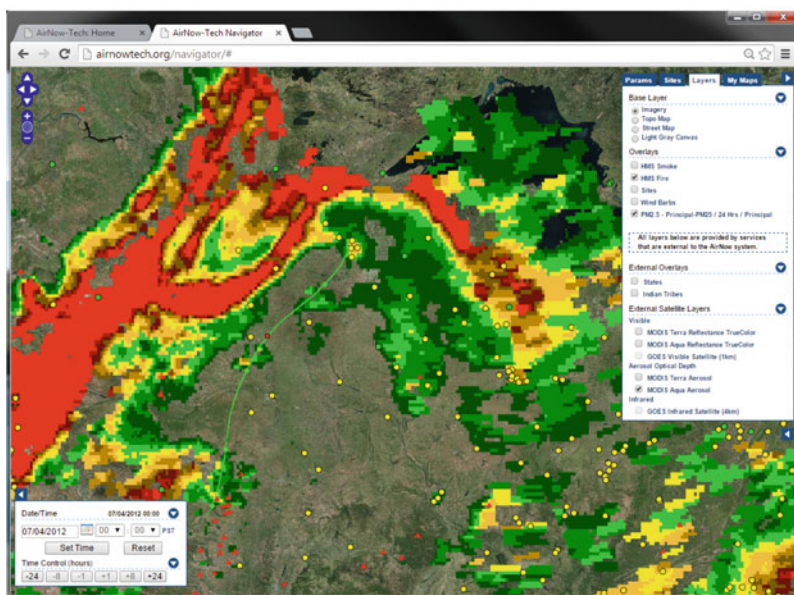
Fig. 6 A typical “lawnmower” flight track (*green line*) to be used by HS3 to sample the environment of a storm superimposed over Worldview’s display of Hurricane Nadine on September 12, 2012. The flight track is designed to examine the extent to which the Saharan air gets wrapped into the storm circulation

meteorological data, smoke plumes, and fire locations. The AirNow user community expressed a strong desire to integrate NASA satellite data into Navigator. With NASA Applied Sciences funding, EPA and STI collaborated with LANCE to incorporate two satellite data sets into Navigator using a WMTS from GIBS, the AOD and True Color imagery from MODIS.

The near real-time capability of GIBS provides Navigator users with a tool to overlay MODIS products, surface air quality and meteorological data, fire location information, and trajectory data on one plot for quick multi-layer analysis of past and current air quality conditions. For example, on July 4, 2012 (Fig. 7), moderate air quality concentrations for $PM_{2.5}$ were observed in southeastern Minnesota. The addition of NASA satellite data from GIBS allows air quality forecasters to overlay NASA MODIS True Color and AOD imagery, trajectory, surface concentration data, and fire locations. GIBS AOD imagery allowed air quality scientists to determine that visible smoke likely played a role in increasing $PM_{2.5}$ concentrations to moderate levels in Minnesota on that day.



a



b

Fig. 7 Screenshots from AirNow-Tech navigator of a visible smoke event on July 4, 2012. Data displayed are: 24-h average $PM_{2.5}$ concentrations (*dots*, color-coded based on the AQI); fire locations from NOAA's Hazard Mapping Service (HMS; *red triangles*); 24-h forward HYSPLIT trajectory ending on July 4, 2012, at 100 m *above* ground level; NASA GIBS MODIS true color imagery (*left*) and Aerosol Optical Depth (*right*) from the Aqua satellite

3.5 FIRMS Fire Email Alerts: Monitoring Protected Forests in Belize

The Fire Information for Resource Management System (FIRMS) fire email alerts are sent in English, French and Spanish to individuals working in government and non-government organizations in over 120 countries. The fire alerts are used by natural resource managers, policy makers, and scientists to support decision making in a number of applications including protecting forests from illegal slash and burn farming, prioritizing limited resources for strategic fire management, supporting tactical fire management (improving location knowledge of a fire) and identifying the source of smoke plumes for air quality management.

In Belize, the non-profit group Friends for Conservation and Development (FCD) uses the fire alerts to help monitor the Chiquibul National Park, on the border with Guatemala. It is the largest protected forest in Belize and home to the biggest Mayan archaeological site in the country. The fire alerts warn of possible encroachments across the border and into the forest by local Guatemalan farmers and are used by FCD to prioritize their limited resources for aerial and ground reconnaissance. The 264,000-acre park is home to a rainforest that is not prone to naturally caused fire therefore detected fires are likely to be caused by humans. Fires in this fragile rainforest often indicate clearing for agriculture. Slash and burn farming can lead to large gaps in the forest canopy, which disturbs the moisture-dependent ecosystem and sometimes leads to irreversible changes in the forest cover. When hotspots/fires are reported in remote areas far from forest trails, FCD sends a plane and spotter for reconnaissance purposes. Knowing the coordinates of a detected fire, just 3 h after satellite overpass is very valuable information for this conservation effort (Vizcarra 2012).

4 Key Lessons Learned

As mentioned in Chap. 8, LANCE is managed by ESDIS and steered by a User Working Group (UWG). Recommendations from the UWG and feedback from users² guide the development of LANCE. End user lessons learned are summarized here:

- Interactions with end users indicate they want NRT data and imagery to be easy to find, freely available, and in easy to use formats. This finding is not new but it is one that is regularly revisited as technologies improve.
- End users want to integrate imagery with other geographic data without the overhead of having to ingest and stage data. Mashup maps, a combination of geographic datasets from various sources brought together for viewing on the Internet as a new map, are increasingly popular. GIBS are empowering users to deploy map mashup solutions or pull the latest imagery into their desktop, mobile

² Correspondence and informal interviews with users and feedback from users through the NASA EOSDIS User Support Tool.

or online mapping tools (as shown in the EPA example in Section 3.4). GIBS' reliance on open imagery standards such as the WMTS and Keyhole Markup Language (KML) are a key factor in the growth of NRT imagery access.

- Some users want information not data. Where feasible, catering to this requirement will result in uptake by users who would probably not otherwise access satellite data. For example, the FIRMS email alerts provide information only when a fire is detected in a user-defined area of interest. Gallery images or bookmarked events in Worldview also go a long way to meeting this 'information' requirement—particularly when shared as part of a blog/social media or a popular article.
- File size is particularly important for users with low bandwidth, Rapid Response subset images and Worldview image downloads currently make up the bulk of files downloaded from LANCE. This is because they effectively 'bookmark' user-requested geo-referenced images that are relatively small and easy to download.
- Scientists studying geophysical events in NRT appreciate the capability to view full resolution browse imagery to rapidly assess situations (for example, to identify the source of a dust plume) and to help decide which data granules to download. The ability to browse full resolution imagery in Worldview and then download underlying data from the EOS Clearing House (ECHO) provides a convenient method for search and order.
- It is important to manage user expectations of what can and cannot be seen in the NRT products. For example, an appreciation of the spatial resolution of dataset is important; users are accustomed to being able to zoom into high-resolution imagery in clients such as Google Earth. This can leave some users frustrated as MODIS imagery has maximum spatial resolution of 250 m, with most products at 500 m, 1, 5 and 10 km. Other instruments have lower resolutions, such as OMI at 25 km and AIRS at 11 and 37 km. To some extent, the frustration can be allayed through explanations on the website and Frequently Asked Questions. In the future, integration of co-incident high and moderate resolution data will also ease this frustration for users.
- Confidence in a satellite-derived product is linked to a user's experience; educating users about the potential and limitations of a dataset will improve this experience. For example the MODIS hotspot/fire detections, distributed through FIRMS are provided as coordinates that represent the center of an approximately 1 km pixel, flagged as containing one or more hotspots/fires within that pixel. The "location" is the center point of the pixel, not necessarily the coordinates of the actual fire—a fact that needs to be kept in mind when a user is in the field looking for a fire.
- Exposure to sample products or case studies is likely to increase uptake and usage (Trigg and Roy 2007). Users need to understand which products are likely to be useful as well as how to use them. In an effort to guide users, LANCE worked with the science teams to develop a table of potentially useful products for NRT applications/hazards and disasters with links to stories in the NASA Earth Observatory (<http://earthobservatory.nasa.gov>) to help users understand what can be seen in an image, in a narrative.

5 Conclusion

This chapter provides examples of how LANCE global NRT data and imagery are serving the needs of the applications community and enabling users to make better decisions. The success of LANCE and breadth of NRT applications illustrated here has been made possible through the NASA's investment in algorithm development, science applications development and the LANCE NRT infrastructure described in Chap. 8. An important dimension of this system, and a distinct advantage in terms of data quality, is having science teams oversee the expedited algorithms, monitor the instrument and algorithm performance and help identify the potential use and limitations of the data sets.

Although use of LANCE data and imagery is growing, a general lack of awareness of the availability of these NRT products and their potential utility, still limits uptake by potential users. It is expected that this will change as user experiences become more streamlined, and blogs and social media provide more links to NRT imagery.

In the near future, users will be able access clients that stream coincident imagery from low/moderate-resolution (like MODIS, AIRS, OMI and MLS) and high-resolution sensors, and this will take the user experience to the next level. The integration of high-spatial—low-temporal resolution imagery with imagery of low/moderate-spatial resolution but high-temporal resolution will increase the utility of both types of data. For example, a user may identify the occurrence of fire, burned area or flood using MODIS but may struggle to determine the spatial extent of the event. Being able to add a co-incident layer of high-resolution imagery will help the user improve their confidence in what they see and provide a more accurate quantification of areal extent.

This chapter highlights how LANCE products are successfully being used, by the groups outlined in Table 2, for a wide range of applications. In addition to AIRS, MLS, MODIS and OMI there are other instruments that could provide data to complement the existing suite of products, if they were available in NRT with LANCE-type capabilities. There is therefore a case for near real-time data capability to become a standard option for global data access.

References

- Aquila V, Oman LD, Stolarski RS et al (2012) Dispersion of the volcanic sulfate cloud from a Mount Pinatubo-like eruption. *J Geophys Res* 117:D06216. doi:10.1029/2011JD016968
- Becker-Reshef I, Justice C, Sullivan M et al (2010a) Monitoring global croplands with coarse resolution earth observations: the Global Agriculture Monitoring (GLAM) Project. *Remote Sens* 2:1589–1609. doi:10.3390/rs2061589
- Becker-Reshef I, Vermote E, Lindeman M, Justice C (2010b) A generalized regression-based model for forecasting winter wheat yields in Kansas and Ukraine using MODIS data. *Remote Sens Environ* 114:1312–1323. doi:10.1016/j.rse.2010.01.010

- Bian H, Colarco PR, Chin M et al (2013) Source attributions of pollution to the Western Arctic during the NASA ARCTAS field campaign. *Atmos Chem Phys* 13:4707–4721. doi:10.5194/acp-13-4707-2013
- Carn SA, Krueger AJ, Krotkov NA et al (2008) Tracking volcanic sulfur dioxide clouds for aviation hazard mitigation. *Nat Hazards* 51:325–343. doi:10.1007/s11069-008-9228-4
- Chin M, Ginoux P, Kinne S et al (2002) Tropospheric aerosol optical thickness from the GOCART model and comparisons with satellite and sun photometer measurements. *J Atmos Sci* 59:461–483. doi:10.1175/1520-0469(2002)059<0461:TAOTFT>2.0.CO;2
- Colarco P, da Silva A, Chin M, Diehl T (2010) Online simulations of global aerosol distributions in the NASA GEOS-4 model and comparisons to satellite and ground-based aerosol optical depth. *J Geophys Res* 115:D14207. doi:10.1029/2009JD012820
- Darmenov A, da Silva AM (2013) The Quick Fire Emissions Dataset (QFED)—documentation of versions 2.1, 2.2 and 2.4. NASA Technical Report Series on Global Modeling and Data Assimilation 32
- Jedlovec G (2013) Transitioning research satellite data to the operational weather community: The SPoRT Paradigm [Organization Profiles]. *Geosci Remote Sens Mag IEEE* 1:62–66. doi:10.1109/MGRS.2013.2244704
- Justice CO, Townshend JRG, Holben BN, Tucker CJ (1985) Analysis of the phenology of global vegetation using meteorological satellite data. *Int J Remote Sens* 6:1271–1318. doi:10.1080/01431168508948281
- Justice CO, Townshend JRG, Vermote EF et al (2002) An overview of MODIS Land data processing and product status. *Remote Sens Environ* 83:3–15. doi:10.1016/S0034-4257(02)00084-6
- Justice CO, Román MO, Csiszar I et al (2013) Land and cryosphere products from Suomi NPP VIIRS: overview and status. *J Geophys Res Atmos* 118:1–13. doi:10.1002/jgrd.50771
- Krueger AJ, Krotkov NA, Yang K et al (2009) Applications of satellite-based sulfur dioxide monitoring. *IEEE J Sel Top Appl Earth Obs Remote Sens* 2:293–298. doi:10.1109/JSTARS.2009.2037334
- Masuoka E, Roy D, Wolfe R et al (2011) MODIS land data products: generation, quality assurance and validation. *L Remote Sens Glob Environ Change* 11:509–531
- Murphy K, Justice CO, Lowe D et al (2012) LANCE user working group meeting summary. *Earth Obs* 24:19–21
- Nowottnick E, Colarco P, Ferrare R et al (2010) Online simulations of mineral dust aerosol distributions: comparisons to NAMMA observations and sensitivity to dust emission parameterization. *J Geophys Res* 115:D03202. doi:10.1029/2009JD012692
- Nowottnick E, Colarco P, da Silva A et al (2011) The fate of Saharan dust across the Atlantic and implications for a central American dust barrier. *Atmos Chem Phys Discuss* 11:8337–8384. doi:10.5194/acpd-11-8337-2011
- Randles CA, Colarco PR, da Silva A (2013) Direct and semi-direct aerosol effects in the NASA GEOS-5 AGCM: aerosol-climate interactions due to prognostic versus prescribed aerosols. *J Geophys Res Atmos* 118:149–169. doi:10.1029/2012JD018388
- Trigg SN, Roy DP (2007) A focus group study of factors that promote and constrain the use of satellite-derived fire products by resource managers in southern Africa. *J Environ Manag* 82:95–110. doi:10.1016/j.jenvman.2005.12.008
- Tucker CJ, Holben BN, Elgin JH, McMurtrey JE (1981) Remote sensing of total dry-matter accumulation in winter wheat. *Remote Sens Environ* 11:171–189. doi:10.1016/0034-4257(81)90018-3
- Vizcarra N (2012) <https://earthdata.nasa.gov/featured-stories/featured-research/orbiting-watchtowers>. Accessed 10 April 2015

Use of Satellite Image Derived Products for Early Warning and Monitoring of the Impact of Drought on Food Security in Africa

Christophe Sannier, Sven Gilliams, Frédéric Ham and Erwann Fillol

Abstract

African and other countries in the world suffer from regular occurrence of extreme weather events of which droughts form a significant part. This is seriously affecting the ability of those countries to cover their population needs in food supply and to maintain their livelihood. However, the pattern of droughts is extremely variable both temporally and spatially and it is crucial that decision makers be informed in advance of the extent and location of potential drought conditions to target relief measures.

Approaches to food security monitoring based on the temporal and spatial analyses of Satellite image derived products are presented. These approaches demonstrate that the extent and severity of a drought can effectively be characterised in near real time. Examples of previous work in Zambia showed the benefit of integrating historical agricultural statistics with satellite derived products to better attribute vegetation development variability to agricultural production thus providing a means to predict potential crop production levels for the current growing season. Other work in Namibia, Niger, Senegal, South Sudan and Botswana shows that such techniques can be used to monitor rangeland primary production levels for a given season.

Lessons from the implementation of these approaches operationally are summarized, emphasizing the importance of institutional support.

C. Sannier (✉)

Systèmes d'Information à Référence Spatiale (SIRS), Parc de la Cimaise I,
27 rue du Carrousel, 59650 Villeneuve d'Ascq, France
e-mail: Christophe.sannier@sirs-fr.com

S. Gilliams

Vlaamse Instelling Technologish Onderzoek (VITO), Boeretang 200, 2400 Mol, Belgium

F. Ham · E. Fillol

Fundación Acción Contra el Hambre (ACF Spain), c/ Duque de Sevilla, 3, 28002 Madrid, Spain

© Springer Science+Business Media New York 2015

C. D. Lippitt et al. (eds.), *Time-Sensitive Remote Sensing*,
DOI 10.1007/978-1-4939-2602-2_12

183

Keywords

Crop production · Rangeland conditions · Biomass · NDVI · Vegetation biophysical variables · Time series analysis

1 Introduction

African and other countries in the world suffer from regular occurrence of extreme weather events of which droughts form a significant part. This is seriously affecting the ability of those countries to cover their population needs in food supply and to maintain their livelihood assets.

However, the pattern of droughts is extremely variable both temporally and spatially and it is crucial that decision makers be informed in advance of the extent and location of potential drought conditions to target relief measures. Figure 1 below shows the variability of Maize production in Zambia between 1981 and 2005 with an average of just over 1MT over the period considered, the actual annual production can vary by a factor of 4. Considering that maize is the main staple crop in Zambia, with a rapidly growing population, early indication on the status of the growing season is considered as strategic information by the Zambian government.

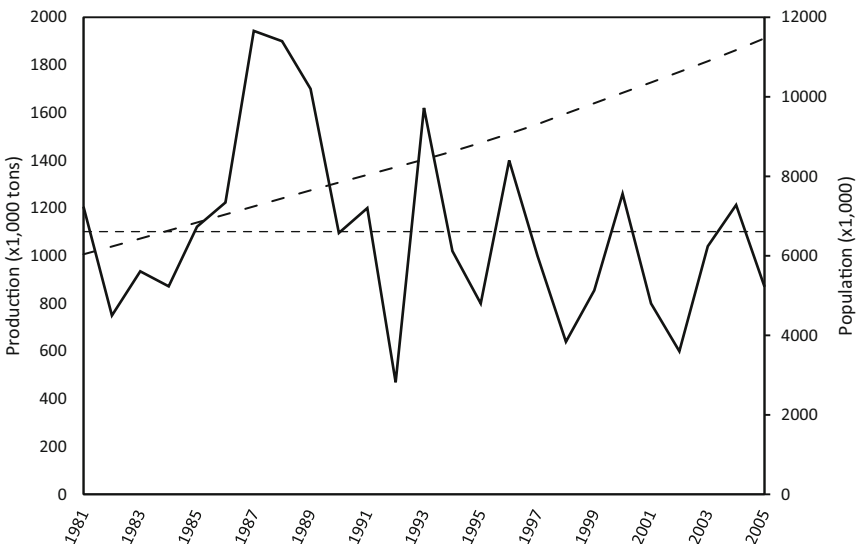


Fig. 1 Maize production in Zambia 1981–2005 (— maize production, - - - - average production, - . - . population, source FAO). Note that population is increasing, while maize production is not

set up by international (FAO-GIEWS¹, USAID-FEWS-NET² and WFP-VAM³), regional (e.g. AgrHyMet centre, RMCRD⁴, SADC⁵) and national organizations (mainly meteorological departments). Most of these systems rely on several components and other sources of information than just remote sensing of vegetation activity (Hutchinson 1991). They normally include some or all of the following aspects:

1. Socio-economic and market analysis based on desk and field data acquisition
2. Rainfall monitoring
3. Agro-meteorological modeling products
4. Vegetation status monitoring

Points 1–3 are focusing either on field based or meteorological data and are outside the scope of this book. Therefore, this chapter will further focus on the link between vegetation status monitoring and food security.

Surprisingly, despite the fact that “Food insecurity is likely to increase under climate change, unless early warning systems and development programs are used more effectively” (Brown and Funk 2008), a bibliographical search on food security and remote sensing reveals very few hits particularly in recent years. This may be because much of the research has been directed toward retrieval of biophysical parameters from satellite imagery to monitor vegetation: fraction of Absorbed Photosynthetically Active Radiation (fAPAR), Leaf Area Index (LAI) or Dry Matter Productivity (DMP) rather than on developing research on better methods for early warning of droughts for food security. Another factor may have been the drop in funding for agricultural research with a shift toward environmental research in western countries since the late 90s. This is now perhaps likely to change with the recent surge in agriculture commodity prices. As a result, a number of initiatives were launched at the highest political level such as the G20⁶ action plan on food price volatility and Agriculture⁷ particularly in the context of climate change when the world agricultural production is likely to be increasingly erratic due to more frequent extreme weather events including droughts (Lobell et al. 2008).

In Africa, early characterization of droughts is crucial if drought impacts on food security are to be mitigated. Although a review of existing methodologies used in these systems shows that the use of remotely sensed imagery plays an essential part in the process, the products derived are often difficult to interpret. Additional

¹ Food and Agriculture Organization’s Global Information and Early Warning System on food and agriculture.

² United States Agency for International Development (USAID) Famine Early Warning System Network.

³ World Food Programme’s Vulnerability Analysis and Mapping.

⁴ Regional Center for Mapping of Resources for Development.

⁵ Southern African Development Community.

⁶ The group of 20 major economies.

⁷ <http://un-foodsecurity.org/node/1115>.

analyses are required to derive indicators that can convey the appropriate information to decision makers in layman terms.

Approaches based on the temporal and spatial analyses of satellite image derived products have been developed. Even though droughts are considered as slow onset disasters, the time sensitive element of the remote sensing data used is at two levels:

- Long term archives are necessary for these approaches to be successfully implemented and the longer the time series, the more reliable the indicators developed become;
- Indicator products need to be made available to decision makers as early as possible before the end of the growing season for them to take appropriate action (e.g. import cereals in case of serious drought before prices are too high).

2 Common Characteristics of Vegetation Status Monitoring and Drought Early Warning Systems in Africa

As indicated previously, bibliographical references on this topic are scarce. However, a good source of information about the state of the art in this area is found in the Crop and Rangeland Monitoring (CRAM) workshops that regularly takes place in Nairobi, Kenya⁸.

Most early warning systems for food security make use of vegetation status products. In its simplest way, they will consist of 10-day maximum value composites of vegetation indices derived from high temporal resolution satellite images to comply with the time sensitive aspect of the information to be provided (AVHRR⁹, SPOT¹⁰ VEGETATION, MERIS¹¹ or MODIS¹²).

The most widely used satellite derived indicator of vegetation activity is the Normalized Difference Vegetation Index (NDVI, Tucker 1979). However, new approaches are now being increasingly used such as the Enhanced Vegetation Index (EVI) for MODIS (Huete et al. 2002) or the use of biophysical variables resulting from radiative transfer model inversion with fAPAR/LAI products (Knyazikhin et al. 1999; Gobron et al. 2005; Rossi et al. 2008; Baret et al. 2007). Several studies have demonstrated the use of vegetation indices to assess crop yields or rangeland primary production (Prince and Astle 1986; Kennedy 1989; Diallo et al. 1991; Prince 1991; Rasmussen 1992; Carfagna and Gallego 2006). For the non-technical user, vegetation indices or LAI/fAPAR maps as shown in Fig. 2 are difficult to interpret. Without further information, it can only be said from looking at the map that some

⁸ <http://mars.jrc.ec.europa.eu/mars/News-Events/3rd-CRAM-Workshop>.

⁹ Advanced Very High Resolution Radiometer.

¹⁰ Système Pour l'Observation de la Terre.

¹¹ MEdium Resolution Imaging Spectrometer.

¹² MODOerate resolution Imaging Spectroradiometer.

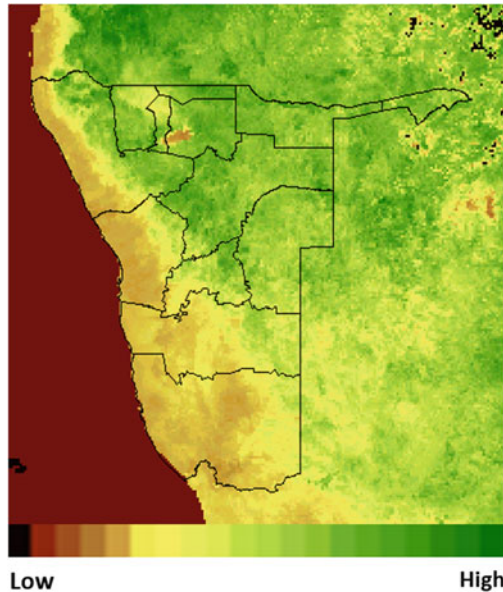


Fig. 2 National oceanic and atmospheric administration (NOAA) advanced very high resolution radiometer (AVHRR) normalized difference vegetation index (NDVI) image of Namibia for the second 10-day period of 2000

areas appear greener than others. However, this does not necessarily mean that those areas exhibit better conditions. Firstly, because the relationship between vegetation indices and vegetation condition is not explicit and secondly, there may be different relationships for each vegetation type. Previous studies (Kogan 1990; Maselli et al. 1993) have shown the influence of geographic variations on the interpretation of the NDVI.

In order to relate vegetation indices or fAPAR/LAI to vegetation conditions, there is a need to compare the current value at a given location with historical data. Only then will it be possible to determine whether the vegetation conditions are better or worse than normal. Current operational early warning systems such as GIEWS or FEWS-NET have set up operational early warning systems which compare current NDVI images with the previous 10-day period or with the mean image for the period considered (Le Compte 1989; Hutchinson 1991; Lambin et al. 1993). The first approach only helps determine whether vegetation is greening up or not and does not really help assess the actual vegetation conditions. The second approach is also very simple but relies on the temporal variation of the NDVI for a location and a given 10-day period being normally distributed. This assumption may be unreasonable because the lower limit of the NDVI is bounded by the response for bare soil. Kogan (1990) took a different approach and defined a Vegetation Condition Index (*VCI*) as:

$$VCI = 100 \left(\frac{NDVI - NDVI_{\min}}{NDVI_{\max} - NDVI_{\min}} \right) \quad (1)$$

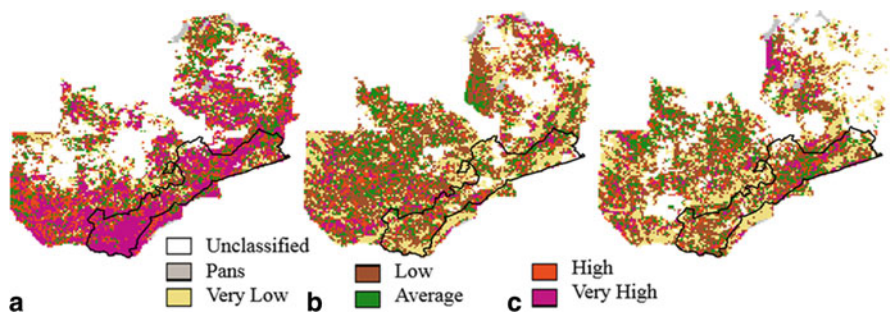


Fig. 3 Vegetation productivity indicator (VPI) maps of Zambia for (a) 1988 with 1.9 Mt of Maize produced (b) 1982 with 0.7 Mt of Maize produced and (c) 2002 with 0.6 Mt of maize produced

where $NDVI_{max}$ and $NDVI_{min}$ are the maximum and minimum NDVI values in the time series, for the dekad. This assumes that the current range represents the maximum possible variation and that all values of the NDVI within the range occur with the same frequency and therefore have the same probability. This also maybe an unrealistic assumption.

Sannier et al. (1998) proposed an alternative method to compare the current NDVI with the historical NDVI archive to assess vegetation condition with a Vegetation Productivity Indicator (VPI). The method estimates the statistical distribution of the NDVI empirically from the available data without limiting assumptions and is sensitive to the background vegetation type. The VPI is expressed as a probability p to get a lower NDVI value:

$$VPI = p = \frac{m}{n + 1} \quad (2)$$

where m is the current NDVI rank in the time series and n is the number of years. Therefore, a low probability corresponds to low vegetation conditions. The method was applied to NDVI, but could also be applied to other vegetation indices or fAPAR/LAI. Figure 3 shows VPI maps of Zambia for selected growing seasons illustrating the relation with maize production.

Time series profiles as shown in Fig. 4 can also be produced from time series of images against the VPI template indicating how a season is progressing for selected locations. These together with maps can then be integrated in bulletins produced during the growing season and disseminated to stakeholders.

3 Crop Monitoring for Food Security

3.1 Context

As mentioned in the introduction, throughout the past decades a number of crop monitoring systems using remote sensing data as input have been developed at global to

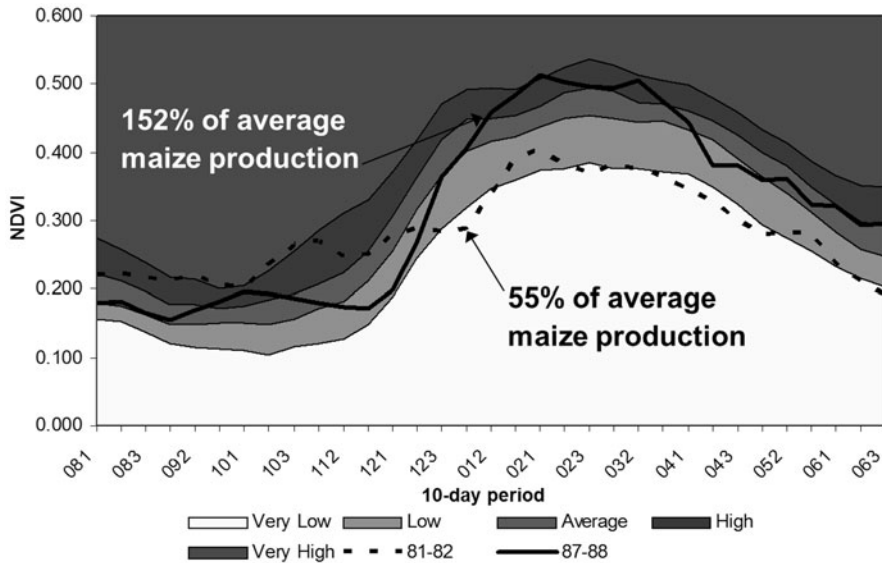


Fig. 4 Comparison of the vegetation productivity indicator (VPI) in two different seasons (1981–1982 and 1987–1988) in Zambia for the same location in the Kalomo district

regional and national scale. Crucial for these systems is to get the correct information in a timely manner on the desk of decision makers. During the 3rd CRAM workshop held in Nairobi, Kenya from 26 to 30 September 2011, this was pointed out and stressed once more. The workshop took place during the 2010–2011 famine in the Horn of Africa which had claimed the lives of thousand in the region. During the conference it was highlighted that analyses based on remote sensing data had already predicted this event, but this information was not picked up by decision makers. As such it was concluded that one of the challenges of the early warning community still remains to find the right way to convey relevant information in a timely and understandable manner to decision makers¹³. The following sections describe an approach on how this can be achieved by close collaboration with local experts.

3.2 Remote Sensing Time Series Analysis for Crop Monitoring

The focus of this section is on approaches used in the Crop Yield and Vegetation Monitoring Service of the Global Monitoring for Food Security (GMFS¹⁴) project. GMFS is part of the ESA’s contribution to the European Union/ESA Global Monitoring for Environment and Security (GMES-Copernicus) program. The GMFS

¹³ http://mars.jrc.ec.europa.eu/mars/News-Events/3rd-CRAM-Workshop/summary_cram3.

¹⁴ www.gmfs.info.

partnership started in 2003 and consists of seven European institutions with different fields of expertise, in addition to the European partners, there are two regional African partners: the AgrHyMet Centre in Niger and the Regional Centre for Mapping Resources for Development (RCMRD) in Kenya. As stated by Haub and Gilliams (2010), “GMFS aims to provide earth observation based services and encourage partnerships in monitoring food security and related environmental processes in Africa, by concerting efforts to bring data and information providers together, in order to assist stakeholders, nations and international organizations to better implement their policies towards sustainable development.”

The primary data used for the above mentioned service was from the MERIS sensor, covering the period 2002–2012. When contact was lost with the ENVISAT satellite platform carrying the MERIS sensor in April 2012, the GMFS program began to use data from the SPOT-VEGETATION program (1998–present). These long term archives make it possible to compare the current crop status at local regional and continental level with “normal” conditions (i.e. the historical average situation).

As part of the JRC-MARS¹⁵ project VITO developed an analysis tool specially developed to analyze time series data called Software for Processing and Interpretation of Remote sensing Image Time Series (SPIRITS). This tool allows local experts to analyze the long term remote sensing data archives at their disposal and compare time series data with current data. Outputs from this analysis tool are similar to the result shown in Fig. 4. The long term min, max and mean NDVI can be plotted versus the NDVI of the 2009 growing season for selected administrative regions, as well as a similar analysis for Rain Fall Estimates (RFE). The NDVI and RFE profiles were extracted based on an agricultural mask derived from the FAO (Food and Agriculture Organization of the United Nations) AFRICOVER data set (Kalensky 1998).

Thanks to the availability of the full archive of SPOT-VEGETATION data this type of analysis can be done at any time during the growing season for every region in Africa. In fact based on these graphs, decision makers can already see at the start of the season if the vegetation in the arable parts of their region is growing below or above the normal and if the growth is within the min and max range of the historical archive. This provides them with a basis to take early actions during the growing season in case of extreme events.

A second approach using the software tool that is applied within the GMFS project is based upon a cluster analysis. In this analysis the NDVI values for all arable land pixels are compared to the historical mean NDVI value for that specific pixel at a specific time in the growing season. The result as shown in Fig. 6 provides the spatial location, the spatial extent as well as the temporal extent of an anomaly. For the red area in Fig. 5, it can be seen that until around May, the NDVI values were close to the average (grey zone around 0 difference). At the end of June and throughout July there was a serious drop in NDVI values as compared to the historical mean values (drop of around 15 %), but this drop was not permanent since it seems that vegetation had recovered by mid-August.

¹⁵ Joint Research Centre—Monitoring Agriculture with Remote Sensing project.

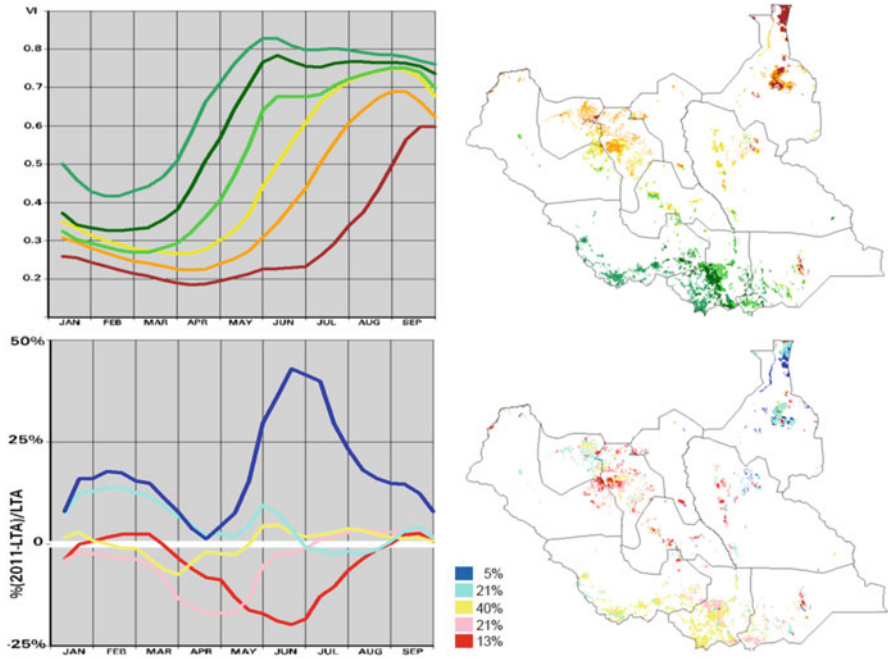


Fig. 5 Global monitoring for food security cluster analysis product, where all pixels with similar characteristics throughout the growing season or as compared to the historical mean are clustered and displayed on a map. The temporal characteristics of each cluster is displayed in the graph

A third and final approach demonstrating the time sensitive element of remote sensing data in crop monitoring systems is the analysis of the start of the growing season. Based on the analysis of the historical archive of the remote sensing data, the average start of the season is calculated. The NDVI response for the current season is then compared with the average NDVI response. Based on this analysis, the time difference between the start of the current and average seasons can be calculated as a number of 10-day periods (or dekads) as shown in Fig. 6.

3.3 User Interactions

The examples shown in the previous section clearly illustrate the importance of maintaining a long, qualitative and complete archive of remote sensing data to provide decision makers with relevant and correct information on drought conditions likely to affect the food security situation in the region considered. The second challenge raised in the conclusion of the CRAM workshop i.e. the time delivery of the data in understandable manner, will be addressed in this section.

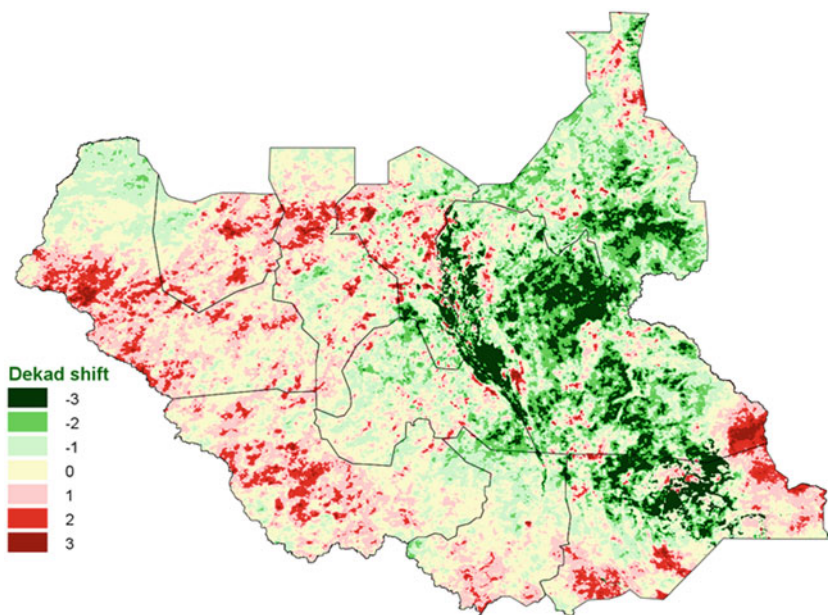


Fig. 6 South Sudan—Crop monitoring information support: Start of growing season analysis using the software for processing and interpretation of remote sensing image time series (SPIRITS) tool. Start of season shift: 2012 compared to (1999–2011) average

GMFS users are the driving force behind the definition of GMFS products (Haub and Gilliams 2010) and implementation of the activities. The interaction between GMFS and the Centre de Suivi Ecologique (CSE) in Senegal provides a demonstration of this approach. The objective of the CSE is to collect, process, analyze and distribute remote sensing products on land, infrastructure and natural resources of Senegal to improve the management of natural resources at all decision levels. As such, CSE is a member of the interdisciplinary group that meets every 10 days during the growing season in Senegal in which they share their remote sensing derived information with the other members of the group (e.g. ministry of agriculture, meteorological department etc.). Since this meeting takes place every second day after a the end of a 10-day period, it is crucial that CSE receives GMFS products before this date with sufficient time left for local experts to analyze the information provided. CSE experts were trained on SPIRITS to ensure they can understand, produce and explain the products provided and perform the analyses they need. Figure 7 illustrates how analyses described in the previous section are published in the bulletins CSE produces every 10 day during the growing season.



Fig. 7 Bulletin production by the Centre de Suivi ecologique integrating the global monitoring for food security approach

4 Rangeland Monitoring for Food Security

4.1 Pasture Production Estimation

Largely dependent on water and pasture availability, the livelihood of pastoral communities in the Sahel region is based on a fragile equilibrium, very sensitive to rainfall variability. In these areas where ACF International (a humanitarian organization committed to ending world hunger) has been working since 1996, the evaluation of available pastoral resources represents fundamental information for pastoralists.

In the Sahel, for a given year, the total rainfall amount falls during a unique rainy season that lasts between 2 and 4 months. Once this period has passed, it is possible to assess the resource availability and forecast the likely adaptation strategies pastoralists and their livestock might adopt during the coming year. Doing so, it is possible to evaluate the level of vulnerability for each area.

In order to address an existing gap for the assessment of pastoral communities' vulnerability, ACF and its partners have been progressively developing a geographic information system (GIS) based tool—the Biogenerator—providing a semi-automated approach to biomass production monitoring.

This tool integrates SPOT-VEGETATION DMP and NDVI products. These products are pre-processed by VITO from 1998 until today, on a 10 days basis and with 1 × 1 km pixel size. DMP [kg/ha/day] is estimated using the SPOT-VEGETATION

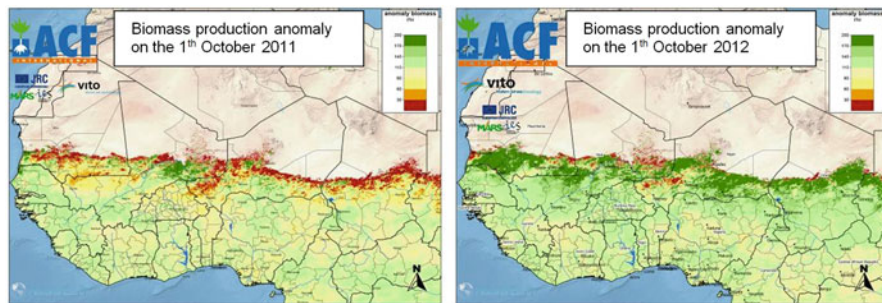


Fig. 8 Spatial comparison between biomass production anomalies in the Sahel region in 2011 and 2012

NDVI temporal profile converted to fAPAR values based on the Monteith's model (Baret et al. 2007).

Three types of outputs are produced by the Biogenerator:

- The biomass production map for each year of the time series;
- The inter annual average biomass production map;
- The biomass production anomaly map for each year of the time series.

The outputs are produced right after the end of the rainy season (end of September, beginning of October). Specifically, the annual biomass production map and the biomass production anomaly can be effectively used in the frame of early warning processes in pastoral areas, while the inter-annual average biomass production map would provide useful information for land and natural resources management for longer terms purposes.

Biomass production anomaly maps for 2011 and 2012 are presented in Fig. 8. The Biomass production deficit is represented by red color while excess is represented by green color. From these two maps, it is easy to observe the huge difference between these two consecutive years. In 2011, the rainy season failed in almost the whole of Sahel while in contrast, 2012 has been one of the most productive years recently. The 1 km² resolution is sufficient for a sub national and local analysis to support an efficient early warning process and response several months before the effects of the rain failure could be felt. In Fig. 9 DMP values over 2011 and 2012 rainy seasons are compared to "normal" year's values for a single pixel chosen in the Ifoghas mountains region in north Mali. In 2011, the rains started earlier but also stopped very early aborting the productive period, while in 2012 rains started later than the normal year but gave much higher production.

The tool was developed and transferred to national authorities in Mali and Niger and is progressively recognized at regional level by governments, non-governmental organizations and United Nations agencies as a reference to anticipate incoming crisis. As the Sahel is heavily affected by climate change, the system could also help

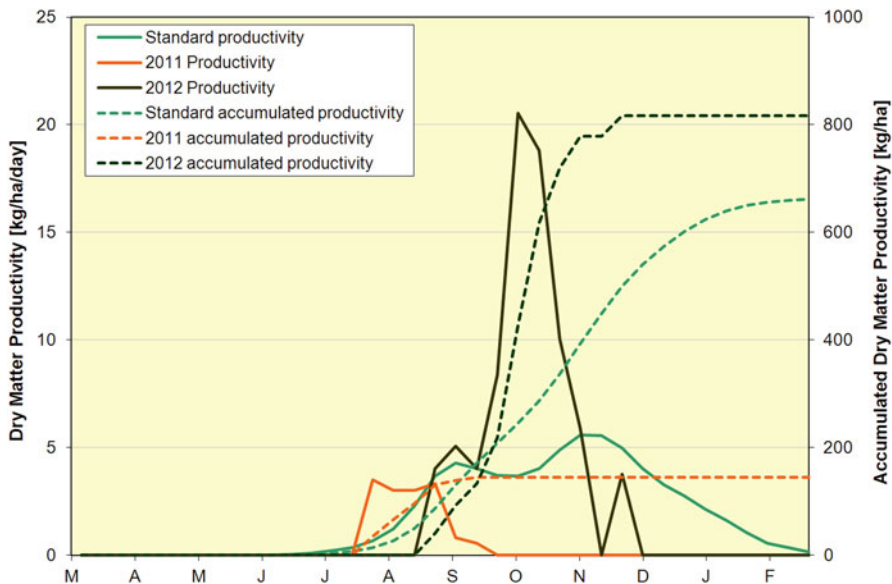


Fig. 9 Comparison of dry matter productivity between years 2011 and 2012 for one pixel in Ifoghas mountains (18°51'09.64"N, 1°45'48.21"E)

analyzing some of climate change induced effects and could become a planning tool to support pastoral population resilience.

4.2 Feed Balance Diagram

The biomass production anomaly consists of a reliable early warning indicator in the pastoral areas of the Sahel. However, the value of this tool is rather limited to quantify the biomass production in order to provide an actual feed balance. A comparison of the Biogenerator output and field data (570 plots measurements realized between 1998 to 2009 in north Mali and Niger) show that it reliably characterize the annual dry matter production quantity ($R^2 = 0.59$, Fillol et al. 2008). However the actual usable and accessible biomass is not directly assessed. As a result, using the output of the Biogenerator could be misleading without applying some additional spatial analysis. Figure 10 shows the different analysis that should be performed in order to provide a more realistic feed balance.

LEVEL 1 is the level directly reached by the Biogenerator. It provides a total quantity of biomass production without distinguishing any degree of palatability and accessibility.

LEVEL 2 introduces the notion of usability/palatability. Applying pastoral potentiality maps on top of biomass production could help getting a closer idea of usable biomass.

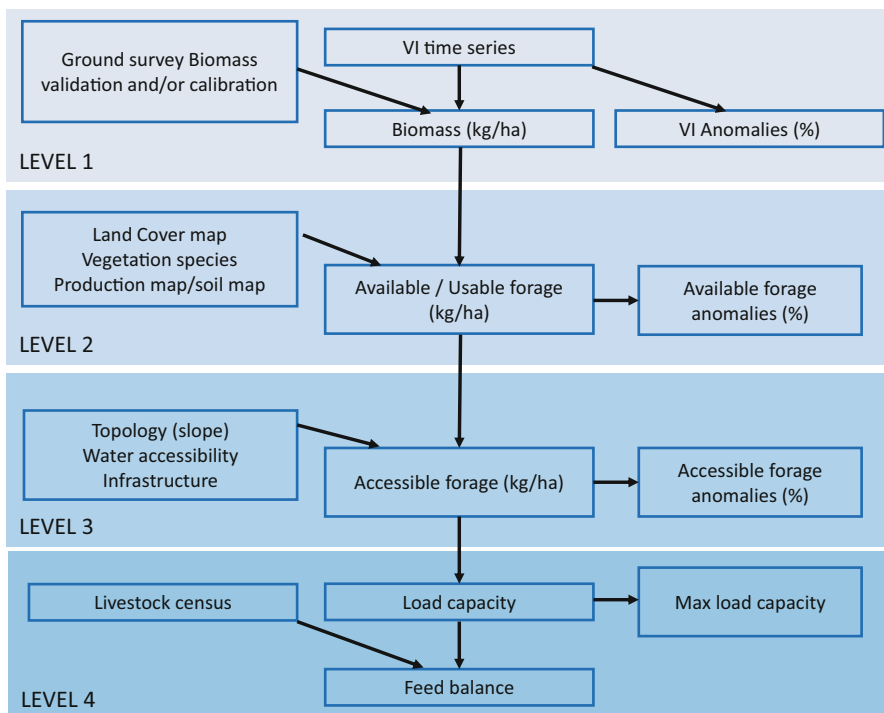


Fig. 10 Feed balance diagram. (Ham F. & Fillol E.)

LEVEL 3 considers the accessibility of the pasture lands with respect to the distance to water and considering topography.

LEVEL 4 would relate the usable and accessible pasture to the number of animals. At this level it would be possible to provide a more realistic feed balance.

This last level is not currently achieved, but ACF is exploring how this could be done through partnerships at local, regional and international levels. This would then provide a means to anticipate more accurately a potential crisis in the Sahel.

5 Conclusions

These approaches demonstrate that the extent and severity of a drought can effectively be characterized for time sensitive applications. Work in Namibia, Niger and Botswana shows that such techniques can be used to monitor rangeland primary production levels for a given season. Examples in Senegal and Zambia showed the benefit of integrating historical agricultural statistics with satellite derived products to better attribute vegetation development variability to agricultural production thus providing a means to predict potential crop production levels for the current growing

season. However, scrutiny of existing operational food security early warning systems show that EO derived vegetation condition map products are not always well integrated with other sources of information. These inputs are still very valuable in providing converging evidence of the presence of drought conditions, but the use of these products for early decision making could be reinforced if the relationship between the severity of the drought and the associated reduction in crop yields or rangeland primary production was better known quantitatively.

To be successful, these approaches need to carefully consider how decisions affecting food security are made and to whom the products are addressed. These considerations emphasize the importance of institutional support.

References

- Baret F, Hagolle O, Geiger B, Bicheron P, Miras B, Huc M et al (2007) LAI, fAPAR and fCover CYCLOPES global products derived from vegetation: part 1: principles of the algorithm. *Remote Sens Environ* 110(3):275–286
- Brown ME, Funk CC (2008) Food security under climate change. *Science* 319:580–581
- Carfagna E, Gallego FJ (2006) Using remote sensing for agricultural statistics. *Int Stat Rev* 73(3):389–404
- Diallo O, Diouf A, Hanan N P, Ndiaye A, Prévost Y (1991) AVHRR monitoring of savanna primary production in Senegal, West Africa: 1987–1988. *Int J Remote Sens* 12:1259–1279
- Fillol E, Metais T, Gómez A (2008) Estimation de la quantité de biomasse sur la zone Sahélienne Mali-Niger par télédétection pour l'aide à la gestion de l'activité pastorale. Paper presented at the 2008 Toulouse Space Show, Pierre Baudis Center, Toulouse, 22–25 April 2008
- Gobron N, Pinty B, Mélin F, Taberner M, Verstraete M, Belward A, Lavergne T et al (2005) The state of vegetation in Europe following the 2003 drought. *Int J Remote Sens* 26(9):2013–2020
- Haub C, Gilliams S (2010) GMFS service integration and know how transfer to Africa. Paper presented at the ESA Living Planet Symposium 2010, Bergen, Norway, 28 June–2 July 2010
- Huete A, Didan K, Miura T, Rodriguez EP, Gao X, Ferreira LG (2002) Overview of the radiometric and biophysical performance of the MODIS vegetation indices. *Remote Sens Environ* 83:195–213
- Hutchinson CF (1991) Uses of satellite data for famine early warning in sub-Saharan Africa. *Int J Remote Sens* 12:1405–1421
- Kalensky ZD (1998) Africover—land cover database and map of Africa. *Can J Remote Sens* 24(3):292–297
- Kennedy P (1989) Monitoring the vegetation of tunisian grazing lands using the normalized difference vegetation index. *Ambio* 18:119–123
- Knyazikhin Y, Glassy J, Privette JL, Tian P, Lotsch A, Zhang Y, Wang Y, Morisette JT, Votava P, Myneni RB, Nemani RR, Running SW (1999) MODIS Leaf Area Index (LAI) and fraction of photosynthetically active radiation absorbed by vegetation (fPAR). Product (MOD15) Algorithm Theoretical Basis Document. http://modis.gsfc.nasa.gov/data/atbd/atbd_mod15.pdf. Accessed 29 Sept 2013
- Kogan FN (1990) Remote sensing of weather impacts on vegetation in non-homogeneous areas. *Int J Remote Sens* 11:1405–1419
- Lambin EF, Cashman P, Moody A, Parkhurst BH, Pax MH, Schaaf CB (1993) Agricultural production monitoring in the sahel using remote sensing: present possibilities and research needs. *J Environ Manag* 38:301–322

- Le Comte DM (1989) Using AVHRR for early warning of famine in Africa. *Photogramm Eng Remote Sens* 55:168–169
- Lobell DB, Burke MB, Tebaldi C, Mastrandea MD, Falcon WP, Naylor RL (2008) Prioritizing climate change adaptation needs for food security in 2030. *Science* 319:607–610
- Maselli F, Conese C, Petkov L, Gilabert MA (1993) Environmental monitoring and crop forecasting in the sahel through the use of NOAA-NDVI data. A case study: Niger 1986–1989. *Int J Remote Sens* 14:3471–3487
- Prince SD (1991) Satellite remote sensing of primary production: comparison of results for sahelian grasslands 1981–1988. *Int J Remote Sens* 12:1301–1311
- Prince SD, Astle WL (1986) Satellite remote sensing of rangelands in Botswana. I. Landsat MSS and herbaceous vegetation. *Int J Remote Sens* 7:1533–1553
- Rasmussen MS (1992) Assessment of millet yields and production in northern Burkina Faso using integrated NDVI from the AVHRR. *Int J Remote Sens* 13:3431–3442
- Rossi S, Weissteiner C, Laguardia G, Kurnik B, Robustelli M, Niemeyer S, Gobron N (2008) Potential of MERIS fAPAR for drought detection. In: Lacoste H, Ouwehand L (eds) *Proceedings of the 2nd MERIS/(A)ATSR User Workshop*, Frascati (Italy), 22–26 September 2008. ESA SP-666, ESA Communication Production Office
- Sannier CAD, Taylor JC, du Plessis W (1998) Real-time vegetation monitoring with NOAA-AVHRR in Southern Africa for wildlife management and food security assessment. *Int J Remote Sens* 19(4):621–639
- Tucker C J (1979) Red and photographic infrared linear combinations for monitoring vegetation. *Remote Sens Environ* 8(2):127–150